Microglial Signalling Cascades Associated with Stroke and Alzheimer's Disease

Claudie Hooper

A thesis submitted to the Institute of Neurology, University College London in candidature for the degree of Doctor of Philosophy in Neuroscience

October 2003

ProQuest LLC
789 East Eisenhower Parkway
P.O. Box 1346
Ann Arbor, MI 48106-1346

Abstract

Microglia, the resident macrophages of the brain, were originally assumed to be passive cells, however increasing evidence suggests that microglia play an active role during development and in neurological disorders. Activated microglia release a variety of toxic inflammatory mediators including reactive nitrogen species, cytokines, glutamate and oxygen free radicals, all of which exert a detrimental effect on neuronal survival if secretion is sustained. Microglial responses depend on the signals received from the surrounding microenvironment. Therefore, in this thesis the effects of albumin, chromogranin A (CgA), β-amyloid (Aβ), ischaemia and combined insults (ischaemia plus albumin or ischaemia plus Aβ) on microglial signalling have been investigated because these activators are associated with the pathology of stroke and/or Alzheimer's disease.

Briefly, albumin was found to induce iNOS expression, to cause the release of glutamate and to elicit a calcium-dependent proliferative response in microglia; events that were mediated by a possible interaction with myosin IX. Interestingly, peritoneal macrophages were unresponsive to the same concentrations of albumin. CgA and Aβ triggered microglial signalling via scavenger receptor-dependent mechanisms. Both activators caused microglia to undergo mitochondrial depolarisation, which precipitated apoptosis. CgA, but not Aβ, also induced iNOS expression and glutamate release. CgA-induced iNOS expression was mediated by the Src kinase-dependent phosphorylation of ERK. Ischaemia *per se* did not elicit any discernable effects on microglial signalling. However, microglia subjected to ischaemia followed by albumin treatment endured mitochondrial depolarisation, which led to apoptosis. Similarly, ischaemia followed by Aβ treatment potentiated the levels of microglial apoptosis and mitochondrial depolarisation induced by Aβ alone. A common characteristic displayed by microglia subjected to albumin, CgA, Aβ, or ischaemia was the ability to induce neuronal death. Thus, manipulation of microglial signalling pathways to reduce reactivity and neurotoxicity may provide novel therapeutic strategies for the amelioration of neurodegeneration in disorders such as stroke and Alzheimer's disease.

TABLE OF CONTENTS

LIST OF TABLES

LIST OF FIGURES

5.0 Investigation of the microglial signalling elicited by CgA or Aβ

6.0 Effects of ischaemia on microglial signalling

Acknowledgements

I would like to thank my principal supervisor Dr Jennifer Pocock for her advice and guidance throughout the course of my studies. I would also like to acknowledge and thank my secondary supervisor Dr Deanna Taylor for her help and support. A special thank you goes to both of them for their limitless help with the preparation of this thesis.

I wish to thank Dr David Baker and Gareth Pryce for their assistance with the fluorescence activated cell sorting and Susan Griffin for the use of the hypoxia chamber. I am also grateful to Sarah, Amanda and Sam for their help in the lab and their friendship throughout my studies.

I would also like to acknowledge the Alzheimer's Research Trust who through the Haberdashers Benevolent Foundation provided funding for this work. Finally, I would like to thank Mum, Dad and Paul for their encouragement and support.

Abbreviations

$\Delta\Psi$	mitochondrial membrane potential
Aβ	amyloid-β protein
AD	Alzheimer's disease
AIDS	auto-immuno-deficiency-syndrome
AIF	apoptosis inducing factor
Alb	albumin
AMPA	2-amino-3-hydroxy-5-methylisoxazole-4-propionic acid
ANOVA	analysis of variance
ANT	adenine nucleotide translocator
APAF-1	apoptosis protease activating factor-1
ApoE	apolipoprotein E
APP	amyloid precursor protein
Ara-C	cytosine arabinofuranoside
ATP	adenosine triphosphate
BACE	β site APP cleaving enzyme
BAPTA	1,2-bis(2-aminophenoxy)ethane-N,N,N',N' tetra-acetic acid
BBB	blood brain barrier
BDNF	brain derived neurotrophic factor
BSA	bovine serum albumin
Ca^{2+}	calcium ion
CAA	cerebral amyloid angiopathy
CgA	chromogranin A
CGC	cerebellar granule cells
CM	conditioned medium
CREB	cAMP response element binding protein
CSK	C-terminal Src kinase
cNOS	constitutive nitric oxide synthase
CNS	central nervous system
CNQX	6-cyano-7-nitroquinoxaline-2,3-dione
CO_2	carbon dioxide
COX	cyclo-oxygenase
CSF	cerebrospinal fluid
Cyt *c*	cytochrome *c*
DAB	diaminobenzidine tetrahydrochloride
DMEM	dulbeccos modified eagles medium
DMSO	dimethyl-sulphoxide

DNA	deoxyribonucleic acid
DPX	distyrene, tricresyl phosphate and xylene mounting medium
ECL	enhanced chemi-luminescence
ELISA	enzyme linked immunosorbant assay
eNOS	endothelial nitric oxide synthase
ER	endoplasmic reticulum
ERK	extracellular signal regulated kinase
FACS	fluorescence activated cell sorting
FAD	familial Alzheimer's disease
FADD	FAS-associated death domain protein
$FADH_2$	flavin adenine dinucleotide (reduced)
FCS	foetal calf serum
FITC	fluorescien isothiocyanate
Fv	fraction v
G protein	Guanine nucleotide binding protein
GABA	gamma-aminobutyric acid
GFAP	glial fibrillary acidic protein
5-HT	serotonin
H^+	hydrogen ion
HCHWA-D	hereditary cerebral haemorrhage with amyloidosis, dutch type
Hoechst 33342	2'-{-4-ethoxyphenyl}-5-{-4-methyl-1-piperazinyl}-2,5'bi-1-H-benzimidazol
HPLC	high performance liquid chromatography
HRP	horse radish peroxidase
ICAM-1	intercellular adhesion molecule 1
ICE	interleukin 1β converting enzyme
IFNγ	interferon gamma
IL	interleukin
iNOS	inducible nitric oxide synthase
IP_3	inositol trisphosphate
FCCP	carbonyl cyanide *p*-(trifluoromethoxy)phenylhydrazone
JC1	5,5'6,6'-tetraethylbenzimidazole carbo-cyanine iodide
K^+	potassium ion
LDL	low density lipo-protein
LPA	lysophosphatidic acid
LPS	lipopolysaccharide
LTD	long term depression
LTP	long term potentiation

MALDI	matrix assisted laser desorption ionisation
MAP	microtubule associated protein
MAPK	mitogen activated protein kinase
MCA	middle cerebral artery
MCP-1	monocyte chemoattractant protein 1
MEK	MAP kinase kinase
MEM	minimum essential medium
MFI	mean fluorescence intensity
Mg^{2+}	magnesium ion
mGluR	metabotropic glutamate receptor
mRNA	messenger ribonucleic acid
MHC	major histocompatability complex
MK801	5-methyl-10,11-dihydro-5H-dinezo[a,d]cyclohepten-5,1-imine hydrogen maleate
MS	multiple sclerosis
MSPG	(±)-α–methyl-4(4-sulphonophenyl)glycine
N9	N9 microglial cell line (mouse)
Na^+	sodium ion
NAD^+	nicotinamide adenine dinucleotide (oxidised)
NADH	nicotinamide adenine dinucleotide (reduced)
$NADP^+$	nicotinamide adenine dinucleotide phosphate (oxidised)
NADPH	nicotinamide adenine dinucleotide phosphate (reduced)
NCAM	neural cell adhesion molecule
NFT	neurofibrillary tangle
NGF	nerve growth factor
NFκβ	nuclear factor κβ
NMDA	N-methyl-D-aspartate
NOS	nitric oxide synthase
nNOS	neuronal nitric oxide synthase
NO	nitric oxide
OD	optical density
PBS	phosphate buffered saline
PD	Parkinson's disease
PE	phycoerythrin
PHF	paired helical filament
PI	propidium iodide
PIP_2	phosphatidylinositol bisphosphate
PKA	protein kinase A

PKC	protein kinase C
PLC	phospholipase C
Poly I	poly inosinic acid
PPADS	pyridoxal-phosphate-6-azophenyl-2'-4'-disulphonic acid
PP2	4-amino-5-(4-chlorophenyl)-7-(t-butyl)pyrazolo[3,4-d]pyramidine
PS	presenilin
PT	permeability transition pore
PTH	phenylthiohydantoin
Ptx	pertussis toxin
PVDF	polyvinylidene di-fluoride
RAS	rat sarcoma viral oncogene homologue
RAF	RAS activated kinase
RNA	ribonucleic acid
RSK	ribosomal protein SG kinase of 90 kDa
SBTI	soyabean trypsin inhibitor
SDS	sodium dodecylsulphate
SDS-PAGE	SDS- polyacrylamide gel electrophoresis
SCM	serum containing medium
SFM	serum free medium
SH2	src homology 2
SOS	son of sevenless
TACE	TNF-α converting enzyme
TBS	tris buffered saline
TTBS	tween-20 tris buffered saline
TGF	transforming growth factor
TIA	transient ischaemic attack
TNF	tumour necrosis factor
T-test	student's t-test
UO126	1,4-diamino-2,3-dicyano-1,4-bis (0-aminophenylmercapto) butadiene
UV	ultra violet
VaD	vascular dementia
VCAM	vascular cell adhesion molecule
VDAC	voltage dependent anion channel
VDCC	voltage dependent calcium channels

1.0 Introduction

1.1 General introduction

1.1.1 The central nervous system and glia

The CNS consists of a network of approximately 10^{12} neurones, which facilitate the transmission of action potentials enabling organisms to communicate with their environment (Alberts et al., 2002). Despite the essential function of neurones, about 90% of the cells in the CNS are glia (Sherwood 1993). Glia were originally believed to be passive cells that only acted physically to support neurones, hence the name glia meaning 'glue' (Coyle and Schwarcz 2000). However, glia are now known to play an active role in many central homeostatic processes. Four main types of glia exist, namely oligodendrocytes, astrocytes, ependymal cells and macrophages of the brain (Sherwood 1993), which are commonly termed microglia irrespective of their cerebral location (see below).

Oligodendrocytes comprise several short processes, which wrap themselves around neurones. Oligodendrocytes are responsible for the myelination of neurones in the CNS (Alberts et al., 2002). Oligodendrocytes also regulate extracellular potassium ion concentration (Ransom and Sontheimer 1992) and secrete a number of nerve growth factors including nerve growth factor (NGF), brain derived neurotrophic factor (BDNF) and neurotrophin-3 (Dai et al., 2000). Peripheral axons are myelinated by Schwann cells and these cells in contrast to oligodendrocytes faciliate neuronal regeneration following injury (Torigoe et al., 1996).

Astrocytes are classified into protoplasmic and fibrous astrocytes. Protoplasmic astrocytes display short processes and are associated with grey matter, whereas fibrous astrocytes exhibit long processes and are associated with white matter (Kimelberg and Norenberg 1989). During development astrocytes act as a scaffold

facilitating neuronal migration and synaptogenesis (Ransom and Sontheimer 1992). In the adult astrocytes are involved in the maintenance and permeability of the blood brain barrier (BBB), accordingly astrocytic processes or 'end feet' surround every capillary in the brain (Kimelberg and Norenberg 1989). Astrocytes also support the metabolic requirements of neurones (Magistretti et al., 1999) and play a role in the degradation of a number of neurotransmitters including serotonin, glutamate and gamma-aminobutyric acid (GABA) (Kimelberg and Katz 1985; Kimelberg and Norenberg 1989). Additionally, astrocytes regulate extracellular potassium ion concentration, which is crucial for the propagation of action potentials in neurones (Ransom and Sontheimer 1992). Furthermore, astrocytes play a role in immune functions (Fontana et al., 1984) and are involved in the formation of neural scars (gliosis) following brain injury (Kimelberg and Norenberg 1989).

Ependymal cells line the ventricles and the central canal of the spinal cord (Del Bigio 1995). The functions of ependymal cells remain largely speculative; however these cells possess micro-villi, which beat in a co-ordinated manner. Therefore ependymal cells may be involved in the directional movement of cerebral spinal fluid (CSF). This action is postulated to facilitate the transport of nutrients into the brain and the removal of toxic metabolites. Ependymal cells have also been suggested to serve as an axonal guidance system during early development.

The fourth type of glial cell is the brain macrophage. Several distinct populations of specialised brain macrophage exist (Jordon and Thomas 1988). These cells are located in the ventricular margins, the choroid plexus, the meninges in a perivascular location and in the parenchyma, where they are known as supraependymal cells, epiplexus cells, subarachnoid/ leptomeningeal macrophages, perivascular

macrophages or microglia respectively. Together these unique macrophages guard every surface and area of access to the brain. The ventricular surface is protected by the ventricular macrophages and the macrophages associated with the choroid plexus. Meningeal macrophages guard the pial surface, perivascular macrophages provide protection from blood borne pathogens, whilst microglia protect the internal region of the brain (Jordon and Thomas 1988; Perry 2001). Microglia are the focus of this study and are discussed in detail in section 1.2. In brief, microglia were originally identified as a distinct cell form by Rio Hortega in the 1960's (see review by Jordon and Thomas 1988). Subsequent studies have revealed that microglia are involved in immune surveillance and transform into active phagocytic macrophages in response to neuronal injury or pathogen invasion. In the reactive state microglia release a number of inflammatory mediators, which in excess may contribute to degenerative processes in neurological disorders.

1.1.2 The immune system

The immune system is divided into two functional divisions, the innate and the adaptive immune system (Roit et al., 1987). The innate immune system provides the first line of defence against infectious agents. The innate immune system is made up of the skin, macrophages, neurophils, natural killer cells and soluble factors such as activated complement proteins and lysozyme. Macrophages can be further classified into Kupffer macrophages of the liver, alveolar macrophages of the lung, microglia of the brain and monocytes in the blood (Roit et al., 1987). The adaptive immune system provides a second line of defence and is associated with the production of antibodies. Antibodies facilitate phagocytosis and the activation of complement proteins. Furthermore, antibodies provide an immunological memory; therefore re-infection with the same agent does not culminate in disease (Roit et al., 1987). Macrophages

provide a vital link between the innate and the adaptive immunity, since activated macrophages express major histocompatibility class II antigen (MHC II), thereby facilitating antigen presentation to T cells, a process that is required for the production of antibodies by B cells. Dentritic cells also perform the function of antigen presentation, however in these cells this activity is constitutive and not inducible (Holgate and Church 1995).

1.1.3 The brain, an immunologically privileged site

The brain was originally regarded as an immunologically privileged site due to the inaccessibility of the organ to circulating immune cells and soluble inflammatory mediators. This notion arose from the observation that tissue grafts survived for long periods of time when transplanted to the brain without any evidence of an immune response (Head and Griffin 1985). More recently, the immune privilege has been demonstrated by injecting mycobaterium into the brain parenchyma (Matyszak and Perry 1998). In peripheral organs mycobacterium induces an aggressive immune reaction, whereas in the brain this pathogen fails to initiate such a response. The main factors believed to contribute to the unique immune status of the brain are the presence of the BBB, the lack of a conventional lymphatic drainage system and the expression of low levels of MHC antigens. The latter is in part attributed to the absence of a cerebral dendritic cell population and the quiescent state of the resident microglia (Perry and Gordon 1988; Perry et al., 1997; Perry 1998).

The brain however is not in complete isolation from the peripheral immune system, since circulating blood monocytes (Lawson et al., 1992) and activated T cells (Wekerle et al., 1986) cross the BBB in health and at an accelerated rate in disease. Thus, the BBB is not an impenetrable barrier to the peripheral immune system.

Furthermore, under a variety of pathological conditions microglia upregulate the expression of MHC class II antigens, thereby facilitating antigen presentation to immuno-surveying T cells (Streit et al., 1989; Benveniste et al., 2001). Reactive microglia also secrete a plethora of inflammatory mediators, which serve to coordinate the inflammatory response (Colton and Gilbert 1987; Banati et al., 1993a; Forloni et al., 1997; Bhat et al., 1998; Casal et al., 2002). Therefore, the brain is able to sustain a low-grade inflammatory reaction in which microglia play a key role. However, cerebral immune activity is normally suppressed, this probably serves as a protective mechanism since neurones are post-mitotic and if lost or damaged cannot be replaced.

1.2 Microglia

1.2.1 The origins of microglia

The origins of microglia is an issue that has been highly debated. Proposals suggest that microglia either originate from the mesoderm like peripheral monocytes or from neuroectoderm along with neurones and other glia (Kitamura et al., 1984) (Fig. 1.1). However, the most recent and convincing studies support a monocytic origin. Ling and co-workers demonstrated the hematogenous origin of microglia by injecting carbon labelled monocytes into the peripheral blood stream of postnatal rats before the complete development of the BBB (Ling et al., 1980). Using this approach, labelled microglia were detected in the brains of the recipient rats implying that microglia derive from circulating blood monocytes.

Experiments using rat bone marrow chimeras have also shown that microglia are bone marrow derived as are meningeal and perivascular macrophages (Hickey and

Kimura 1988). In these studies, the haematopoietic progenitor cells of a recipient animal are destroyed and are replaced with cells from a donor animal. The experiment is based on differences in MHC antigen expression, thus bone marrow derived cells can be traced in the chimeric animal (Hickey and Kimura 1988; Perry 2001).

Developmental studies provide additional evidence that microglia exhibit a hematogenous origin. In the developing brain macrophages are initially observed in the choroid plexus (Sturrock 1978) and in the meninges (Boya et al., 1979). These macrophages subsequently migrate along the ventricular surface entering the brain parenchyma where they ultimately transform into ramified microglia with the amoeboid cell form acting as a morphological transitional state. Initial migration events precede the development of the vasculature; however studies undertaken following vessel formation also demonstrate that brain macrophages are derived from blood monocytes with perivascular cells acting as a possible intermediate (Baron and Gallego 1972).

Collectively these findings provide evidence that microglia are of monocytic lineage, but there is still some uncertainty as to whether microglia are a specialised branch of this lineage (Perry 2001). There are two possible scenarios, in one microglia are derived from monocytes and there is no selection bias as to which monocytes enter the CNS. Monocytes having entered the CNS, come under the influence of the specialised micro-environment, which induces microglial morphology and phenotype. The other possibility is that there is a subset of monocytes that are destined for the CNS (Perry 2001).

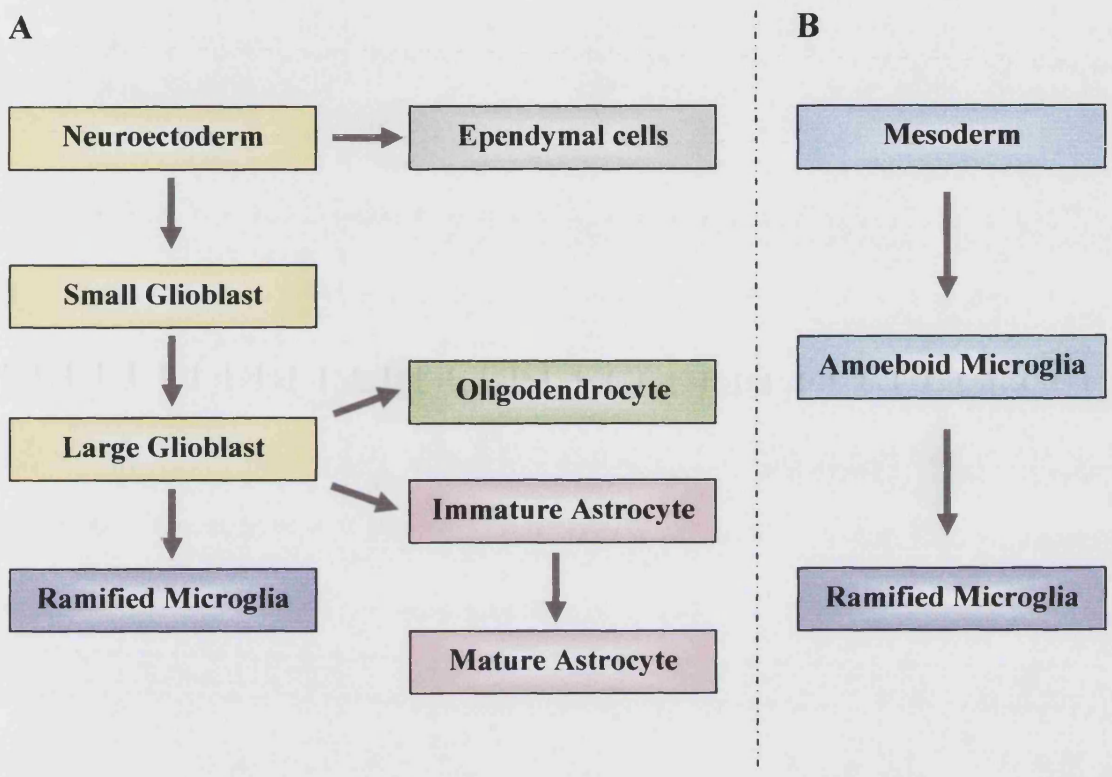

Figure 1.1 Origins of microglia

Proposals suggest that microglia either originate from the neuroectoderm (A) or from the mesoderm like circulating blood monocytes (B).

1.2.2 Microglial phenotypes

In recent years advances in technology have lead to the characterisation of three distinct forms of microglia termed amoeboid, ramified and reactive microglia, all of which serve different functional roles.

1.2.2.1 Amoeboid microglia

Amoeboid microglia are associated with the developing CNS. In rats, amoeboid microglia arise in the last week of gestation and disappear in the second post-natal week (Ling et al., 1980). These cells exhibit a rounded morphology possessing pseudopodia and thin filopodia-like processes and contain numerous lysosomes and phagosomes. During the post-natal period amoeboid microglia are believed to play a role in gliogenesis (Guilian 1987) and tissue histogenesis through the elimination of inappropriate axons (Innocenti et al., 1983).

Through the use of carbon labelled monocytes it has been demonstrated that amoeboid microglia ultimately grow long crenulated processes and transform into ramified microglia (Ling 1979). In support of this, the application of retinoic acid or dimethyl sulphoxide (agents known to accelerate cellular differentiation) to amoeboid microglia *in vitro* stimulates the growth of thin processes several hundred microns in length (Giulian and Baker 1986). These process bearing microglia subsequently lose macrophage associated properties including nonspecific esterase activity, the ability to proliferate, to perform phagocytosis and to bind acetylated low-density lipoprotein, functions which are down-regulated in ramified microglia (Giulian and Baker 1986).

1.2.2.2 Ramified microglia

Ramified microglia are found in abundance in the brain parenchyma and constitute approximately 10-20% of the total population of glial cells in the adult CNS (Vaughan and Peters 1974; Banati 2003). These small oval cells comprise a variable number of branching processes and possess scant cytoplasm. In the adult, the resident population of ramified microglia is maintained through local cell division and the recruitment of circulating blood monocytes (Lawson et al., 1992). These processes contribute almost equally to steady state turnover.

Until recently, ramified microglia were considered to be inactive under physiological conditions. However, it has been demonstrated that microglia exhibit pinocytotic activity and motility within a circumscribed local area (Booth and Thomas 1991). These findings in conjunction with the observations that ramified microglia are evenly distributed throughout the brain parenchyma and express degradative enzymes, led to the hypothesis that these cells function as a CSF cleansing system (Booth and Thomas 1991; Thomas 1992). In this respect, it has been suggested that ramified microglia contribute to the removal of cellular metabolites and the disposal of toxic factors released from damaged neurones. In addition, it has been proposed that ramified microglia limit the spread of diffusible neurotransmitters thereby contributing to the transmission of nerve impulses. Accordingly, microglia express receptors (Zhang et al., 1998; Biber et al., 1999; Taylor et al., 2002, 2003) and re-uptake transporters (Nakajima et al., 2000) for a number of known neurotransmitters.

1.2.2.3 Conversion of ramified microglia into the reactive phenotype

In response to neuronal injury, ramified microglia transform into active macrophages otherwise known as reactive microglia. This phenomenon has been investigated using the axotomized rat facial nucleus model (Kreutzberg 1996). The facial nerve is employed in this paradigm because these cells possess centrally located cell bodies but project axons into the peripheral nervous system. Therefore, microglial activation can be studied in the absence of infiltrating haematogenous cells, since nerve transection leaves the BBB intact.

Using the facial nucleus model it has been shown that in response to neuronal damage ramified microglia proliferate and up-regulate the expression of CR3 complement receptors, major histocompatibilty complex (MHC) class I and II antigens and the intermediate protein vimentin (Graeber et al., 1988a, b, c). Whilst microglia are activated by neuronal damage and regeneration they do not become phagocytic. However, neuronal death induced by injecting ricin into the facial nerve (causing death by retrograde transport) evokes a rapid increase in the expression of MHC class I and II antigens, which is accompanied by the conversion of microglia into phagocytic macrophages (Streit and Graeber 1993). This suggests that factors released from dying neurones are required to induce phagocytic activity. Thus, microglia transform into active macrophages with at least one intermediate form. This form, possessing partial macrophage properties, has been termed the active microglia. In contrast to ramified microglia, activated microglia exhibit stouter processes and thereby resemble the reactive form (phagocytic microglia).

1.2.2.4 Reactive microglia

Reactive microglia are rod-like in appearance, devoid of branching processes and contain an abundance of lysosomes and phagosomes. The reactive cell form represents a transient population of macrophages that are associated with brain injury and neuroinflammation. Following a damaging event, reactive microglia rapidly accumulate at the site of injury (Murabe et al., 1981a). In acute lesions the peak of microglial activation occurs 2-3 days post insult, but if the pathological stimulus persists microglial activations continues (Banati 2003).

Like macrophages, reactive microglia produce a number of inflammatory mediators including super oxide anions, nitric oxide, interleukin 1, interleukin 6, tumour necrosis factor and interferon-γ (Colton and Gilbert 1987; Banati et al., 1993a; Forloni et al., 1997; Bhat et al., 1998; Casal et al., 2002). Interestingly, interleukin 1 induces astrocyte proliferation (Giulian and Baker 1986) and it has been postulated that reactive astrocytes secrete microglial mitogens (Frei et al., 1986). Thus, a complex interplay between microglia and astrocytes is likely to be involved in CNS repair. Reactive microglia also express MHC class II antigens and other surface molecules necessary for antigen presentation including CD40, B7 and ICAM-1 (Streit et al., 1989; Benveniste et al., 2001). Consequently, microglia are considered to be the most potent endogenous antigen presenting cells in the CNS.

1.2.3 Inflammatory mediators secreted by reactive microglia

Reactive microglia secrete a plethora of inflammatory mediators, which are involved in the host's immune response to injury or invading micro-organisms. However, the following discussion is limited to the description of nitric oxide, prostaglandins, superoxide, transforming growth factor β (TGFβ) and the archetypal pro-

inflammatory cytokines tumour necrosis factor (TNFα) and interleukin 1 (IL1). Other inflammatory agents secreted by activated microglia include proteases, interferons (IFN) and colony stimulating factors (CSF) to name but a few (Banati et al., 1993a; Calvo et al., 1996; Yan et al., 1997; Kingham and Pocock 2001).

1.2.3.1 Nitric oxide

Nitric oxide (NO) is an important free radical, which is involved in many physiological processes including microglial and macrophage cytotoxicity, neurotransmission and the regulation of blood pressure (Moncada and Higgs 1993). Synthesis of NO is mediated by the enzyme nitric oxide synthase (NOS), which converts L-arginine into L-citrulline and NO. Three isoforms of NOS have been described, two which possess constitutive calcium dependent activity (cNOS) and one inducible form whose activity is calcium independent (iNOS or type II). However, it should be noted that calcium has been implicated in the signalling pathways leading to iNOS expression (Raddassi et al., 1994; Hoffmann et al., 2003), although activity itself is calcium independent. Constitutive forms of NOS are found in the endothelium (eNOS or type III) (Sessa et al., 1992) and in neurones (nNOS or type I) (Bredt and Snyder 1990; Schmidt et al., 1991), whereas iNOS is expressed in many cell types including microglia, macrophages, and vascular smooth muscle cells (Xie et al., 1992; Koide et al., 1993; Bhat et al., 1998). Unlike cNOSs, which are constitutively expressed and produce small amounts of NO intermittently, iNOS is typically synthesised following exposure to inflammatory stimuli. Many agents induce iNOS expression including LPS (Bhat et al., 1998) and cytokines (Koide et al., 1993). Expression of the iNOS gene is regulated intracellularly by the transcription factors NFκβ, STAT-1 (Murphy 2000) and AP-1 (Kristof et al., 2001).

1.2.3.2 Superoxide

Like all phagocytes, activated microglia possess the ability to synthesise superoxide (Colton and Gilbert 1987; Si et al., 1997; Spranger et al., 1998). This process involves the reduction of molecular oxygen by NADPH oxidase to form superoxide anions (O_2^-). NADPH oxidase is composed of a number of subunits some of which are cytoplasmic, whilst others are membrane bound (Lavigne et al., 2001). Following stimulation, the cytoplasmic components $p47^{phox}$, $p67^{phox}$, $p40^{phox}$ (where phox stands for phagocyte oxidase) and the small GTPase p21Rac1 translocate to the plasma membrane where they form a complex with flavocytochrome b_{558}, a membrane tethered heterodimer composed of $gp91^{phox}$ and $p22^{phox}$ (Abo et al., 1992; Wallach and Segal 1996; Leuson et al., 1996).

Superoxide provides the starting material for a vast assortment of reactive oxidant species, which are all effective bactericidal agents (Holgate and Church 1995; Guyton and Hall 1996). Superoxide dismutase converts superoxide to hydrogen peroxide, which subsequently reacts with newly formed superoxide to form hydroxyl radicals (Holgate and Church 1995). Hydrogen peroxide also reacts with myeloperoxidase in the presence of halides to produce oxidants such as hypochlorite (Holgate and Church 1995; Guyton and Hall 1996). Furthermore, superoxide readily reacts with NO resulting in the production of peroxynitrite ($ONOO^-$) (Ischiropoulos et al., 1992). Peroxynitrite is a potent antimicrobial agent, which renders lipid, thiol, amine or phenol containing bacterial bio-molecules inactive. Thus, superoxide derivatives in combination with reactive nitrogen species provide a powerful line of defence against foreign bodies.

1.2.3.3 Prostaglandins

Prostaglandins are another inflammatory mediator secreted by activated microglia (Minghetti and Levi 1995; Pyo et al., 1999; Pinteaux et al., 2002). Prostaglandins mediate a wide variety of physiological responses including platelet aggregation, kidney function, vasodilation and gastric cytoprotection (Rang et al., 1999; Dubois et al., 1998; Vane et al., 1998; Hinz and Brune 2001). Furthermore, prostaglandin synthesis is upregulated during inflammation, where they mediate vasodilation and potentiate the effects of painful stimuli by sensitising C fibres. Prostaglandins are also implicated in the production of fever; accordingly high concentrations of prostaglandins are found in the CSF during infection (Rang et al., 1999).

Prostaglandins are derivatives of arachidonic acid, a fatty acid that is liberated from the plasma membrane by the action of phospholipases. Arachidonic acid is subsequently metabolised by cyclooxygenase (COX) to form prostaglandin H_2 from which the other prostaglandins (PGI_2, PGE_2, PGD_2, $PGF_2\alpha$, thromboxane) are produced by the actions of specific prostaglandin synthases (Dubois et al., 1998; Rang et al., 1999; Hinz and Brune 2001). COX exists in two isoforms COX-1 and COX-2 (Vane et al., 1998; Rang et al., 1999). COX-1 is found in most cells as a constitutive enzyme, which synthesises prostaglandins involved in normal homeostatic processes. In contrast, the synthesis of COX-2 is induced in inflammatory cells by specific inflammatory stimuli; therefore prostaglandins generated by this enzyme are associated with pathology. However, it should be noted that COX-2 is constitutively expressed in some neurones, where it may be involved in nerve transmission. Furthermore, prostaglandins generated by a constitutively active form of COX-2 are involved in ovulation and in the birth process (Dubois et al., 1998; Vane et al., 1998).

For many years non-steroidal anti-inflammatory drugs (NSAIDs) have been prescribed for the treatment of arthritis and other chronic inflammatory disorders. These drugs work by selectively inhibiting the activity of COX enzymes. More recently, epidemiological studies have demonstrated that NSAIDs reduce the risk of developing AD (McGeer et al., 1996; Stewart et al., 1997), which suggests that COX-2 is upregulated in this neurological disorder.

1.2.3.4 Tumour necrosis factor

Tumour necrosis factor α (TNFα) is representative of a large family of cytokines including TNFβ (lymphotoxin), FasL and CD40L. These cytokines exert effects on the inflammatory response, cell death and proliferation (Vilcek and Lee 1991). Furthermore, the over production of TNF family members is associated with septic shock and autoimmune disorders.

TNFα and TNFβ share approximately 30 % sequence homology (Pennica et al., 1984) and bind to the same cell surface receptors (Aggarwal et al., 1986). Two distinct TNF receptors exist; TNFR1 and TNFR2, which possess molecular masses of 55 and 75 kDa respectively. TNFR1 is associated with apoptotic cell death. This receptor contains an 80 amino acid sequence designated the 'death domain', which is required for the induction of apoptosis. In contrast, TNFR2 has been demonstrated to play a role in the proliferation of T cells. TNFR2 bears no sequence homology to TNFR1, which implies that the receptors couple to different second messenger pathways (Tewari and Dixit 1996). Interestingly, TNFα is primarily produced by macrophages and microglia, whereas TNFβ is predominantly secreted by activated lymphocytes (Aggarwal et al., 1986). Microglia also express both TNFR1 and

TNFR2 suggesting that secreted TNFα may exert autocrine effects on these cells (Dopp et al., 1997). TNFα is cleaved from a transmembranous precursor by TNFα converting enzyme (TACE) (Black et al., 1997). Following cleavage TNFα assembles into homotrimeric complexes (Smith and Baglioni 1987). Interestingly, recent evidence suggests that the membrane anchored form of TNFα is the most efficacious species of this cytokine (Grell et al., 1995).

1.2.3.5 Interleukin 1

Interleukin 1 (IL1) is the general name for two distinct proteins, IL1α and IL1β. These cytokines are synthesised as 31-33 kDa pro-cytokines that share approximately 26 % amino acid identity (March et al., 1995). Cleavage of IL1α is mediated by calpain, a calcium dependent cysteine protease (Carruth et al., 1991). In contrast, IL1β is cleaved by IL1β converting enzyme (ICE), which was the first identified member of the caspase family of cysteine proteases. IL1α and IL1β are believed to exert identical actions. Signalling is mediated by an 80 kDa cell surface receptor (IL1R1), which requires association with an accessory protein (AcP) for activity (Rothwell and Luheshi 2000). A second 68 kDa receptor (IL1R11) also binds IL1α and IL1β, but does not mediate signal transduction. The third member of the IL1 family is a naturally occurring receptor antagonist (IL1Ra), which binds IL1R1 but fails to trigger association with AcP (Rothwell and Luheshi 2000).

In the periphery, IL1 plays a pivotal role in inflammatory processes. IL1 promotes the responses of B and T cells to antigen, it increases the synthesis of leucocyte adherence factors on endothelium and induces the secretion of other cytokines (Rang et al., 1999; Goldsby et al., 2001). In the CNS, IL1 is involved in neuro-inflammation

(Rothwell and Luheshi 2000) and the induction of fever (Guyton and Hall 1996). Cells known to secrete IL1 include macrophages, microglia, fibroblasts, astrocytes and oligodendrocytes. Interestingly, cells of monocytic lineage such as microglia, predominantly secrete the IL1β isoform (Thornberry et al., 1992). Microglia also express IL1R1 and IL1R11, therefore secreted IL1 may exert feedback effects on these cells (Pinteaux et al., 2002).

1.2.3.6 Transforming growth factor

There are three isoforms of transforming growth factor-beta, TGF-β 1, 2 and 3, which play similar biological roles. TGFβ is involved in angiogenesis, in the regulation of growth and development and in inflammation and repair (Clark and Coker 1998; Ling and Robinson 2002). Following injury, TGFβ attracts and activates macrophages and then promotes macrophages to apoptose after tissue debris and invading microorganisms have been engulfed. TGFβ subsequently promotes angiogenesis and the deposition of extracellular matrix, which closes the wound (Ling and Robinson 2002). The vital anti-inflammatory properties of TGFβ are illustrated by the fact that less than 50 % of TGFβ1 knock out mice die in utero and the remainder succumb to uncontrolled inflammation 1-2 weeks after birth (Kulkarni et al., 1993). Similarly, TGFβ2 (Sanford et al., 1997) and TGFβ3 (Proetzel et al., 1995) knockout mice die rapidly in the postnatal period.

TGFβ isoforms are generally secreted as latent precursors, requiring activation before they can exert biological activity (Clark and Coker 1998). Recently, thrombospondin β (Crawford et al., 1998) and plasmin (Lyons et al., 1990) have been implicated in the processing of latent TGFβ. Signalling is mediated by two membrane receptors (type I

and type II) that possess serine/threonine kinase activity (Eickelberg 2001). In the presence of TGFβ, type I and II TGFβ receptors form a heterotetrameric complex and the type II receptor transphosphorylates and activates the type I receptor (Eickelberg 2001). Type I receptors subsequently initiate the phosphorylation of downstream targets, which include the Smad family of transcription factors (Moustakas et al., 2000) and MAPK (Eickelberg 2001). Microglia express type I and type II TGF β receptors (Jones et al., 1998), which suggest that microglia are responsive to this cytokine.

1.2.4 Receptors expressed by microglia

Microglia express a number of cell surface receptors including complement receptors (Ford et al., 1995), Fc receptors (Vedeler et al., 1994), mannose receptors (Marzolo et al., 1999), thrombin receptors (Möller et al., 2000), scavenger receptors (SR) (Paresce et al., 1996) and receptors for advanced glycation end products (RAGE) (Yan et al., 1996). However, the following discussion is limited to the description of scavenger receptors and RAGE since these receptors pertain to this study.

1.2.4.1 Scavenger receptors

SR are a family of macrophage cell surface glycoproteins that exhibit broad ligand specificity; hence they have been likened to 'molecular flypaper' (Kriger 1992). SR ligands include modified lipoproteins such as oxidised and acetylated LDL, polyinosinic acid, fucoidan, and LPS (Goldstein et al., 1979; Krieger 1992). Almost all SR ligands are polyanionic molecules, although not all negatively charged molecules bind to SR (Krieger 1992). Cloning studies have recently revealed the existence of a broad family of SR that have been classified into six sub-groups (A-F)

based on their putative tertiary structure (Peiser and Gordon 2001). The SR-A subgroup comprises SRA-1, SRA-2, SRA-3 and macrophage receptor containing a collegenous domain (MARCO). CD36 and SR-B1 constitute the SR-B sub-group, whilst dSR-C1, CD68, lectin like oxidised low density lipoprotein receptor-1 (LOX-1) and endothelial cell scavenger receptor (SREC) are the sole members of SR-C, SR-D, SR-E and SR-F respectively (Peiser and Gordon 2001).

Cellular functions of scavenger receptors include the phagocytosis of invading micro-organisms (Suzuki et al., 1997) and apoptotic cells (Platt et al., 1999). SR have also been implicated in cell adhesion (Post et al., 2002), Alzheimer's disease (AD) (Paresce et al., 1996; Honda et al., 1998), stroke (Honda et al., 1998) and in the formation of lipid engorged foam cells in atherosclerosis (Goldstein et al., 1979; Krieger 1992). Furthermore, SR have been found to initiate intracellular signalling cascades (Pollaud-Cherion et al., 1998; Whitman et al., 2000), which implies that these receptors may possess the ability to induce gene transcription and thereby modulate cellular function.

1.2.4.2 RAGE

RAGE is a member of the immunoglobulins superfamily of cell surface molecules that includes neural cell adhesion molecule (NCAM), vascular cell adhesion molecule (VCAM) and intracellular adhesion molecule (ICAM) (Neeper et al., 1992; Schmidt et al., 1992). Several other advanced glycation end product (AGE) receptors have been identified including lactoferrin (Schmidt et al., 1992; Li et al., 1995), oligosccharyl transferase complex protein 48 (OST-48; AGE-R1) (Ming et al., 1996), 80KH protein (AGE-R2) (Ming et al., 1996), galectin-3 (AGE-R3) (Zhu et al., 2001) and lysozyme (Li et al., 1995).

Advanced glycation end products result from the non-enzymatic reaction of glucose or other reducing sugars with amino groups of proteins and lipids (glycation) (Brownlee 1995). AGE accumulate with age and at an accelerated rate in diabetes (Brownlee 1995). The accumulation of AGE has also been implicated in the pathogenesis of AD, since RAGE binds β-amyloid (Aβ) and RAGE is over expressed in AD (Yan et al., 1996, 1997). The interaction between AGE and their receptors elicit a variety of biological responses including microglial chemotaxis (Yan et al., 1997), cytokine secretion (Dukic-Stefanovic et al., 2003) and free radical production (Brownlee 1995; Dukic-Stefanovic et al., 2003). The signalling cascades coupled to RAGE remain largely uncharacterised, although it has been shown that ligation of RAGE causes ERK and NFκβ activation in microglia (Dukic-Stefanovic et al., 2003) and THP-1 monocytes (Yeh et al., 2001).

1.2.5 The fate of reactive microglia

Two opposing hypothesis describe the ultimate fate of reactive microglia following a damaging event. The first theory supposes that reactive microglia proliferate, perform their immunological function then revert back to a quiescent ramified phenotype (Jordon and Thomas 1988). The second hypothesis predicts that reactive microglia degenerate (Jones et al., 1997). Cell death can be divided into two forms known as apoptosis or necrosis. It is not known which form of cell death reactive microglia undergo *in vivo*, although microglia have been shown to endure a non-classic form of apoptosis following facial nerve axotomy (Jones et al., 1997). Apoptotic microglia are also found around senile plaques in AD (Lassmann et al., 1995; Yang et al., 1998). Nevertheless, microglia may succumb to different types of cell death after specific pathological insults.

1.2.5.1 Apoptosis

Apoptosis or 'programmed cell death' is responsible for the ordered removal of aged or damaged cells without the initiation of an inflammatory reaction (Kroemer et al., 1998). Consequently, apoptosis occurs under physiological and pathophysiological conditions. Apoptosis is characterised by distinct biochemical changes, including DNA fragmentation and chromatin condensation caused by the activation of endonucleases (Kroemer et al., 1998). Apoptotic cells also undergo membrane blebbing and phosphatidylserine residues are flipped from the inner to the outer leaflet of the plasma membrane, both of these processes facilitate cellular engulfment by macrophages (Kroemer et al., 1998). Other features of apoptosis include cellular shrinkage, caspase activation and mitochondrial dysfunction (Kroemer et al., 1998).

1.2.5.2 Caspases

To date 13 mammalian caspases have been identified, which have distinct roles in apoptosis (caspase 2, 3, 6, 7, 8, 9, 10) and inflammation (caspase 1, 4, 5, 11, 12, 13) (Thornberry and Lazebnik 1998). Caspases are cysteine proteases that are expressed as pro-enzymes containing three domains, including an NH_2 terminal, a large subunit (20 kDa) and a small subunit (10 kDa) (Thornberry and Lazebnik 1998; Hengartner 2000). Caspase activation involves the proteolytic processing between domains and the association of the large and the small subunit. A large body of evidence supports a cascade model for caspase activation. Initiator caspases such as caspase 8 and 9 are believed to instigate the cascade, leading to the activation of effector caspases, which include caspase 3, 6 and 7 (Thornberry and Lazebnik 1998). Caspases cause cell death by cleaving proteins necessary for cell survival including DNA repair enzymes and cytoskeletal proteins such as gelsolin and fodrin (Schulz et al., 1999; Hengartner 2000). Caspases also cleave nuclear lamins, which causes nuclear shrinkage

(Hengartner 2000). Furthermore, caspases cleave negative regulators of apoptosis including Bcl-2, which is an inhibitor of the large mitochondrial conductance channel associated with apoptosis known as the mitochondrial permeability transition pore (PT) (Thornberry and Lazebnik 1998).

1.2.5.3 The role of the mitochondrion in apoptosis

Apoptosis is often preceded by a reduction in mitochondrial membrane potential ($\Delta\Psi$; mitochondrial depolarisation), which is caused by the opening of the PT (Zamzami et al., 1996; Green and Reed 1998). The structure of the PT remain only partially defined, however it is known to comprise the inner mitochondrial membrane protein adenine nucleotide translocator (ANT) and the outer membrane protein porin (otherwise known as voltage dependent anion channel; VDAC) (Green and Read 1998) (Fig. 1.2). The opening of the PT triggers the dissipation of the proton gradient created by the electron transport chain. This subsequently causes the uncoupling of oxidative phosphorylation and the shutdown of mitochondrial biogenesis (Zamzami et al., 1996; Kroemer et al., 1998; Green and Reed 1998). The opening of PT also causes the release of cytochrome *c* (Yang and Cortopassi 1998; Earnshaw 1999; Zhu Y et al., 2002) and apoptosis inducing factor (AIF) (Earnshaw 1999; Susin et al., 1999). Cytochrome *c* plays a dual role in cellular homeostasis, since it is an integral part of the respiratory chain, whilst at the same time it is a potent inducer of apoptosis. Cytochrome *c* in conjunction with apoptosis proteases activating factor (APAF-1) and pro-caspase 9 form an 'apoptosome' (Saleh et al., 1999; Yuchen et al., 1999). This complex promotes the activation of caspase 9, which in turn activates other caspases that collectively orchestrate the execution of apoptosis. AIF causes DNA fragmentation and chromatin condensation. Furthermore, AIF potentiates cytochrome *c* and caspase 9 release from the mitochondria (Susin et al., 1999).

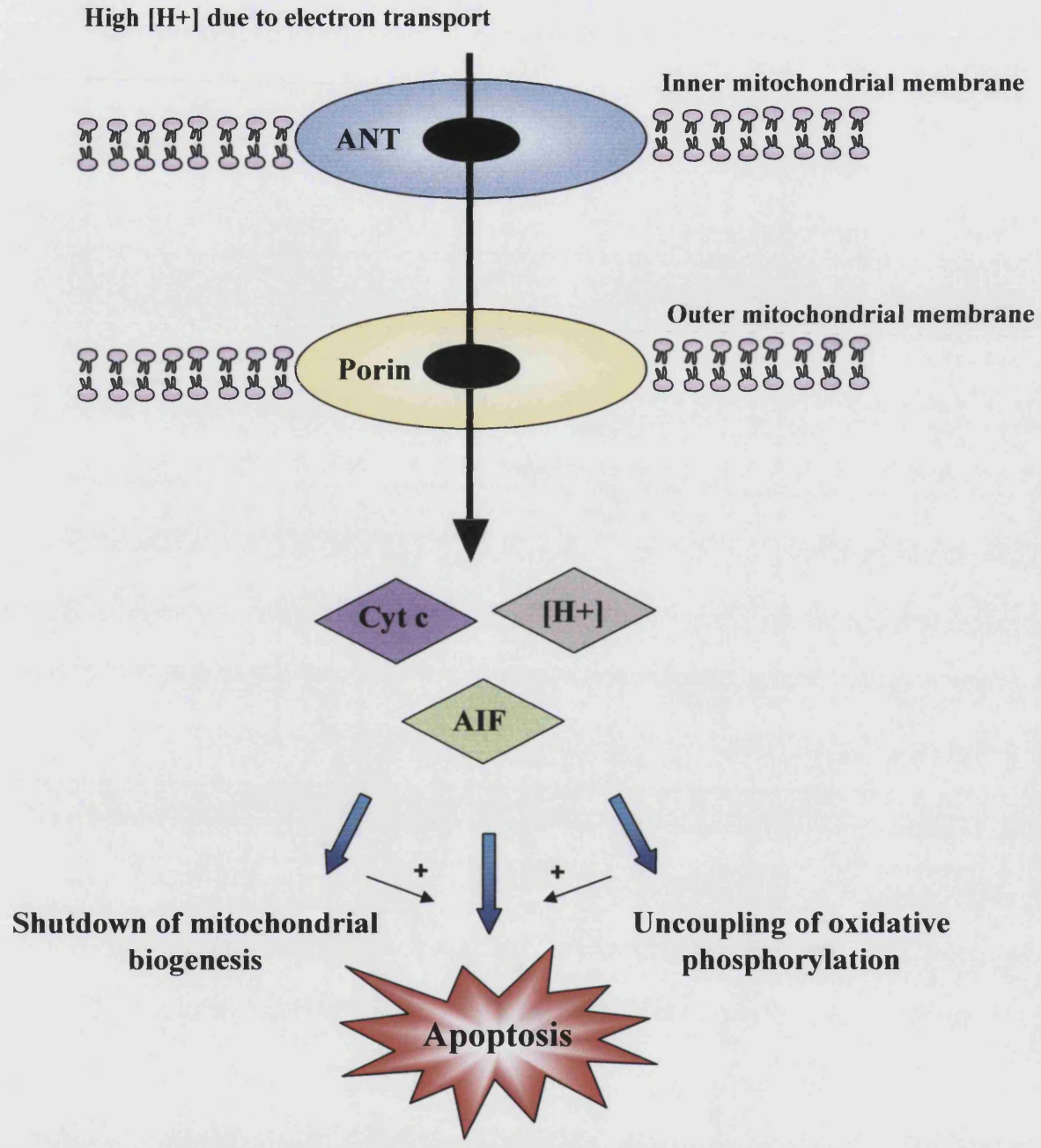

Figure 1.2 Proposed structure of the mitochondrial PT pore

Apoptosis is often preceded by a reduction in mitochondrial membrane potential, which is caused by the opening of a large conductance channel known as the PT pore. The PT pore is postulated to comprise of the inner mitochondrial membrane protein adenine nucleotide translocator (ANT) and the outer membrane protein porin. The opening of the PT pore triggers the dissipation of the proton gradient created by the electron transport chain. This causes the uncoupling of oxidative phosphorylation and the shutdown of mitochondrial biogenesis. The opening of PT also causes the release of cytochrome *c* (Cyt c) and apoptosis inducing factor (AIF), which together orchestrate apoptosis.

1.2.5.4 Necrosis

Necrosis is induced by biochemical or physical damaging events such as abrupt anoxia or heat (Kroemer et al., 1998). Necrosis is characterised by cytoplasmic and mitochondrial swelling and ultimately cellular lysis, which results in the leakage of cellular contents. This in turn creates a toxic environment for neighbouring cells and exacerbates tissue damage either directly or via the recruitment of inflammatory cells (Kroemer et al., 1998) (table 1.1).

Apoptosis	Necrosis
Physiological or pathological	Always pathological
Processes tightly regulated	Processes poorly regulated
Plasma membrane remains intact until late	Plasma membrane becomes disrupted early
No leakage of cell content	Leakage of cell content
Little or no inflammation	Inflammation
DNA fragmentation	Cytoplasmic swelling
Chromatin condensation	Mitochondrial swelling
Mitochondrial dysfunction	Cell lysis
Caspase activation and protein degradation	
Membrane blebbing	
Cellular shrinkage	

Table 1.1 Comparison of the features of apoptosis versus necrosis

Apoptosis occurs under physiological and pathological conditions, whereas necrosis is associated with pathological situations. Apoptosis involves a tightly regulated series of events, which lead to cell death, whereas necrosis is poorly regulated (Kroemer et al., 1998).

1.3 Intracellular signalling pathways

A number of ubiquitous second messengers mediate a plethora of cellular responses in a wide variety of cells. In this project the signalling molecules that were studied with respect to microglial signalling include guanine nucleotide binding proteins (G proteins), calcium, members of the Src family of protein kinases, and ERK a member of the MAPK family.

1.3.1 G proteins

In the resting state (receptor unoccupied) G proteins exist as a hetero α, β, γ trimer, with GDP bound to the α subunit (Rang et al., 1999). When a G protein coupled receptor is occupied by an agonist a conformational change occurs causing the receptor to acquire high affinity for the α, β, γ trimer (Fig. 1.3). Association of the α, β, γ trimer with the receptor causes the bound GDP to dissociate and be replaced with GTP. This in turn causes the dissociation of the α–GTP subunit from the β, γ dimer. The α-GTP entity is the active form of a G protein. There are four main types of G protein, G_s, G_i, G_q and G_{12}, which are classified according to the properties of the α subunit (Simon et al., 1991). G_s proteins stimulate the activity of adenylate cyclase and therefore promote the production of cAMP, whereas G_i proteins inhibit adenylate cyclase and thereby prevent cAMP production (Rang et al., 1999). G_q proteins activate phospholipase C β (see section 1.3.2.1 for a detailed description), whilst the precise intracellular cascades through which G_{12} proteins signal are unknown (Fields and Casey 1997). G protein activity is terminated by the intrinsic GTPase activity of the α-subunit, which catalyses the hydrolyses of GTP to GDP.

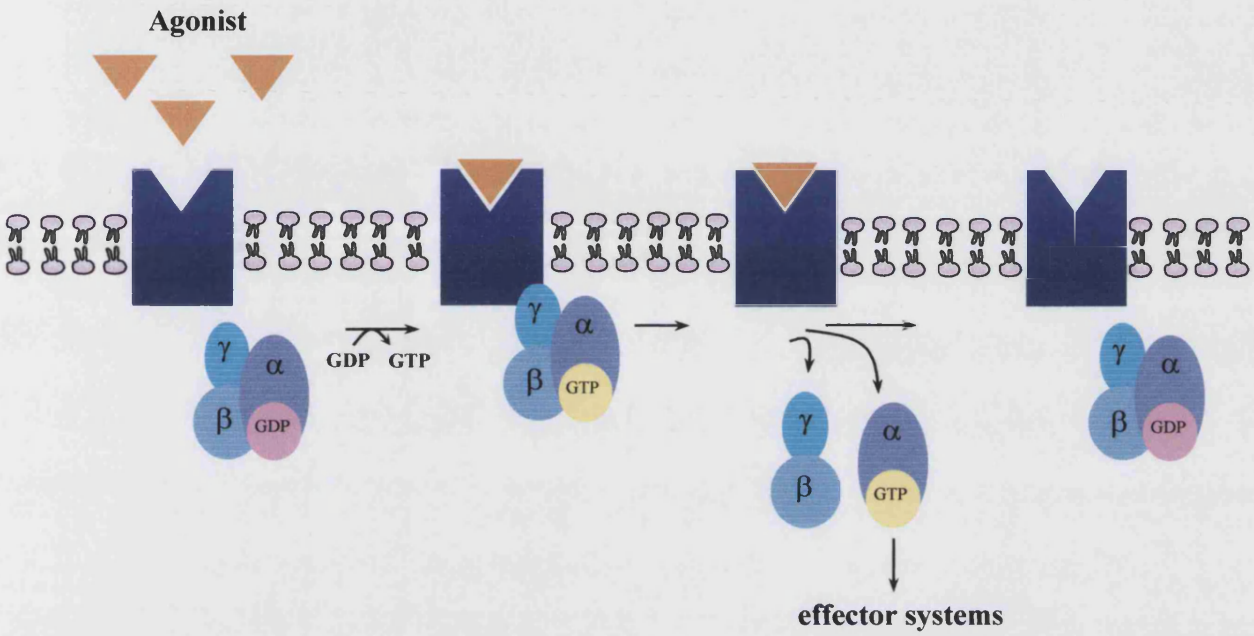

Figure 1.3 Mechanism of G protein signalling

In the resting state (receptor unoccupied) G proteins exist as a hetero α, β, γ trimer, with GDP bound to the α subunit. When a G protein coupled receptor is occupied by an agonist a conformational change occurs causing the receptor to acquire high affinity for the α, β, γ trimer. Association of the α, β, γ trimer with the receptor causes the bound GDP to dissociate and be replaced with GTP. This in turn causes the dissociation of the α-GTP subunit from the β, γ dimer. The α-GTP entity is the active form of a G protein, which subsequently activates downstream effector systems. G protein activity is terminated by the intrinsic GTPase activity of the α-subunit, which catalyses the hydrolysis of GTP to GDP resulting in the reformation of the α, β, γ trimer.

The differences in G protein structure can be exploited using bacterial toxins and therefore these toxins provide ideal experimental tools (Alberts et al., 2002). Cholera toxin catalyses the transfer of ADP ribose to $G_s\alpha$, which results in the persistent activation of $G_s\alpha$. Conversely, pertussis toxin catalyses ADP ribosylation of $G_i\alpha$, which prevents G_i proteins from interacting with receptors, therefore G proteins remain in the inactive GDP form unable to initiate down stream signalling (Alberts et al., 2002).

1.3.2 Calcium

Calcium is a crucial intracellular signalling molecule that mediates many aspects of cellular function including proliferation, muscle contraction and secretory processes (Henzi and MacDermott 1992; Alberts et al., 2002). The endoplasmic reticulum (ER) is the main source of intracellular calcium and release can either be induced by inositol trisphosphate (IP_3) or through calcium-dependent calcium release, which involves ryanodine receptors (Imagawa et al., 1987; Henzi and MacDermott 1992; Berridge 1993; Alberts et al., 2002). The depletion of calcium stores may also induce an influx of calcium across the plasma membrane, a phenomenon known as store operated calcium entry (also known as capacitative calcium entry) (Berridge 1993; Duta 2000). The purpose of this is believed to be the replenishment of store calcium.

1.3.2.1 IP_3 calcium release pathway

IP_3 signalling involves the breakdown of phosphatidylinositol bisphosphate (PIP_2), which is a phospholipid that is located in the inner half of the plasma membrane lipid bilayer (Alberts et al., 2002). Breakdown of PIP_2 is mediated by the membrane bound enzymes phospholipase C β (PLCβ) or phospholipase C γ (PLCγ). PLCβ is activated

by G_q, whereas PLCγ comprises Src homology 2 (SH2) domains and is activated by receptor tyrosine kinases or non receptor tyrosine kinases which include members of the Src family (Berridge 1993; Carpenter and Ji 1999; Kim et al., 2000; Berg et al., 2002). In addition to activating PLCγ, tyrosine kinases often initiate the activation of rat sarcoma viral oncogene homologue (RAS) and the subsequent activation of ERK, which alters cellular activity through the transcription of specific genes (Berridge 1993). A third member of the PLC family PLCδ has also been reported, although the mode of action of this enzyme is currently unknown (Berridge 1993).

PLCβ or PLCγ cleave PIP_2 to generate diacylglycerol (DAG) and IP_3, two signalling molecules that elicit divergent intracellular signalling cascades (Alberts et al., 2002) (Fig. 1.4). DAG induces the phosphorylation of protein kinase C (PKC), which is a calcium-dependent enzyme that modulates the expression of various genes. In contrast, IP_3 is a small water soluble molecule that leaves the plasma membrane and diffuses through the cytoplasm, where it releases calcium from the ER by binding to IP_3 gated calcium release channels. Signalling is terminated by the action of phosphatases, which rapidly dephosphorylate IP_3. In addition, calcium is pumped back into the ER by sarcoplasmic-endoplasmic reticulum Ca^{2+}ATPases (SERCAs) (Alberts et al., 2002; Berg et al., 2002). Calcium signalling is also terminated by the action of the high capacity Na^+/Ca^+ exchanger located in the plasma membrane (Berg et al., 2002). IP_3 signalling can be studied *in vitro* using inhibitors of phospholipase C such as U73122 (Heemskerk et al., 1997; Pollaud-Cherion et al., 1998; Tokmakov et al., 2002).

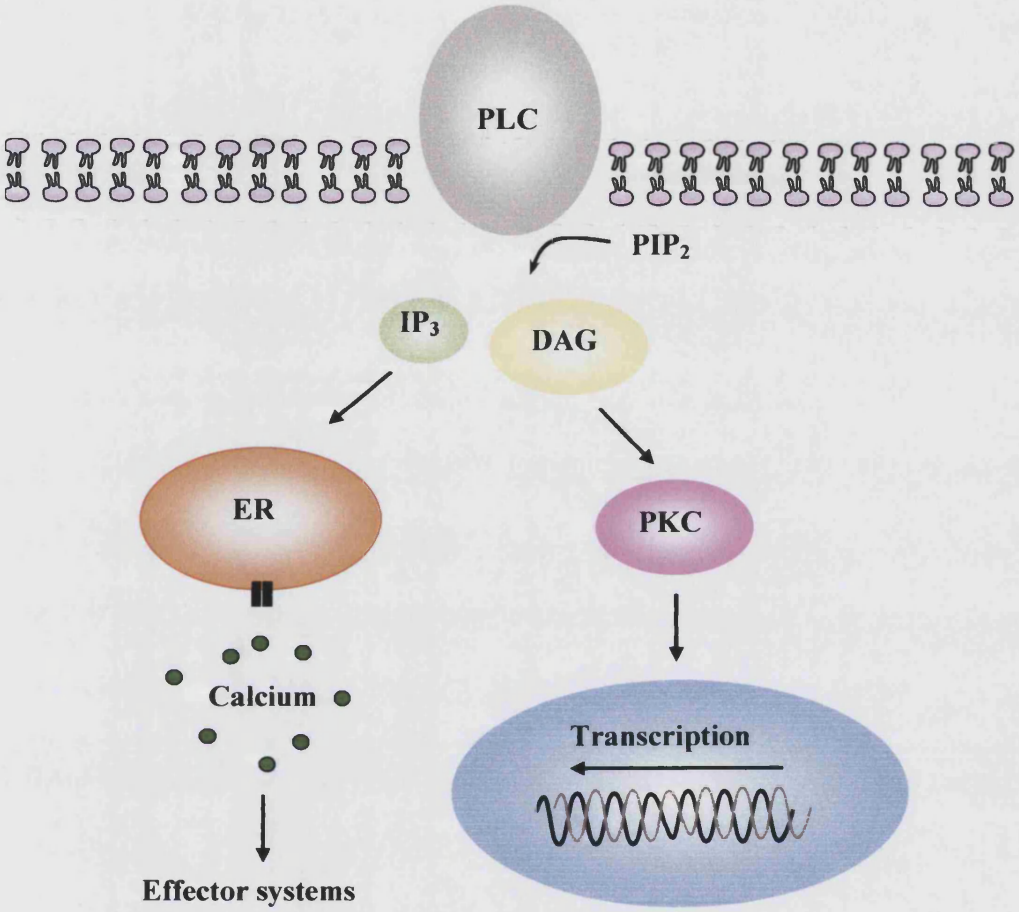

Figure 1.4 Mechanism of PLC signalling

PLCβ or PLCγ cleave PIP_2 to generate DAG and IP_3. DAG induces the phosphorylation of PKC, which modulates the expression of various genes. In contrast, IP_3 triggers the release of calcium from the ER by binding to IP_3 gated calcium release channels.

1.3.3 Extracellular signal regulated kinase

Extracellular signal regulated kinase (ERK) is a member of the mitogen activated protein kinase (MAPK) family. ERK mediates a multitude of cellular functions and is activated by G protein coupled receptors, receptor tyrosine kinases (Alberts et al., 2002) and ionotrophic receptors (Perkinton et al., 1999; 2002). An unusual feature of ERK is that it requires the phosphorylation of a tyrosine and a threonine residue for full activity (Alberts et al., 2002; Daum et al., 1994; Seger and Krebs 1995). ERK activation is mediated by a muti-step chain of events. Firstly, the small adaptor molecule Grb_2 binds to an activated receptor via its SH2 domain (Fig. 1.5). The guanine nucleotide exchange factor son of sevenless (SOS) then binds to Grb_2 forming a complex which leads to the activation of RAS. RAS subsequently activates RAS activated kinase (RAF), which in turn activates MEK 1 and 2 (MAPK kinase), the kinase responsible for the phosphorylation and activation of ERK (Alberts et al., 2002; Daum et al., 1994; Seger and Krebs 1995). In mammals two isoforms of ERK have been identified, which are known as ERK 1 (p44) and ERK 2 (p42). These isoforms share approximately 90 % homology and induce similar cellular functions (Seger and Krebs 1995).

Following activation ERK migrates from the cytoplasm to the nucleus where it relays downstream signals through the activation of various transcription factors including c-Myc, c-Fos, c-Jun. Elk-1 and ATF-2 (Shaywitz and Greenberg 1999; Adams and Sweatt 2002). In the nucleus, c-Fos can combine with c-Jun to form the gene regulatory protein AP-1 (Alberts et al., 2002). AP-1 in turn induces the transcription of a number of other genes whose products mediate cellular responses. Another substrate of ERK is ribosomal protein SG kinase of 90 kDa (RSK) (Shaywitz and Greenberg 1999; Adams and Sweatt 2002). Upon activation, RSKs, of which there

are three isoforms (RSK1-3), translocate to the nucleus where they phosphorylate and activate the cAMP response element binding protein (CREB), a transcription factor that was traditionally associated with cAMP and protein kinase A (PKA) activity. ERK also possesses the ability to modulate phospholipase A_2 activity and to regulate the activity of the potassium ion channel Kv4.2 (Adams and Sweatt 2002).

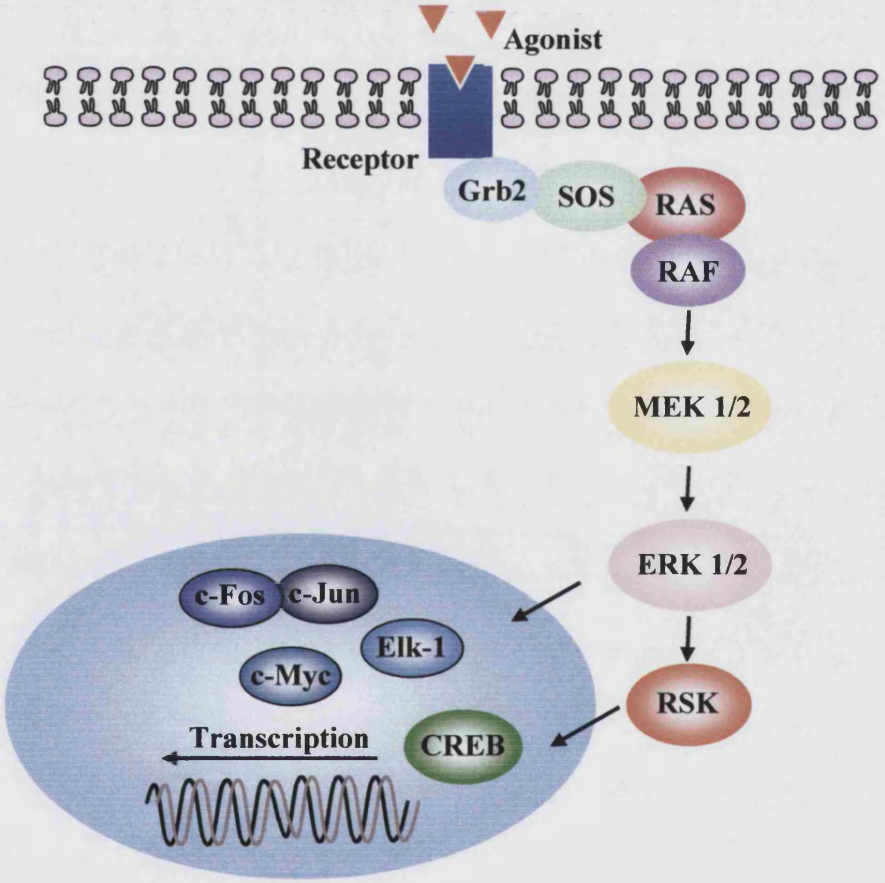

Figure 1.5 Signalling cascade leading to the activation of ERK

Grb_2 binds to an activated receptor via its SH2 domain. SOS then binds to Grb_2 forming a complex which leads to the activation of RAS. RAS subsequently activates RAF, which in turn activates MEK 1/2, the kinase responsible for the activation of ERK 1/2. Following activation ERK translocates to the nucleus where it induces the transcription of specific genes through the activation of various transcription factors including c-Myc, c-Fos, c-Jun. Elk-1 and ATF-2. c-Fos and c-Jun often combine to form the AP-1 complex, which in turn mediates the transcription of a subset of genes. RSKs are another substrate of ERK. Upon activation RSKs translocate to the nucleus where they mediate the activation of the transcription factor CREB.

ERK signalling can be studied *in vitro* using inhibitors such as UO126 (Favata et al., 1998) or PD98059 (Alessi et al., 1995). These agents inhibit MEK 1 and 2 thereby preventing the downstream activation of ERK. UO126 inhibits the active and inactive form of MEK 1 and 2 (Favata et al., 1998), whereas PD98059 only inhibits the inactive forms of the kinase (Alessi et al., 1995).

Other members of the MAPK family include p38 and stress activated protein kinases, which are also known as Jun N-terminal kinases (JNKs) (Tibbles and Woodett 1999; Hagemann and Blank 2001). These kinases modulate gene expression following exposure to toxins, physical stress or cytokines (Tibbles and Woodett 1999).

1.3.4 Src kinases

Src kinases belong to the non-receptor tyrosine kinase family of proteins (Alberts et al., 2002). These tyrosine kinases function in a similar way to receptor tyrosine kinases such as the epidermal growth factor (EGF) receptor except that their kinase domain is non-covalently associated with the receptor and is encoded by a separate gene. As expected, inactive Src kinases are closely associated with the inner leaflet of the plasma membrane and are held in place by protein-protein interactions and by covalently attached lipid groups. This sub-cellular location therefore enables Src kinases to mediate membrane proximal phosphorylation events (Alberts et al., 2002).

Members of the Src kinase family possess a kinase domain, a SH2 and a SH3 domain. In the inactive state Src activity is suppressed by C-terminal Src kinase (CSK) an intracellular kinase that phosphorylates a specific tyrosine residue (Tyr 527) (Pawson 1995). Phosphorylation creates a binding site for the SH2 domain, which prevents association with phosphorylated tyrosine residues on activated

receptors. Furthermore, the SH3 domain folds in such a way that protein-protein interactions are precluded, whilst the kinase domain is locked in an inactive conformation (Pawson 1995). Two mechanisms have been proposed for Src activation; either dephosphorylation of Tyr 527 destabilises the inactive Src complex releasing the SH2 and SH3 domains and activating the kinase domain, alternatively high affinity ligands compete for the auto-inhibitory interactions (Pawson 1995).

At present nine members of the Src kinase family have been identified, which include Src, Lyn, Yes, Fgr, Fyn, Lck, Hck and Blk (Alberts et al., 2002; Kefalas et al., 1995; Superti-Furga 1995). Src, Fyn, Yes, and Yrk are expressed in a broad range of cell types, whereas expression of Blk, Fgr, Hck, Lck and Lyn is restricted to specific haematopoietic cell lineages (table 1.2). Src kinase family members play a role in bone maintenance, learning and memory and in the regulation of cytoskeletal structures involved in exocytosis and phagocytosis (Kefalas et al., 1995; Superti-Furga 1995). Signalling via the Src family of kinases can be studied *in vitro* using the inhibitor PP2 (Hanke et al., 1996; Salazar et al., 1999).

Kinase	Platelet	Monocyte	Granulocyte	Macrophage	T-cell	B-cell
Blk		+	+	+		+
Fgr		+	+	+		
Hck		+	+	+		
Lck					+	+
Lyn	+	+		+		+

Table 1.2 Expression pattern of Src kinases in cells of haematopoietic lineage
Src, Fyn, Yes, and Yrk are widely expressed, whereas expression of Blk, Fgr, Hck, Lck and Lyn is restricted to cells of haematopoietic lineage.

1.4 Neurones

As mentioned previously, neurones constitute a vital component of the CNS. The CNS comprises hundreds of thousands of neuronal pathways that link together to form a complex network and it is inevitably neuronal damage induced by reactive microglia or other means, which precipitates the clinical symptoms of stroke, AD and other neurological disorders.

1.4.1 *In vitro* neuronal models

To dissect cellular and molecular neuronal interactions it has been necessary to develop models that provide a simplified replica of the *in vivo* situation. Such models include brain slices and cultures of cells isolated from specific regions of the brain. In this thesis cerebellar granule neurones were used as a neuronal model. Cerebellar granule neurones are a popular preparation for studying neuronal signalling because these cells can be easily isolated from the cerebellum. Moreover, cerebellar granule neurones constitute the majority of cells in the cerebellum (Anderson et al., 1992; Korbo et al., 1993) and develop post-natally (Jacobson 1991). This means that preparations can be made from neonatal animals and cultures are granule cell rich. Granule neurones are also predominantly glutamatergic (Pearce et al., 1987; Aronica et al., 1993; Archibald et al., 1998; Pocock and Nicholls 1998) and glutamate is intimately involved in neurodegenerative processes. Thus, cerebellar granule neurones provide a robust model for studying the neurotoxic properties of microglial conditioned medium on glutamatergic neurones.

1.4.2 The structure and circuitry of the cerebellum

The cerebellum from the Latin meaning 'little brain' is involved in the control of balance, eye movements and muscle tone. Furthermore, the cerebellum plays a role in the planning and coordination of skilled voluntary movements (Sherwood 1993). The cerebellar cortex comprises three distinct layers, the molecular cell layer, the Purkinje cell layer and the granule cell layer (Fig. 1.6) (Kiernan 1998). The molecular cell layer contains basket cell interneurones, but is largely a synaptic zone containing branching Purkinje cell dendrites and axons of the granule cells. The Purkinje cell layer consists of a single row of cell bodies, while the granule cell layer consists of closely packed granule and Golgi cell interneurones. The mossy fibers are the main operational input into the cerebellum, carrying afferent information from the periphery and other brain centres (Kiernan 1998).

Mossy fibers form excitatory glutamatergic synapses with granule cells in the granule layer. Climbing fibers provide another afferent input into the cerebellum; these fibers originate exclusively from the brain stem. Climbing fibers form excitatory glutamatergic synapses with up to ten Purkinje cells. Purkinje cells process the excitatory inputs received from the climbing fibers and granule cells and the inhibitory inputs received from the basket cells. Subsequently, Purkinje cells relay these neuronal signals to the deep cerebellar nuclei. Since Purkinje cells are GABAergic, basket cell input effectively excites the deep nuclei through disinhibition (Bastain et al., 1999).

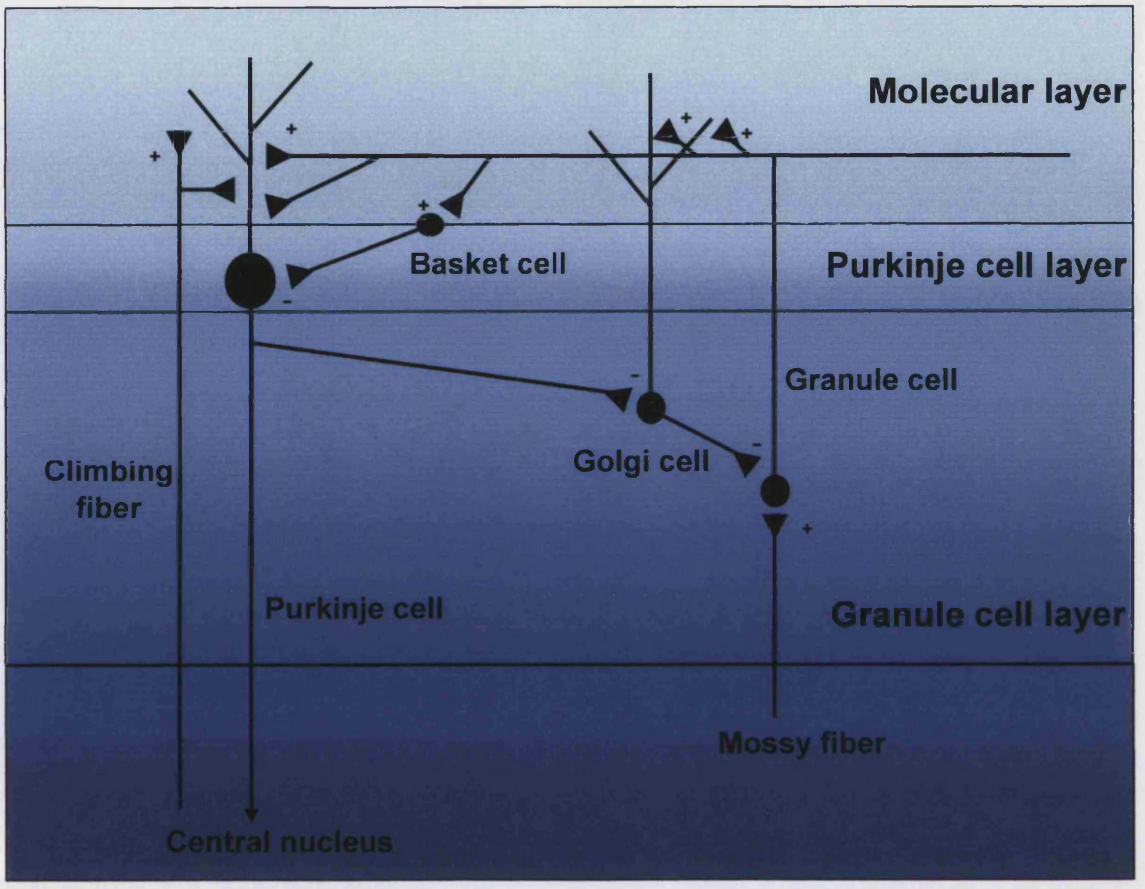

Figure 1.6 Layers of the cerebellar cortex

The cerebellar cortex comprises three distinct layers, namely the molecular cell layer, the Purkinje cell layer and the granule cell layer. The molecular cell layer contains basket cell interneurones, but is largely a synaptic zone containing Purkinje cell dendrites and axons of the granule cells. The Purkinje cell layer consists of a single row of cell bodies, while the granule cell layer consists of closely packed granule and Golgi cell interneurones. The mossy fibers are the main operational input into the cerebellum. Climbing fibers form another excitatory glutamatergic input. Excitatory glutamatergic synaptic connections and inhibitory GABAergic connections are depicted by (+) and (-) respectively (adapted from Kiernan 1998).

1.5 Ischaemia

Ischaemia describes the reduced supply of oxygen (hypoxia) and glucose (hypoglycaemia) for ATP synthesis and the diminished removal of lactic acid. The main cause of cerebral ischaemia is stroke, which results in irreversible brain injury (an infarction). Stroke is the third most common cause of death in the developed world after cancer and heart attack, with an incidence of 1 in 40 and a mortality rate of approximately 30 % (Marsden and Fowler 1998). The consequences of a stroke depend on which part of the brain is damaged and the extent of the damage, although stroke patients often present with weakness or paralysis down one side of the body, speech impediments or disturbed vision.

1.5.1 Stroke

There are two main types of stroke termed intracerebral haemorrhagic stroke and ischaemic stroke, the latter is subdivided into focal and global ischaemia (Sharp et al., 1998). Intracerebral haemorrhagic stroke occurs when a cerebral blood vessel bursts. Focal ischaemia results when an artery that supplies blood to the brain becomes blocked. Focal ischaemia is characterised by an irreversibly damaged core surrounded by an area known as the penumbra exhibiting constricted blood flow and partially preserved energy metabolism. Over time and in the absence of treatment the penumbra becomes irreversibly damaged due to ongoing cytotoxic processes (Sharp et al., 1998). Transient ischaemic attacks (TIA) or 'mini strokes' are another form of focal ischaemia (Marsden and Fowler 1998). TIAs are caused by a brief interruption of the brain's blood supply. The symptoms of a TIA last under 24 hours and patients generally make a full recovery, however TIAs often precede a full blown stroke, therefore patients require urgent medical attention. Global ischaemia describes

complete ischaemia to the entire brain, which can be caused by cardiac arrest or severe hypotension (Sharp et al., 1998).

1.5.2 Risk factors for stroke

Hypertension is the principal risk factor for stroke and intracerebral haemorrhage. Other risk factors include cigarette smoking, obesity, atrial fibrillation and atherosclerosis (Marsden and Fowler 1998; Wolf and D'agostino 1998). Atrial fibrillation is a disorder in which the atria do not contract efficiently; therefore there is an increased tendency for blood to pool and clot in the heart (Guyton and Hall 1996). Atherosclerosis is a progressive arterial disease that can lead to occlusion of affected vessels (Sherwood 1993). Atherosclerosis develops from atheromas, which are benign tumours of smooth muscle cells located in blood vessel walls. These cells migrate from the muscular layer to a position just beneath the endothelial lining, where they continue to divide and enlarge. Cholesterol and other lipids accumulate in the abnormal smooth muscle cells to produce a plaque that protrudes into the blood vessel lumen (Sherwood 1993). Blood borne macrophages subsequently infiltrate atherosclerotic lesions where they accumulate massive amounts of lipid and thereby contribute to plaque volume (Krieger 1992). Thus, hypercholesterolemia also increases the risk of stroke, furthermore diabetics are known to have an increased susceptibility to atherosclerosis and therefore stroke (Wolf and D'Agostino 1998). As atherosclerotic plaques enlarge, they often break through the weakened endothelial barrier, thereby exposing blood to the underlying collagen (Sherwood 1993). This process triggers platelets to initiate the clotting cascade, which subsequently leads to the production of a thrombus. The thrombus may enlarge until it completely blocks the blood vessel (Sherwood 1993). Alternatively, the thrombus may break away from its site of attachment to form a free floating clot known as an embolus. Emboli travel

through the circulation until they lodge in small blood vessels resulting in an ischaemic episode (Sherwood 1993).

1.5.3 Brain metabolism and the primary effects of ischaemia

The brain comprises 2 % of total body mass and yet accounts for 15 % of total body metabolism (Guyton and Hall 1996), therefore the brain exhibits a high requirement for metabolic substrates. Glucose is the energy substrate of preference for most organs including the brain, however if necessary fructose, galactose, fatty acids or amino acids can be oxidised to produced ATP (Sherwood 1993; Guyton and Hall 1996). The energy produced from cerebral respiration is consumed to maintain neuronal and glial integrity. This includes the preservation of ionic gradients, axonal transport and biosynthesis, whilst the remaining energy is used for electrochemical activity (Guyton and Hall 1996).

Most tissues of the body can go without oxygen for several minutes, during which cells obtain energy from the anaerobic metabolism of glucose and glycogen (Guyton and Hall 1996). However, the brain is not capable of sustaining anaerobic metabolism since neurones exhibit a high metabolic rate; in addition glycogen and fat stores in the brain are slight. Thus, a cessation in cerebral blood flow causes unconsciousness within 5-10 seconds and ischaemic injury (Guyton and Hall 1996). Ischaemic injury is a consequence of disrupted of ionic gradients, the accumulation of glutamate in the extracellular space, excitotoxicity and acidosis (Fig. 1.7).

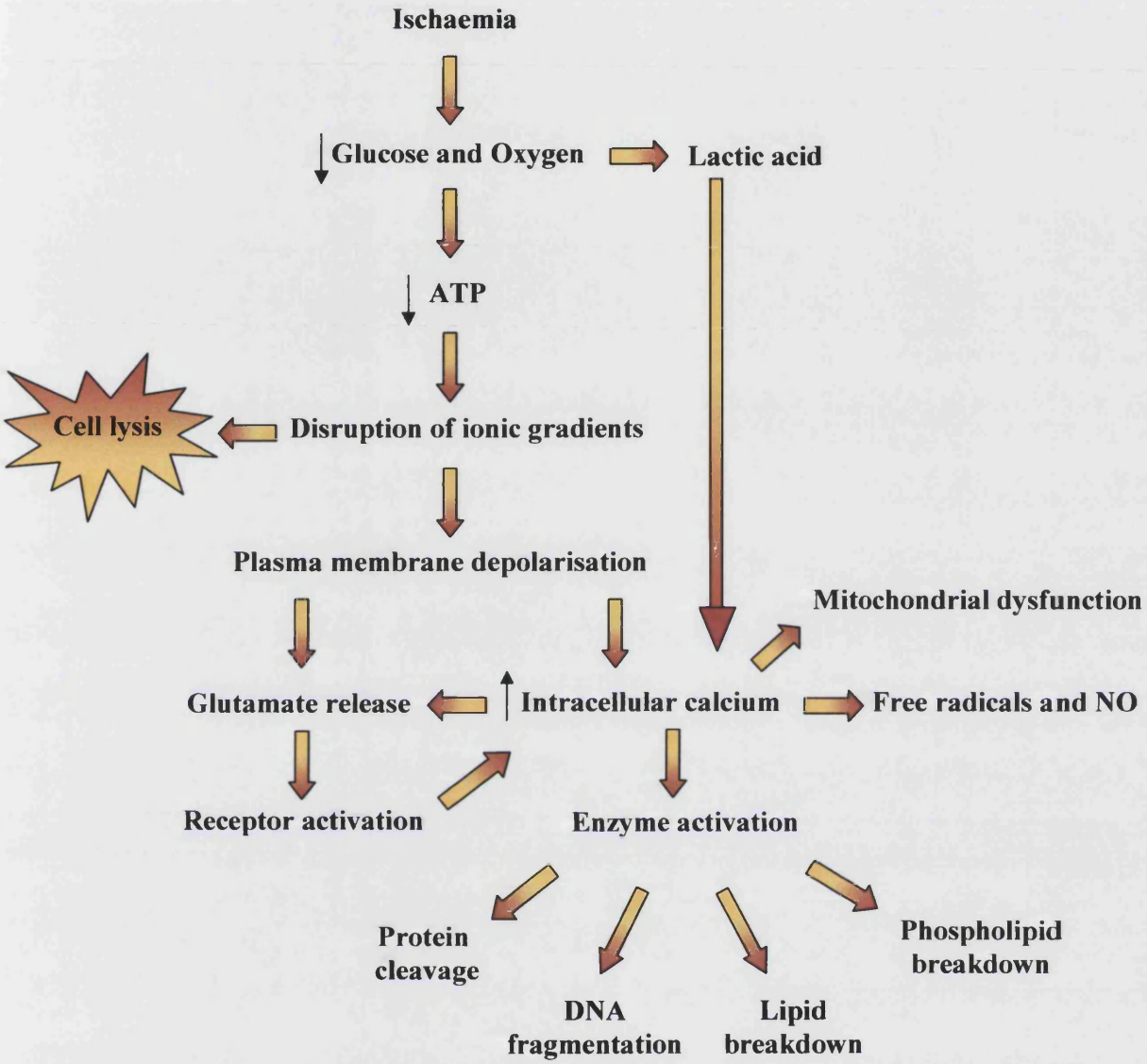

Figure 1.7 Overview of signalling pathways triggered by ischaemia

Ischaemia triggers energy depletion and the disruption of ionic gradients, which results in cell membrane depolarisation. Depolarisation subsequently triggers cell swelling and lysis, glutamate release and a rise in intracellular calcium. Signalling downstream of calcium includes the activation of proteases, endonucleases, lipases and phospholipases. Other pathogenic cascades triggered by excess calcium include the generation of free radicals and mitochondrial dysfunction. The accumulation of lactic acid, a by-product of anaerobic metabolism, also contributes to intracellular calcium overload in ischaemia.

1.5.4 Ionic gradients and ischaemia

Ionic gradients across cell membranes are required for the conduction of action potentials, the regulation of cell volume and the transport of nutrients and metabolites (Sherwood 1993). Ionic gradients are maintained by the sodium-potassium ATPase. The ATPase operates as an anti-porter, actively pumping sodium (Na^+) out of the cell against a steep electrochemical gradient, whilst potassium (K^+) is pumped in (Alberts 2002). For every molecule of ATP hydrolysed, three Na^+ are pumped out and two K^+ are pumped in. Consequently, the concentration of K^+ is typically 10–20 times higher inside the cell than ouside (internal [K+] ≈ 160 mM, external [K+] ≈ 8 mM), whereas the converse is true for Na^+ (internal [Na+] ≈ 18 mM, external [K+] ≈ 135 mM).

Approximately 30 % of a cell's energy requirement is used to fuel the Na^+-K^+ ATPase (Alberts et al., 2002). Thus, in ischaemia the lack of ATP prevents the Na^+-K^+ ATPase from operating and Na^+ / K^+ balance is disrupted across cell membranes. Consequently, neurones and glia depolarise, creating a large osmotic gradient and water enters the cell (the influx of Na^+ and Cl^- is much greater than the efflux of K^+) (Dirnagl et al., 1999). The ensuing oedema inhibits perfusion of the surrounding tissue thereby contributing to neuronal injury (Dirnagl et al., 1999). Furthermore, depolarisation triggers voltage dependent calcium channels (VDCC) to open, which in turn evokes the release of glutamate and other neurotransmitters into the extracellular space (Dirnagl et al., 1999). Depolarisation also induces the reversed operation of neuronal and glial glutamate uptake carriers, which augments the accumulation of extracellular glutamate (Szatkowski and Atwell 1994; Takahashi et al, 1997; Katsumori et al., 1999; Rossi et al., 2000). In addition, spreading depression exacerbates glutamate release (Willis and Grossman 1981; Sharp et al., 1998). Spreading depression is a slow moving wave of glial and neuronal depolarisation,

which is associated with a massive efflux of potassium and glutamate into the extracellular space. Waves of spreading depression pass through the ischaemic penumbra travelling at a rate of 2-5 mm/min (Willis and Grossman 1981).

1.5.5 Excitotoxicity and ischaemia

Excitatory neurotransmission is a normal physiological process mediated by the neurotransmitter glutamate (Choi 1988, 1992; Rang et al., 1999). However, in excess glutamate is destructive and literally 'excites' neurones to death by a process known as excitotoxicity (Choi 1988, 1992; Rang et al., 1999). Glutamate mediates its actions through three types of receptor designated N-methy-D-aspartate (NMDA), 2-amino-3-hydroxy-5-methylisoxazole-4-propionic acid (AMPA) and metabotropic glutamate receptors (mGluRs) (Rang et al., 1999). AMPA receptors are often subdivided into two pharmacological subtypes termed AMPA and kainate receptors (KA). The functions of AMPA and kainate receptors appear to be similar but their distribution in the brain is different (Rang et al., 1999).

The excitotoxic actions of glutamate are predominantly mediated by NMDA receptors (Choi 1988, 1992; Feldman et al., 1997; Rang et al., 1999). Under physiological conditions NMDA receptors are involved in long-term potentiation (LTP) and long-term depression (LTD), phenomena that are mediated by calcium influx (Rang et al., 1999). In ischaemia the chronic activation of NMDA receptors facilitates the entry of neurotoxic levels of calcium into cells, which subsequently leads to excitotoxicity (Choi 1988, 1992; Rang et al., 1999; Lynch and Guttmann 2001). Normally, NMDA receptors are blocked by magnesium, however this block is voltage dependent and is relieved by membrane depolarisation (Rang et al., 1999), which is a characteristic feature of ischaemia (Dirnagl et al., 1999). The activation of

AMPA/KA and mGluRs also contribute to intracellular calcium overload in ischaemia. AMPA/KA receptors are normally involved in fast synaptic neurotransmission, which is mediated by sodium entry into post-synaptic neurones (Rang et al., 1999). Therefore, during ischaemia the persistent influx of sodium through these receptors triggers the sustained opening of VDCC (Sharp et al., 1998). Some KA/AMPA receptors also flux calcium (Hollmann et al., 1991); moreover ischaemia can trigger the upregulation of KA/AMPA receptor subunits that specifically gate calcium (Pellegrini-Giampietro et al., 1992). AMPA and NMDA receptor function is modulated by mGluRs (Rang et al., 1999). Activation of mGluRs triggers the release of calcium from intracellular stores via an IP_3 dependent mechanism (Rang et al., 1999). Thus, mGluRs probably contribute to calcium toxicity in ischaemia as well. Other excitatory neurotransmitters such as acetylcholine and dopamine induce the influx of calcium into neurones, therefore augmenting glutamate-dependent cellular injury during ischaemia (Sharp et al., 1998).

Calcium overload in ischaemia activates lipases, endonucleases, proteases and phospholipases, which catalyse the breakdown of lipids, DNA, proteins and phospholipids respectively (Feldman et al., 1997; Sharp et al., 1998). A key consequence of phospholipase activation is the liberation of arachidonic acid (Sharp et al., 1998). Arachidonic acid damages the BBB (Kontos et al., 1980), inhibits glutamate uptake by glia (Yu et al., 1987) and provides the starting material for the production of prostaglandins and leukotrienes (Rang et al., 1999), factors that are involved in inflammatory processes. Other pathogenic cascades triggered by calcium overload include the generation of free radicals and the synthesis of NO (Feldman et al., 1997; Sharp et al., 1998). Furthermore, the synthesis of ATP is curtailed as a consequence of calcium sequestration by mitochondria (Budd and Nicholls 1996).

1.5.6 Lactic acidosis and ischaemia

During ischaemia the absence of an adequate energy source leads to the anaerobic metabolism of glucose, which results in the accumulation of lactic acid (Berg et al., 2002). Lactic acid is a strong organic acid and therefore dissociates into lactate and a hydrogen ion (H^+) at physiological pH. The presence of excess H^+ in tissues subsequently causes acidosis. Lactic acidosis in ischaemia triggers a rise in intracellular Ca^{2+} by inhibiting efflux by ATP driven transport and passive Na^+/Ca^{2+} exchange (Café et al., 1993). Therefore, lactic acidosis contributes to intracellular calcium overload. Acidosis also augments free radial reactions in ischaemia (Café et al., 1993). The detrimental role of acidosis in ischaemia is supported by the finding that pre-ischaemic hyperglycaemia potentiates post-ischaemic damage, which has been attributed to the intensification of lactic acidosis (Schurr 2002). Consequently, clinicians monitor and control blood glucose levels in patients undergoing cardiopulmonary bypass surgery or neurological procedures (Schurr 2002).

1.5.7 Cell death in ischaemia

Excitotoxicity and ischaemia *per se* induce plasma membrane failure and cell swelling; therefore cells are most likely to undergo necrosis in ischaemia. However, studies have identified molecular signatures of apoptosis in the ischaemic brain, including the translocation of cytochrome *c* from the mitochondria to the cytosol (Schulz et al., 1999), the activation of caspase 3 (Namura et al., 1998; Ni et al., 1998) and DNA fragmentation (Heron et al., 1993; Ni et al., 1998). Moreover, caspase inhibitors reduce infarct size following ischaemia (Hara et al., 1997; Endres et al., 1998). Therefore, it is likely that both necrotic and apoptotic cascades are elicited in ischaemia and some cells may even undergo a 'mixed' form of death (Barinaga et al., 1998).

1.5.8 Role of microglia in ischaemia

Microglia are found in abundance in the ischaemic penumbra (Morioka et al., 1993; Rupalla et al., 1998). Reactive microglia are detectable 20 minutes after reperfusion whilst the strongest microglial reaction is apparent 4-6 days post insult but can persist for up to 4 weeks (Morioka et al., 1991). *In vivo* studies have shown that ischaemia triggers microglia to retract their long processes and upregulate the expression of CR3, ED-1 and MHC class I and II antigens (Kato et al., 1995, 1996). It is generally believed that microglia exacerbate ischaemic injury through the release of neurotoxic inflammatory mediators such as TNFα (Barone et al., 1997; Park et al., 2002), IL (Rothwell et al., 1997), NO (Park et al., 2002; Suzuki et al., 2002; Zhu et al., 2002a) and superoxide (Spranger et al., 1998). Accordingly, microglial activation precedes neuronal death in ischaemic lesions (Lees 1993; Rupalla et al., 1998) and neuronal death is reduced by inhibiting microglial activation (Tikka et al., 2001). Furthermore, hypothermia, which affords neuroprotection in ischaemia, appears to work by inhibiting microglial activation (Kumar and Evans 1997). Collectively, these findings suggest that microglia play an intrinsic role in ischaemic damage. However, an alternative hypothesis supposes that reactive microglia play a protective role in ischaemia through the phagocytosis of neuronal debris (Gehrmann et al., 1995) and the secretion of growth factors (Gehrmann et al., 1995; Watanabe et al., 2000).

Waves of spreading depression provide a secondary stimulus for microglial activation in the penumbra; inasmuch as potassium triggers microglial proliferation (Schlichter et al., 1996) whilst glutamate induces activation (Tikka et al., 2001). Paradoxically, activated microglia secrete prodigious quantities of glutamate (Piana and Fontana 1994; Kingham et al., 1999 Barger and Basile 2001), therefore activated microglia may actually augment excitotoxic injury by contributing to the extracellular pool of

glutamate (Lees 1993). ATP originating from injured cells may also contribute to microglial activation in the penumbra (Chow et al., 1997; Hide et al., 2000; Möller et al., 2000; Shigemoto-Mogami et al., 2001). Moreover, ATP induces microglial chemotaxis, which may underlie the accumulation of microglia in damaged brain regions (Honda et al., 2001). Additionally, exposure to blood borne elements such as albumin (Si et al., 1997), thrombin (Möller et al., 2000a; Ryu et al., 2000) or complement fragments (Nolte et al., 1996; Möller et al., 1997) may initiate microglial activation if the BBB is damaged (Kato and Walz 2000) and this is one aspect of ischaemia that was explored in this thesis. Studies have shown that the BBB is disrupted in approximately 50 % of stroke patients and damage is most pronounced in the first two weeks of illness (Hornig et al., 1983).

In addition to activating microglia, focal ischaemia triggers circulating blood monocytes and neutrophils to enter the brain (Perry et al., 1997). In fact, it has been proposed that microglia co-ordinate the recruitment of circulating leucocytes through the secretion of cytokines (Kato and Walz 2000). Neutrophils are the first invading cells to be recruited to the lesion (Kato and Walz 2000). Monocytes follow suit and become the predominant cell type five to seven days after ischaemia (Kato and Walz 2000). The recruitment of circulating leucocytes is achieved through the expression of adhesion molecules on the cerebral endothelium including intercellular adhesion molecule 1 (ICAM-1) and P and E selectin (Sharp et al., 1998; Kato and Walz 2000). Upon entry into the brain, neutrophils and monocytes are guided towards the infarct by chemotactic cytokines, examples of which include interleukin 8 (Mukaida et al., 1998) and monocyte chemo-attractant protein 1 (MCP-1) (Wang et al., 1995). Thus, it is conceivable that inflammatory mediators released from monocytes and neutrophils augment the endogenous microglial reaction apparent in ischaemia.

1.6 Alzheimer's disease

1.6.1 Types of dementia

Dementia is a generic term that describes chronic or progressive dysfunction of cortical or subcortical structures resulting in complex cognitive decline (Ritchie and Lovestone 2002). Dementia can be sub-classified into Alzheimer's disease (AD), frontotemporal dementia (Pick's disease), dementia with Lewy bodies, vascular dementia or dementia secondary to another disease process such as auto-immuno-deficiency-syndrome (AIDS) (Ritchie and Lovestone 2002). Moreover, patients often present with mixed state dementia, which is caused by a combination of different types of dementia.

1.6.2 Characteristics of Alzheimer's disease

AD is a progressive neurodegenerative disorder affecting 5-10 % of the elderly population (Ladner and Lee 1998). Alzheimer's patients suffer memory loss, disorientation, confusion, impaired concentration and a decline in cognitive function. Postmortem examination of Alzheimer's brain tissue demonstrates a marked atrophy of the cortical gyri, particularly in the frontal and temporal lobes of the cortex. Neuronal loss is also apparent in the amygdala, the hippocampus, the locus coeruleus, the raphe nucleus and the nucleus basalis of Meynert (Strange 1992). Thus, many neurotransmitter systems are involved in neuropathology and thereby the clinical presentation of the disease. The defining hallmarks of AD include senile plaques and neurofibrillary tangles (NFTs), which were first described by Alois Alzheimer in 1907 (see review by Selkoe 1994). These histopathological structures are concentrated predominantly in the hippocampus and the cortex of afflicted individuals (Crowther 1990).

NFTs comprise paired helical filaments (PHF) of an abnormal form of tau, an axonal microtubule associated protein (MAP) (Iqbal et al., 1994). Normally, tau is involved in tubulin polymerization and microtubule stabilization and is phosphorylated at two to three sites (Goedart 1993). However, in AD tau becomes phosphorylated at six to eight sites. Consequently, tau dissociates from microtubules and aggregates into PHFs forming NFTs. The reduced binding of phospho-tau to microtubules results in the impairment of vital cellular processes such as axonal transport (Brion 1992; Berg et al., 2002), which ultimately culminates in the degeneration of affected neurones. Thus, masses of NFTs are often observed extraneuronally presumably as a residue of dead neurones (Brion 1992).

Senile plaques mainly consist of extracellular deposits of Aβ, a peptide produced from the proteolytic cleavage of β-amyloid precursor protein (APP). In AD several types of senile plaque are apparent including neuritic, diffuse and burned out plaques (Delaere et al., 1991; Feldman et al., 1997). Neuritic plaques possess dense extracellular deposits of Aβ surrounded by dystrophic and degenerating neurites, reactive astrocytes and microglia. Diffuse plaques represent the early stages of plaque formation and contain Aβ but no degenerating neurites. In contrast, burned out plaques possess a dense core of Aβ but no degenerating neurites and are regarded as the final stages of plaque formation. Presumably, after the dystrophic neurites degenerate, their remains are phagocytosed by plaque associated microglia (Vehmas et al., 2003).

1.6.3 APP and its cleavage to yield Aβ

APP is derived from a single gene, from which alternative splicing gives rise to a family of proteins containing either 695, 751, or 770 amino acids (Schellenberg 1995). Following RNA splicing, APP is inserted into the cell membrane so that there is a single transmembrane domain containing part of the Aβ peptide (Kang et al., 1987). The remainder of the protein is arranged such that there is a short cytoplasmic segment and an extensive extracellular region (Kang et al., 1987). The structure of APP suggests that this protein may function as a receptor or a growth factor (Rossjohn et al., 1999). Mutations in the APP gene are responsible for a very small proportion of AD cases, therefore attention has turned to the abnormal processing of APP as a contributory factor to the pathogenesis of AD.

APP is subject to proteolytic processing at three sites by the action of α, β and γ secretase (Checler 1995). Cleavage by α secretase releases an extracellular region of APP (APPsα), which exhibits neurotrophic and neuroprotective properties (Coughlan and Breen 2000). APPsα also plays a role in neuronal cell differentiation and neurite outgrowth (Coughlan and Breen 2000). In contrast, the joint action of β and γ secretase releases the harmful Aβ peptide (Fig. 1.8) (Checler 1995). Thus, the generation of APPsα and Aβ are mutually exclusive. Therefore, an increase in Aβ production parallels a decrease in the production of neuroprotective APPsα, which may render cells more susceptible to the actions of neurotoxins and indeed Aβ itself (Coughlan and Breen 2000). Intense efforts have been directed towards the identification of α, β, and γ secretase. Consequently, ADAM 10 (Lammich et al., 1999) and TACE (Bauxbaum et al., 1998b) have been reported to mediate α-cleavage of APP. The aspartyl protease BACE has been demonstrated to mediate β cleavage

(Vasser et al., 2001), whilst a multi-protein complex consisting of presenilin-1 (Wolfe et al., 1999), nicastrin (Li et al., 2003), Aph-1 and Pen-2 (Taylor-Kimberly et al., 2003) is thought to be involved in γ cleavage (De Strooper 2003). An intriguing property of γ secretase is that it performs proteolysis in the middle of a transmembrane domain.

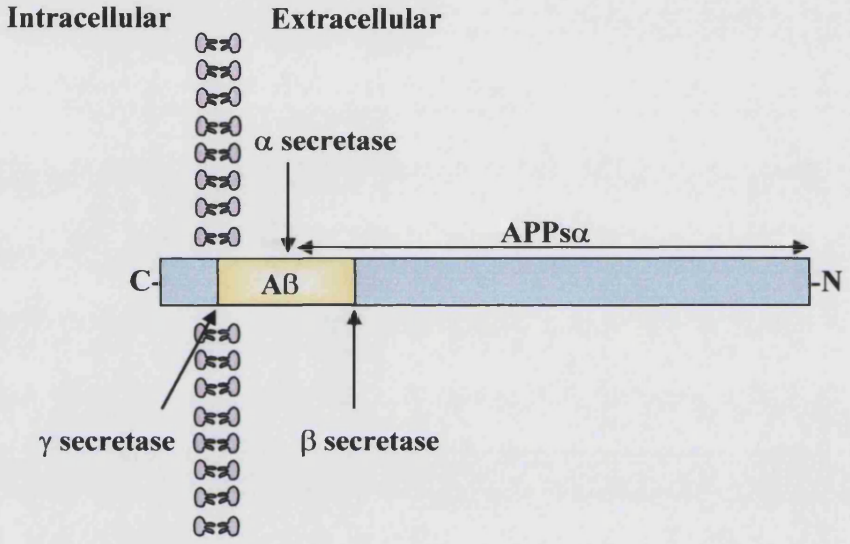

Figure 1.8 Sites of APP processing

APP (depicted by blue bar) is subject to proteolytic processing at three sites by α, β and γ secretase. Cleavage by α secretase releases the majority of the extracellular segment of APP (APPsα), which is neuroprotective. In contrast, the joint action of β and γ secretase releases the harmful Aβ peptide (depicted by yellow bar). (N, N-terminus; C, C-terminus).

Cleavage by β and γ secretase is not highly precise, hence Aβ varies between 39-42 amino acids in length. After cleavage Aβ exhibits a random coil conformation, however the protein gradually adopts an insoluble β-sheet structure, which is deposited in the form of senile plaques (Soto 1999). *In vitro* studies have

demonstrated that the 42 mer aggregates more readily than the shorter species of Aβ and is therefore the most pathogenic cleavage product (Suzuki et al., 1994). Another fragment frequently used in experimental paradigms is $A\beta_{(25-35)}$, which is the biologically active fragment of the full length species of Aβ. At physiological pH $A\beta_{(25-35)}$ readily aggregates into a β-sheet conformation and therefore does not require 'aging' before use (Pike et al., 1993; Terzi et al., 1994a,b). $A\beta_{(25-35)}$ was the form of Aβ used in this study.

1.6.4 Theories of increased Aβ production

It is thought that Aβ is involved in normal physiological processes because Aβ shares sequence homology with the tachykinin family of neuropeptides (Yanker et al., 1990). Furthermore, low concentrations of Aβ exert a neurotrophic effect on undifferentiated hippocampal neurones (Whitson et al., 1990). Thus, plaque formation in AD and subsequent neuropathological events may be related to increases in the activities of β and γ secretase. Alternatively, the formation of plaques may be due to decreased clearance of Aβ from the CSF (Feldman et al., 1997).

1.6.5 Genetics of Alzheimer's disease

AD is a genetically heterogeneous disorder, a conclusion that is not surprising given the prevalence of the disorder. Population survey studies have demonstrated that 25 – 40 % of AD cases have a genetic link and in most circumstances the disease is inherited as an autosomal dominant trait (van Broeckhoven 1995).

1.6.5.1 Early onset Familial Alzheimer's disease

Early onset forms of Familial Alzheimer's disease (FAD) typically present before the age of 65 and have been linked to mutations in APP, presenilin-1 (PS-1) and presenilin-2 (PS-2). All three mutations adversely affect APP processing and result in the production of insoluble Aβ, which is deposited in the form of senile plaques.

1.6.5.2 APP gene mutations

Early in the search for genes involved in the pathogenesis of AD, researchers discovered that patients suffering from Down Syndrome (DS) exhibited senile plaques and NFTs (Wisniewski et al., 1985). Moreover, as the life span of DS patients has increased due to improvements in treatment and care, many patients now develop dementia before the age of forty (Kolata 1985; Hardy and Higgins 1992). Aged DS sufferers regress from a person with limited intelligence to a person who is disoriented, unable to comprehend or speak, all of which are symptoms associated with AD. The cause of DS is non-disjunction of chromosome 21, which results in the inheritance of three copies of this chromosome instead of the normal pair (Alberts et al., 2002). These findings were the first to suggest that a gene on chromosome 21 might be responsible for the onset of some cases of AD.

Important progress in the genetics of AD occurred with the cloning and mapping of APP to a site on chromosome 21 (Robakis et al., 1987; St George-Hyslop et al., 1987; Tanzi et al., 1987). Subsequently, several kindreds have been identified which express APP mutations. Families have been identified in which the valine at position 717 is mutated to isoleucine, phenylalanine or glycine (London mutation) (Goate et al., 1991; Hardy and Higgins 1992). This mutation is situated three amino acid residues away from amino acid 43 of the Aβ peptide. Cells transfected with APP

containing either isoleucine or phenylalanine at this position, do not secrete abnormal quantities of Aβ, but secrete an increased ratio of the highly pathogenic 1-42 species (Suzuki et al., 1994). Two Swedish kindreds have also been identified whom exhibit a double mutation in the APP gene (Mullan et al., 1992). In this family the lysine at position 670 and the adjacent methionine at position 671 are mutated to aspartate and leucine respectively. These amino acids are located at the putative α secretase site, at the beginning of the Aβ sequence. Cells transfected with an APP gene bearing this double mutation secrete significantly more Aβ than cells transfected with wild type APP, which probably serves to fuel plaque formation (Citron et al., 1992).

1.6.5.3 Presenilin gene mutations

The second gene identified to contribute to the pathogenesis of AD is located on chromosome 14 and is known as presenilin-1 (PS-1; S182) (Sherrington 1995; Wisnieski et al., 1995). Already 15 different mutations associated with AD have been mapped to this gene. The precise functions of PS-1 remain unknown, however PS-1 mutations increase the production of the long form of Aβ (1-42) (Murayama et al., 1999). Moreover, PS-1 exhibits proteolytic activity and is thought to be a prime component of the γ secretase complex (Wolfe et al., 1999; De Strooper 2003). Increased levels of PS-1 are detectable in the senile plaques in AD, Hereditary Cerebral Haemorrhage with Amyloidosis, Dutch type (HCHWA-D) and DS, which suggests that PS-1 plays a common role in these related disorders (Wisniewski et al., 1995). Initial studies of the PS-1 gene suggested the existence of other genes with similar sequences. This led to the identification of a novel gene, which was termed presenilin-2 (PS-2; E5-1) (Rogaev et al., 1995). Mutations in the PS-2 gene are associated with four early onset FAD cases belonging to an extended pedigree of

Italian origin and three pedigrees with (Volga) German ancestry. Thus, PS-1 and PS-2 may be members of a large family of proteins involved in the pathogenesis of AD.

1.6.5.4 Late onset Familial Alzheimer's disease

Late onset FAD typically presents after the age of 65 and is influenced by variation in a fourth gene encoding ApoE (Wisniewski 1992). Normally, ApoE is involved in the maintenance of lipoprotein structure and the regulation of lipoprotein metabolism (Gurr 1993; Guyton and Hall 1996). Most organs produce ApoE, the largest pool of ApoE mRNA is found in the liver whilst the second largest amount is associated with the brain. In the brain ApoE is mainly secreted by astrocytes (Boyles et al., 1985; Pitas et al., 1987).

There are three major alleles of the ApoE gene, designated ApoE4, ApoE3 and ApoE2 (Feldman et al., 1997). Expression of ApoE4 enhances the likelihood of developing AD (Corder et al., 1993). Research demonstrates that ApoE4 binds Aβ and promotes its deposition into senile plaques (Wisniewski et al., 1992). Conversely, ApoE3 and E2 have been postulated to exert a protective effect against the development of AD (Strittmatter et al., 1994). These isoforms possess the ability to bind tau and prevent aberrant phosphorylation. Consequently, ApoE2 and E3 impede the generation of PHF and the formation of NFTs (Strittmatter et al., 1994). Thus, over a lifetime, the expression of the ApoE4 may significantly increase the incidence of AD, thereby giving rise to late onset AD in genetically predisposed individuals.

1.6.6 Theories of Alzheimer's disease pathogenesis

There is no question that AD pathology is characterised by the presence of senile plaques, NFTs and neuronal loss, however the precise sequence of events underlying pathogenesis remains unknown. Probably the most influential theory to date has been the amyloid cascade hypothesis (Hardy and Allsop 1991; Hardy 1992). According to this theory APP synthesis and or processing become abnormal due to a combination of genetic and environmental factors, which results in the formation of senile plaques. The presence of plaques subsequently exerts a deleterious effect on neuronal survival, leading to the development of PHFs and NFTs. Thus, over time, the gradual accumulation of these histopathological features is believed to cause neuronal death and neurotransmitter deficits ultimately culminating in dementia.

The amyloid cascade hypothesis still dominates the field of Alzheimer research. However, the hypothesis has been criticised on the grounds that diffuse amyloid deposits are present in non-demented elderly individuals (Braak and Braak 1991; Delaere et al., 1991). In addition, some AD patients exhibit NFTs but no amyloid deposits (Braak and Braak 1991). In light of this, the existence of senile plaques cannot be considered as an absolute pre-requisite for the formation of NFTs. An alternative hypothesis supposes that the formation of plaques and tangles is a consequence of neurodegeneration. Recent evidence demonstrates that neuronal loss in AD is caused by the aberrant re-entry of neurones into the cell cycle (Nagy 2000). Since neurones are terminally differentiated, cell cycle re-entry results in the failure of regulatory mechanisms. Thus, some neurones undergo apoptotic cell death, whereas in apoptotic incompetent neurones, the active kinases cause Aβ formation and the aberrant phosphorylation of tau.

1.6.7 Cell death in Alzheimer's disease

The exact cause of neuronal death in AD is unknown, but there is mounting evidence that suggests apoptosis plays a key role. Cultured neurones treated with Aβ exhibit morphological and biochemical characteristics of apoptosis, including membrane blebbing, compaction of nuclear chromatin and DNA fragmentation (Loo *et al*, 1993). Presenilin 1 and 2 mutations promote neuronal apoptosis through the disruption of intracellular calcium homeostasis (Bauxbaum et al., 1998a; Tanzi 1998). Similarly, administration of anti–APP antibody (Rohn et al., 2000) and over expression of wild type APP trigger apoptotic neuronal death (Uetsuki et al., 1999).

Many caspases have been implicated in Aβ mediated neurodegeneration. Aβ has been shown to induce an ER specific apoptotic pathway involving caspase 12. Caspase 12 resides in the ER and is activated by ER stress, including perturbation of calcium homeostasis (Nakagawa et al., 2000). Caspase 2 has also been implicated in Aβ mediated neuronal death. Accordingly, down regulation of caspase 2 with anti-sense oligonucleotides prevents Aβ mediated cell death and neurones from caspase 2 null mice are resistant to Aβ (Troy et al., 2000). Other reports have shown that Aβ cross links Fas, a member of the TNF receptor family, which causes the recruitment of FAS associated death domain protein (FADD) and the subsequent activation of caspase 8 (Irvins et al., 1999). Moreover, a novel cytotoxic APP fragment is generated by the action of caspase 8 and the resultant fragment called C31 is a potent inducer of apoptosis (Lu et al., 2000). Oxidative stress (Soledad et al., 2000) and excitotoxicity (Migual-Hidelgo et al., 2002) are other pathogenic mechanisms that have been implicated in Aβ mediated neurodegeneration. Both oxidative stress and excitotoxicity can initiate apoptosis. Oxidative stress causes mitochondrial damage,

which leads to apoptosis, whilst excitotoxicity is associated with intracellular calcium overload and the subsequent activation of caspases (Honig and Rosenberg 2000). Thus, apoptosis may elicit the final steps in neuronal death following oxidative stress or excitotoxic insults. This provides a unifying theory that takes into consideration the existence of other pathogenic mechanisms evident in AD.

1.6.8 The role of microglia in Alzheimer's disease

Immunoglobulins and T cells are not detectable in AD brain, which indicates that humoral or classical cell mediated immunity are not involved in AD pathology (Eikelenboom et al., 2002). Furthermore, adhesion molecules are not upregulated on the endothelial cells that constitute the BBB implying that peripheral leucocytes are not recruited into the CNS as occurs in stroke (Eikelenboom et al., 2002). However, the presence of activated microglia in and around senile plaques suggests that some form of inflammatory reaction does occur in AD (Itagaki et al., 1989; Haga et al., 1989; Le et al., 2001; Vehmas et al., 2003). Indeed microglial activation may represent a specialised CNS response to injury or foreign bodies, inasmuch as microglial activation is a graded response with the extent of activation depending on the severity of the insult. Thus, in the CNS the benefits of inflammation appear to be carefully balanced with the deleterious effects of such a reaction on neuronal survival. The primary role of activated microglia in AD has been the focus of much debate and has led to the development of two contrasting hypotheses. The first theory supposes that microglia play a beneficial role in AD. Accordingly, activated microglia secrete TGFβ, a cytokine that exhibits anti-inflammatory and neurotrophic properties (Justica et al., 2001). Moreover, microglia have been shown to phagocytose degenerating neurites (Vehmas et al., 2003) and amyloid deposits (Shaffer et al., 1995; Paresce et al., 1996; Paresce et al., 1997; Kopec and Carroll 1998); processes which may serve

to slow the progression of AD. Aβ has also recently been demonstrated to exhibit chemotactic properties (Yan et al., 1996; Nakai et al., 1998; Le et al., 2001; Tiffany et al., 2001), which may account for the accumulation of phagocytic microglia in and around senile plaques *in vivo*. Nevertheless, the accumulation of large deposits of Aβ in AD suggests that microglia are largely unsuccessful in their endeavours to remove extracellular Aβ. The second theory supposes that microglia contribute to amyloidogeneisis and the deposition of senile plaques and thereby play a deleterious role in AD (Haga et al., 1989; Frackowiak et al., 1992). Consistent with this, activated microglia upregulate APP expression (Banati et al., 1993b) and have been reported to release Aβ *in vitro* (Bitting et al., 1996). Moreover, imaging studies show that reactive microglia are apparent at an early stage in AD, which extends the conception that microglia are merely debris removing phagocytes and supports the notion that microglia contribute to pathology (Cagnin et al., 2001; Banati 2003).

Regardless of the primary role of reactive microglia in AD, microglia contribute to cerebral inflammation. Studies have demonstrated the presence of a wide variety of inflammatory mediators in senile plaques, many of which are produced by reactive microglia (table 1.3) (McGeer and McGeer 1997, 1999; Kingham and Pocock 2000). *In vitro*, reactive microglia also secrete a number of other potent neurotoxins including glutamate (Piana and Fontana 1994; Kingham et al., 1999; Barger and Basile 2001), superoxide (McDonald et al., 1997; Si et al., 1997) and NO (Bhat et al., 1998; Kingham et al., 1999). Consistent with the latter, nitrated proteins are detectable in AD tissue, which is associated with the formation of peroxynitrite from superoxide and NO (Smith et al., 1997). Paradoxically, numerous factors associated with senile plaques including Aβ (Li et al., 1996; McDonald et al., 1997; Combs et

al., 2001), cytokines (Ding et al., 1997; Hellendall and Ting 1997; Possel et al., 2000), chromogranin A (Taupenot et al., 1996; Kingham et al., 1999) and thrombin (Möller et al., 2000) induce microglial activation. Thus, it is feasible that a self-sustaining vicious cycle is instigated, which leads to heightened microglial activation accompanied by the production of more microglial derived inflammatory factors. Since inflammatory mediators cannot distinguish friend from foe, neurones in the local vicinity of the plaques may incur 'bystander' damage, thereby exacerbating neurodegenerative processes. In support of this, reactive microglia trigger neuronal death in mixed culture systems *in vitro* (Kingham et al., 1999; Combs et al., 2001). Furthermore, microglial derived IL1 triggers the activation of astrocytes (Giulian and Baker 1986), which in turn may impair astrocytic sequestration of glutamate and potassium thereby exacerbating neuronal dysfunction in AD.

The presence of inflammation in AD is corroborated by epidemiological studies, which have demonstrated that non-steroidal anti-inflammatory drugs (NSAIDs) reduce the risk of developing AD (McGeer et al., 1996; Stewart et al., 1997). Interestingly, NSAID administration is associated with a 65 % reduction in plaque associated activated microglia (Mackenzie and Munoz 1998). NSAIDs work by selectively inhibiting the activity of COX enzymes (COX-1 and COX-2). COX-1 is constitutively expressed in all cells, whereas COX-2 is expressed during chronic inflammatory reactions. Therefore, it seems likely that COX-2 is over expressed in AD probably by plaque associated microglia.

	Microglia	Astrocytes	Neurones
Complement proteins	+	+	+
Complement inhibitors	+		+
Heat shock protein 72 and 27			+
Acute phase proteins			
α1-antichymotrypsin		+	
α1-antitrypsin		+	
α2-macroglobulin		+	+
Capthepsins and Cytostatins			
Cathepsin B, D, E, H, L and S	+	+	+
Cytostatins A and C			+
Substrates for Lipoprotein receptors			
Apoliprotein E	+	+	+
LPR		+	+
Lipoprotein lipase			+
Cytokines and growth factors			
bFGF	+	+	
TGFβ1	+	+	
IL1	+	+	+
IL6	+	+	+
MCP-1	+	+	
Thrombin and plasmin systems			
Thrombin	+	+	
Tissue plasminogen activator	+	+	+
Urokinase plasminogen activator	+	+	+
Proteoglycans			
Heparin sulphate proteoglycan	+	+	+
Chondroitin sulphate proteoglycan	+	+	
Other			
ICAM-1		+	
Chromogranin A			+

Table 1.3 Factors associated with senile plaques

Astrocytes, microglia and neurones release factors that co-localise with senile plaques. The origins of the factors are denoted with a + (McGeer and McGeer 1997, 1999; Kingham and Pocock 2000).

1.7 The interplay between Stroke and Alzheimer's disease

1.7.1 Stroke as a risk factor for Alzheimer's disease

Stroke patients have been demonstrated to exhibit an increased susceptibility to AD (Tatemichi et al., 1994; Kokmen et al., 1996; Moroney et al., 1996; Desmond et al., 2000; Madureira et al., 2001). The clinical determinants of dementia include the location and the severity of the stroke and host characteristics including age and level of education (Desmond et al., 2000). Moreover, it has been shown that amyloidogeneis and tau pathology are induced by hypo-perfusion in ischaemically damaged areas of the brain (Gehrmann et al., 1995; Kim et al., 1998; Nihashi et al., 2001; Kalaria 2002). Indeed, Alois Alzheimer originally described the presence of vascular changes in the first recorded case of AD in 1907 (see review by Kalaria 2002). More recently, a large majority of AD patients examined at autopsy have been demonstrated to bear stroke like lesions or infarcts that range from haemorrhage to cerebral amyloid angiopathy (CAA) (Kalaria et al., 1996; Desmond et al., 2000). CAA describes the deposition of amyloid in the walls of cerebral arteries and arterioles, a process that may weaken the vasculature thereby increasing the risk of haemorrhage or thrombus occlusion. Stroke may also prime microglia to subsequent pathological insults. Therefore, 'stroke primed' microglia may exhibit an accentuated response to Aβ or other factors associated with AD, which in turn may exacerbate neuronal injury and promote cognitive decline at an accelerated rate in comparison to the 'normal' progression of AD (Pocock et al., 2001). This was one of the hypotheses investigated in this thesis.

1.7.2 The relationship between vascular dementia and Alzheimer's disease

The complex relationship between stroke and AD is emphasised by the fact that the second most frequent form of dementia is vascular dementia (VaD). VaD is caused by cerebral infarction and is characterised by white matter lesions (Kalaria et al., 2002). It has been proposed that AD and VaD are a continuum of the same disease, with pure AD and VaD representing the two extremes (Kalaria 2002). Consequently, patients often present with 'mixed dementia', which is characterised by clinical features of both AD and VaD. Thus, 'mixed dementia' is associated with CAA, micro-infarcts and small vessel disease (atherosclerosis) as well as senile plaques and tau pathology (Table 1.4).

Description	Identifying features
Pure AD	Plaque and neurofibrillary pathology
Plaque only AD	Lack of neurofibrillary pathology
AD with severe CAA	AD with vascular amyloid deposition
CAA with plaques	Mild AD with vascular involvement
AD with vascular lesions	AD with vascular lesions including micro-infarcts
VaD with AD changes	VaD predominates with AD pathology
VaD with small vessel disease	VaD with prominent micro-vascular changes
Pure VaD	Infarction with white matter lesions

Table 1.4 The continuum of AD and VaD

It has been proposed that AD and VaD are a continuum of the same disease, with pure AD and VaD representing the two extremes (Kalaria 2002).

1.7.3 APP mutants and stroke

Interestingly, APP gene mutations often precipitate in a disorder bearing stroke as the main clinical phenotype. In contrast, to APP mutations causing AD, the stroke causing mutations are located within the Aβ sequence and it has been shown that these mutants protect Aβ from proteolytic degradation (Tsubuki et al., 2003). The first such mutation was described at position 22 of Aβ, where a glutamine residue is substituted for a glutamic acid residue. This mutation results in hereditary cerebral haemorrhage with amyloidosis, Dutch type (HCHWA-D), an autosomal dominant disease, clinically defined by recurrent strokes, vascular dementia and fatal cerebral bleeding in the fifth and sixth decades of life (Luyendijk et al., 1988; Levy et al., 1990). Furthermore, two different mutations termed the Artic and the Italian mutation have been described at position 22 of the Aβ peptide (Ghiso and Frangione 2001). The Artic mutation results from the substitution of glutamic acid for glycine and causes early onset AD with prominent vascular pathology, whilst the Italian mutation triggered by the substitution of glutamic acid for lysine, causes dementia with cerebral haemorrhage. Other APP mutants include the Flemish mutation in which an alanine to glycine substitution occurs at position 21 of the Aβ peptide (Hendriks et al., 1992). Patients bearing this mutation present with dementia associated with cerebral haemorrhage. Together these disorders provide evidence that common genetic abnormalities underlie stroke and AD.

1.8 Aims of the study

The aims of this study were to investigate the signalling cascades elicited in cultured microglia using *in vitro* models of stroke and AD. Microglia are the resident macrophages of the brain. These cells play a role in immuno-surveillance and protect

the brain against invading pathogens. However, there is increasing evidence that chronic microglial activation contributes to neurodegeneration in diseases such as stroke (Lees 1993; Kumar and Evans 1997; Rupalla et al., 1998; Tikka et al., 2001) and AD (McGeer et al., 1996; Stewart et al., 1997) and this was the fundamental premise for this study.

In this thesis the effects of albumin on microglia were investigated (chapter 4), the rationale being that microglia are normally exposed to low levels of albumin. However, if the BBB is compromised as occurs in stroke (Hornig et al., 1983) and in some cases of AD (Alafuzoff et al., 1983; Skoog et al., 1998) then microglia are exposed to large increases in this plasma protein. Next the signalling cascades elicited in microglia following treatment with Aβ or chromogranin A were investigated since both proteins are associated with senile plaques in AD (Feldman et al., 1997; Munoz 1991; Yasuhara et al., 1994; Rangon et al., 2003) (chapter 5). The microglial signalling cascades triggered by ischaemia were also explored (chapter 6). Additionally, the effects of ischaemia followed by albumin or Aβ treatment were studied because it was postulated that stroke may heighten the reactivity of microglia to subsequent pathological insults (Pocock et al., 2001). Furthermore, the effects of microglial conditioned medium on neurones were investigated in an attempt to model the interplay between microglia and neurones *in vivo* (chapter 4, 5, 6).

2.0 Materials and Methods

2.1 Materials

The following section lists the materials used and the company that supplied them.

All bench grade chemicals used in this thesis were from Sigma (Dorset, UK).

Material	Supplier
Adenosine 5' phosphatase (ATPase)	Sigma (Dorset, UK)
Albumin (#A6272)	Sigma (Dorset, UK)
Albumin agarose complex (#A3790)	Sigma (Dorset, UK)
Ampicillin,	Sigma (Dorset, UK)
Avidin-biotin complex	Vector Laboratories (Peterborough, UK)
β-amyloid	Bachem (Essex, UK)
BAPTA	Sigma (Dorset, UK)
Bradford protein assay reagent kits	Perbio Science (Chesire, UK)
Cell titer 96 AQ_{ueous} one solution proliferation assay	Promega (Southampton, UK)
CgA	Scientific Marketing Associates (Hertfordshire, UK)
CNQX (6-cyano-7-nitroquinoxaline-2,3-dione)	Tocris Cookson (Bristol, UK)
CO_2 gas	BOC gases (Guildford, UK)
5 % CO_2 - 95 % N_2 gas	BOC gases (Guildford, UK)
Cytosine arabinofuranoside	Sigma (Dorset, UK)
DNAase	Sigma (Dorset, UK)
Donkey anti-goat IgG (HRP) (#2020)	Autogen Bioclear (Wiltshire, UK)
DPX mountant	VWR International (Leicester, UK)
Dulbeccos modified eagles medium (DMEM)	Sigma (Dorset, UK)
Earle's balanced salts solution (EBSS)	Life Technologies (Paisley, UK)
Enhanced chemiluminescence reagent (ECL)	Amersham Pharmacia (Buckinghamshire, UK)
FITC-albumin (#A9771)	Sigma (Dorset, UK)
FITC-mouse anti-CD45	Serotec (Oxford, UK)
FITC-mouse anti-ED-1	Serotec (Oxford, UK)
Fluoroscein diacetate,	Sigma (Dorset, UK)
Foetal calf serum	Life Technologies (Paisley, UK)
Formaldehyde	VWR International (Leicester, UK)
Fraction V (#A6414)	Sigma (Dorset, UK)

Material	Supplier
Fura-2	Molecular Probes (Leiden, The Netherlands)
Glass coverslips	Scientific Laboratory Supplies (Nottingham, UK)
Glutamate dehydrogenase	Sigma (Dorset, UK)
Goat anti-COX-2 (#1746)	Autogen Bioclear (Wiltshire, UK)
Goat anti-mouse IgG (HRP) (#2005)	Autogen Bioclear (Wiltshire, UK)
Goat anti-rabbit IgG (HRP) (#2004)	Autogen Bioclear (Wiltshire, UK)
Goat anti-TNFα (#1351)	Autogen Bioclear (Wiltshire, UK)
Griess reagent	Sigma (Dorset, UK)
Hoechst 33342 (2'[epoxyphenyl]-5-[4-methyl-1-piperazinyl]-2,5'-bi-1H-benzimidazol)	Sigma (Dorset, UK)
JC-1 (5,5'6,6'-tetraethylbenzimidazole carbo-cyanine iodide)	Molecular Probes (Leiden, The Netherlands)
LPS (lipopolysaccharide)	Sigma (Dorset, UK)
Methanol	VWR International (Leicester, UK)
Minimum essential medium (MEM)	Life Technologies (Paisley, UK)
MK801 (5-methyl-10,11-dihydro-5H-dinezo[a,d]cyclohepten-5,1-imine hydrogen maleate)	Tocris Cookson (Bristol, UK)
Mouse anti-β actin (#A5441)	Sigma (Dorset, UK)
Mouse anti-CD11b (OX-42)	Serotec (Oxford, UK)
Mouse anti-ED-1 (MCA341)	Serotec (Oxford, UK)
Mouse anti-GFAP (#G3893)	Sigma (Dorset, UK)
Mouse anti-p-ERK (#7383)	Autogen Bioclear (Wiltshire, UK)
MSPG [(±)-α–methyl-4(4-sulphonophenyl)glycine]	Tocris Cookson (Bristol, UK)
N9 microglia	Dr P R Castagnoli (CNR Cellular and Molecular Pharmacology Centre, Milan, Italy)
$NADP^+$	Sigma (Dorset, UK)
NADPH	Sigma (Dorset, UK)
Neutralising anti-RAGE antibody	Dr L Denner (Texas Biotechnology Corporation, Texas, USA)
Nitrate reductase	Sigma (Dorset, UK)
Nunc maxi-sorp cell culture plates	Scientific Laboratory Supplies (Nottingham, UK)
Oxygen trap (ischaemia chamber)	Chromatography Research Supplies (Louisville, UK)

Material	Supplier
PE-mouse anti-CD11b	Serotec (Oxford, UK)
Penicillin	Sigma (Dorset, UK)
Percoll (#P1644)	Sigma (Dorset, UK)
Pertussis toxin	Centre for Applied Microbiology and Research (Wiltshire, UK)
Pluronic acid	Sigma (Dorset, UK)
Poly I	Sigma (Dorset, UK)
PPADS (pyridoxal-phosphate-6-azophenyl-2'-4'-disulphonic acid)	Sigma (Dorset, UK)
PP2	Calbiochem (Nottingham, UK)
Propidium iodide	Sigma (Dorset, UK)
Protein A/G plus agarose (#2003)	Autogen Bioclear (Wiltshire, UK)
PVDF membrane (Immobilon-P-polyvinylidene di-fluoride)	Sigma (Dorset, UK)
Rabbit anti-iNOS (#610333)	BD Biosciences Pharmingen (Oxford, UK)
Rabbit anti-TGFβ (#7892)	Autogen Bioclear (Wiltshire, UK)
Rabbit anti-total ERK (#9102)	New England Biolabs (Herfordshire, UK)
SDS polyacrylamide gels (10 %)	Bio-Rad (Hertfordshire, UK)
Sheath fluid	BD Biosciences (Oxford, UK)
Soya bean trypsin inhibitor	Sigma (Dorset, UK)
TGFβ1 Emax enzyme linked immunosorbent assay (ELISA) kits (#G7591)	Promega (Southampton, UK)
Tissue culture plasticware	Scientific Laboratory Supplies (Nottingham, UK)
TNFα Quantikine ELISA kits (#RTA00)	R & D systems (Oxford, UK)
TSA-3 astrocytes	Gareth Pryce (Department of Neuroinflammation, Institute of Neurology, University College London, London, UK)
UO126	Promega (Southampton, UK)
U73122	Sigma (Dorset, UK)
Wistar rats (bred and reared in house)	Charles River UK (Kent, UK)

2.2 Methods

2.2.1 Cell culture

2.2.1.1 Preparation of microglia

Primary cultures of microglia were prepared from the brains of 3-6 day old Wistar rats (Kingham and Pocock 2000). Animals were killed by cervical dislocation and decapitation in accordance with the Scientific Procedures Act, UK, 1986. Brains (minus cerebellum) were removed into ice cold phosphate buffered saline (PBS; 140 mM NaCl, 5mM KCl, 25 mM $NaHPO_4$, 11 mM glucose, pH 7.4), mechanically dissociated, pelleted by centrifugation (500 x g) then resuspended in 70 % percoll (10 ml). A gradient was produced by overlaying this cell suspension with 35 % percoll (10 ml) followed by PBS (10 ml). The percoll gradient was then centrifuged (1250 x g) for 45 minutes and the microglial cells were extracted from the 35 % - 70 % percoll interface (Fig. 2.1).

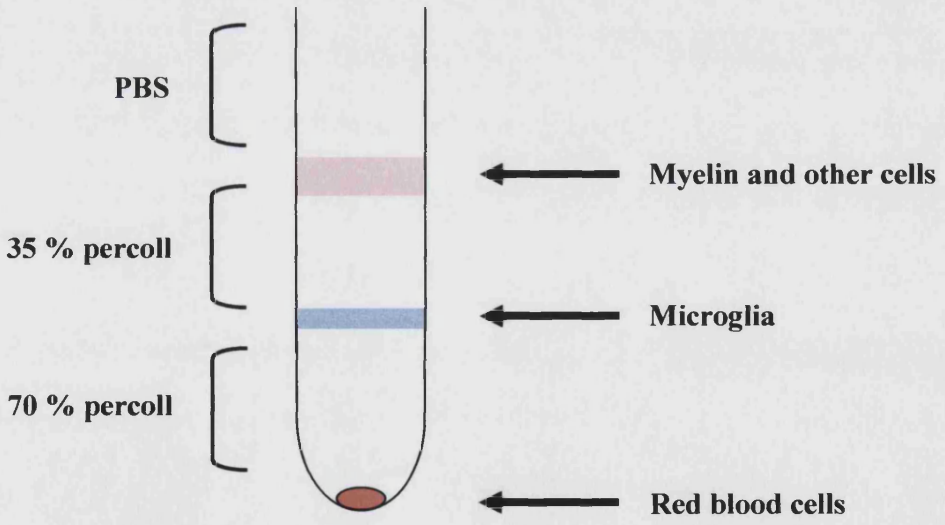

Figure 2.1 Schematic diagram of a percoll gradient

Following centrifugation, red blood cells form a pellet at the bottom of the tube. Microglia collect at the 35 %- 70 % percoll interface. Myelin and other cells gather at the 35 % percoll – PBS interface.

Cells were washed with PBS, pelleted by centrifugation (500 x g) then resuspended in culture medium (Minimum essential medium (MEM) supplemented with 25 mM KCl, 30 mM glucose, 25 mM $NaHCO_3$, 1 mM glutamine, 10 % foetal calf serum, 100 U/ml penicillin, 100 µg/ml streptomycin and 6 µg/ml ampicilin). Cells were plated at a density of 6 x 10^5 cells/well on 35 mm culture dishes or at 6 x 10^4 cells/well on 13 mm glass coverslips in 24 well plates. Microglia were maintained at 37 °C in a humidified atmosphere of 5 % CO_2 in air and were used after 1 day *in vitro*.

2.2.1.2 Preparation of peritoneal macrophages

Macrophages were isolated from the peritoneal cavities of neonatal (3-6 day old) or adult (> 6 months) Wistar rats (Soares et al., 1998). Animals were killed by carbon dioxide induced anoxia followed by decapitation in accordance with the Scientific Procedures Act, UK, 1986. Macrophages were harvested from the peritoneal cavity using sterile Earle's balanced salt solution (EBSS; 30 ml). The peritoneal lavage fluid was subsequently centrifuged (500 x g) for 5 minutes to pellet the cells. Cells were resuspended in culture medium (composition described in section 2.2.1.1) then plated at a density of 6 x 10^5 cells/well on 35mm culture dishes or at 6 x 10^4 cells/well on 13 mm glass coverslips in 24 well plates. Peritoneal macrophages were maintained at 37 °C in a humidified atmosphere of 5 % CO_2 in air and were used after 1 day *in vitro*.

2.2.1.3 Preparation of cerebellar granule neurones

Cerebellar granule neurones were prepared from 3-6 day old Wistar rats (Kingham et al., 1999). Animals were killed by cervical dislocation and decapitation in accordance with the Scientific Procedures Act, UK, 1986 and cerebella were removed into chilled solution A (100 mM PBS, 0.3 % fatty acid free BSA, 10 mM glucose, 0.38 % $MgSO_4.7H_2O$). Cerebella were mechanically dissociated then incubated in trypsin

(0.25 %) for 20 minutes at 37 °C. Solution B (100 mM PBS, 0.3 % fatty acid free BSA, 10 mM glucose, 0.38 % $MgSO_4.7H_2O$, 16 U/ml DNAase, 0.5 mg/ml soybean trypsin inhibitor; 20 ml) was subsequently added to the cell suspension and the cells were pelleted by centrifugation (500 x g) for 5 minutes. The resultant cell pellet was re-suspended in solution C (100 mM PBS, 0.3 % fatty acid free BSA, 10 mM glucose, 0.38 % $MgSO_4.7H_2O$, 100 U/ml DNAase, 0.05 mg/ml soybean trypsin inhibitor; 2 ml), then placed on top of an aliquot of EBSS/BSA (Earles's balanced salt solution with 26 mM $NaHCO_3$, 3 mM $MgSO_4.7H_2O$, 4 % fatty acid free albumin; 5 ml) and centrifuged (500 x g) for 10 minutes. Finally, cells were resuspended in culture medium (composition described in section 2.2.1.1), then plated at a density of 6×10^5 cells/well on 13 mm glass coverslips in 24 well plates. Prior to use, coverslips were soaked in 100 % ethanol for a minimum of 2 days, baked at 180 °C for 24 hours then coated in poly-d-lysine (15 mg/l) for one hour at 37 °C. Cerebellar granule neurones were maintained at 37 °C in a humidified atmosphere of 5 % CO_2 in air. After 1 day *in vitro*, the culture medium was replaced with fresh medium supplemented with cytosine arabinofuranoside (Ara C: 10 μM) to prevent excessive astrocyte proliferation. Cerebellar granule neurones were used after 7 days *in vitro*.

2.2.1.4 Growth and maintenance of the N9 microglial cell line

The N9 microglial cell line was originally derived from embryonic day 13 mouse microglial cultures (Corradin et al., 1993). Stocks of N9 cells were preserved in freezing medium (10 % DMSO, 90 % FCS) and stored at - 80 °C. A working stock of N9 cells was maintained in culture medium (DMEM supplemented with 4.4 mM $NaHCO_3$, 50 μM β-mercaptoethanol, 5 % foetal calf serum, 50 U/ml penicillin and 50 μg/ml streptomycin) at 37 °C in a humidified atmosphere of 5 % carbon dioxide in

air. N9 cells were passaged weekly (1 in 10) using a sterile cell scraper and plated when required at a density of 2.5 x 10^5 cells/well on 35 mm culture dishes or at 4 x 10^4 cells/well on 13 mm glass coverslips in 24 well plates. Plated N9 cells were routinely used after 1 day *in vitro*.

2.2.1.5 Growth and maintenance of the TSA-3 astrocytic cell line

The TSA-3 astrocytic cell line was originally derived from neonatal day 2 murine astrocytic cultures derived from Biozzi ABH mice (Personal communication: Gareth Pryce). Stocks of TSA-3 astrocytes were preserved in freezing medium (10 % DMSO, 90 % FCS) and stored at - 80 °C. A working stock of TSA-3 astrocytes was maintained in culture medium (DMEM supplemented with 4.4 mM NaHCO3, 50 μM β-mercaptoethanol, 5 % foetal calf serum, 50 U/ml penicillin and 50 μg/ml streptomycin) at 37 °C in a humidified atmosphere of 5 % carbon dioxide in air. TSA-3 astrocytes were passaged twice a week (1 in 10) using a sterile cell scraper and plated when required at a density of 2.5 x 10^5 cells/well on 35 mm culture dishes or at 4 x 10^4 cells/well on 13 mm glass coverslips in 24 well plates. Plated astrocytes were routinely used after 1 day *in vitro*.

2.2.1.6 Treatment of primary, N9 microglia and peritoneal macrophages

Primary microglia, N9 microglia or peritoneal macrophages were treated with albumin or fraction V (at defined concentrations) for 2 hours in serum free medium (SFM), after which the SFM was replaced with serum containing medium (SCM) for the remainder of the experimental period. In other experiments, primary or N9 microglia were treated with CgA, $A\beta_{(25-35)}$ or LPS (at defined concentrations) in SCM for the stipulated time periods. In experiments using inhibitors, primary or N9

microglia were incubated with the agent (at defined concentrations) in SFM or SCM before the addition of the appropriate activator and also during subsequent treatment with the activator (table 2.1).

Inhibitor and concentration (s) used	Action	Time	References
Aminoadipate (2.5 mM)	Xc^- transporter inhibitor	1 hour	Piani and Fontana 1994 Kingham et al., 1999
AMT-HCL (0.3 μM)	iNOS inhibitor	1 hour	Kingham et al., 1999
BAPTA-AM (1-10 mM)	Intracellular calcium chelator	45 mins	Nolte et al., 1996 Hoffmann et al., 2003
Neutralising RAGE antibody (200 μg/ml)	RAGE antagonist	1 hour	Yeh et al., 2001
Pertussis toxin (Ptx) (1-2 μg/ml)	Gi/0 inhibitor	18 hours	Post et al., 2002
Poly I (0.1-0.5 μg/ml)	Scavenger receptor antagonist	45 mins	Post et al., 2002 Whitman et al., 2000 Husemann et al, 2001
PP2 (50 nM-500nM)	Src kinase inhibitor	1 hour	Hanke et al., 1996 Salazar and Rozengurt 1999
UO126 (1-20 μM)	ERK inhibitor	30 mins	Favata et al., 1998
U73122 (0.5-2 μM)	Phospholipase C inhibitor	1 hour	Heemskerk et al., 1997 Pollaud-Cherion et al., 1998 Tokmakov et al., 2002

Table 2.1 Description of inhibitors

Cells were pre-incubated with inhibitors for the defined period of times at concentrations stipulated in the text and figure legends (within range stated in table). Inhibitors were also incubated with the cells during exposure to the appropriate activator.

2.2.1.7 Depletion of microglial conditioned medium

Microglial conditioned medium was depleted of proteinaceous factors by boiling the conditioned medium for 45 minutes. The medium was then applied to neuronal cultures (see section 2.2.1.8). TNFα and TGFβ were immuno-depleted from microglial conditioned medium using goat anti-TNFα or rabbit anti-TGFβ1, 2, 3 antibodies respectively. Aliquots (500 µl) of conditioned medium were incubated with antibody (2 µg) for 3 hours at 4 °C with end over end rotation. Protein A/G agarose was then incubated with the microglial conditioned medium for 1 hour at 4 °C with constant rotation (Zhao and Eghbali-Webb 2001). Next, the immune complex was removed by centrifugation at 13 000 x g for 2 minutes. The supernatant was subsequently collected then added to cerebellar granule neurones. In other experiments, ATP was depleted from microglial conditioned medium using ATPase. Aliquots (500 µl) of microglial conditioned medium were incubated with ATPase (0.5 U/ml) for 2 hours at 37 °C. The medium was subsequently added to cerebellar granule neurones.

2.2.1.8 Treatment of cerebellar granule neurones

After 7 days *in vitro*, half of the culture medium (200 µl) was removed from the neuronal cultures and replaced with microglial or macrophage conditioned medium (200 µl) or 'depleted' conditioned medium (200 µl) for 24 hours. In experiments using inhibitors, neurones were pretreated with the broad spectrum purinergic receptor antagonist PPADS (100 µM) or the glutamate receptor antagonists CNQX (20 µM), MK801 (10 µM) and MSPG (200 µM) for 1 hour before microglial conditioned medium was added. The inhibitors were also present during the exposure to microglial conditioned medium.

2.2.1.9 Simulation of ischaemia in vitro

Ischaemia was modelled by exposing primary microglia or N9 microglial cells to 95 % N_2 in 5 % CO_2 in the presence of Dulbeccos modified Eagles medium (DMEM) lacking glucose, pyruvate and foetal calf serum (ischaemia medium) (Pringle et al., 1997; Lyons and Kettenmann 1998; Yenari and Giffard 2001). Microglia bathed in ischaemia medium were placed in a humidified glass chamber located within a 37 ° C incubator. The chamber was airtight and comprised two modified valves, which enabled gas to be let into or out of the chamber. Oxygen was removed from the chamber, by flushing with a mixture of 95 % N_2, 5 % CO_2 for 30 minutes. The gas was passed through an oxygen trap (0.25 inches, model 1000) to remove any residual oxygen from the delivery pipe before reaching the chamber. Resazurin was used as an oxygen indicator, in the absence of oxygen resazurin indicator strips change from red/pink to white. Microglia were exposed to ischaemia for 3 hours before 'reperfusion'. Reperfusion involved changing the medium from 'ischaemia medium' to 'normal' culture medium containing glucose and serum (see section 2.2.1.1 for the composition). Microglia were then maintained at 37 °C in a humidified atmosphere of 5 % CO_2 in air (normoxic) for the stipulated time periods. Additionally, after the ischaemic insult some cultures were exposed to Aβ (45 μM) in SCM (+ glucose) for defined periods of time, whilst others were exposed to fraction V (1 mg/ml) in SFM medium (+ glucose) for 2 hours, then SCM (+ glucose) for the remainder of the experimental period.

2.2.2 Immunocytochemistry

To check for purity cultures of microglia or peritoneal macrophages were stained with OX-42, an antibody which recognises the CR3 complement receptor (CD11b/CD18) (Graeber et al., 1989) and ED-1, an antibody that recognises a lysosomal protein (Graeber et al., 1990; Slepko and Levi 1996). High levels of ED-1 are associated with macrophages and activated microglia, whilst low levels of expression are associated with quiescent ramified microglia (Graeber et al., 1990; Slepko and Levi 1996). The presence of astrocytes in the microglial preparations was also assessed by staining for GFAP, an astrocytic marker (Eliasson et al., 1999). Additionally, the presence of contaminating microglia and astrocytes in cerebellar granule neurone cultures was assessed by staining with OX-42 and GFAP respectively.

Microglia and peritoneal macrophages were cultured for 1 day *in vitro* then fixed with methanol at 4 °C for 5 minutes, whereas cerebellar granule cells were cultured for 7 days before being fixed. Cells were washed in three changes of PBS then blocked in normal horse serum (diluted 1 in 40 in PBS) for 45 minutes at room temperature. Samples destined for ED-1 staining were permeabilised by adding triton (0.1 %) to the blocking solution. Cells were incubated with the respective primary antibody (mouse anti-CD11b, mouse anti-ED-1, mouse anti-GFAP) diluted in blocking reagent (1 in 500) for 18 hours at 4 °C. All incubations were performed in a humidified chamber to prevent excessive evaporation. Control cultures were also set up to test the specificity of the staining, in which cells were incubated in blocking buffer in the absence of primary antibody. Following primary antibody treatment, cells were washed in four changes of PBS, then incubated with an anti-mouse IgG secondary antibody conjugated to biotin (1 in 200) for 2 hours at 4 °C. Subsequently, cells were

washed in three changes of PBS and incubated with a pre-formed avidin-biotin horseradish peroxidase (HRP) complex for 1 hour at room temperature. To visualise the staining, cells were washed extensively in PBS and incubated with diaminobenzidine tetrahydrochloride (DAB) for 5 minutes at room temperature. Cells were then bathed in PBS for 5 minutes to allow the staining to develop, after which the cells were counterstained with haematoxylin for 1 minute. Cells were subsequently washed in water then dehydrated through an ethanol gradient (70-100 %) before being immersed in xylene for 3 minutes. Finally, cells were mounted onto glass slides using distyrene, tricresyl phosphate and xylene mounting medium (DPX). Immunoreactive cells were counted on three coverslips per treatment on three independent occasions (each coverslip comprised 10 fields of view). Immunoreactive cells were expressed as a percentage of the total number of cells counted as demonstrated by haematoxylin staining.

2.2.3 Fluorescent activated cell sorting

2.2.3.1 FACSCalibur flow cytometer

Fluorescent activated cell sorting (FACS) was performed using a Becton and Dickinson FACSCalibur flow cytometer (Fig. 2.2). Flow cytometers enable the physical and antigenic properties of individual cells to be assessed. Cells are channelled through a single beam of light produced by an argon laser. The light is subsequently disrupted and detected as forward (FS) or side scattered (SS) light. Forward scattered light reflects the size of a cell, whereas side scattered light provides an indication of granularity. Cells can also be stained with fluorescent antibodies directed against cell surface or intracellular antigens. The fluorochromes absorb light from the laser beam then emit light in different regions of the spectrum. The cytometer subsequently measures the intensity of fluorescent signal emitted from

each cell. The main advantage of FACS over immunocytochemistry is that thousands of cells can be analyzed in a relatively short space of time.

The argon-ion laser situated in the cytometer produces light at a wavelength of 488 nm. The light is directed through a focussing lens onto the cells. The forward scattered light is measured by the forward scatter diode. The side scattered light and the fluorescent emissions are gathered by the collection lens, which is positioned perpendicularly to the light source. The side scattered light and the fluorescent beams are subsequently focussed through a series of optical filters then spectrally split by specific dichroic mirrors. Green/yellow light characteristic of fluoroscein isothiocyanate (FITC) staining passes to the FL1 photomultiplier tube. In addition, a fraction (10 %) of the FL1 signal provides the side scatter measurement. Yellow/Orange light characteristic of phycoerythrin staining (PE) is reflected to the FL2 photomultiplier tube. Red light that is associated with peridinin chlorophyll protein (PerCP) staining is channelled to the FL3 photomultiplier tube. Finally, the optical signals received are converted into electrical data. In this thesis data was analysed using CELLQUEST software.

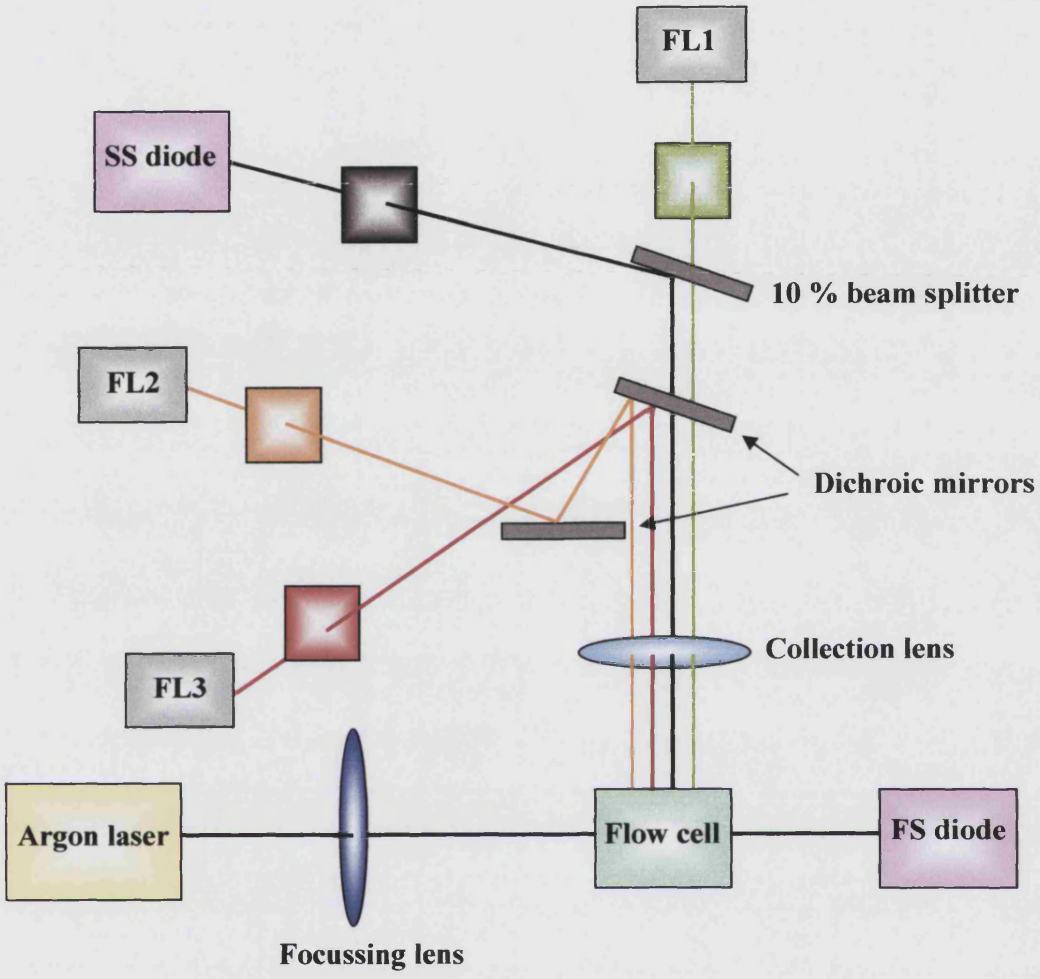

Figure 2.2 Schematic diagram of the flow cytometer

Light passes through the focussing lens and on to the cells. Scattered and emitted light is collected as indicated. Optical outputs are subsequently converted into electrical signals.

2.2.3.2 FACS analysis

Primary microglia and peritoneal macrophages were analysed for the expression of the CR3 complement receptor (CD11b/CD18), ED-1 and CD45 using FACS. Primary microglia and peritoneal macrophages were cultured for 1 day *in vitro* following isolation. The cells were then harvested by cell scraping, pelleted and fixed with formaldehyde (8 %) in phosphate buffered saline. Samples destined for ED-1 staining were permeabilised by adding triton (0.1 %) to the fixative. Following fixing, the cells were pelleted and resuspended in the appropriate primary antibody conjugate (PE-mouse anti-CD11b; 1 in 20, FITC-mouse anti-CD45; 1 in 10, FITC-mouse anti-ED-1; neat) and incubated for 1 hour at room temperature. Finally, cells were pelleted and resuspended in sheath fluid, then analysed by flow cytometry in accordance with the manufacturer's instructions. Experiments were performed in triplicate, therefore the results shown are representative of a single experiment consisting of data collected from 4000 cells.

2.2.4 Western blotting

2.2.4.1 Preparation of cell lysates

Following the appropriate treatment, cells were harvested in lysis buffer (20 mM Tris-acetate, 1 mM EDTA, 1 mM EGTA, 10 mM sodium β-glycerophosphate, 1 mM sodium orthovanadate, 5 % glycerol, 1 % Triton X-100, 0.27 M sucrose, 1 mM benzamidine, 4 μg/ml leupeptin, 0.1 % β-mercaptoethanol, pH 7.4) then incubated on ice for 10 minutes. Following the incubation, samples were centrifuged (13500 x g) for 5 minutes (Kingham and Pocock 2000) and the resultant supernatants were collected. Protein concentrations of supernatants were determined according to the method of Bradford (Bradford 1976) using bovine serum albumin as a standard (Fig.

2.3). In brief, samples (2 µl) were mixed with Bradford reagent (1 ml) and the optical density (OD) was read after 20 minutes at 595 nm.

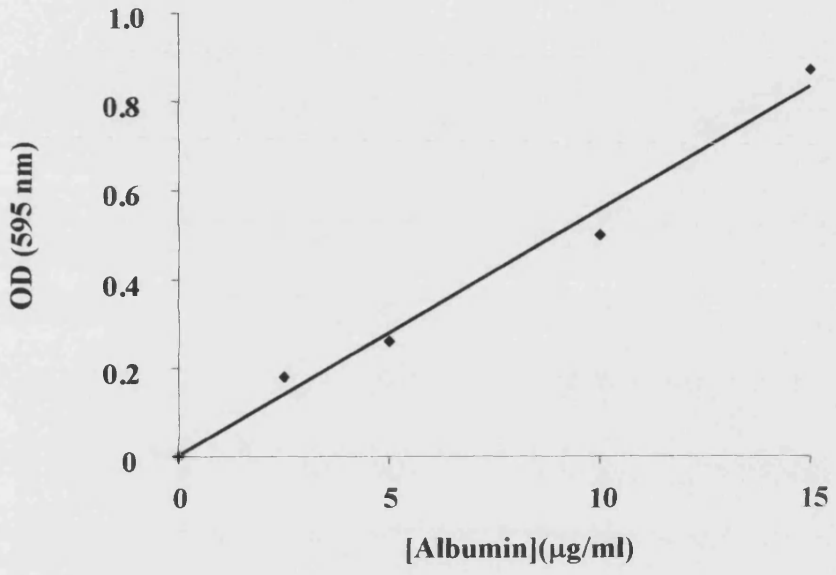

Figure 2.3 Representative standard curve of protein concentration against OD
Albumin standards (0-15 µg/ml) were incubated with Bradford reagent and the OD was measured at 595 nm.

2.2.4.2 SDS polyacrylamide gel electrophoresis

Proteins from cell lysates were resolved by SDS polyacrylamide electrophoresis (SDS-PAGE) using a Bio-Rad mini-protean 2 electrophoresis cell (BioRad, UK). Prior to electrophoresis, samples were boiled for 5 minutes, mixed with laemelli sample buffer (1 % SDS, 10 % glycerol, 2.5 % β-Mercaptoethanol, 125 mM Tris/HCl, 1 % bromophenol blue, pH 6.8; 30 – 40 µg/well) then loaded on to Bio-Rad SDS-PAGE Tris-HCl precast gels (10 %). Electrophoresis was performed at 180 volts for 1 hour in the presence of running buffer (125 mM Tris, 1M glycine, 0.01 % SDS).

2.2.4.3 Electrophoretic protein transfer

Gels were equilibrated in transfer buffer (25 mM Tris, 192 mM glycine, 0.01 % SDS, 20 % methanol) for 10 minutes. Meanwhile, a PVDF (Immobilon-P) membrane was activated by immersion in chilled methanol for 1 minute. The gel and the membrane were then assembled in the transfer cassette and the proteins were transferred using a Bio-Rad mini trans blot electrophoretic transfer cell (BioRad, UK). Transfer was performed at 80 volts for 2 hours or at 22 volts for 16 hours.

2.2.4.4 Immunoblotting

Membranes were washed in Tween-20 Tris buffered saline (TTBS; 10 mM Tris-HCl, 150 mM NaCl, 0.5 % Tween-20, pH 7.4) for 15 minutes. Membranes were then incubated with blocking buffer (TTBS, 5 % nonfat dried milk) for 2 hours at room temperature to minimise non-specific binding. Membranes were subsequently incubated with primary antibody (rabbit anti-iNOS; 1:5000, goat anti-COX-2; 1:750, or mouse anti-p-ERK; 1:750) for 2 hours at room temperature. Following the incubation with primary antibody, membranes were washed in four changes of TTBS. Next membranes were incubated for a further 2 hours at room temperature with the corresponding secondary antibody conjugated to HRP (goat anti-rabbit IgG; 1:500, donkey anti-goat IgG; 1 in 1000, or goat anti-mouse IgG; 1:1000). Finally, membranes were washed in four changes of TTBS and the proteins of interest were detected using enhanced chemiluminescence. To ensure equal protein loading membranes were reprobed with either mouse anti-β actin (1:1000), or rabbit anti-total ERK (1:500). Western blots were performed in triplicate and therefore the blots shown are representative of a single experiment. Densitometry was performed using Gel Pro software (Version 3.1) in accordance with the manufacturer's instructions.

2.2.5 Albumin 'binding protein' precipitation

N9 microglia, peritoneal macrophages, TSA-3 astrocytes or cerebellar granule neurones were harvested in RIPA lysis buffer (150 mM NaCl, 50 mM Tris, 1 % NP40, 0.5 % sodium deoxycholate, 0.1 % SDS, 1 mM benzamidine, 4 μg/ml leupeptin, 0.1 % β-mercaptoethanol, pH 7.4) then incubated on ice for 5 hours. Following the incubation, samples were sonicated for 1 minute then centrifuged (13500 x g) for 5 minutes and the resultant supernatants were collected. Albumin conjugated to agarose beads (12 μl) was incubated with cell lysates (1 mg/ml) for 3 hours at 4 °C with end over end rotation. The beads were subsequently pelleted by centrifugation (13500 x g) then washed in three changes of RIPA buffer. Following the last wash the precipitated proteins were resuspended in laemelli sample buffer, then boiled for 5 minutes to elute the proteins of interest from the agarose complex. Next proteins were resolved using a Bio-Rad SDS-PAGE Tris-HCl precast gel (10 %). The proteins were then transferred on to a PVDF membrane, which was stained with coumassie blue to enable protein visualisation.

2.2.6 Protein sequencing

2.2.6.1 N-terminal protein sequencing

N-terminal sequencing of the putative albumin 'binding protein' isolated from N9 microglia was performed by Dr Fox (Alta Bioscience, Birmingham University, UK). The protein of interest immobilized on a PVDF membrane and stained with coumassie was subjected to repetitive cycles of Edmun degradation. Edmun degradation sequentially removes one amino acid from the N-terminus of a protein (Berg et al., 2002). The method employs phenyl isothiocyanate, which reacts with the uncharged terminal group of the protein to form a phenylthiocarbamoyl derivative.

Then under mildly acidic conditions a cyclic phenylthiohydantoin (PTH) derivative of the terminal amino acid is liberated. PTH-amino acids are subsequently identified using high performance liquid chromatography (HPLC) against a standard mixture of PTH-amino acids.

2.2.6.2 MALDI fingerprinting

Matrix assisted laser desorption and ionization (MALDI) fingerprinting was performed by Dr Packman (PNAC facility, Cambridge University, UK). The putative albumin 'binding protein' isolated from N9 microglia was resolved on a Bio-Rad SDS-PAGE Tris-HCl precast gel (10 %) and stained with coumassie. The protein was then enzymatically digested with trypsin. Peptides were extracted from the digestion buffer and desalted using a Millipore C18 ZipTip according to the manufacturer's instructions. Subsequently, peptides were identified by tandem mass spectrometry using a ThermoFinnigan LCQ classic mass spectrometer with static nanospray source. Basically, the peptide fragments were accelerated down a flight tube. The mass to charge ratio of an individual peptide is related to the time it takes to reach a detector. Therefore, the identity of a protein can be elucidated by comparing the trypsin fingerprints with known sequences on a database. Database searching was done with Mascot and only statistically significant hits were considered.

2.2.7 Measurement of glutamate

The presence of glutamate in culture medium was assessed by fluorometric quantification of NADPH, which is produced through the reaction of glutamate with $NADP^+$ in the presence of glutamate dehydrogenase (Nicholls and Sihra 1986). This reaction yields one mol of NADPH for every mol of glutamate; therefore NADPH levels are directly proportional to glutamate concentrations in the medium.

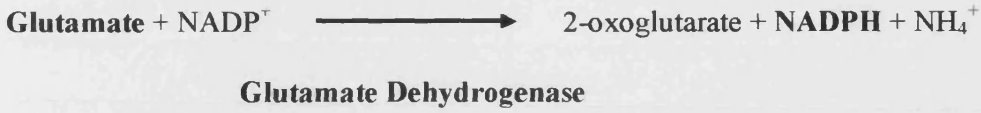

Culture medium (100 µl) was diluted in basic medium (153 mM NaCl, 3.5 mM KCl, 1.3 mM $CaCl_2$, 1.2 mM $MgCl_2$, 0.4 mM KH_2PO_4, 5 mM $NaHCO_3$, 1.2 mM Na_2SO_4, 5 mM glucose, 20 mM TES, pH 7.4; 900 µl), then incubated with $NADP^+$ (1 mM) for 2 minutes at 37 °C. Samples were subsequently incubated with glutamate dehydrogenase (32.4 U/ml) for 8 minutes at 37 °C. NADPH levels were determined using a Perkin Elmer fluorimeter with excitation set at 340 nm and emission greater than 400 nm was collected. The concentration of glutamate was determined against a standard curve (Fig. 2.4). Glutamate experiments were performed in triplicate on samples isolated on three independent occasions.

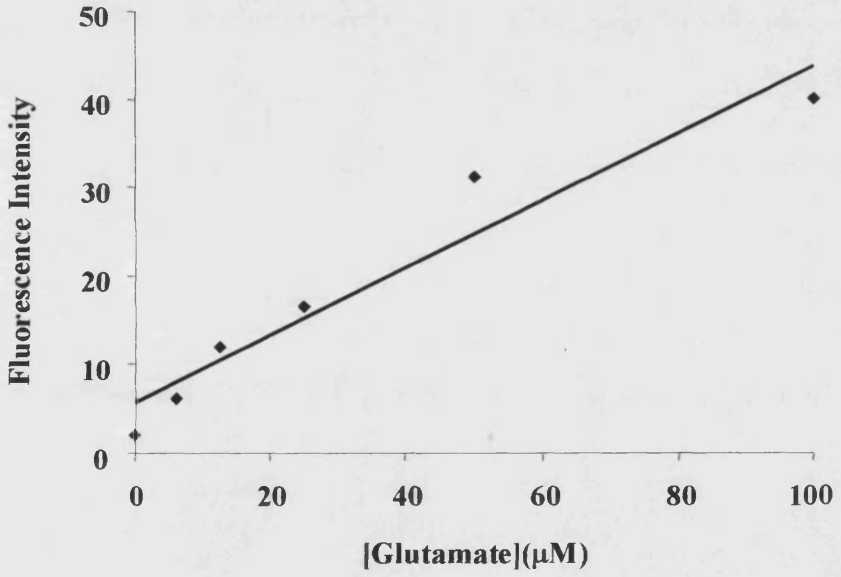

Figure 2.4 Representative standard curve of glutamate concentration against fluorescence intensity. Glutamate standards were treated with $NADP^+$ then glutamate dehydrogenase. NADPH levels were subsequently measured at a wavelength of 340 nm and emission greater then 400 nm was collected.

2.2.8 Measurement of nitrite

In aqueous solution NO is rapidly oxidised to nitrite and nitrate. Therefore, the presence of NO in the culture medium was assessed by spectrophotometric quantification of nitrite using Griess reagent (Kingham et al., 1999). To avoid underestimation of NO production, nitrate was converted to nitrite using nitrate reductase. The Griess assay is based on the production of a diazonium salt by the reaction of nitrite with sulphanilamide in acidic solution. The sulfanilamide diazonium salt subsequently reacts with naphthylethylenediamine producing a diazonium chromophore that can be detected at 540 nm.

$$\textbf{Nitrate } (NO_3^-) + NADPH \xrightarrow[\textbf{Nitrate Reductase}]{} \textbf{Nitrite } (NO_2^-) + NADP^+ + H_2O$$

To determine nitrite concentrations, culture medium was incubated with nitrate reductase (0.028 U/ml) and β NADPH (100 μM) for 15 minutes at 37 °C in the dark. Lactate dehydrogenase (111 U/ml) and sodium pyruvate (110 mg/ml) were subsequently added for 10 minutes at 37 °C to consume any residual NADPH. Griess reagent (0.1 % naphthylethylenediamine, 1 % sulfanilamide, 5 % H_3PO_4) was then added and the OD was read at 540 nm. The efficiency of conversion of nitrate to nitrite was determined against a standard nitrate curve (Fig. 2.5). Nitrite experiments were performed in triplicate on samples isolated on three independent occasions.

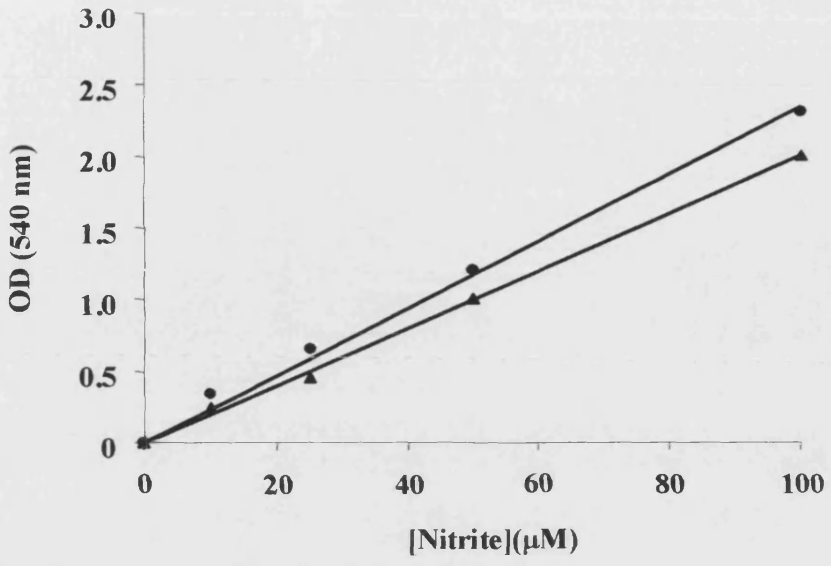

Figure 2.5 Representative standard curve of nitrite concentration against OD
Nitrite standards (circles) were incubated with Griess reagent and the OD was measured at 540 nm. To demonstrate the efficiency of conversion of nitrate to nitrite, nitrate standards (triangles) were converted to nitrite using β-NADPH and nitrite reductase. OD was subsequently measured at 540 nm.

2.2.9 Measurement of TNFα

The presence of TNFα in culture medium was assessed using a 'TNFα Quantikine ELISA (enzyme linked immunosorbent assay) kit' (Xaus et al., 2000; Choi et al., 2002). Assays were performed by Ms Fleur Jones (Cell Signalling Laboratory, Department of Neuroinflammation, Institute of Neurology, UCL) in accordance with the manufacturer's instructions. In brief, cell culture supernatants (50 μl) were diluted in calibration buffer (100 μl) before being added to an ELISA plate containing assay diluent (50 μl/ well). The plate was agitated for one minute and then incubated at room temperature for 2 hours. Next, the plate was washed in four changes of wash buffer (40 μl/well), then primary TNFα antibody conjugated to HRP (100 μl/well)

was added and incubated with the samples for 2 hours at room temperature. The plate was subsequently washed in four changes of wash solution (40 µl/well) then substrate solution (100 µl/well) was incubated with the samples for a further 30 minutes. Finally, the OD was read at 450 nm with the reference filter set to 570 nm to correct for plate imperfections. The concentration of TNFα was determined against a standard curve (Fig. 2.6). Experiments were performed in triplicate on samples isolated on three independent occasions.

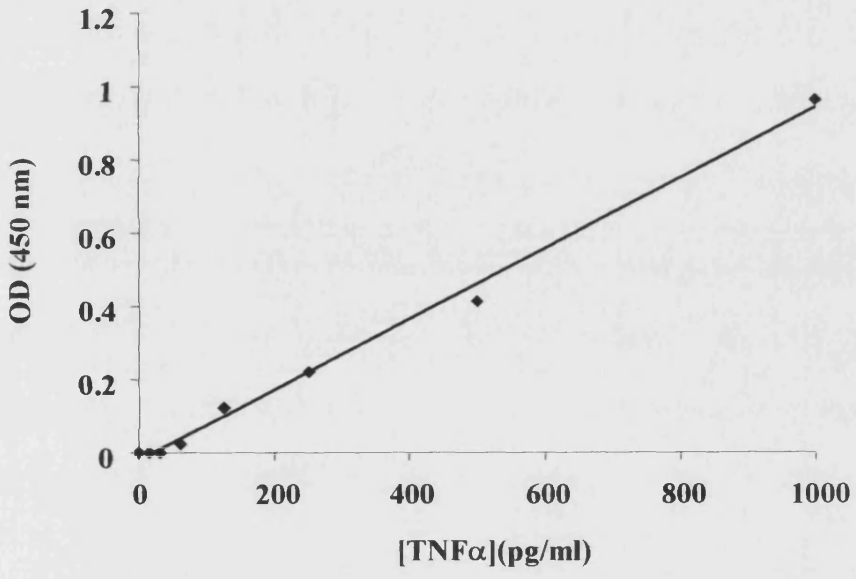

Figure 2.6 Representative standard curve of TNFα concentration against OD

TNFα standards were added to an ELISA plate and treated in accordance with the manufacturer's instructions. OD was subsequently measured at 450 nm with the reference filter set at 620 nm.

2.2.10 Measurement of TGFβ

The presence of TGFβ in culture medium was assessed using a 'TGFβ1 Emax ELISA kit' (Bruno et al., 1998). Assays were performed by Ms Fleur Jones in accordance with the manufacturer's instructions. In brief, a nunc maxi-sorp cell culture plate was coated with TGFβ monoclonal antibody (100 µl/well) overnight at 4 °C. Next the plate was washed in five changes of wash buffer (40 µl/well) then blocking reagent was incubated with the plate for a further 35 minutes at 37 °C. The plate was subsequently washed in five changes of wash buffer (40 µl/well) then cell culture supernatants (100 µl/well) were added to the plate and incubated at room temperature for 1.5 hours with shaking. Following the incubation period, the plate was washed in 5 changes of wash buffer then primary TGFβ polyclonal antibody (100 µl/well) was added and incubated with the samples for 2 hours at room temperature with shaking. Next the plate was washed in five changes of wash buffer (40 µl/well), after which TGFβ HRP conjugate (100 µl/well) was added and incubated for 2 hours at room temperature with shaking. Finally, the plate was washed in five changes of wash buffer (40 µl/well) before TMB one solution (100 µl/well) was added to the wells. The plate was then left at room temperature for 15 minutes before the reaction was terminated by the addition of hydrochloric acid (1M; 100 µl/well). The OD was read at 450 nm with the reference filter set to 620 nm to correct for plate imperfections. The concentration of TGFβ was determined against a standard curve (Fig. 2.7). Experiments were performed in triplicate on samples isolated on three independent occasions.

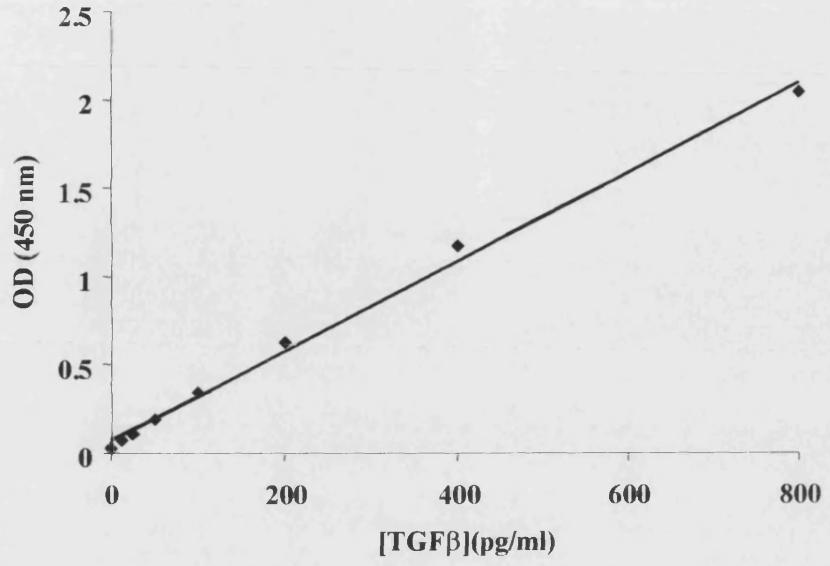

Figure 2.7 Representative standard curve of TGFβ concentration against OD

TGFβ standards were added to an ELISA plate and treated as per the manufacturer's instructions. OD was subsequently measured at a wavelength of 450 nm with the reference filter set to 570 nm.

2.2.11 Measurement of cell proliferation

Under pathological conditions microglia proliferate resulting in the production of identical daughter cells (Graeber et al., 1988c). In this thesis, proliferation was assessed by counting the number of cells present per field of view. Cells were counted on three coverslips per treatment on three independent occasions (each coverslip comprised 10 fields of view). In addition, proliferation was assessed using the 'Cell titer 96 Aq_{ueous} one solution proliferation assay kit' (Vairano et al., 2002; Wang et al., 2002). This proliferation assay is based on the reaction between NADH, which is produced by proliferating cells as a consequence of increased respiration and MTS (3-(4,5-dimethylthiazol-2-yl)-5-(3-carboxymethoxyphenyl)-2-(4-sulfophenyl)-

2H-tetrazolium). The reaction results in the formation of a coloured formazan end product that can be assessed spectrophotometrically. The amount of formazan product generated, as measured by the absorbance at 492 nm is directly proportional to the number of proliferating cells in culture. The kit was used according to the manufacturer's instructions. In brief, cell proliferation reagent (50 µl) was added to culture medium (200 µl) bathing treated and untreated primary microglia, N9 microglia or peritoneal macrophages at the appropriate time points. Cells were incubated in the presence of reagent for 4 hours at 37 °C. Samples (50 µl) were then removed from the cultures and the absorbance was read at 492 nm. Proliferation assays were performed in triplicate. Samples were collected from cells isolated on three independent occasions.

2.2.12 Fluorescence microscopy

Fluorescence microscopy was used to assess intracellular calcium fluxes, mitochondrial membrane depolarisation, cellular viability, cellular death and FITC labelled albumin uptake.

2.2.12.1 Fluorescence imaging system

Single cell fluorescence imaging was performed using an Olympus 1X70 epi-fluorescence microscope coupled to a Perkin Elmer Life Science Resources Merlin imaging system (version 1.863) unless otherwise stated (see section 2.2.12.7). Using this set up, cells loaded with a fluorescent dye were illuminated with UV light, the exact excitation wavelength obtained using a Perkin Elmer Life Science Resources SpectraMaster monochromator (Pocock and Evans 2000). UV light from the monochromator passes through a light tube to a dichroic mirror, which reflects light

through an objective lens and on to the cells. The emitted light is then channelled back to a dichroic filter, which allows light of a particular wavelength to travel to a 12 bit digital camera. The camera comprises a set of light sensitive diodes, each of which digitises the intensity of fluorescence it receives. This results in the generation of computerised images and graphical representations of the data (Fig. 2.8).

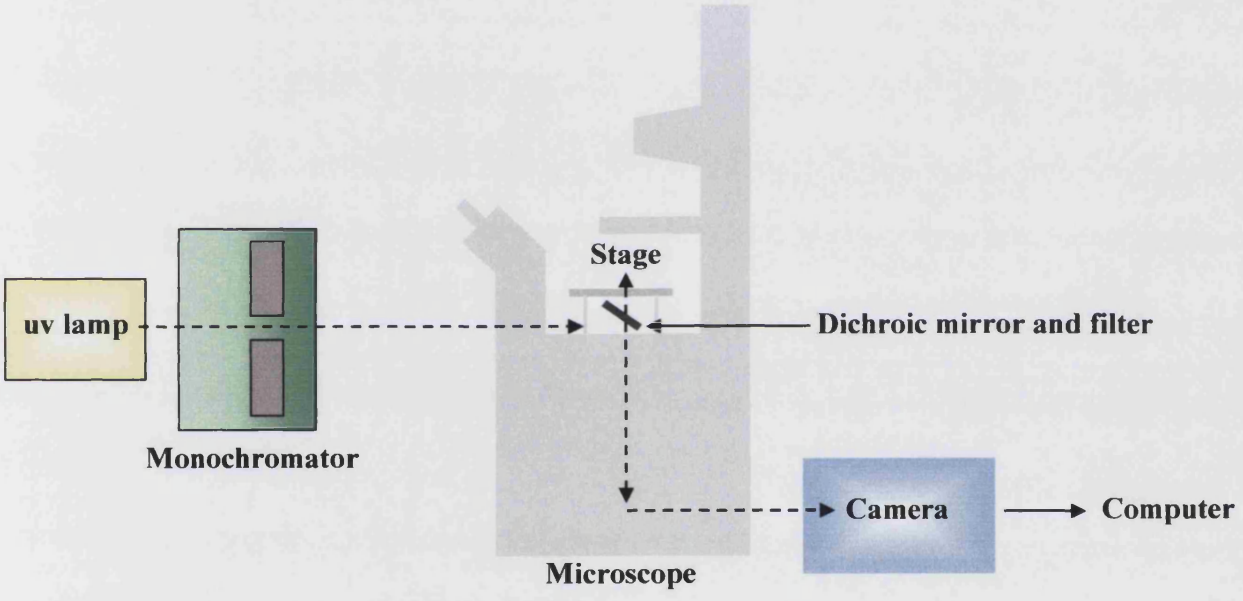

Figure 2.8 Schematic diagram of the imaging system

Cells loaded with a fluorescent dye can be illuminated with UV light, the exact excitation wavelength obtained using a monochromatic filter. UV light passes through a light tube to a dichroic mirror, which reflects light through an objective lens and on to the cells. The emitted light is channeled back to a dichroic filter, which allows light of a particular wavelength to travel to a digital camera then on to a computer.

Imaging was performed under conditions of very low ambient light to prevent dye bleaching (Pocock and Evans 2000). The major advantages of fluorescence imaging over a fluorometer are that recording can be made from individual cells. Recordings can also be made from specific cell types allowing elimination of data from contaminating cells. Furthermore, imaging allows recordings to be made from many cells simultaneously; therefore it is possible to determine the homogeneity of a response (Pocock and Evans 2000).

2.2.12.2 Introduction to calcium imaging

A number of fluorescent dyes are available which can be used to appraise calcium ion fluxes at the sub-cellular level (reviewed by Tsien 1988; Hallet et al., 1999; Pocock and Evans 2000). These dyes are sub-classified into single or dual wavelength (ratiometric) dyes based on their fluorescent properties. Single wavelength dyes are excited by a single wavelength and emit at a single wavelength. Examples of single wavelength dyes include quin-2, calcium green and fluo 3. In contrast, dual wavelength calcium indicators use two excitation or emission wavelengths. This enables a ratio of the shift in excitation or emission intensity to be calculated, which is proportional to the calcium concentration within the cell. Frequently used dual wavelength dyes include fura-2 and indo-1. A number of advantages are associated with the use of dual wavelength dyes. For example, artifactual changes in fluorescence generally only affect one of the excitation or emission wavelengths and are therefore easily detectable, the concentration of the dye is not critical and calibration of the system is possible, thus calcium concentrations can be easily determined.

In this study the ratiometric fluorescent probe fura-2 (AM modified) was used to perform single cell calcium imaging. Fura-2 contains a ligand binding moiety which is based on the calcium chelator EGTA, therefore this dye displays a very high affinity for calcium over it's most fierce competitor magnesium. In the acetoxymethyl ester (AM) form, fura-2 readily penetrates cell membranes, rendering redundant the need for micro-injection which can be detrimental to cell survival and time consuming. Once inside the cell fura-2 is de-esterified by endogenous esterases, which consequently prevents the dye leaching back out across the cell membrane.

In the absence of calcium, fura-2 exhibits an excitation maxima of 380 nm. The excitation maxima shifts in the presence of calcium from 380 nm to 340 nm (Fig 2.9). In contrast, the emission peak is 510 nm in the presence or absence of calcium. Therefore, it is the intensity of the emissions elicited by excitation at both 380 and 340 nm that is used to calculate the ratio. The intensity of the emission after illumination at 340 nm is divided by the intensity of fluorescence resulting from illumination at 380 nm. The value of this ratio is dependent on the concentration of free calcium in the cell. A high ratio indicates that there is a high concentration of calcium within the cell, whereas a low ratio is indicative of low calcium.

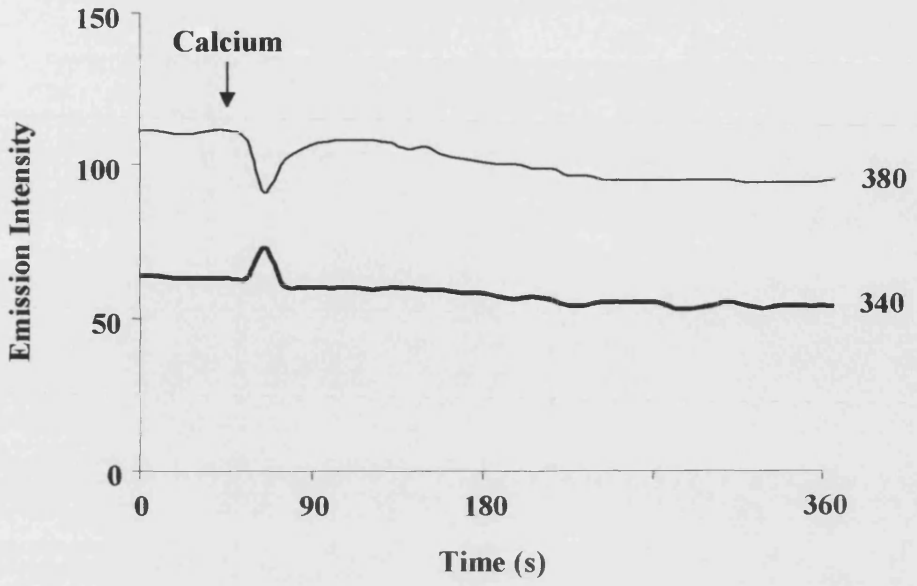

Figure 2.9 Emission profile of fura-2 in the presence of calcium

In the presence of calcium the excitation maxima of fura-2 shifts from 380 nm to 340 nm.

2.2.12.2.1 Assessment of intracellular calcium fluxes

Changes in intracellular calcium were assessed using the fluorescent probe fura-2 (Pocock et al., 1998; Mőller et al., 2001). Cells on coverslips were loaded with fura-2 (5 μM) in the presence of pluronic acid (0.02 %) for 45 minutes at 37 °C in the dark. Coverslips were then inserted into a thermostatically controlled holder set to 37 °C and basic medium was added (150 μl). The dye was subsequently excited at 340 nm and 380 nm and emission greater than 510 nm was collected. Compounds diluted in basic medium (50 μl) were added directly to the cells whilst a continual sequence of images was recorded. Data from a minimum of 10 cells per field of view was analysed and values were expressed as 340/380 nm fluorescence ratios. Experiments were performed in triplicate therefore the results shown are representative of a single experiment.

2.2.12.3 Assessment of mitochondrial membrane polarisation

Mitochondrial depolarisation was assessed using 5,5'6,6'-tetraethylbenzimidazole carbo-cyanine iodide (JC-1), a fluorescent dye which is sensitive to changes in mitochondrial membrane potential (Kingham and Pocock 2000). Cells on coverslips were incubated with basic medium containing JC-1 (5 μM) for 10 minutes at 37 °C in the dark. Coverslips were then inserted into a thermostatically controlled holder set to 37 °C and basic medium was added (150 μl). Mitochondrial polarisation was subsequently assessed at 490 nm with emission greater than 520 nm collected. In cells possessing polarised mitochondria, JC-1 exists in the aggregated form, which emits at 585 nm and appears as punctate red/orange mitochondrial staining on a green cytoplasmic surround. In cells possessing depolarised mitochondria, JC-1 exists in the monomeric form, which emits at 527 nm and appears as green mitochondrial staining indistinguishable from the green cytoplasm (Salvoli et al., 1997). Cells possessing depolarised mitochondria were counted on three coverslips per treatment on three independent occasions (each coverslip comprising 10 fields of view). Microglia exhibiting depolarised mitochondria were expressed as a percentage of the total number of cells counted per field.

2.2.12.4 Assessment of cell membrane integrity

Cell membrane integrity was assessed using the fluorescent dyes fluoroscein diacetate and propidium iodide (Jones and Senft 1985; Kingham et al., 1999). Cells on coverslips were incubated with basic medium containing fluoroscein diacetate (15 μg/ml) and propidium iodide (5 μg/ml) for 10 minutes at 37 °C in the dark. Cell viability was subsequently assessed at 380 nm with emission greater than 505 nm collected. Fluoroscein diacetate is metabolised in healthy cells to form a fluorescent

product, which emits at 530 nm, staining live cells green. Propidium iodide, however, penetrates dead cells possessing compromised plasma membranes where it intercalates between the bases of DNA and emits at 600 nm appearing red. Live and dead cells fluorescing green or red respectively were counted on three coverslips per treatment on three independent occasions (each coverslip comprised 10 fields of view). Dead cells were expressed as a percentage of the total number of cells counted per field.

2.2.12.5 Assessment of apoptosis

Apoptosis was assessed using the fluorescent dye 2'[epoxyphenyl]-5-[4-methyl-1-piperazinyl]-2,5'-bi-1H-benzimidazol (Hoechst 33342) (Rivera et al., 1998; Kingham et al., 1999). Hoechst 33342 binds to the minor groove of DNA with a preference for AT sequences (Portugal and Waring 1988). Cells on coverslips were fixed in formaldehyde (4 %) in phosphate buffered saline at 4 °C, then incubated with Hoechst 33342 (17.8 μM) for 10 minutes at 20 °C in the dark. Nuclear morphology was subsequently appraised at 365 nm with emission greater than 490 nm collected. Following staining, apoptotic cells possess brightly stained pyknotic nuclei, whereas, non apoptotic cells possess large weakly stained nuclei. Apoptotic cells were counted on three coverslips per treatment on three independent occasions (each coverslip comprised 10 fields of view). Apoptotic cells were expressed as a percentage of the total number of cells counted per field.

2.2.12.6 Assessment of apoptosis and necrosis

Hoescht 33342 and propidium iodide staining was used to distinguish necrotic and apoptotic cells (Thuret et al., 2003). Cells on coverslips were incubated with basic medium containing Hoescht 33342 (17.8 μM) and propidium iodide (5 μg/ml) for 10 minutes at 37 °C in the dark. Cell viability was subsequently assessed at 380 nm with emission greater than 505 nm collected. Apoptotic cells were counted as those cells possessing brightly stained pyknotic nuclei as demonstrated by Hoescht 33342 staining. Late apoptotic cells also stained with propidium iodide in addition to exhibiting pyknotic nuclei. Necrotic cells were counted as those cells possessing propidium iodide staining accompanied with large unstained nuclei as demonstrated by Hoescht 33342. Healthy cells were counted as cells possessing large unstained nuclei as demonstrated by Hoescht 33342 with no propidium iodide staining. Cells were counted on three coverslips per treatment on three independent occasions (each coverslip comprised 10 fields of view). Apoptotic and necrotic cells were expressed as a percentage of the total number of cells counted per field.

2.2.12.7 FITC albumin uptake

Microglia or peritoneal macrophages were incubated with FITC labelled albumin (0.5 mg/ml) in SFM for 1 hour at either 37 °C or 4 °C (Tabernero et al., 2002a, b). Cells were then washed in three changes of PBS and examined with a Zeiss epi-fluorescence microscope coupled to an Axiovision imaging system (version 3.1). Phase contrast and fluorescent images of the cells were immediately photographed with an exposure time of 30 seconds.

2.2.13 Statistical analysis

To compare a single treatment with a control group, a two sided, unpaired T-test was used. Comparison of two or more treatments with a control group (or other treatment) was made using a one way analysis of variance (ANOVA) in combination with the Tukey post test. P values < 0.05 were considered statistically significant.

3.0 Characterisation of primary cultures

3.1 Introduction

3.1.1 Preparation of microglial cultures

Microglia can be isolated from the brain using percoll density gradients (Havenith et al., 1998; Kingham and Pocock 2000); alternatively microglia can be harvested based on their differential adhesive properties by agitating mixed glial cultures after 7-12 days *in vitro* (Nolte et al., 1996; McDonald et al., 1997; Möller et al., 2000a, b; Casal et al., 2002). In this thesis microglia were prepared using percoll gradients because this method yields extremely pure microglial cultures (Kingham et al., 1999; Kingham and Pocock 2000). Furthermore, the microglia are less activated since they are in culture for very short periods of time (Slepko and Levi 1996).

3.1.2 Identification of microglia

Microglial identification has been hampered due to the lack of microglial specific antigens; all antibodies used for the detection of microglia are raised against macrophage specific antigens. However, recent advances in microglial identification have been achieved using FACS. Using this approach ramified parenchymal microglia have been demonstrated to possess the phenotype $CD11b^{+}CD45^{low}$, whilst other CNS macrophages and peripheral macrophages exhibit the phenotype $CD11b^{+}CD45^{high}$ (Ford et al., 1995; Becher and Antel 1996). A number of other techniques are available for the identification of microglia, although these procedures fail to distinguish microglia from macrophages (due to the lack of microglial specific markers). Thus, it is not surprising that these techniques preferentially label reactive and amoeboid microglia, which are more akin to active macrophages than ramified microglia. Nevertheless, ramified microglia can be detected using monoclonal antibodies raised against macrophage specific antigens. OX-42 (Graeber et al., 1989) and MAC-1 (Perry et al., 1985) recognise the CR3 complement receptor (CD11b/CD18) in rat and murine microglia respectively. The 2.4G2 antibody

recognises the Fc receptor and F4/80 binds an unknown antigen on murine ramified microglia (Perry et al., 1985). Alternatively, ED-1 an antibody that recognises a lysosomal protein can be used to stain microglia (Graeber et al., 1990; Slepko and Levi 1996). High levels of ED-1 expression are associated with activated microglia whilst low levels of expression are associated with quiescent ramified microglia (Graeber et al., 1990; Slepko and Levi 1996). Furthermore, identification of ramified microglia can be achieved using Rio Hortega's original silver staining technique, phosphatase staining or lectin binding. Lectins are carbohydrate binding proteins that selectively label microglia through the recognition of d-galactose. Commonly used lectins include B4 isolectin (Murabe and Sano 1981a), mistletoe lectin (Streit and Kreutzberg 1987) and agglutinin-120 (Suzuki et al., 1988).

Techniques are also available for the identification of reactive and amoeboid microglia, however these procedures do not stain ramified microglia. Such procedures include staining for non-specific esterases (Murabe and Sano 1981b; Giulian and Baker 1986) or the intermediate filament vimentin (Graeber et al., 1988a). Alternatively, fluorescently labelled acetylated low-density lipoprotein (LDL) can be used which selectively labels LDL receptors expressed by reactive microglia (Giulian and Baker 1986).

3.1.3 Preparation of cerebellar granule cells

Cerebellar granule neurones constitute approximately 94 % of the cells in the human (Anderson et al., 1992) and rat (Korbo et al., 1993) cerebellum; therefore it is easy to prepare pure cultures of granule neurones from the undifferentiated cerebellum without contamination from other neuronal cell types (Gallo et al., 1982; Pearce et al., 1987). Furthermore, contamination by glia can be minimised by supplementing the culture

medium with the mitotic inhibitor cytosine arabinofuranoside (Gallo et al., 1982; Xu and Chuang 1987).

3.1.4 Identification of cerebellar granule cells

At present there are no known cerebellar granule neurone specific markers, therefore in this thesis granule cells were identified according to morphological criteria. Following plating cerebellar granule cells appear rounded, however after 7 days *in vitro* granule cell somas form clusters and extend cable like neurites. It is interesting to note that 7 day old cerebellar granule neurones exhibit other features of mature neurones including expression of glutamatergic (Pearce et al., 1987; Aronica et al., 1993; Archibald et al., 1998; Pocock and Nicholls 1998), serotinergic, adrenergic and histaminergic receptors (Xu and Chuang 1987). Moreover, mature granule neurones express voltage dependent calcium channels (Pocock et al., 1995) and display synaptic connectivity (Xu and Chuang 1987). Since cultured granule cells lack afferent mossy fiber input they require depolarising conditions for survival (Gallo et al., 1987). This was achieved *in vitro* by supplementing the medium with potassium chloride (20-40 mM).

3.1.5 Summary of results

Primary microglial cultures isolated by percoll density gradient were rich in resting microglia as determined by OX42, CD45 and ED-1 staining. Microglia exhibited low granularity reflecting a down-regulated phenotype and cultures did not contain any contaminating astrocytes. Peritoneal macrophage cultures were also found to be extremely pure, although these cells were more activated than microglia. Furthermore, staining revealed that cerebellar granule cell cultures exhibited minimal contamination from glia.

3.2 Immunological profiling of the microglial cultures

The purity of microglial cultures was assessed by immunocytochemistry using a number of monoclonal antibodies. Microglia were stained with OX-42, which recognises the CR3 complement receptor (CD11b/CD18) (Graeber et al., 1989) and ED-1 an antibody that recognises a lysosmal protein (Graeber et al., 1990; Slepko and Levi 1996). Furthermore, the presence of astrocytes in the microglial cultures was assessed by staining for glial fibrillary acidic protein (GFAP), which is an astrocytic marker (Eliasson et al., 1999). Macrophages isolated from the peritoneal cavity of adult (> 6 months) rats were also stained with OX-42 and ED-1 to check for purity.

Immunocytochemistry revealed that the vast majority of microglia and macrophages exhibited CR3 (CD11b) reactivity as demonstrated by OX-42 staining (Fig. 3.1A,B). Approximately half of the microglial cells in the cultures expressed ED-1, whereas the majority of macrophages expressed this lysosomal antigen. Furthermore, microglial cultures did not contain any GFAP positive astrocytes. Control cultures that were not exposed to primary antibody did not exhibit any positively stained cells, which demonstrates that the staining is specific. Taken together, these results suggest that the microglial and macrophage cultures are extremely pure.

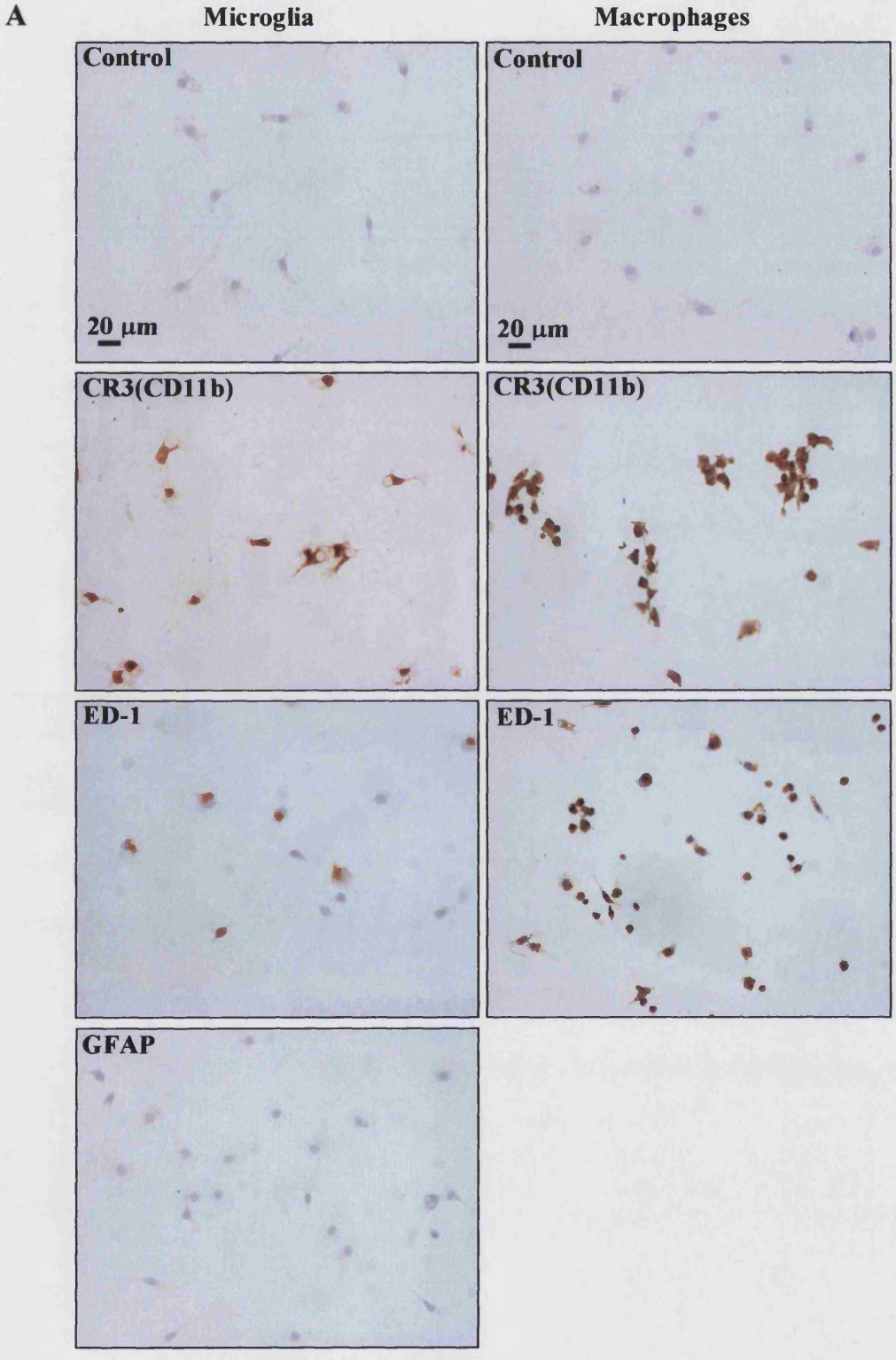

Figure 3.1 (see overleaf for figure legend)

B

	% Immunoreactivity		
	CR3 (CD11b)	**ED-1**	**GFAP**
Microglia	99 ± 1.4	55.2 ± 6.2	0
Macrophages	96.5 ±4.6	95.7 ± 5.6	N/A

Figure 3.1 Immunological profile of microglial and peritoneal macrophage cultures

A: Microglia and peritoneal macrophages (isolated from adult rats) were stained with antibodies recognizing CR3(CD11b) (OX-42), ED-1 or GFAP after 24 hours in culture. Primary antibodies were detected using anti-mouse IgG secondary antibody conjugated to biotin. The staining was subsequently visualized by incubating the cells with a pre-formed avidin-biotin horseradish peroxidase (HRP) complex for 1 hour at room temperature, followed by treatment with DAB. Cells were counterstained with haematoxylin to provide an estimation of total cell number. Control cells were processed omitting the incubation with primary antibody. **B**: The values represent the mean number of positively stained cells present per field of view ± sem.

A number of disadvantages are associated with immunocytochemical staining. Firstly, it cannot be used to quantify levels of receptor expression and secondly it cannot be used to distinguish microglia from other CNS macrophages (or peripheral macrophages) due to the lack of microglial specific antigens. Recent advances in microglial identification have been made using FACS. This technique enables quantification of receptor expression through the measurement of fluorescent staining intensity. Therefore, using FACS ramified parenchymal microglia have been demonstrated to possess the phenotype $CD11b^{+}CD45^{low}$. In contrast, peripheral macrophages and CNS macrophages found in the meninges, the subarachnoid space, the choroid plexus or in a perivascular location possess the phenotype $CD11b^{+}CD45^{high}$ (Ford et al., 1995; Becher and Antel 1996). The immunological profile of the microglial cells was subsequently assessed according to these parameters. In this way, the presence of other CNS macrophages in the microglial cultures could be appraised. Microglia were also stained with ED-1 to further characterise the activational state of the cells and to complement immunocytochemical data. Macrophages isolated from the peritoneal cavity of neonatal (3-6 day old) or adult (> 6 months) rats were used as positive controls, the former providing aged matched equivalents to the microglia.

FACS analyses revealed that most microglia (80.4 %) and macrophages isolated from neonatal (98.1 %) or adult (95.8 %) rats expressed CD11b (Fig 3.2). Macrophages derived from neonatal rats exhibited a mean fluorescence intensity (MFI) which was twice as great as the microglial value, whereas macrophages isolated from adult rats possessed a MFI that was approximately 19 times as great. Therefore, macrophages derived from neonatal rats express less CD11b than their adult counterparts; however, in general macrophages express considerably more CD11b than microglia.

Only a small proportion of microglia (21.8 %) displayed CD45 reactivity, which is consistent with the report published by Ford et al., (1995) (Fig. 3.3). In contrast, the majority of macrophages isolated from neonatal (98.1 %) or adult (93.9 %) rats expressed CD45. Macrophages derived from neonatal tissue exhibited a MFI that was twice as great as the microglial value, whilst macrophages isolated from adult tissue possessed a MFI that was about 21 times as great. Thus, macrophages isolated from neonatal rats express less CD45 than macrophages derived from adult rats, although macrophages *per se* express higher levels of CD45 than microglia.

A fairly large number of microglia were shown to express ED-1 (63.6 %), albeit at extremely low levels (Fig. 3.4). Furthermore, most macrophages isolated from neonatal (98.9 %) or adult (99.4 %) rats expressed ED-1. Macrophages isolated from either age rat exhibited similar MFIs and these values were approximately 14 fold higher than the MFI obtained with microglia. This indicates that macrophages generally express much more ED-1 than microglia.

The forward scatter (FSC) and side scatter (SSC) of 'aged matched' microglia and peritoneal macrophages (isolated from 3-6 day old rat pups) were subsequently compared. FSC reflects the size of a cell, whilst SSC provides a measure of intracellular granularity. FACS analysis revealed that microglia and peritoneal macrophages are comparable in size, but microglia are considerably less granular (Fig. 3.5).

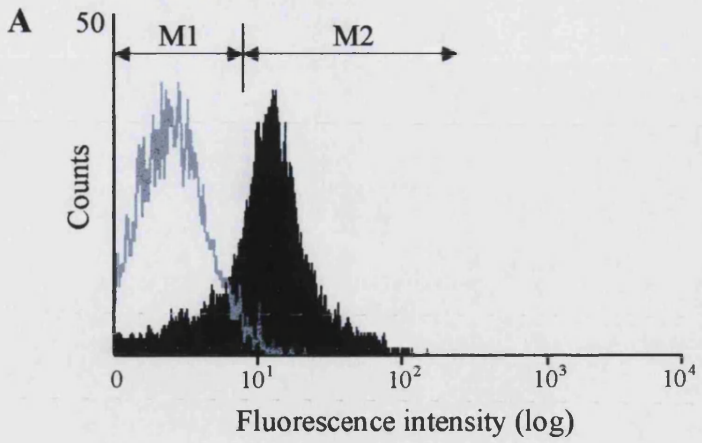

	%	MFI
M1 unlabelled	96.3	2.4
M2 labelled	80.4	19.8

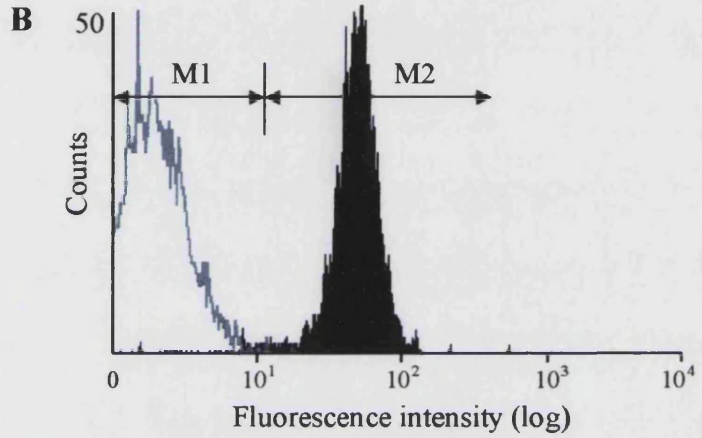

	%	MFI
M1 unlabelled	99.4	2.0
M2 labelled	98.1	40.6

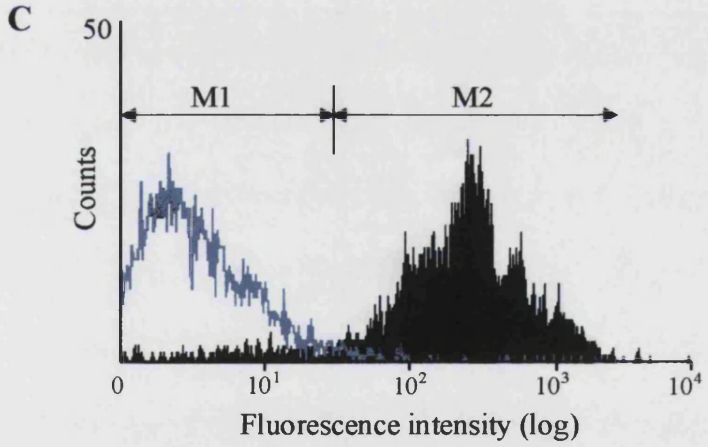

	%	MFI
M1 unlabelled	97.9	3.6
M2 labelled	95.8	372

Figure 3.2 Expression of CD11b by microglia and peritoneal macrophages

Representative FACS plots of CD11b expression. Microglia and peritoneal macrophages were isolated and left in culture for 24 hours. The cells were subsequently harvested, fixed then analysed by flow cytometry. **A**: Expression of CD11b by microglia isolated from 3-6 day old rats. **B**: Expression of CD11b by peritoneal macrophages isolated from 3-6 day old rats. **C**: Expression of CD11b by peritoneal macrophages isolated from adult rats. The CD11b labelled cells are represented by the black shaded populations, whereas the unlabelled cells are depicted by the grey line (%: % of cells in M1 or M2 region, MFI: mean fluorescence intensity).

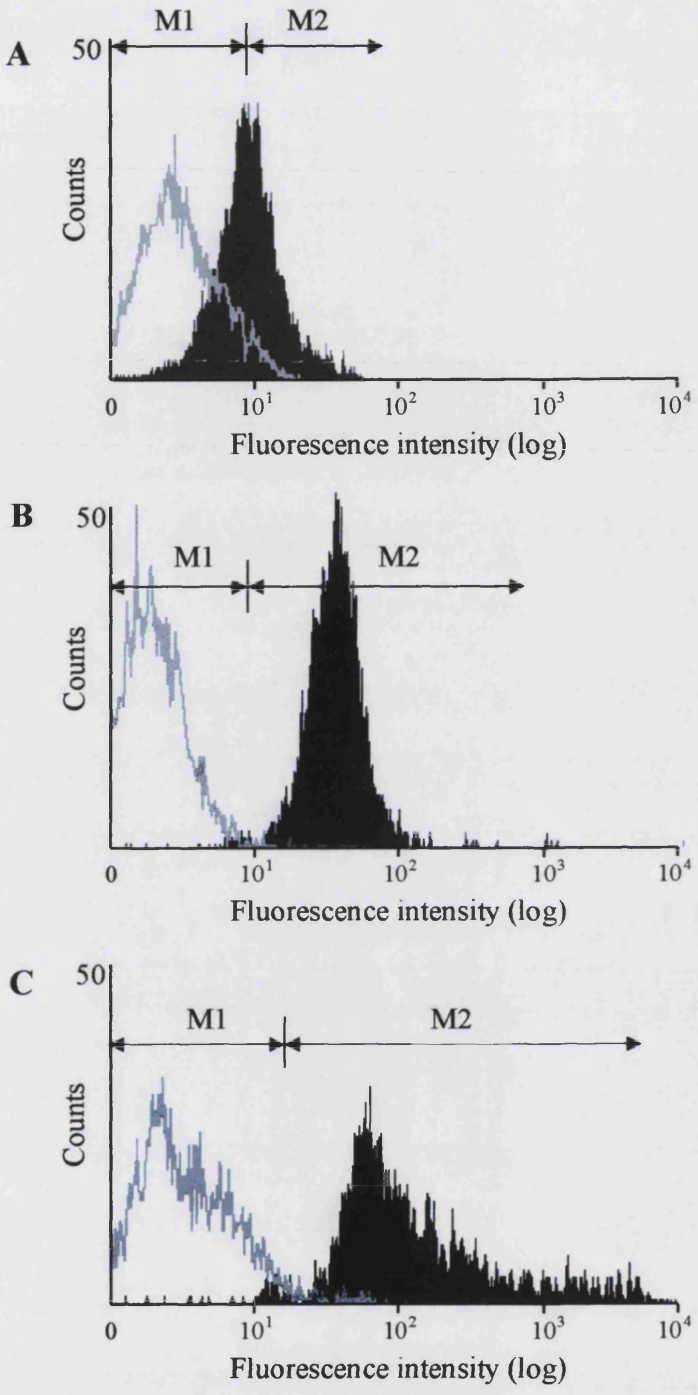

	%	MFI
M1 unlabelled	97.6	3.6
M2 labelled	21.8	26.9

	%	MFI
M1 unlabelled	99.4	2.1
M2 labelled	98.1	50.7

	%	MFI
M1 unlabelled	92	4.59
M2 labelled	93.9	570

Figure 3.3 Expression of CD45 by microglia and peritoneal macrophages

Representative FACS plots of CD45 expression. Microglia and peritoneal macrophages were isolated and left in culture for 24 hours. The cells were subsequently harvested, fixed then analysed by flow cytometry. **A**: Expression of CD45 by microglia isolated from 3-6 day old rats. **B**: Expression of CD45 by peritoneal macrophages isolated from 3-6 day old rats. **C**: Expression of CD45 by peritoneal macrophages isolated from adult rats. The CD45 labelled cells are represented by the black shaded populations, whereas the unlabelled cells are depicted by the grey line (%: % of cells in M1 or M2 region, MFI: mean fluorescence intensity).

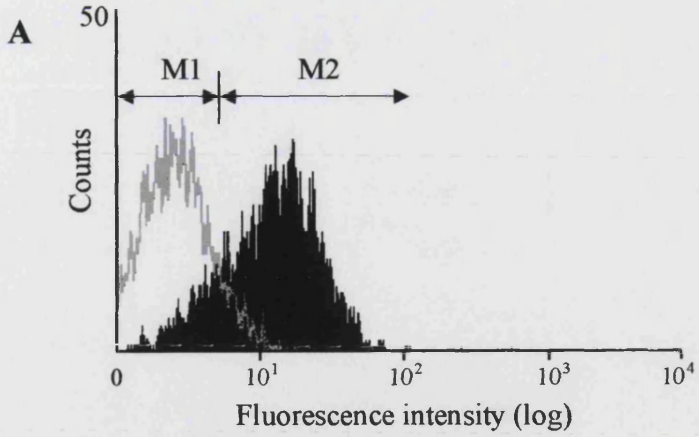

	%	MFI
M1 unlabelled	99.4	2.87
M2 labeled	63.6	20.8

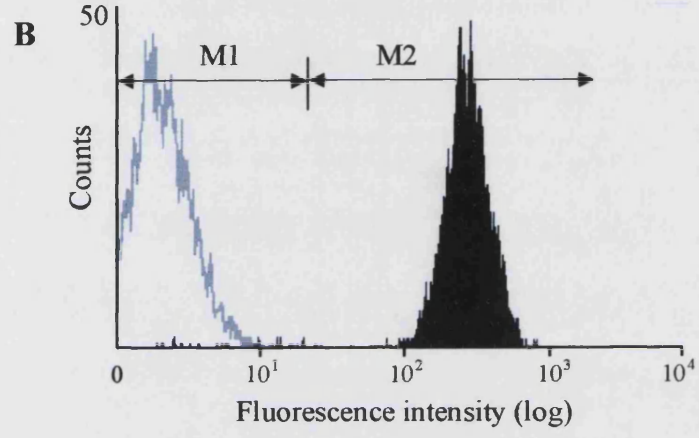

	%	MFI
M1 unlabelled	99.9	2.35
M2 labelled	98.9	288

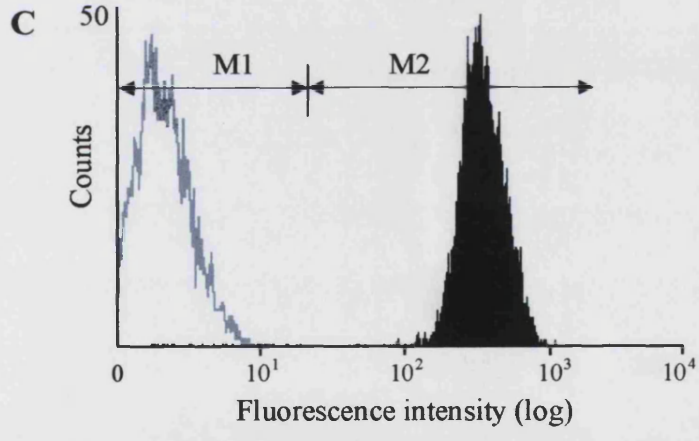

	%	MFI
M1 unlabelled	99.9	2.35
M2 labelled	99.4	365

Figure 3.4 Expression of ED-1 by microglia and peritoneal macrophages

Representative FACS plots of ED-1 expression. Microglia and peritoneal macrophages were isolated and left in culture for 24 hours. The cells were subsequently harvested, fixed then analysed by flow cytometry. **A**: Expression of ED-1 by microglia isolated form 3-6 day old rats. **B**: Expression of ED-1 by peritoneal macrophages isolated from 3-6 day old rats. **C**: Expression of ED-1 by peritoneal macrophages isolated from adult rats. The ED-1 labelled cells are represented by the black shaded populations, whereas the unlabelled cells are depicted by the grey line (%: % of cells in M1 or M2 region, MFI: mean fluorescence intensity).

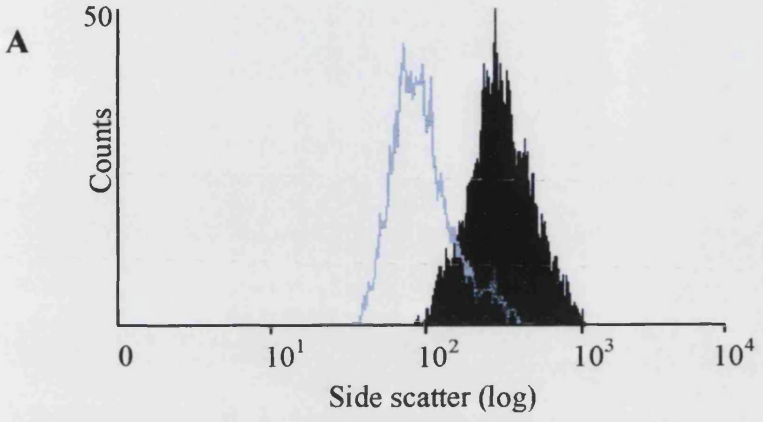

	Mean SSC
microglia	101.3
macrophage	315.7

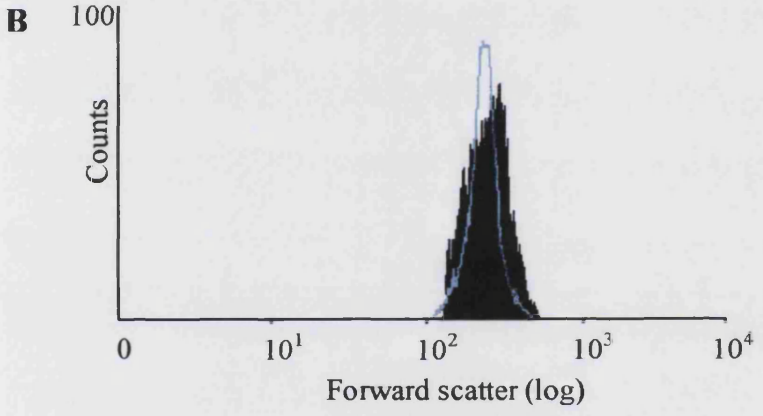

	Mean FSC
microglia	230.5
macrophage	248.2

Figure 3.5 Size and granularity of microglia and peritoneal macrophages

Representative FACS plots of size and granularity of microglia and macrophages. Microglia and peritoneal macrophages were isolated from 3-6 day old rats and left in culture for 24 hours. The cells were subsequently harvested, fixed then analysed by flow cytometry. **A**: Comparison of microglial and peritoneal macrophage side scatter (SSC) as an indication of intracellular granularity. **B**: Comparison of microglial and peritoneal macrophage forward scatter (FSC) as a measure of cell size. The microglial cell population is represented by the grey line, whereas the peritoneal macrophage population is depicted by the black shaded population.

3.3 Assessment of cerebellar granule neurone preparation purity

The presence of contaminating microglia and astrocytes in the cerebellar granule neuronal cultures was assessed by immunocytochemistry. Microglia and astrocytes were stained with antibodies recognizing CR3/CD11b (OX-42) and GFAP respectively, whilst neurones were identified according to morphological criteria. Immunocytochemistry revealed that cerebellar granule neuronal cultures contained very few microglia and astrocytes (Fig. 3.6A,B). Moreover, control cultures that were not exposed to primary antibody did not exhibit any positively stained cells, which demonstrates that the staining is specific. These findings indicate that the cerebellar granule neuronal cultures are extremely pure.

A

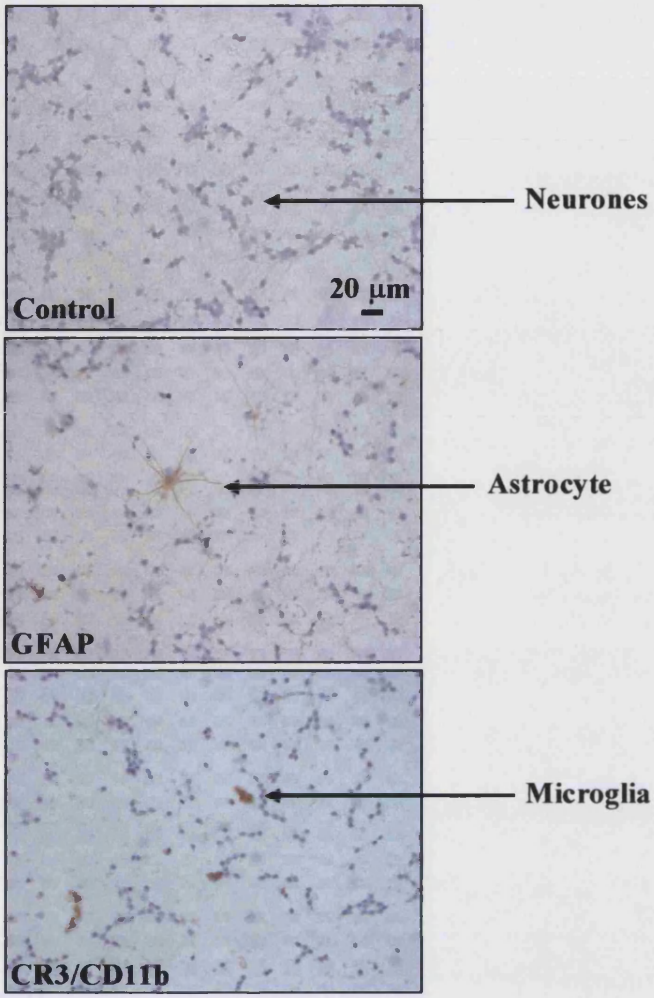

B

	% of total
Neurones	95.5 ± 0.02
Microglia (CR3/CD11b)	3.1 ± 0.02
Astrocytes (GFAP)	1.4 ± 0.01

Figure 3.6 Purity of cerebellar granule neurone cultures

A: Cultures of cerebellar granule neurones were stained with antibodies recognizing CR3/CD11b or GFAP after 7 days in culture to identify microglia and astrocytes respectively. Primary antibodies were detected using anti-mouse IgG secondary antibody conjugated to biotin. The staining was subsequently visualized by incubating the cells with a pre-formed avidin-biotin horseradish peroxidase (HRP) complex for 1 hour at room temperature, followed by treatment with DAB. Cells were counterstained with haematoxylin to provide an estimation of total cell number and neurones were identified according to morphological criteria. Control cultures were processed omitting the incubation with primary antibody. **B**: The values represent the mean number of cells present per field of view ± sem

3.4 Discussion

Microglial, peritoneal macrophage and cerebellar granule neurone cultures were found to be almost entirely pure. Therefore, the results presented in this thesis can be interpreted with confidence, since the responses are likely to reflect a true representation of each cell type.

3.4.1 Microglial cultures

Microglial cultures were demonstrated to comprise of parenchymal microglia as demonstrated by FACS. Using this technique parenchymal microglia can be identified because these cells exhibit the phenotype $CD11b^{+}CD45^{low}$, whereas other CNS macrophages and peripheral macrophages exhibit the phenotype $CD11b^{+}CD45^{high}$ (Ford et al, 1995). This is useful to note since each distinct population of macrophages in the brain (supraependymal cells, epiplexus cells, subarachnoid/ leptomeningeal macrophages, perivascular macrophages or microglia) exhibit different morphological characteristics and perform different functions (Jordon and Thomas 1988; Streit 2002).

CD45 also known as leucocyte common antigen was identified as the first and prototypical transmembrane protein tyrosine phosphatase (Sasaki et al., 2001). Cell signalling depends on the subtle balance between tyrosine kinases and tyrosine phosphatases, which in concert control phosphorylation and dephosphorylation events (Berg et al., 2002). CD45 is expressed by all nucleated haematopoieic cells except erythrocytes and platelets. CD45 is a critical positive regulator of T and B cell receptor mediated signalling, which is required for the activation of lymphocytes (Sasaki et al., 2001). The main role described for CD45 in macrophages is the regulation of integrin mediated adhesion (Roach et al., 1997). Therefore, the finding that microglia express less CD45 than macrophages probably reflects the down-regulated phenotype of microglia.

Likewise, microglia were demonstrated to express less CD11b and ED-1 than macrophages. CD11b is part of CR3 complement receptor (CD11b/CD18), which is involved in phagocytosis (Dana et al., 1991; Ueda et al., 1994), cell adhesion and chemotaxis (Dana et al., 1991), whilst ED-1 binds an unknown lysosomal antigen, which is also involved in phagocytosis (Damoiseaux et al., 1994). Thus, the finding that microglia express low levels of CD11b and ED-1 substantiates the notion that microglia exhibit a quiescent down-regulated phenotype and is in accord with previous findings (Kingham et al., 1999). Interestingly, macrophages isolated from neonates express less CD11b and CD45 than macrophages isolated from adults. This might be because macrophages isolated from adult rats have been exposed to more antigen and are consequently more activated.

Analysis of side scatter demonstrated that microglia were less granular than macrophages. Granularity provides a measure of intracellular inclusions such as phagosomes and endosomes and therefore provides further evidence that microglia are less activated than macrophages. In summary, these findings illustrate that microglial cultures mainly comprise of resting parenchymal microglia with no contamination from astrocytes or other CNS macrophages. In addition, experimental data revealed that peritoneal macrophage cultures are extremely pure.

3.4.2 Cerebellar granule neuronal cultures

Immunocytochemical staining demonstrated that cerebellar granule cell cultures contain minimal contamination form microglia and astrocytes. Given that the cerebellum comprises mainly of granule cells (Anderson et al., 1992; Korbo et al., 1993) it is likely that these cells represent the majority of the neuronal population in the cultures. Contamination by glia was minimized by adding Ara C to the culture medium. Ara C is a

drug used in the treatment of cancer; it is an analogue of the naturally occurring nucleoside 2'deoxycytidine and is therefore incorporated into DNA to a limited extent, but it's main cytotoxic action is the inhibition of DNA polymerase (Rang et al., 1999). Under normal culture conditions neurones do not divide, therefore Ara C preferentially inhibits glial DNA synthesis because these cells retain the propensity to replicate. Consequently, glial proliferation is prevented and the cultures are neurone rich, which in accord with previous findings (Kingham et al., 1999).

3.4.3 Conclusion

Results presented in this chapter exemplify that the methods used in this thesis enable the preparation of pure microglial, macrophage and cerebellar granule cell cultures. Thus, these primary cultures provide a robust model for studying cell signalling and microglial-neuronal interactions. Moreover, microglia were demonstrated to exhibit a down-regulated phenotype, thereby providing a large window for activation.

4.0 Investigation of microglial signalling elicited by albumin

4.1 Introduction

This chapter explores the signalling cascades elicited in microglia following treatment with albumin. The effects of albumin were studied because this plasma protein has been implicated in stroke (Hornig et al., 1983), AD (Alafuzoff et al., 1983; Skoog et al., 1998) and multiple sclerosis (Gay and Esiri 1991) in cases where BBB damage is evident. The effects of albumin on peritoneal macrophages were also investigated, the rationale being that macrophages are accustomed to high concentrations of albumin, whilst microglia are subjected to much lower levels of this protein. The concentration of albumin in the blood ranges from 35-50 mg/ml (Diem 1962; reviewed by Nadal et al., 2001), whilst the concentration in peritoneal fluid ranges from 12.5-25 mg/ml (Kelton et al., 1978; Barber et al., 1990). In contrast, the concentration of albumin in the CSF is considerably lower and ranges from 35-50 μg/ml (reviewed by Nadal et al., 2001).

4.1.1 Physiological roles of albumin

Albumin is a 66 kDa protein that constitutes approximately 50 % of all plasma proteins (reviewed by Nadal et al., 2001). Albumin exhibits a globular shape and at physiological pH, its surface is covered by a number of charged groups accounting for its water solubility. An important function of albumin is to bind fatty acids and thereby make them more soluble in aqueous solutions such as plasma (reviewed by Nadal et al., 2001). Each albumin molecule possesses 3 primary, 3 secondary and 63 tertiary fatty acid binding sites (Spector et al., 1969). Albumin binds almost all fatty acids released into the blood from adipose cells including palmitic acid, oleic acid, linoleic acid and steric acid. The form of albumin that comprises attached fatty acids is known as fraction V, owing to the separation method by which it is extracted. Fraction V can be further sub-divided into serum and plasma albumin, which are derived from coagulated or un-coagulated blood respectively (reviewed by Nadal et al., 2001). Consequently, serum albumin comprises

bound coagulation factors such as lysophosphatidic acid (LPA), which is a phospholipid that is released from platelets during coagulation (reviewed by Nadal et al., 2001). Other physiological roles of albumin include the maintenance of blood pressure and the buffering of blood pH (Sherwood 1993).

4.1.2 Effects of albumin on 'brain' cells

Recently, a group from Japan have demonstrated that serum, plasma and fatty acid free albumin potentiate phorbal myristate acetate (PMA) induced superoxide production in microglia (Si et al., 1997). The same group have identified the active sequence of albumin to be a 12mer that is located near the N-terminus on the outer surface of the protein (Nakamura et al., 2000). In astrocytes, plasma and serum albumin (fraction V) evoke calcium waves and a calcium-dependent proliferative response (Nadal et al., 1995; 1997). However, these effects are due to the presence of an unidentified polar lipid that is normally bound to both the plasma and serum forms of albumin (fraction V). This lipid is unlikely to be the calcium mobilizing phospholipid LPA (Möller et al., 2001) since plasma and serum albumin (fraction V) are equi-potent (Nadal et al., 1995). Nevertheless, the protein component of albumin irrespective of the presence of attached lipids promotes the uptake of calcium into intracellular stores (Nadal et al., 1996). From a functional point of view, this may serve to potentiate the effects of calcium mobilizing agonists such as glutamate and bradykinin.

Other studies have shown that essentially fatty acid free albumin stimulates the synthesis of oleic acid (a fatty acid) from glucose and lactate through a mechanism involving the transcription factor SREBP-1 (Tabernero et al., 2002a). Astrocyte derived oleic acid subsequently induces neuronal phospholipid synthesis, which in turn promotes axonal growth (Tabernero et al., 2001). Therefore, albumin may play a role in axonal sprouting in

the fetus when the concentration of albumin is known to be much higher than in the adult (Tabernero et al., 2001). Furthermore, astrocytes (Tabernero et al., 2002a) and neurones (Tabernero et al., 2002b) have been reported to internalize albumin. Essentially fatty acid free albumin also increases the oxidation of glucose or lactate through the pyruvate dehydrogenase catalysed reaction in both astrocytes (Tabernero et al., 1999) and neurones (Tabernero et al., 2002b). This results in the increased production of acetyl coenzyme A (acetyl Co A) without affecting the rate of pyruvate oxidation through the citric acid cycle. This phenomenon is believed to be a consequence of intracellular fatty acid sequestration since fatty acids are known to inhibit pyruvate dehydrogenase.

From these studies it is clear that the protein component of albumin triggers several distinct cellular functions and can therefore be considered as an agonist in its own right. Interestingly, in healthy individuals reactive microglia are evident in areas where the BBB is absent. These areas are collectively known as the circumventricular organs, which include the pineal gland, the median eminence, the subfornical organ, the area postrema, the subcommissural organ, the organum vasculosum of the lamina terminalis and the pituitary gland (Cagnin et al., 2001, Perry 2001). This provides evidence that plasma proteins such as albumin may mediate microglial activation *in vivo*.

4.1.3 Summary of results

Treatment of microglia with essentially pure rat serum albumin containing 0.005 % fatty acids and 0.005 % immunoglobulins (hereafter referred to as albumin) induced iNOS expression and glutamate release, whilst exerting no effect on COX-2 expression. Furthermore, albumin triggered microglia to proliferate. These findings were mirrored using rat fraction V serum albumin (hereafter referred to as fraction V), suggesting that albumin bound fatty acids, lipids or immunoglobulins do not contribute to cell signalling. Lipopolysaccharide (LPS) was shown to induce iNOS expression, COX-2 expression and glutamate release in microglia, although LPS did not trigger microglia to proliferate.

Peritoneal macrophages isolated from neonatal or adult rats were resistant to the concentrations of albumin or fraction V used to activate microglia. Even at a concentration of 12 mg/ml, albumin or fraction V failed to induce glutamate release or proliferation in these cells. However, peritoneal macrophages isolated from neonatal or adult rats expressed iNOS when exposed to 12 mg/ml of albumin or fraction V. Albumin or fraction V also failed to induce COX-2 expression in macrophages, even at concentrations of 12 mg/ml. Interestingly, LPS (2 μg/ml) induced iNOS and COX-2 expression in macrophages but did not potentiate glutamate release or proliferation.

The microglial signalling cascades that mediate albumin or fraction V-induced iNOS expression, glutamate release and proliferation were subsequently studied using a number of inhibitors. iNOS expression was attenuated by UO126, which suggests that signalling is mediated by ERK. Consistent with this, the phosphorylated forms of ERK 1 and 2 were detectable in microglia but not macrophages (isolated from neonatal or adult rats) treated with albumin or fraction V. Glutamate release was prevented by aminoadipate, suggesting a role for the Xc^- transporter in secretion. Proliferation was inhibited by BAPTA, U73122

or PP2. This indicates that the proliferative response is calcium dependent and that release is mediated through IP_3 gated stores via a Src kinase-dependent mechanism. Accordingly, albumin or fraction V evoked calcium release from thapsigargin-sensitive intracellular stores in N9 microglia and release was inhibited by U73122 or PP2. Albumin or fraction V treatment did not induce changes in intracellular free calcium in macrophages isolated from neonatal or adult rats. Conversely, fraction V induced calcium transients in TSA-3 astrocytes, whereas albumin exerted no discernable effects on intracellular free calcium in these cells.

In a parallel experiment, conditioned medium harvested from albumin or fraction V treated microglia was demonstrated to be neurotoxic. Neuronal death was not attenuated by the iNOS inhibitor, AMT-HCl or a cocktail of glutamate receptor antagonists (MK801, CNQX and MSPG). These results suggest that neuronal death is NO and glutamate independent. In contrast, boiling the microglial conditioned medium afforded neuroprotection, which suggests that the neurotoxic agent(s) are heat labile. Neurotoxin release from microglia occurred 6 hours after the addition of albumin or fraction V and the neurotoxicity of the conditioned medium increased with time.

Finally, albumin was demonstrated to bind to myosin heavy chain IX in N9 microglia. Albumin was also found to bind to myosin heavy chain IX in TSA-3 astrocytes and cerebellar granule neurones. This suggests that myosin heavy chain IX may serve as a non-conventional receptor in these cells through which albumin mediates signalling. Conversely, albumin did not appear to bind to myosin heavy chain IX in peritoneal macrophages isolated from adult rats. Myosin IX has recently been implicated in phagocytosis, consistent with this microglia but not macrophages internalised FITC labelled albumin in a temperature sensitive fashion.

4.2 Albumin induces iNOS expression in microglia

Microglia were analysed for iNOS expression following exposure to albumin. Microglia were treated with albumin in serum free medium (SFM) for 2 hours. The SFM was then replaced with serum containing medium (SCM) for the remainder of the experimental period. This activation protocol was used in all subsequent experiments described in this chapter. Therefore, it should be emphasised that the time points described in the text include the initial 2 hour incubation with albumin in SFM. Microglia were treated with albumin in SFM because serum contains endogenous albumin, fatty acids, lipids and other factors that may synergise with the exogenously applied albumin.

Western blot analyses revealed that albumin (0.1-2 mg/ml) induced a dose dependent increase in iNOS expression after 24 hours in culture (Fig. 4.1A). All blots were cropped to depict the area of interest; iNOS was visualised as a single band exhibiting a molecular weight of 130 kDa (Bhat et al., 1998; Kingham et al., 1999; Combs et al., 2001; Bhat and Fan 2002). In contrast, iNOS was not present in untreated microglia at the same time point (basal). Similarly, iNOS was undetectable in microglia treated with SFM for 2 hours (without albumin) then SCM for 22 hours (SFM). Analysis of β-actin levels demonstrated that the observed changes were not due to differences in protein loading. β-actin was visualised as a single band possessing a molecular weight of 42 kDa (Clancy et al., 2000; Kingham and Pocock 2000).

To confirm that residual fatty acids, lipids or immunoglobulins bound to albumin were not responsible for inducing iNOS, the effects of fraction V on iNOS expression were investigated (Fig. 4.1B). As with albumin, microglia were treated with fraction V in SFM for 2 hours. The SFM was then replaced with SCM for the remainder of the experiment.

Fraction V (1 mg/ml) induced similar levels of iNOS expression as albumin after 24 hours in culture as demonstrated by Western blotting. The effect of the known microglial activator, LPS on iNOS expression was also investigated (Fig. 4.1B). In all experiments described in this chapter microglia were treated with LPS (2 μg/ml) in SCM for the designated length of time. Western blotting revealed that microglia treated with LPS (2 μg/ml) expressed comparable levels of iNOS as those cells treated with albumin (1 mg/ml) or fraction V (1 mg/ml) after 24 hours in culture. Time course analysis revealed that iNOS was initially detectable 6 hours after the addition of albumin (1 mg/ml) or fraction V (1 mg/ml) (Fig. 4.1C). iNOS expression was found to increase with time and the activators induced identical expression profiles temporally. In contrast, iNOS was undetectable in microglia treated with SFM for 2 hours then SCM for 46 hours.

In a parallel experiment, nitrite, a stable breakdown product of NO was measured in microglial conditioned medium. Nitrite was not detectable above control levels ('basal' or 'SFM') in medium collected 48 hours after albumin (1 mg/ml) or fraction V (1 mg/ml) treatment (table 4.1). Similarly, negligible amounts of nitrite were present in medium collected from microglia treated with LPS (2 μg/ml) for 48 hours. This was not due to assay failure since nitrite was detectable in culture medium collected from activated macrophages (see table 4.3).

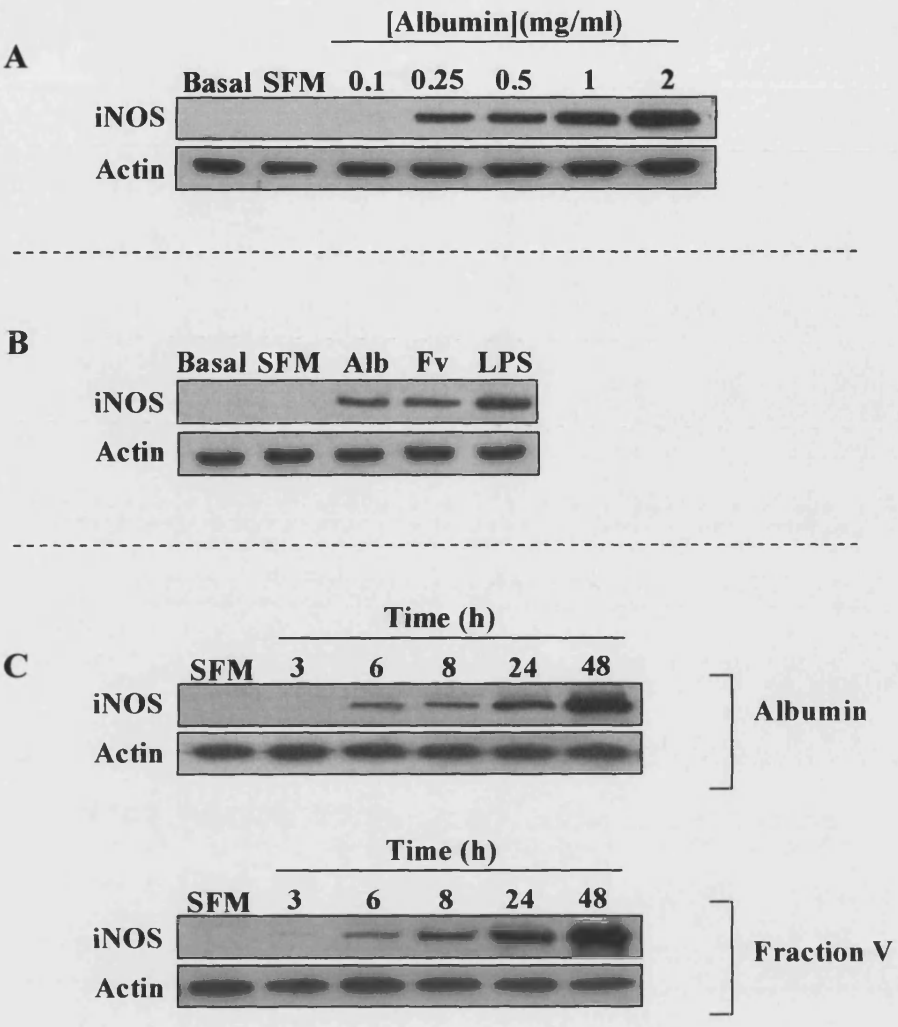

Figure 4.1 iNOS expression in microglia

Representative Western blots of iNOS expression in microglial cell lysates. **A**: Microglia were treated with increasing concentrations of albumin (0.1-2 mg/ml) in SFM for 2 hours. The SFM was then replaced with SCM for 22 hours before lysates were prepared. Control lysates were prepared from microglia left untreated for 24 hours (basal) or microglia exposed to SFM for 2 hours then SCM for 22 hours (SFM). **B:** Microglia were exposed to albumin (Alb: 1 mg/ml) or fraction V (Fv: 1 mg/ml) in SFM for 2 hours, after which the SFM was replaced with SCM for a further 22 hours before lysis. Lysates were also prepared from microglia treated with LPS (2 μg/ml) in SCM for 24 hours. Control lysates were prepared from microglia treated as described in A. **C**: Microglia were treated with albumin (1 mg/ml) or fraction V (1 mg/ml) in SFM for 2 hours. The SFM was then replaced with SCM for a further 1, 4, 6, 22 or 46 hours before lysis. Control lysates were prepared from microglia subjected to SFM for 2 hours then SCM for 46 hours (SFM). Lysates were subjected to Western blot analysis using an antibody raised against iNOS (1:5000), which in turn was detected by goat anti-rabbit IgG (HRP) (1:500). To ensure equal protein loading blots were reprobed with an antibody recognising β-actin (1:1000) followed by exposure to goat anti-mouse IgG (HRP) (1:1000).

Treatment	[Nitrite](nM/μg protein)
Basal	1.04 ± 0.03
SFM	0.94 ± 0.03
Albumin (1 mg/ml)	1.29 ± 0.20
Fraction V (1 mg/ml)	1.12 ± 0.02
LPS (2 μg/ml)	1.13 ± 0.03

Table 4.1 Nitrite release from microglia

Nitrite concentrations (nM/μg of protein) were measured in microglial conditioned medium using Griess reagent. Microglia were treated with albumin (1 mg/ml) or fraction V (1 mg/ml) in SFM for 2 hours. The SFM was then replaced with SCM for a further 46 hours before medium was collected. Medium was also collected from microglia treated with LPS (2 μg/ml) in SCM for 48 hours. Control medium was collected from microglia left untreated for 48 hours (basal) or microglia exposed to SFM for 2 hours then SCM for 46 hours (SFM). The values shown represent the mean concentration in nM/μg of protein ± SEM of data from experiments performed in triplicate. Statistical analysis was performed using ANOVA followed by the Tukey post test. According to this test there was no statistical difference between the treatments.

The signalling pathways that mediate albumin or fraction V induced iNOS expression were subsequently studied using a number of inhibitors. At the concentrations used in these experiments the inhibitors (pertussis toxin, 2 μg/ml; BAPTA-AM, 10 μM; U73122, 2 μM; PP2, 100 nM; UO126, 5 μM) did not induce morphological changes or detachment from the coverslips. Confirmation that the inhibitors were not toxic was obtained using propidium iodide and fluoroscein diacetate. Propidium iodide penetrates dead or damaged cells possessing compromised plasma membranes where it intercalates between the bases of DNA and fluoresces upon excitation. In contrast, fluoroscein diacetate is metabolised by healthy cells to form a fluorescent product and therefore provides an estimation of the total number of viable cells.

Microglia were treated with the inhibitors in SFM for 2 hours. The SFM was then replaced with SCM supplemented with the appropriate concentration of inhibitor for a further 22 hours before staining. Microglial cultures exposed to the inhibitors contained very few propidium iodide positive cells after 24 hours in culture (table 4.2). Similarly, microglial cultures left untreated for 24 hours (basal) or cultures treated with SFM for 2 hours then SCM for 22 hours (SFM) contained few cells exhibiting propidium iodide staining. These findings emphasize that at the concentrations used the inhibitors were not toxic to the microglia.

Treatment	% of propidium iodide stained cells
Basal	2.1 ± 1.1
SFM	2.0 ± 1.6
Pertussis toxin (2 μg/ml)	1.4 ± 0.4
BAPTA-AM (10 μM)	1.6 ± 0.3
U73122 (2 μM)	1.9 ± 0.7
PP2 (100 nM)	2.2 ± 0.6
UO126 (5 μM)	2.1 ± 2.1

Table 4.2 Analysis of inhibitor toxicity using propidium iodide

Inhibitor treated microglia were stained with propidium iodide and fluoroscein diacetate to provide an estimation of toxicity. Microglia were treated with inhibitors (pertussis toxin, 2 μg/ml; BAPTA-AM, 10 μM; U73122, 2 μM; PP2, 100 nM; UO126, 5 μM) in SFM for 2 hours. The SFM was then replaced with SCM supplemented with the appropriate concentration of inhibitor for a further 22 hours before staining. Control microglia were either left untreated for 24 hours of were treated with SFM for 2 hours then SCM for 22 hours before staining. Dead cells possessing propidium iodide staining were expressed as a percentage of the total number of cells counted (cells possessing propidium iodide staining or fluoroscein diacetate staining). The values shown represent the mean ± SEM of data from experiments performed in triplicate. Statistical analysis was performed using ANOVA followed by the Tukey post test. According to this test there was no statistical difference between the treatments.

Western blot analyses revealed that pre-treating microglia with pertussis toxin (Ptx: 2 μg/ml) a $G_{i/O}$ protein inhibitor, BAPTA-AM (10 μM) a membrane permeable calcium chelator, U73122 (2 μM) a phospholipase C inhibitor or PP2 (100 nM) a Src kinase inhibitor did not modulate iNOS expression induced by albumin (1 mg/ml) or fraction V (1 mg/ml) (Fig. 4.2A). Furthermore, microglia treated with the inhibitors alone did not express significantly different levels of iNOS from control ('basal' or 'SFM'). Conversely, pre-treating microglia with UO126 (5 μM) an ERK inhibitor dramatically attenuated iNOS expression induced by albumin (1 mg/ml) or fraction V (1 mg/ml). Maximal inhibition was obtained with a concentration of 5 μM and at this concentration microglia treated with UO126 alone contained similar levels of iNOS as controls ('basal' or 'SFM'). Densitometric analysis was used to quantify the iNOS bands. To correct for slight variations in protein loading the intensity of the iNOS bands were normalised with respect to β-actin levels. Using this approach UO126 (5 μM) was demonstrated to cause a four fold reduction in the levels of iNOS expression induced by albumin (1 mg/ml) or fraction V (1 mg/ml) (Fig. 4.2B).

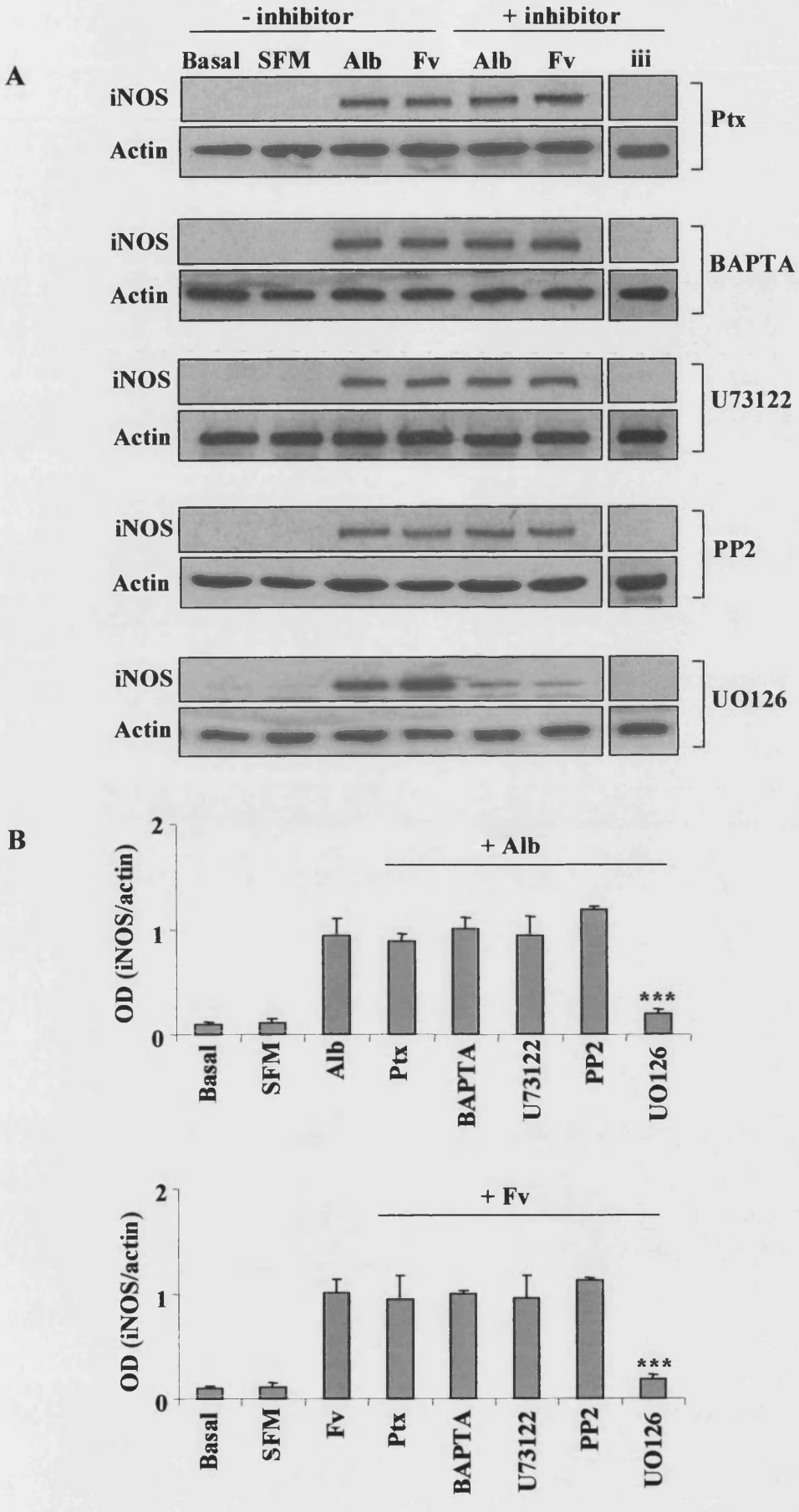

Figure 4.2 (see overleaf for figure legend)

Figure 4.2 Modulation of albumin or fraction V induced iNOS expression in microglia
Representative Western blots of iNOS expression in microglial cell lysates. **A**: Microglia were treated with albumin (1 mg/ml) or fraction V (1 mg/ml) in SFM for 2 hours. The SFM was then replaced with SCM for 22 hours before lysates were prepared. In addition, microglia were treated with albumin (Alb: 1 mg/ml) or fraction V (Fv: 1 mg/ml) in SFM in the presence of pertussis toxin (Ptx; 2 μg/ml), BAPTA (10 μM), U73122 (2 μM), PP2 (100 nM) or UO126 (5 μM). At 2 hours the SFM was replaced with SCM supplemented with the appropriate concentration of inhibitor for a further 22 hours before lysates were prepared. Lysates were also prepared from microglia treated with the inhibitors (iii: Ptx; 2 μg/ml, BAPTA; 10 μM, U73122; 2 μM, PP2; 100 nM, UO126; 5 μM) in the absence of albumin or fraction V. Control lysates were prepared from microglia left untreated for 24 hours (basal) or microglia exposed to SFM for 2 hours then SCM for 22 hours (SFM). Lysates were subjected to Western blot analyses using an antibody raised against iNOS (1:5000). To ensure equal loading blots were re-probed using an antibody recognising β-actin (1:1000). **B**: Densitometric analysis of iNOS and β-actin bands was performed and levels of iNOS were normalised with respect to β-actin levels. Statistical analysis was performed using ANOVA followed by the Tukey post test. *** $P > 0.001$ vs 'albumin' or 'fraction V' treated respectively.

Since UO126 inhibited albumin or fraction V induced iNOS expression, the presence of phospho-ERK was assessed in microglial lysates. Western blot analyses revealed that albumin (1 mg/ml) elicited a rapid phosphorylation of ERK 1 and 2 (Fig. 4.3A). Phospho-ERK was detectable as a doublet (Bhat et al., 1998; McDonald et al., 1998; Combs et al., 2001; Bhat and Fan 2002). The bands exhibited molecular weights of 42 and 44 kDa respectively, corresponding to ERK 1 (p44) and ERK 2 (p42). Phospho-ERK was initially detectable 30 minutes after albumin treatment and expression increased with time. Maximal phosphorylation was reached at 1 hour, followed by a decline in phosphorylation reaching lower levels by 48 hours post treatment.

Parallel time courses using microglia treated with SFM for 2 hours then SCM revealed that ERK phosphorylation did not significantly increase over the experimental period (Fig. 4.3A). This demonstrates that the increases in ERK phosphorylation are due to the addition of albumin and not the medium changes. Furthermore, analysis of total ERK indicated that these results were not due to differences in protein loading. Total ERK recognises both the unphosphorylated and phosphorylated forms of ERK. Total ERK is also visualised as a doublet. Like phospho-ERK the bands exhibit molecular weights of 42 and 44 kDa respectively. Microglia treated with fraction V (1 mg/ml) in SFM for 1 hour were also found to express comparable levels of phospho-ERK as those cells treated with albumin (1 mg/ml) (Fig. 4.3B).

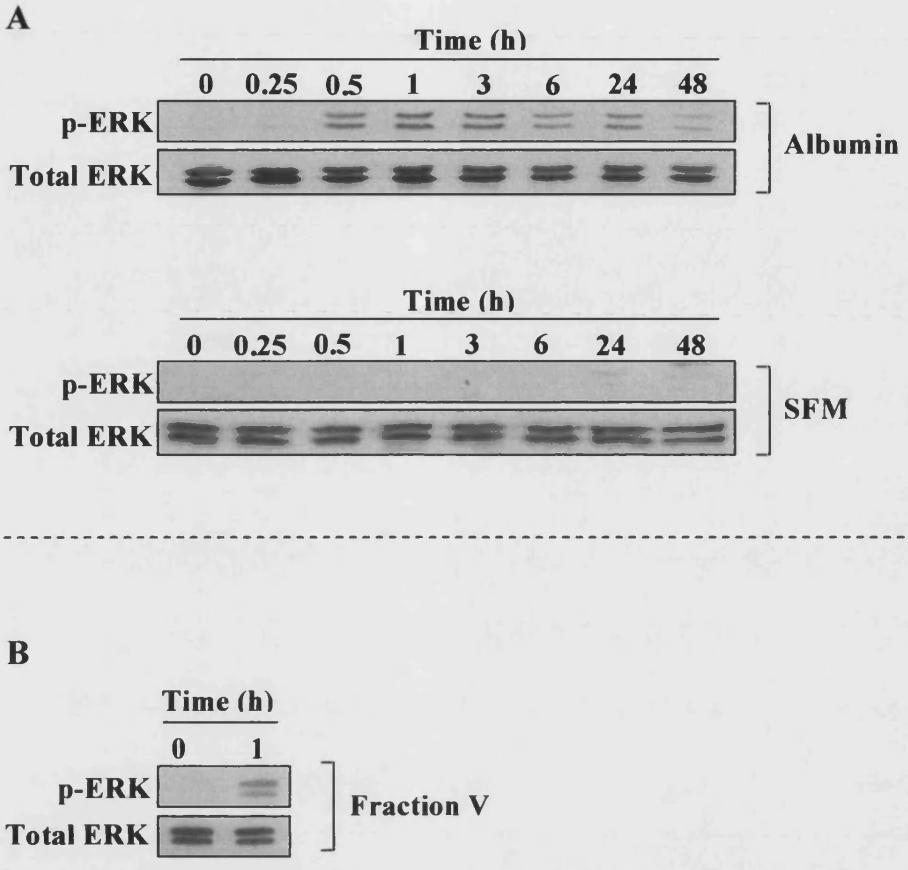

Figure 4.3 Albumin or fraction V evokes ERK phosphorylation in microglia

Representative Western blots of ERK phosphorylation in microglial cell lysates. **A**: Microglia were treated with albumin (1 mg/ml) in SFM and lysates were prepared after 0.25, 0.5 or 1 hour. At 2 hours the SFM was removed from the remaining cultures and replaced with SCM. Lysates were then prepared after a further 2, 4, 22 or 46 hours. Control lysates were prepared from microglia treated with SFM then SCM at the same time points (SFM). **B**: Lysates were prepared from microglia treated with fraction V (1 mg/ml) in SFM for 0 or 1 hour. Lysates were subjected to Western blot analyses using an antibody raised against phospho-ERK (1:750), which in turn was detected by goat anti-mouse IgG (HRP) (1:1000). To ensure equal loading blots were re-probed using an antibody recognising total ERK (1:500) followed by exposure to goat anti-rabbit IgG (HRP) (1:500).

The finding that albumin induced iNOS expression in microglia led to the question as to whether peripheral macrophages are responsive to albumin considering that they are exposed to high concentrations of albumin under physiological conditions. Subsequently, the effects of albumin or fraction V on peritoneal macrophage iNOS expression were investigated. In these experiments, macrophages were isolated from the peritoneal cavity of neonatal or adult rats; the former providing ages matched equivalents to the microglia. In all experiments described in this chapter macrophages were treated with albumin or fraction V in SFM for 2 hours, after which the SFM was replaced with SCM for the rest of the experimental period.

Western blot analyses revealed that peritoneal macrophages isolated from neonatal or adult rats were resistant to the concentrations of albumin or fraction V (2 mg/ml or less) that evoked iNOS expression in microglia (Fig. 4.4A). Exposure to 12 mg/ml of albumin or fraction V for 24 hours was required to induce iNOS expression in these cells. Furthermore, iNOS was undetectable in macrophages left untreated for 24 hours (basal) or macrophages treated with SFM for 2 hours then SCM for 22 hours (SFM). The effect of the classical activator, LPS on macrophage iNOS expression was also studied. As with microglia, macrophages were treated with LPS (2 μg/ml) in SCM in all experiments. Western blot analyses revealed that macrophages treated with LPS (2 μg/ml) for 24 hours expressed similar levels of iNOS as those cells treated with albumin (12 mg/ml) or fraction V (12 mg/ml) (Fig. 4.4B).

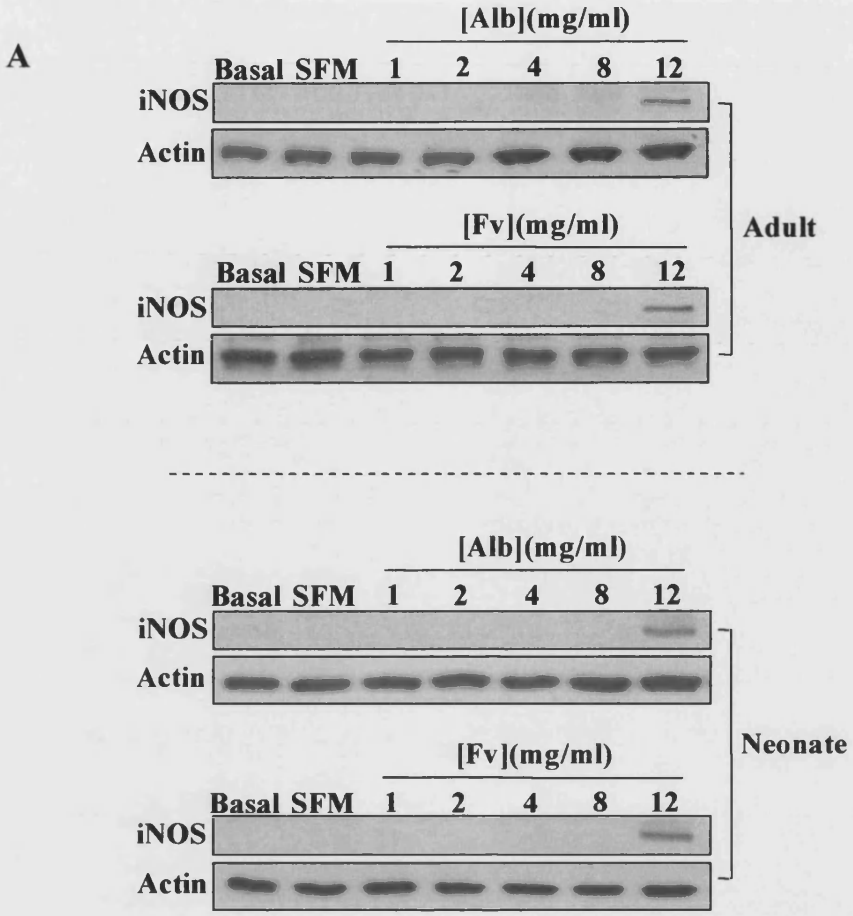

Figure 4.4 (see overleaf for figure legend)

Figure 4.4 iNOS expression in peritoneal macrophages

Representative Western blots of iNOS expression in peritoneal macrophage cell lysates. **A**: Peritoneal macrophages isolated from neonatal or adult rats were treated with increasing concentrations of albumin (Alb: 1-12 mg/ml) or fraction V (Fv: 1-12 mg/ml) in SFM for 2 hours. The SFM was then replaced with SCM for 22 hours before lysates were prepared. Control lysates were prepared from macrophages left untreated for 24 hours (basal) or macrophages exposed to SFM for 2 hours then SCM for a further 22 hours (SFM). **B**: Macrophages were exposed to albumin (Alb: 1 mg/ml) or fraction V (Fv: 1 mg/ml) in SFM for 2 hours, after which the SFM was replaced with SCM for 22 hours before lysis. Lysates were also prepared from macrophages treated with LPS (2 μg/ml) in SCM for 24 hours. Control lysates were prepared from macrophages treated as described in A. Lysates were subjected to Western blot analysis using an antibody raised against iNOS (1:5000). To ensure equal protein loading blots were reprobed with an antibody recognising β-actin (1:1000).

Culture medium collected from macrophages isolated from neonatal or adult rats was subsequently assessed for the presence of nitrite. Significant levels of nitrite were only present in medium collected from macrophages treated with 12 mg/ml of albumin, 12 mg/ml of fraction V or LPS (2 μg/ml) after 24 hours in culture (table 4.3). Considerably lower levels of nitrite were present in medium collected from macrophages treated with lower concentrations of albumin (1-8 mg/ml) or fraction V (1-8 mg/ml). Similarly, low levels of nitrite were present in medium collected from macrophages that were left untreated for 24 hours (basal) or macrophages treated with SFM for 2 hours then SCM for 22 hours (SFM).

In contrast to microglia, macrophages isolated from neonatal or adult rats did not exhibit increases in phospho-ERK expression after treatment with albumin (1 or 12 mg/ml), fraction V (1 or 12 mg/ml) or LPS (2 μg/ml) for 1 hour (Fig. 4.5). Similarly, low levels of phospho-ERK were detectable in macrophages left untreated for 1 hour (basal) or macrophages treated with SFM for 1 hour (SFM). These findings were not attributed to failure of the Western since prominent total ERK bands were visible, which exhibited molecular weights of 42 and 44 kDa respectively. Furthermore, the antibody used recognised p-ERK in microglial lysates (see Fig. 4.3). This indicates that in macrophages ERK is primarily present in the un-phosphorylated form following treatment with albumin, fraction V or LPS.

	Adult	Neonate
Treatment	**[Nitrite](nM/μg)**	**[Nitrite](nM/μg)**
Basal	8.5 ± 8.5	6.1 ± 11.6
SFM	12.7 ± 7.2	17.1 ± 12.4
Albumin (1 mg/ml)	10.9 ± 9.6	7.3 ± 14.3
Albumin (2 mg/ml)	4.9 ± 8.8	3.0 ± 12.1
Albumin (4 mg/ml)	3.6 ± 6.0	3.3 ± 7.6
Albumin (8 mg/ml)	9.7 ± 7.4	3.8 ± 8.0
Albumin (12 mg/ml)	517.7 ± 13.4 ***	507.8 ± 4.7 ***
Fraction V (1 mg/ml)	17.5 ± 17.4	6.8 ± 0
Fraction V (2 mg/ml)	2.2 ± 0.0	14.0 ± 6.4
Fraction V (4 mg/ml)	8.3 ± 24.5	12.4 ± 17.2
Fraction V (8 mg/ml)	10.2 ± 5.5	0 ± 2.03
Fraction V (12 mg/ml)	481.8 ± 14.7 ***	510 ± 6.0 ***
LPS (2 μg/ml)	490.9 ± 16.4 ***	488 ± 3.2 ***

Table 4.3 Nitrite release from peritoneal macrophages

Nitrite concentrations (nM/μg of protein) were measured in macrophage conditioned medium using Griess reagent. Peritoneal macrophages isolated from neonatal or adult rats were treated with albumin (1-12 mg/ml) or fraction V (1-12 mg/ml) in SFM for 2 hours. The SFM was then replaced with SCM for 22 hours before medium was collected. Medium was also collected from macrophages treated with LPS (2 μg/ml) in SCM for 24 hours. Control medium was collected from macrophages left untreated for 24 hours (basal) or macrophages exposed to SFM for 2 hours then SCM for a further 22 hours (SFM). The values shown represent the mean (nM/μg of protein) ± SEM of data from experiments performed in triplicate. Statistical analysis was performed using ANOVA followed by the Tukey post test. *** $P < 0.001$, vs 'basal' or 'SFM'.

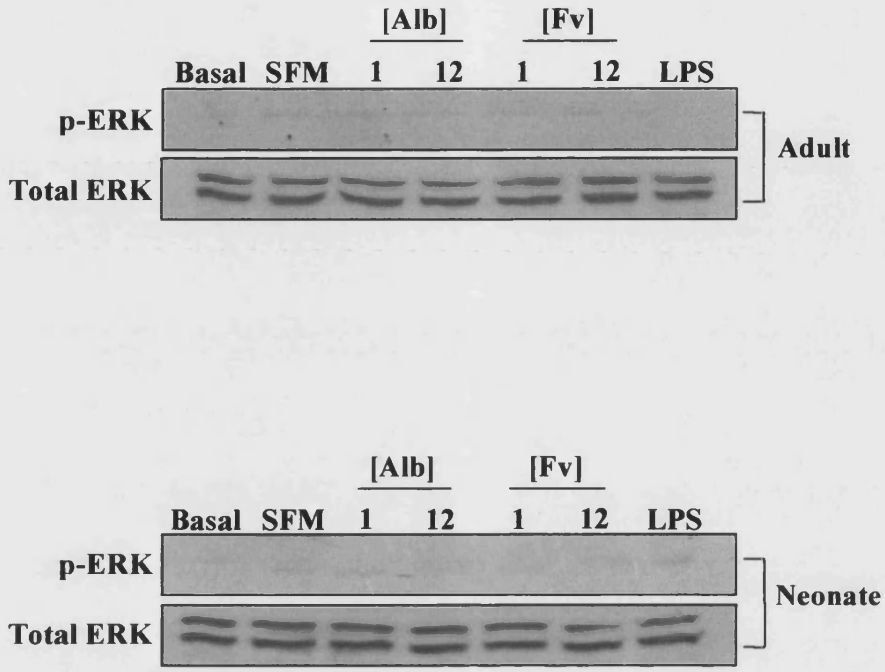

Figure 4.5 Phospho-ERK expression in peritoneal macrophages

Representative Western blots of ERK phosphorylation in macrophage cell lysates. **A**: Peritoneal macrophages isolated from neonatal or adult rats were treated with albumin (Alb: 1 or 12 mg/ml) or fraction V (1 or 12 mg/ml) in SFM and lysates were prepared after 1 hour. Lysates were also prepared from macrophages treated with LPS (2 μg/ml) in SCM after 1 hour. Control lysates were prepared from macrophages left untreated for 1 hour (basal) or macrophages exposed to SFM for 1 hour. Lysates were subjected to Western blot analyses using an antibody raised against phospho-ERK (1:750). To ensure equal loading blots were re-probed using an antibody recognising total ERK (1:500).

4.3 Albumin does not induce COX-2 expression in microglia

Microglia were assessed for COX-2 expression following exposure to albumin. Western blotting revealed that neither albumin (0.1-2 mg/ml) nor fraction V (1 mg/ml) evoked COX-2 expression in microglia after 24 hours in cultures (Fig. 4.6A). In contrast, COX-2 was detectable in microglia treated with LPS (2 μg/ml) for 24 hours. COX-2 was visible as a single protein band exhibiting a molecular weight of 72 kDa (Chen et al., 1999; Dean et al., 1999; Pyo et al., 1999; Clancy et al., 2000). COX-2 was absent in microglia left untreated for 24 hours (basal) or microglia treated with SFM for 2 hours then SCM for 22 hours (SFM). Furthermore, time course analysis demonstrated that COX-2 was undetectable in microglial lysates 3, 8 or 48 hours after albumin (1 mg/ml) or fraction V (1 mg/ml) treatment (Fig. 4.6B). Therefore, microglial signalling induced by albumin does not involve COX-2, although COX-2 expression can be induced by independent signalling pathways.

The ability of albumin or fraction V to induce COX-2 expression in peritoneal macrophages was also assessed. Western blot analyses revealed that peritoneal macrophages isolated from neonatal or adult rats did not express COX-2 following exposure to albumin (1 or 12 mg/ml) or fraction V (1 or 12 mg/ml) for 24 hours (Fig. 4.6C). Conversely, macrophages treated with LPS (2 μg/ml) for 24 hours did upregulate the expression of this inflammatory mediator.

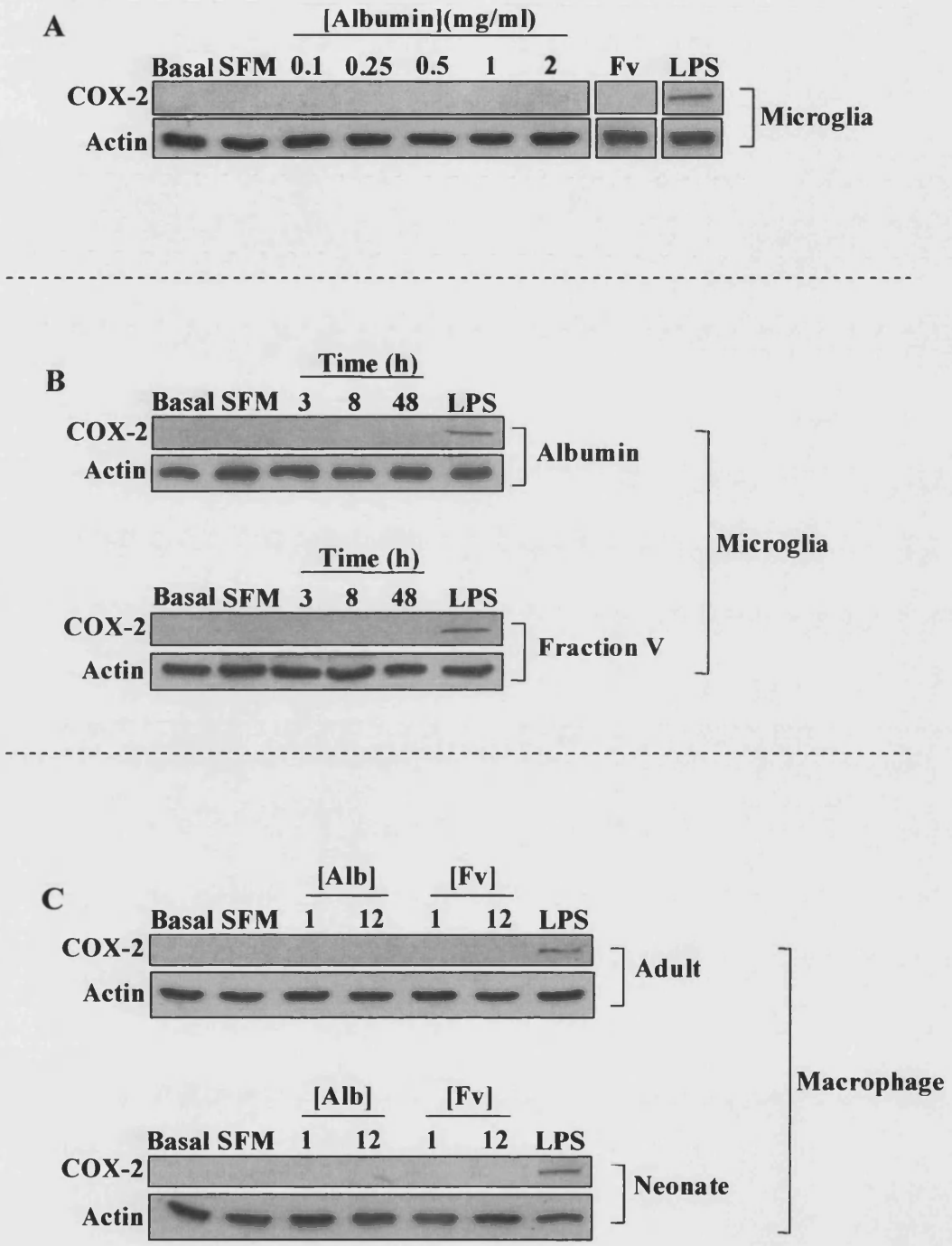

Figure 4.6 (see overleaf for figure legend)

Figure 4.6 COX-2 expression in microglia or peritoneal macrophages

Representative Western blots of COX-2 expression in microglial or peritoneal macrophage cell lysates. **A**: Microglia were treated with increasing concentrations of albumin (0.1-2 mg/ml) or fraction V (Fv: 1 mg/ml) in SFM for 2 hours. The SFM was then replaced with SCM for 22 hours before lysates were prepared. Lysates were also prepared from microglia treated with LPS (2 μg/ml) in SCM for 24 hours. Control lysates were prepared from microglia left untreated for 24 hours (basal) or microglia exposed to SFM for 2 hours then SCM for 22 hours (SFM). **B:** Microglia were treated with albumin (Alb: 1 mg/ml) or fraction V (Fv: 1 mg/ml) in SFM for 2 hours. The SFM was then replaced with SCM for a further 1, 6, or 46 hours before lysis. Lysates were also prepared from microglia treated with LPS (2 μg/ml) in SCM for 24 hours. Control lysates were prepared from microglia left untreated for 48 hours (basal) or microglia exposed to SFM for 2 hours then SCM for 46 hours (SFM). **C**: Peritoneal macrophages isolated from neonatal or adult rats were treated with albumin (Alb: 1 or 12 mg/ml) or fraction V (Fv: 1 or 12 mg/ml) in SFM for 2 hours. The medium was then replaced with SCM for 22 hours before lysis. Lysates were also prepared from macrophages treated with LPS (2 μg/ml) in SCM for 24 hours. Control lysates were prepared from macrophages treated as described in A. Lysates were subjected to Western blot analysis using an antibody raised against COX-2 (1:750), which in turn was detected by donkey anti-goat IgG (HRP) (1:1000). To ensure equal protein loading blots were reprobed with an antibody recognising β-actin (1:1000) followed by exposure to goat anti-mouse IgG (HRP) (1:1000).

4.4 Albumin induces glutamate release from microglia

Previous studies have demonstrated that activated microglia secrete large quantities of glutamate (Piani and Fontana 1994; Kingham et al., 1999; Barger and Basile 2001). Furthermore, albumin treated neurones have been reported to release glutamate into the extracellular milieu (Tabernero et al., 2002b). These findings prompted the effects of albumin on glutamate release from microglia to be evaluated.

Microglia treated with albumin (0.1- 2 mg/ml) were demonstrated to release glutamate in a dose dependent fashion after 24 hours in culture (Fig. 4.7A). Glutamate concentrations ranged from 127 ± 45.5 to 904 ± 14 nM/μg of protein. In contrast, glutamate was present at much lower concentrations in medium collected from microglia left untreated for 24 hours (basal) or microglia treated with SFM for 2 hours then SCM for 22 hours (SFM) (Basal: 11.5 ± 18.4 nM/μg of protein, SFM: 61.1 ± 21.7 nM/μg of protein). In addition, microglia exposed to fraction V (1 mg/ml) or LPS (2 μg/ml) released similar levels of glutamate as those cells treated with albumin (1 mg/ml) after 24 hours in culture (Fig. 4.7B) (Fv: 709.9 ± 15.7 nM/μg of protein, LPS: 733 ± 41 nM/μg of protein, albumin: 698.3 ± 52.7 nM/μg of protein). Time course analyses revealed that glutamate was initially detectable 3 hours after the addition of albumin (1 mg/ml) or fraction V (1 mg/ml) (Fig. 4.7C). Furthermore, the concentration of glutamate in the medium increased with time and both activators were found to induce similar profiles of glutamate release temporally.

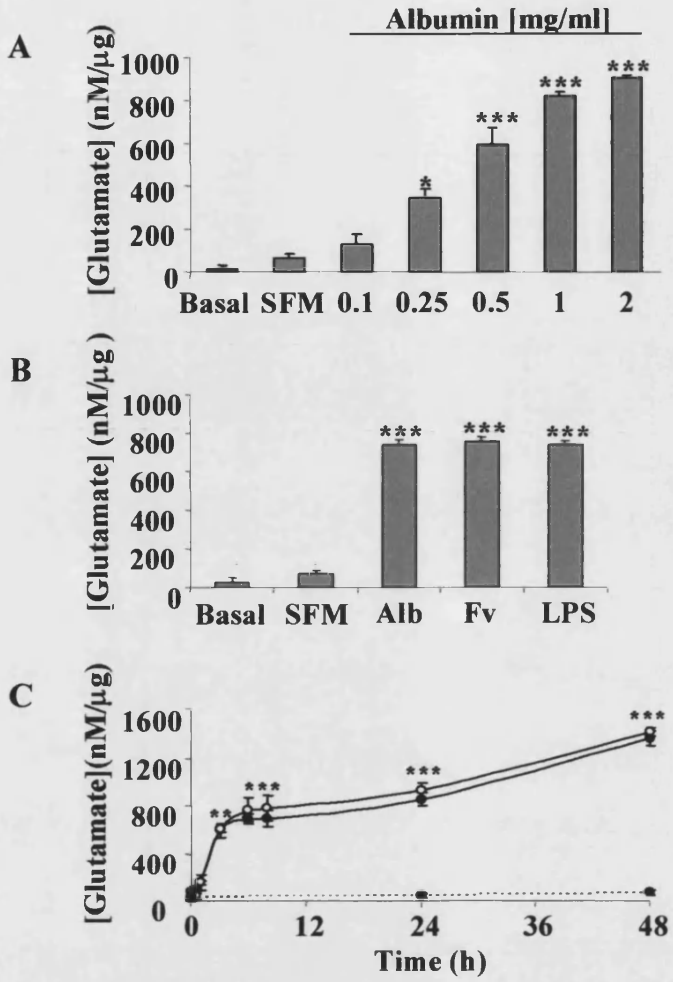

Figure 4.7 Assessment of glutamate release from microglia

Glutamate concentrations (nM/µg of protein) were measured in microglial conditioned medium using a fluorometric assay. **A**: Microglia were treated with increasing concentrations of albumin (0.1-2 mg/ml) in SFM for 2 hours. The SFM was then replaced with SCM for 22 hours before the medium was collected. Control medium was collected from microglia left untreated for 24 hours (basal) or microglia treated with SFM for 2 hours then SCM for 22 hours (SFM). **B**: Microglia were treated with albumin (Alb: 1 mg/ml) or fraction V (Fv: 1 mg/ml) in SFM for 2 hours. The SFM was then replaced with SCM for 22 hours before the medium was collected. In addition, medium was collected from microglia were treated with LPS (2 µg/ml) in SCM for 24 hours. Control medium was collected from microglia treated as described in A. **C**: Microglia were treated with albumin (1 mg/ml: open circles) or fraction V (1 mg/ml: closed circles) in SFM and medium was collected after 0.25, 0.5, or 1 hour. At 2 hours the SFM was removed from the remaining cultures and replaced with SCM. Medium was then collected after a further 1, 2, 4, 6, 22 or 46 hours. Control medium was collected from microglia treated with SFM, then SCM at the same time points (dotted line). The values shown represent the mean (nM/µg of protein) ± SEM of data from experiments performed in triplicate. Statistical analysis was performed using ANOVA followed by the Tukey post test. * $P < 0.05$, ** $P < 0.01$, *** $P < 0.001$ vs control (A, B: control describes 'basal' or 'SFM'; C: control describes time 0).

To verify that glutamate release was not due to cell membrane disruption, albumin or fraction V treated microglia were stained with propidium iodide and fluoroscein diacetate. Microglial cultures exposed to albumin (2 mg/ml) or fraction V (2 mg/ml) contained very few cells that stained with propidium iodide after 48 hours in culture (table 4.4). Similarly, microglia left untreated for 48 hours (basal) or microglia treated with SFM for 2 hours then SCM for 46 hours (SFM) contained few cells exhibiting propidium iodide staining. This suggests that glutamate release induced by albumin or fraction V occurs via a regulated pathway and is not due to loss of microglial cell membrane integrity.

The signalling pathways that mediate albumin or fraction V induced glutamate release were investigated using a range of inhibitors. Previously, it has been demonstrated that glutamate secretion can be mediated by the cysteine-glutamate antiporter (Xc^- transporter) in activated microglia (Piani and Fontana 1994; Kingham et al., 1999). Subsequently, the effect of the Xc^- transporter antagonist aminoadipate on glutamate release was studied. Additionally, the effect of the iNOS inhibitor AMT-HCl was investigated to determine whether NO is involved in glutamate secretion. Pre-treating microglia with aminoadipate (2.5 mM) reduced albumin (1 mg/ml) or fraction V (1 mg/ml) induced glutamate release to control levels ('basal' or 'SFM') (Fig. 4.8A,B). In contrast, pre-treating microglia with AMT-HCl (0.3 μM) did not modulate glutamate release induced by either activator (Fig. 4.8A,B). Furthermore, medium collected from microglia treated with the inhibitors alone did not contain significantly different levels of glutamate from controls ('basal' or 'SFM').

The effects of pertussis toxin (Ptx; 2 μg/ml), BAPTA-AM (10 μM), U73122 (2 μM), PP2 (100 nM), or UO126 (5 μM) on albumin or fraction V induced glutamate release were also explored. However, these inhibitors did not modulate glutamate release elicited by albumin (1 mg/ml) or fraction V (1 mg/ml) treatment (Fig. 4.8A,B). Moreover, medium collected from microglia treated with the inhibitors alone did not contain significantly different levels of glutamate from controls ('basal' or 'SFM').

The effect of albumin or fraction V on glutamate release from peritoneal macrophages was subsequently investigated. As before, macrophages were isolated from neonatal and adult rats. However, glutamate was not present above control levels ('basal' or 'SFM') in medium collected 24 hours after the addition of albumin (1, 2 or 12 mg/ml) or fraction V (1, 2 or 12 mg/ml) (table 4.5). Medium obtained from macrophages treated with LPS (2 μg/ml) for 24 hours also contained a similar level of glutamate to that of control ('basal' or 'SFM'). Furthermore, there were no differences between the results obtained with macrophages isolated from neonatal or adult rats.

Macrophages isolated from neonatal or adult rats were stained with propidium iodide and fluoroscein diacetate to determine whether disturbances in cell membrane integrity were responsible for the high basal levels of glutamate, which may have subsequently masked the effects of the activators. Staining revealed that macrophage cultures left untreated for 24 hours (basal) or cultures treated with SFM for 2 hours then SCM for 22 hours (SFM) contained few propidium iodide positive cells (table 4.6). Furthermore, macrophage cultures exposed to albumin (12 mg/ml) or fraction V (12 mg/ml) contained very few cells that stained with propidium iodide after 24 hours in culture. These results suggest that glutamate release is not due to loss of macrophage cell membrane integrity.

	Basal	SFM	Albumin	Fraction V
% of propidium iodide stained microglia	1.1 ± 1.2	1.2 ± 1.2	1.4 ± 0.2	2.0 ± 0.9

Table 4.4 Analysis of microglial membrane integrity

Microglia were stained with propidium iodide and fluoroscein diacetate to provide an estimation of cell membrane integrity. Microglia were treated with albumin (2 mg/ml) or fraction V (2 mg/ml) in SFM for 2 hours. The SFM was then replaced with SCM for 46 hours before staining was performed. Control microglia were either left untreated for 48 hours (basal) or were treated with SFM for 2 hours then SCM for a further 46 hours (SFM) before staining. Cells possessing propidium iodide staining were expressed as a percentage of the total number of cells counted (cells possessing propidium iodide staining or fluoroscein diacetate staining). The values shown represent the mean ± SEM of data from experiments performed in triplicate. Statistical analysis was performed using ANOVA followed by the Tukey post test. According to this test there was no statistical difference between the treatments.

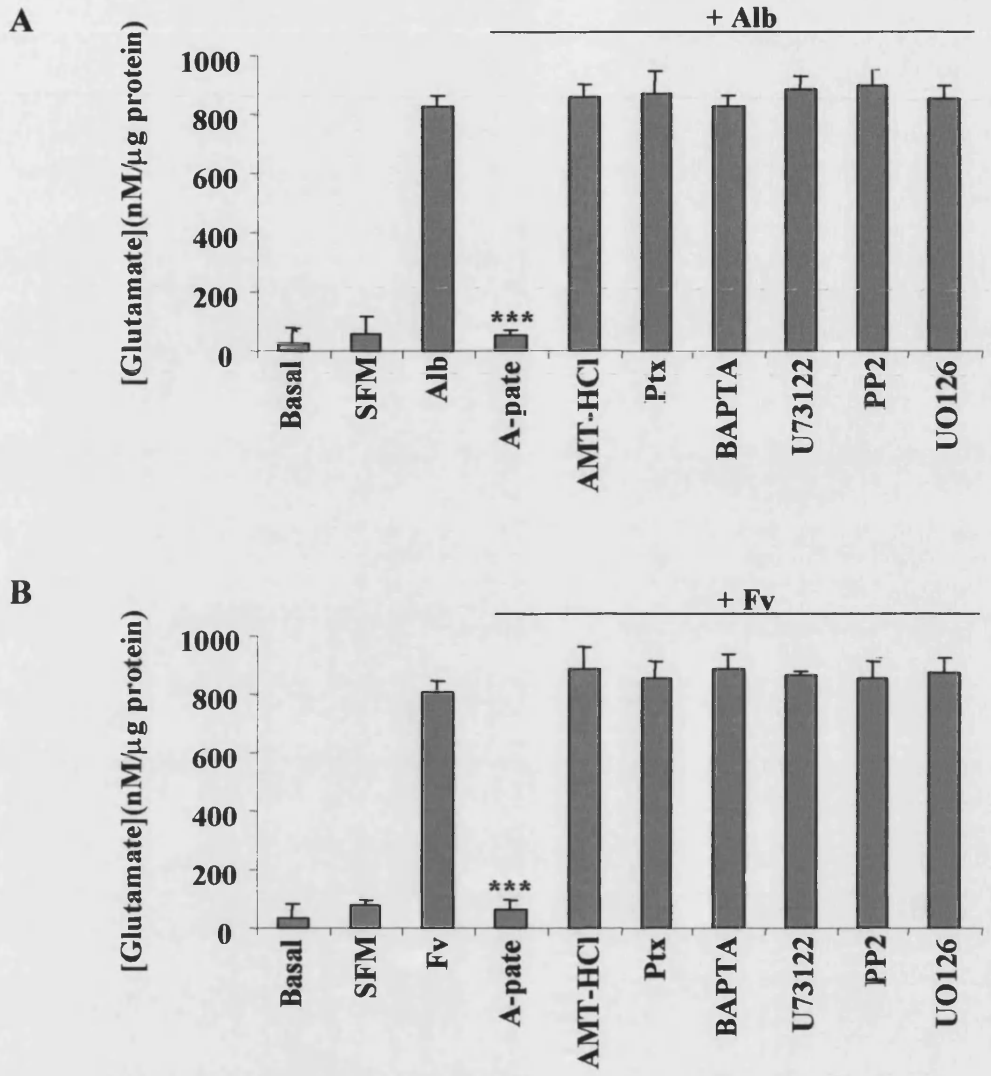

Figure 4.8 Modulation of albumin or fraction V induced glutamate release from microglia

Glutamate concentrations (nM/μg of protein) were measured in microglial conditioned medium using a fluorometric assay. Microglia were treated with albumin (Alb: 1 mg/ml) (**A**) or fraction V (Fv: 1mg/ml) (**B**) in SFM for 2 hours. The SFM was then replaced with SCM for 22 hours before medium was collected. In addition, microglia were treated with albumin (Alb: 1 mg/ml) or fraction V (Fv: 1 mg/ml) in SFM in the presence of aminoadipate (A-pate: 2.5 mM), AMT-HCl (0.3 μM) pertussis toxin (Ptx: 2 μg/ml), BAPTA-AM (10 μM), U73122 (2 μM), PP2 (100 nM) or UO126 (5 μM). At 2 hours the SFM was replaced with SCM supplemented with the appropriate concentration of inhibitor for 22 hours before medium was collected. Control medium was collected from microglia left untreated for 24 hours (basal) or microglia exposed to SFM for 2 hours then SCM for 22 hours (SFM).The values shown represent the mean (nM/μg of protein) ± SEM of data from experiments performed in triplicate. Statistical analysis was performed using ANOVA followed by the Tukey post test. *** $P < 0.001$ vs albumin (Alb) or fraction V (Fv) treated respectively.

	Adult	Neonate
Treatment	**[Glutamate](nM/μg)**	**[Glutamate](nM/μg)**
Basal	260 ± 16.6	245 ± 4.2
SFM	255 ± 17.5	265 ± 4.6
Albumin (1 mg/ml)	245 ± 16.1	256 ± 11.9
Albumin (2 mg/ml)	255 ± 21.2	260 ± 14.6
Albumin (12 mg/ml)	255 ± 15.5	262 ± 5.9
Fraction V (1 mg/ml)	250 ± 15.7	248 ± 14.6
Fraction V (2 mg/ml)	266 ± 24.3	246 ± 19.4
Fraction V (12 mg/ml)	254 ± 17.7	261 ± 13.7
LPS (2 μg/ml)	267 ± 12.1	249 ± 7.1

Table 4.5 Glutamate release from peritoneal macrophages

Glutamate concentrations (nM/μg of protein) were measured in peritoneal macrophage conditioned medium using a fluorometric assay. Peritoneal macrophages isolated from neonatal or adult rats were treated with albumin (1, 2 or 12 mg/ml) or fraction V (1, 2 or 12 mg/ml) in SFM for 2 hours. The SFM was then replaced with SCM for 22 hours before the medium was collected. Medium was also collected from macrophages treated with LPS (2 μg/ml) in SCM for 24 hours. Control medium was collected from macrophages left untreated for 24 hours (basal) or macrophages exposed to SFM for 2 hours then SCM for 22 hours (SFM). The values shown represent the mean (nM/μg of protein) ± SEM of data from experiments performed in triplicate. Statistical analysis was performed using ANOVA followed by the Tukey post test. According to this test there was no statistical difference between the treatments.

% of propidium iodide stained cells	Basal	SFM	Albumin	Fraction V
Macrophages (neonatal)	1.5 ± 1.2	1.6 ± 1.4	1.3 ± 0.6	1.1 ± 1.5
Macrophages (adult)	1.7 ± 1.3	1.3 ± 1.1	1.6 ± 0.9	1.5 ± 1.7

Table 4.6 Analysis of peritoneal macrophage membrane integrity

Peritoneal macrophages isolated from neonatal or adult rats were stained with propidium iodide and fluorescein diacetate to provide an estimation of cell membrane integrity. Macrophages were treated with albumin (12 mg/ml) or fraction V (12 mg/ml) in SFM for 2 hours. The SFM was then replaced with SCM for 22 hours before staining was performed. Control macrophages were either left untreated for 24 hours (basal) or were treated with SFM for 2 hours then SCM for 22 hours (SFM) before staining was performed. Cells possessing propidium iodide staining were expressed as a percentage of the total number of cells counted (cells possessing propidium iodide staining or fluoroscein diacetate staining). The values shown represent the mean ± SEM of data from experiments performed in triplicate. Statistical analysis was performed using ANOVA followed by the Tukey post test. According to this test there was no statistical difference between the treatments.

4.5 Albumin induces microglial proliferation

It was noticed that 24 hours after the addition of albumin, microglial cultures contained a greater number of cells than controls ('basal' or 'SFM'). Subsequently, proliferation was quantified by counting the number of microglia present per field of view. Using this approach albumin (0.1-2 mg/ml) was confirmed to induce a dose dependent increase in microglial number after 24 hours in culture (Fig. 4.9A). Furthermore, albumin treated microglia displayed an increase in the number of processes radiating from their cell bodies, whereas control microglia ('basal' or 'SFM') were amoeboid in appearance exhibiting just a few short processes (Fig. 4.9B).

Albumin induced microglial proliferation was investigated further using the Cell titer 96 Aq_{ueous} one solution proliferation assay kit (cell titer assay). Using this technique, albumin (0.1-2 mg/ml) was also found to induce a dose dependent increase in proliferation after 24 hours in culture (Fig. 4.10A). Since these results corroborated the data obtained by cell counting, the cell titer assay was used in isolation in subsequent proliferation experiments described in this chapter. The effects of fraction V or LPS on microglial proliferation were subsequently studied. Microglia exposed to fraction V (1 mg/ml) proliferated to a similar extent as microglia treated with albumin (1 mg/ml) after 24 hours in culture (Fig. 4.10B). Conversely, microglia treated with LPS (2 μg/ml) for 24 hours did not proliferate above control levels ('basal' or 'SFM'). Next the time course of albumin or fraction V induced proliferation was investigated. This experiment revealed that albumin (1 mg/ml) or fraction V (1 mg/ml) induced similar proliferation profiles temporally. Microglial proliferation was initially detectable between 16-24 hours after albumin (1 mg/ml) or fraction V (1 mg/ml) treatment (Fig. 4.10C). The proliferative response then plateaued between 24-48 hours.

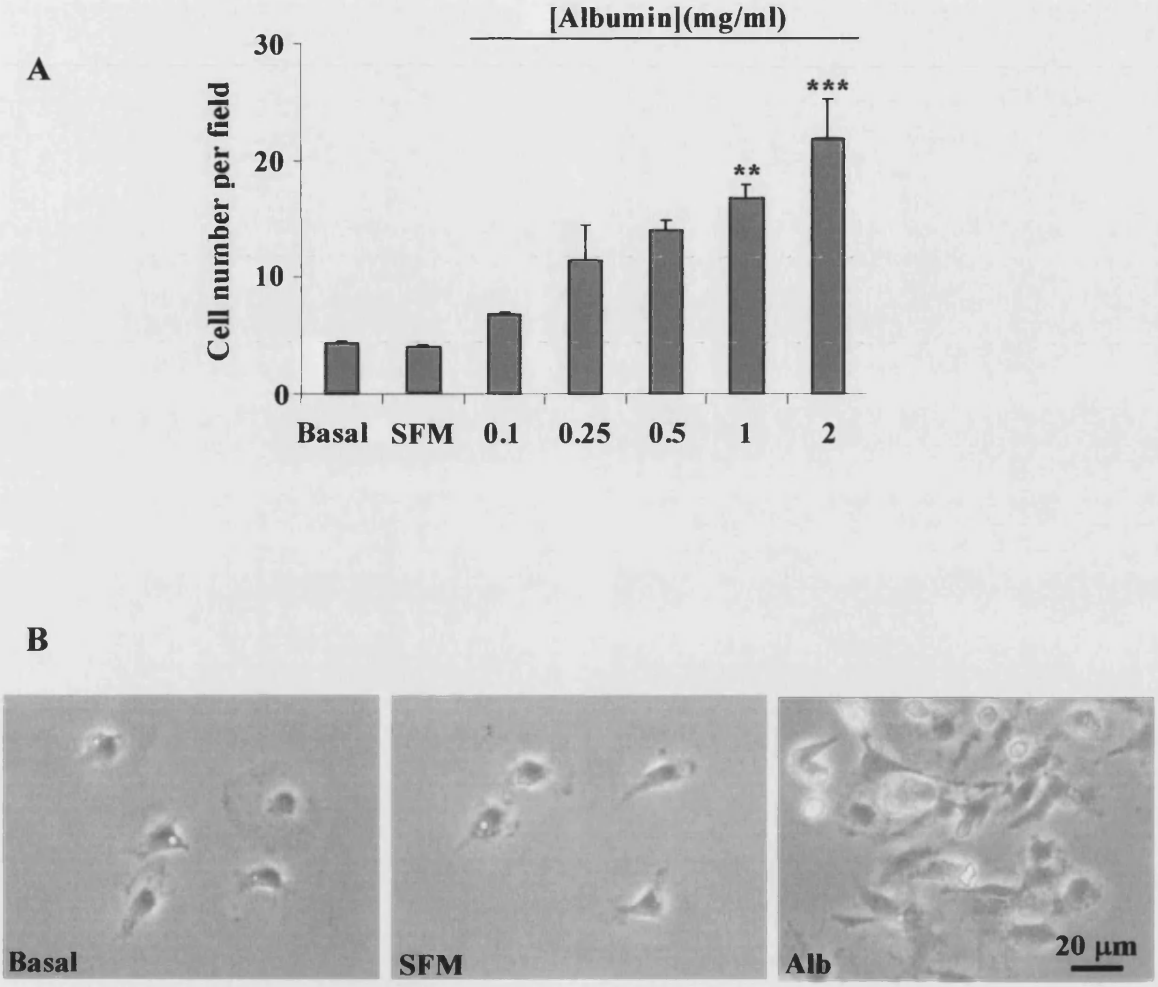

Figure 4.9 Albumin induces microglial proliferation

Microglia proliferation was assessed by counting the number of cells present per field of view. **A**: Microglia were treated with increasing concentrations of albumin (0.1-2 mg/ml) in SFM for 2 hours. The SFM was then replaced with SCM for 22 hours before the cells were counted. Control microglia were either left untreated for 24 hours (basal) or were exposed to SFM for 2 hours then SCM for a further 22 hours (SFM). The values shown represent the mean number of cells present per field ± SEM of data from experiments performed in triplicate. Statistical analysis was performed using ANOVA followed by the Tukey post test. ** $P < 0.01$, *** $P < 0.001$ vs 'basal' or 'SFM'. **B:** The photographs represent control microglia ('basal' or 'SFM') or microglia treated with albumin (Alb: 1 mg/ml) from right to left.

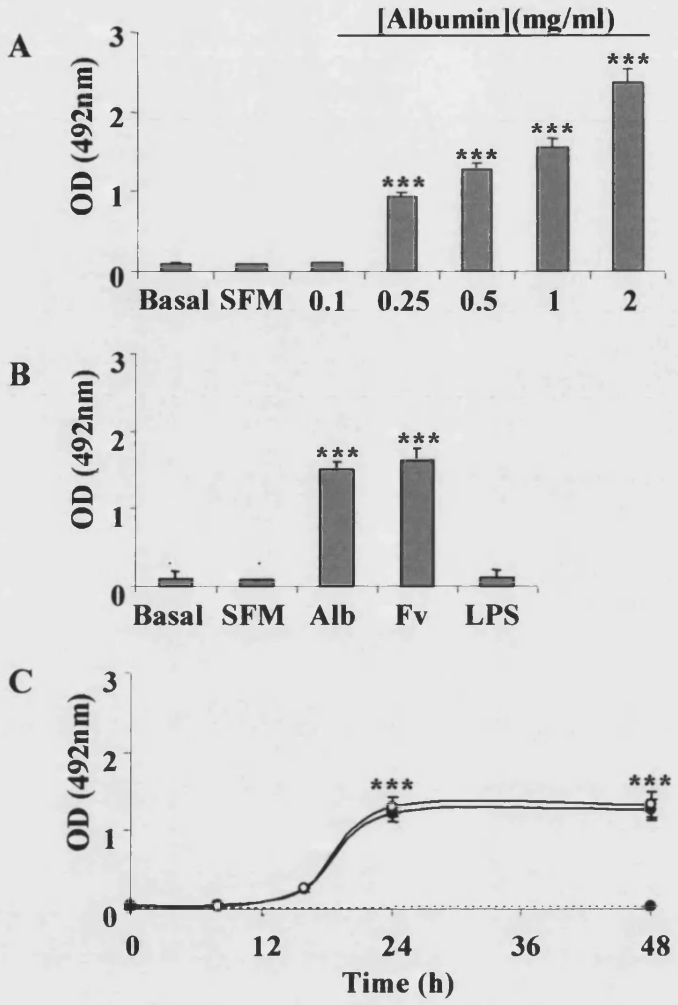

Figure 4.10 Assessment of microglial proliferation

Microglia proliferation was appraised using the cell titer proliferation assay. **A**: Microglia were treated with increasing concentrations of albumin (0.1-2 mg/ml) in SFM for 2 hours. The SFM was then replaced with SCM for 22 hours before the assay was performed. Control microglia were either left untreated for 24 hours (basal) or were exposed to SFM for 2 hours then SCM for 22 hours (SFM) before proliferation was assessed. **B**: Microglia were treated with albumin (Alb: 1 mg/ml) or fraction V (Fv: 1 mg/ml) in SFM for 2 hours. The SFM was then replaced with SCM for 22 hours before the assay was performed. In addition, microglia treated with LPS (2 μg/ml) in SCM for 24 hours were assessed for proliferation. Control microglia were treated as described in A. **C**: Microglia were exposed to albumin (1 mg/ml; open circles) or fraction V (1 mg/ml; closed circles) in SFM for 2 hours. The SFM was then replaced with SCM for 6, 14, 22 or 46 hours before the proliferation assay was performed. Control microglia were subjected to SFM for 2 hours then SCM for 46 hours (SFM) (dotted line). The values shown represent the mean ± SEM of data from experiments performed in triplicate. Statistical analysis was performed using ANOVA followed by the Tukey post test. *** $P < 0.001$ vs control (A,B: control describes 'basal' or 'SFM'; C: control describes time 0).

The signalling cascades that mediate albumin or fraction V induced proliferation were explored using a variety of inhibitors. Pre-treating microglia with AMT-HCl (0.3 μM), pertussis toxin (Ptx: 2 μg/ml) or UO126 (5 μM) did not modulate albumin (1 mg/ml) or fraction V (1 mg/ml) induced proliferation (Fig. 4.11A,B). Furthermore, microglia treated with the inhibitors alone proliferated to a similar extent as control microglia ('basal' of 'SFM'). In contrast, pre-treating microglia with BAPTA-AM (10 μM), U73122 (2 μM) or PP2 (100 nM) reduced albumin (1 mg/ml) or fraction V (1 mg/ml) induced proliferation to control levels ('basal' or 'SFM'). Moreover, these inhibitors did not adversely effect proliferation when incubated with the microglia alone.

Since BAPTA-AM inhibited albumin or fraction V induced proliferation the response was deemed to be calcium dependent, consequently intracellular calcium fluxes were monitored in N9 microglia using fura-2. The N9 cell line is a well characterised microglial cell line, which exhibits similar responses to primary microglia (Corradin et al., 1993; Ferrari et al., 1996; Kingham et al., 1999). Accordingly, albumin (1 mg/ml) or fraction V (1 mg/ml) triggered iNOS expression in N9 microglia, whereas control N9 cells ('basal' or 'SFM') did not express iNOS (Fig. 4.12A). Furthermore, albumin (1 mg/ml) or fraction V (1 mg/ml) induced a large increase in N9 proliferation above control levels ('basal' or 'SFM') (Fig. 4.12B). However, control N9 microglia ('basal' or 'SFM') exhibited a higher basal level of proliferation in comparison to control primary microglia ('basal' or 'SFM'), which was attributed to the fact that the N9 cell line actively proliferates in culture.

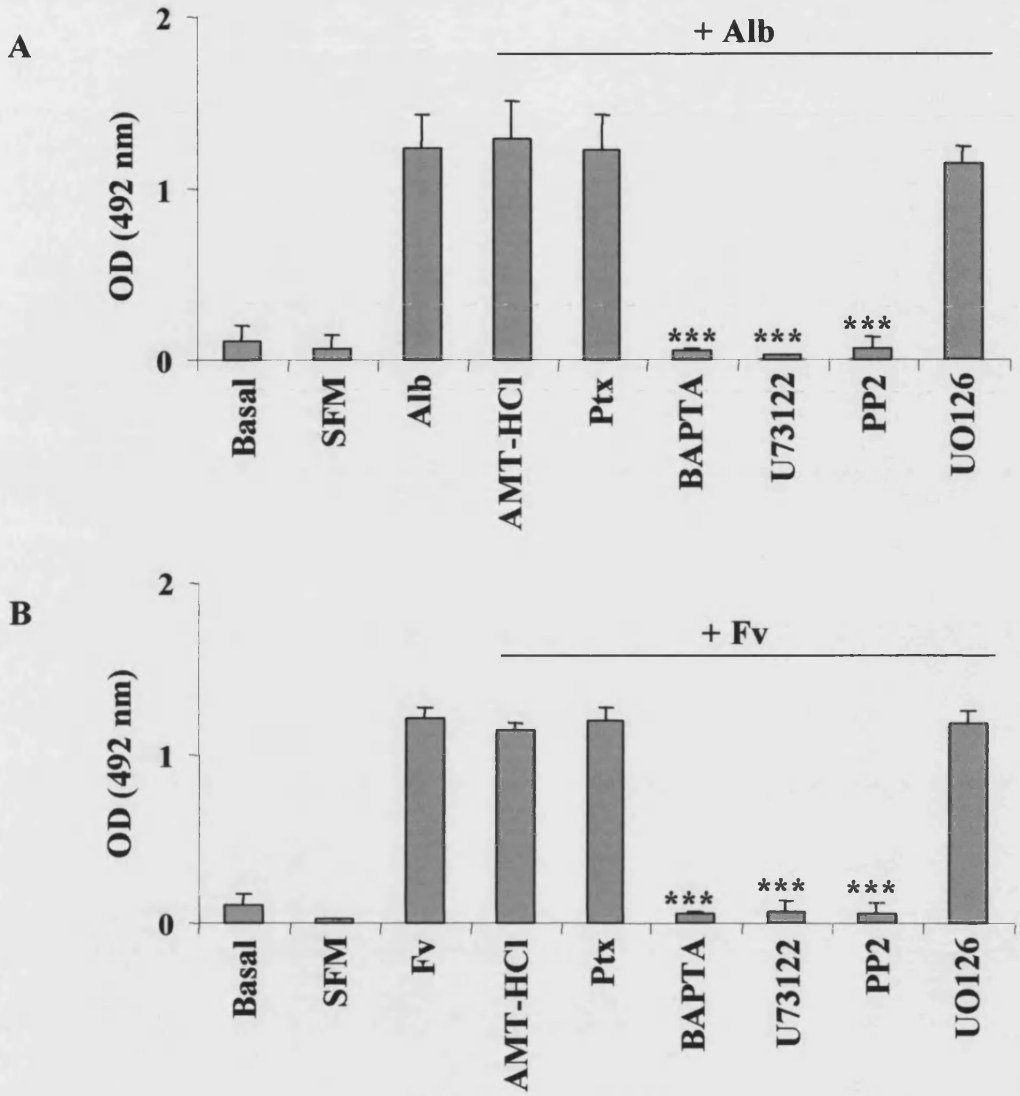

Figure 4.11 Modulation of albumin or fraction V induced microglial proliferation

Microglia proliferation was appraised using the cell titer proliferation assay. Microglia were treated with albumin (Alb: 1 mg/ml) (**A**) or fraction V (Fv: 1mg/ml) (**B**) in SFM for 2 hours. The SFM was then replaced with SCM for 22 hours before the assay was performed. In addition, microglia were treated with albumin (Alb: 1 mg/ml) or fraction V (Fv: 1 mg/ml) in SFM in the presence of AMT-HCl (0.3 μM), pertussis toxin (Ptx: 2 μg/ml), BAPTA-AM (10 μM), U73122 (2 μM), PP2 (100 nM) or UO126 (5 μM). At 2 hours the SFM was replaced with SCM supplemented with the appropriate concentration of inhibitor for a further 22 hours before proliferation was assessed. Control microglia were left untreated for 24 hours (basal) or exposed to SFM for 2 hours then SCM for 22 hours (SFM). The values shown represent the mean ± SEM of data from experiments performed in triplicate. Statistical analysis was performed using ANOVA followed by the Tukey post test. *** $P < 0.001$ vs albumin (Alb) or fraction V (Fv) treated respectively.

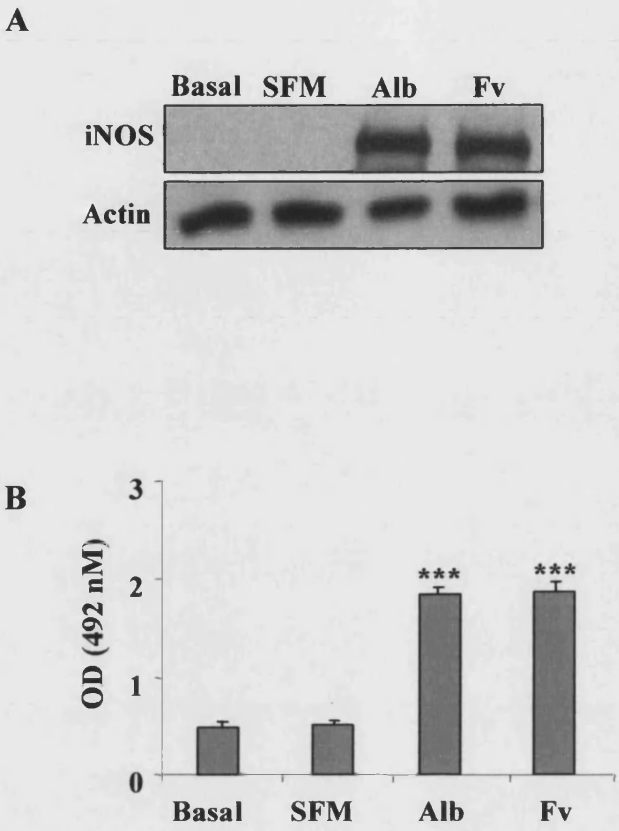

Figure 4.12 Albumin or fraction V induces iNOS synthesis and proliferation in N9 microglia
Representative Western blot of iNOS expression in N9 microglia cell lysates (**A**). N9 Microglia were exposed to albumin (Alb: 1 mg/ml) or fraction V (Fv: 1 mg/ml) in SFM for 2 hours. The SFM was then replaced with SCM for 22 hours before lysates were prepared. Control lysates were prepared from N9 microglia left untreated for 24 hours (basal) or N9 microglia exposed to SFM for 2 hours then SCM for 22 hours (SFM). Lysates were subjected to Western blot analysis using an antibody raised against iNOS. To ensure equal protein loading blots were reprobed with an antibody recognising β-actin. N9 proliferation was appraised using the cell titer proliferation assay (**B**). N9 microglia were treated with albumin (Alb: 1 mg/ml) or fraction V (Fv: 1 mg/ml) in SFM for 2 hours. The SFM was then replaced with SCM for 22 hours before the assay was performed. Control N9 microglia were left untreated for 24 hours (basal) or were exposed to SFM for 2 hours then SCM for 22 hours (SFM). The values shown represent the mean ± SEM of data from experiments performed in triplicate. Statistical analysis was performed using ANOVA followed by the Tukey post test. *** $P < 0.001$ vs control (control describes 'basal' or 'SFM').

Calcium imaging was performed in basic medium in the absence of serum; therefore interference from endogenous albumin in the serum was not a problem. Albumin (1 mg/ml) or fraction V (1 mg/ml) was found to induce a mono-phasic increase in intracellular calcium, whereas calcium transients were not elicited in control N9 microglia (Fig. 4.13). In a subsequent experiment calcium transients induced by albumin (Fig. 4.14) or fraction V (Fig. 4.15) were demonstrated to be dose dependent; a minimum of 0.5 mg/ml of albumin or fraction V was required to elicit a response and maximal responses were obtained with 4 mg/ml of either activator. To ascertain whether calcium fluxes were store mediated, the effect of the Ca^{2+}-ATPase inhibitor thapsigargin on albumin or fraction V-induced calcium transients was explored. The application of thapsigargin (1 μM) elicited an extended calcium response of low amplitude, which returned to baseline after approximately 600 seconds (Fig. 4.16). This phenomenon was attributed to the depletion of intracellular calcium stores occurring as a result of the inhibition of calcium re-uptake. The subsequent application of albumin (1 mg/ml) or fraction V (1 mg/ml) to thapsigargin pre-treated N9 microglia did not elicit increases in intracellular calcium. These findings imply that albumin or fraction V evoke calcium release from intracellular stores. To determine the signalling pathways upstream of calcium release the effects of various inhibitors were studied. Pre-treating microglia with pertussis toxin (Ptx: 2 μg/ml) or UO126 (5 μM) did not modulate albumin (1 mg/ml) (Fig. 4.17) or fraction V (1 mg/ml) (Fig. 4.18) induced calcium transients. Furthermore, the inhibitors did not evoke changes in intracellular calcium when incubated with the microglia alone. In contrast, pre-treating microglia with U73122 (2 μM) or PP2 (100 nM) entirely abated albumin (1 mg/ml) (Fig. 4.17) or fraction V (1 mg/ml) (Fig. 4.18) induced calcium transients. Again, these inhibitors did not evoke changes in intracellular calcium when incubated with the microglia alone.

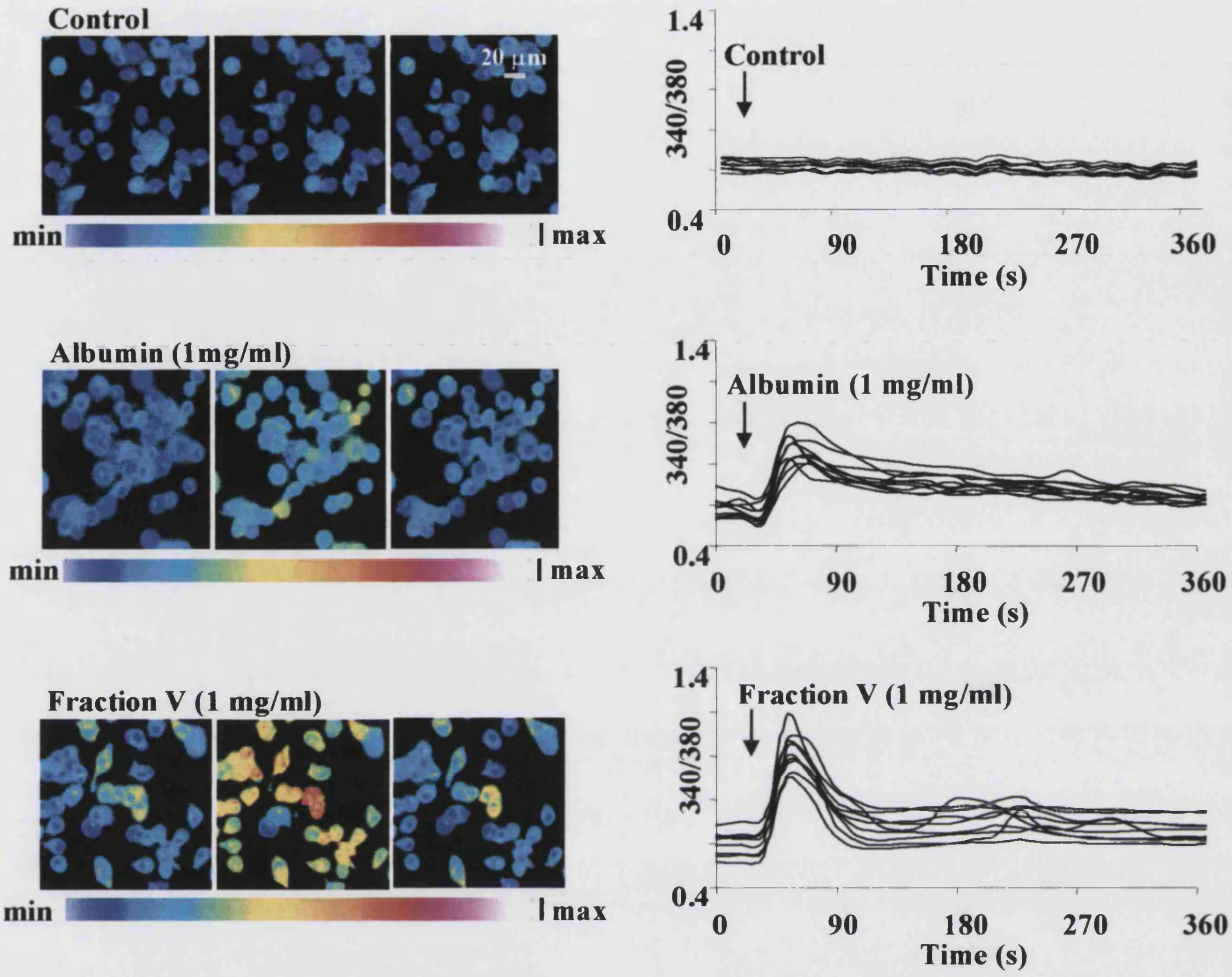

Figure 4.13 Effects of albumin or fraction V on intracellular calcium transients in N9 cells
Representative false colour images and traces depicting intracellular calcium transients evoked in albumin or fraction V treated N9 microglia. N9 microglia were loaded with fura-2 (5 µM) in basic medium for 45 minutes at 37 °C. Cells were subsequently excited with wavelengths of 340 and 380 nm and emission was collected at a wavelength of 510 nm. Albumin (1 mg/ml) or fraction V (1 mg/ml) diluted in basic medium was added to the cells 60 seconds after the commencement of excitation. Control N9 cells were treated with basic medium in the absence of albumin or fraction V at the same time point. Calcium responses were recorded from ten cells and the results were expressed as 340/380 fluorescence ratios. False colour images corresponding to each treatment are also displayed. Images were captured at 0, 70 and 300 seconds (from left to right) and the scale bar provides an indication of intracellular calcium levels.

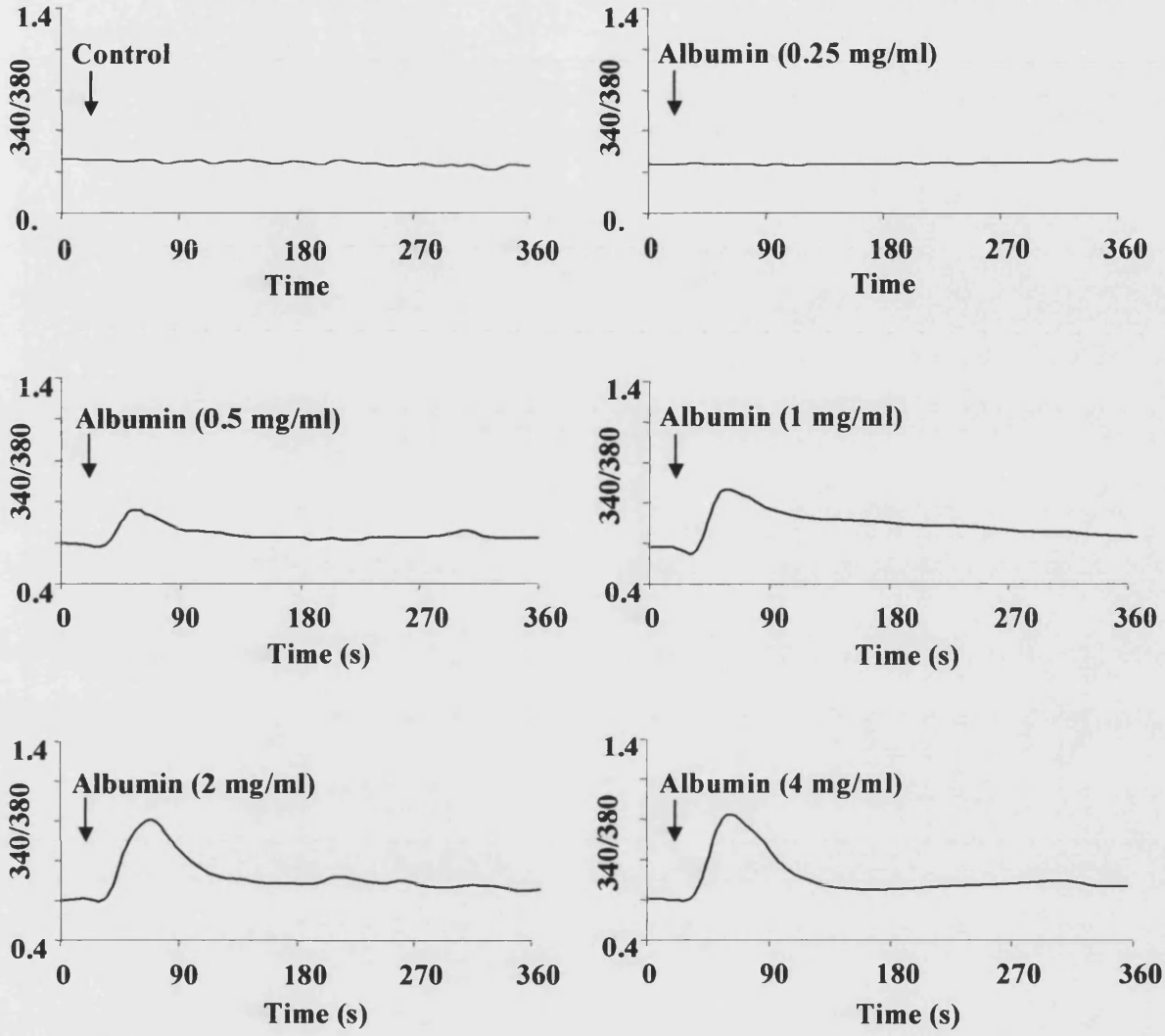

Figure 4.14 Dose dependency of albumin on intracellular calcium transients in N9 cells

Representative traces depicting intracellular calcium transients evoked by increasing concentrations of albumin in N9 microglia. N9 microglia were loaded with fura-2 (5 μM) in basic medium for 45 minutes at 37 °C. Cells were subsequently excited with wavelengths of 340 and 380 nm and emission was collected at a wavelength of 510 nm. Albumin (0.25-4 mg/ml) diluted in basic medium was added to the cells 60 seconds after the commencement of excitation. Control N9 cells were treated with basic medium in the absence of albumin at the same time point. Calcium responses were recorded from ten cells and the results were averaged and expressed as 340/380 fluorescence ratios.

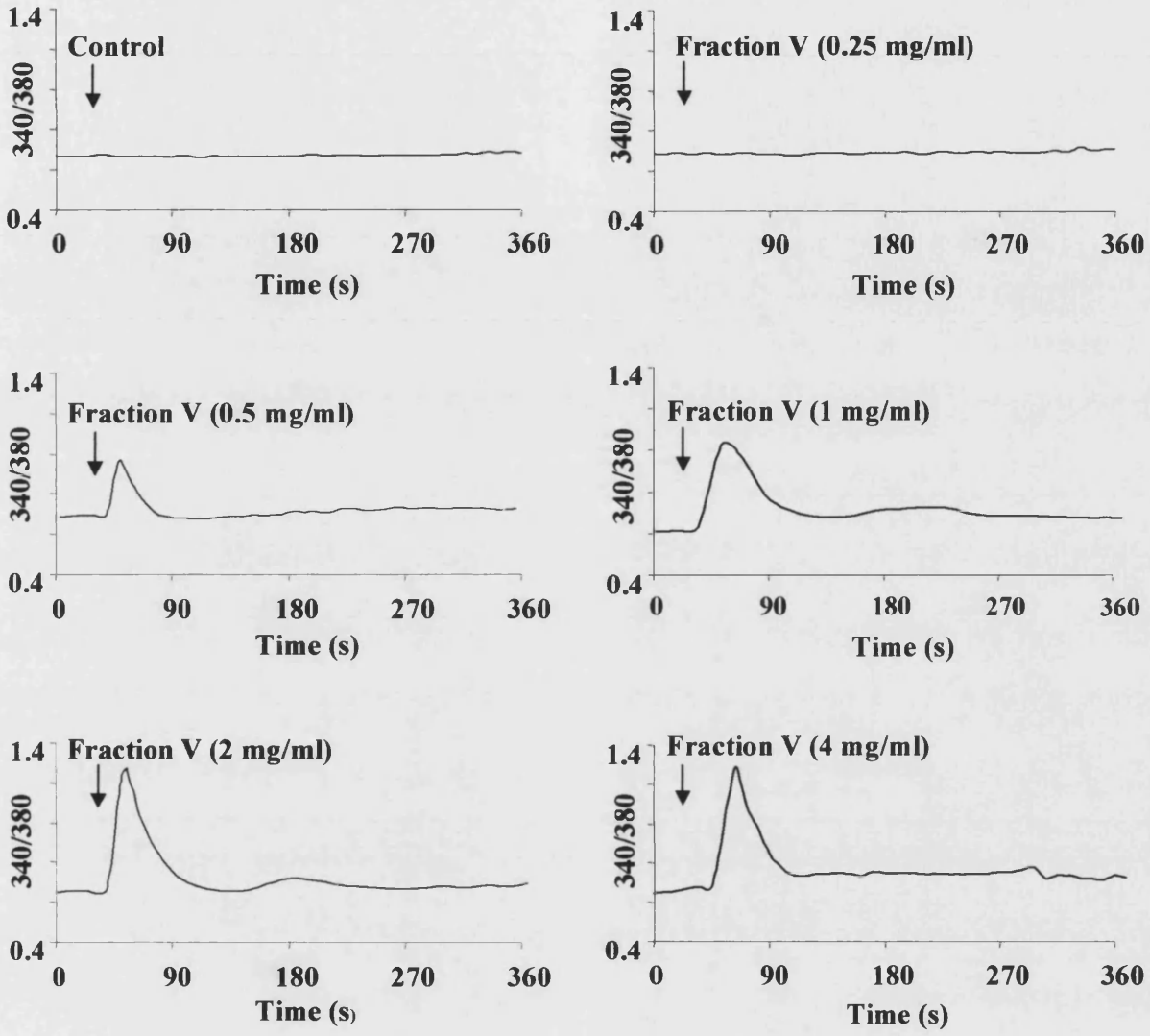

Figure 4.15 Dose dependency of fraction V on intracellular calcium transients in N9 cells
Representative traces depicting intracellular calcium transients evoked by increasing concentrations of fraction V in N9 microglia. N9 microglia were loaded with fura-2 (5 μM) in basic medium for 45 minutes at 37 °C. Cells were subsequently excited with wavelengths of 340 and 380 nm and emission was collected at a wavelength of 510 nm. Fraction V (0.25-4 mg/ml) diluted in basic medium was added to the cells 60 seconds after the commencement of excitation. Control N9 cells were treated with basic medium in the absence of fraction V at the same time point. Calcium responses were recorded from ten cells and the results were averaged and expressed as 340/380 fluorescence ratios.

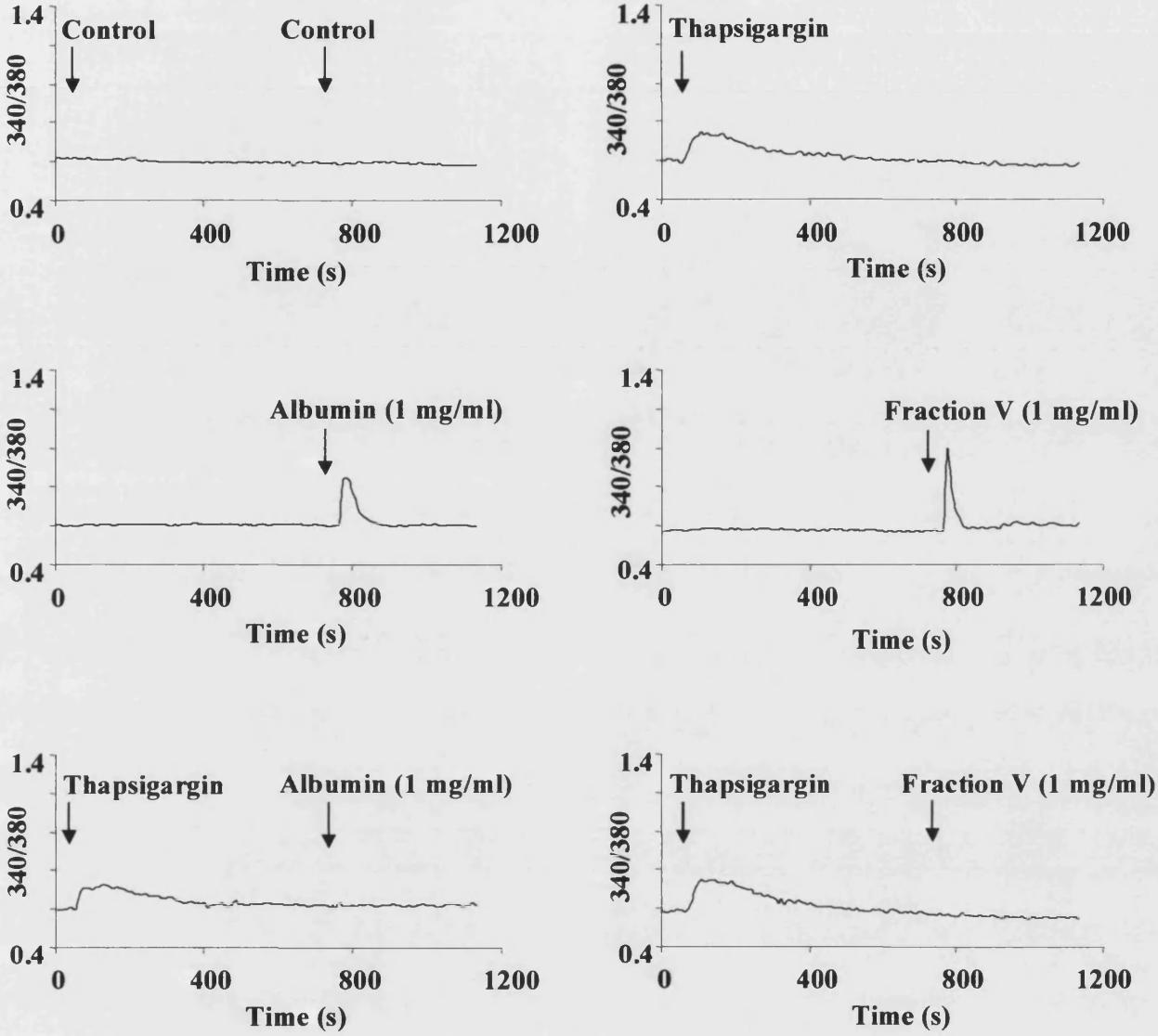

Figure 4.16 Thapsigargin inhibits albumin or fraction V induced calcium fluxes in N9 cells
Representative traces illustrating the effects of thapsigargin on intracellular calcium transients evoked by albumin or fraction V in N9 microglia. N9 microglia were loaded with fura-2 (5 μM) in basic medium for 45 minutes at 37 °C. Cells were subsequently excited with wavelengths of 340 and 380 nm and emission was collected at a wavelength of 510 nm. Albumin (1 mg/ml) or fraction V (1 mg/ml) diluted in basic medium was added to the cells 760 seconds after the commencement of excitation. In addition, N9 microglia were treated with albumin (1 mg/ml) or fraction V (1 mg/ml) in the presence of thapsigargin (1 μM), which was added at 60 seconds. Microglia were also treated with thapsigargin (1 μM) alone. Control microglia were treated with basic medium in the absence of any other stimulus. Calcium responses were recorded from ten cells and the results were averaged and expressed as 340/380 fluorescence ratios.

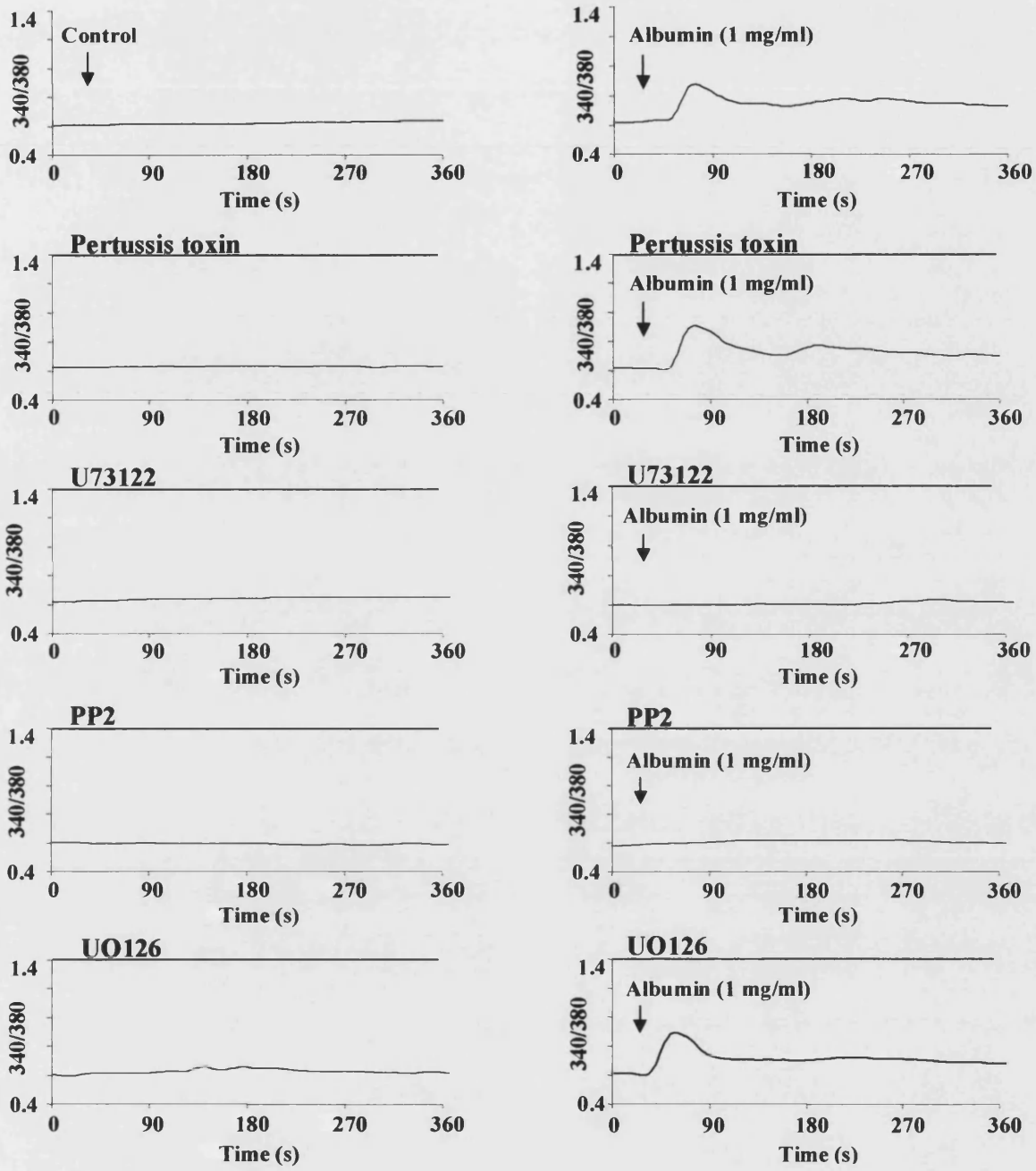

Figure 4.17 Modulation of albumin induced calcium transients in N9 cells

Representative traces depicting the effects of various inhibitors on intracellular calcium transients evoked by albumin in N9 microglia. N9 microglia were loaded with fura-2 (5 μM) in basic medium for 45 minutes at 37 °C. Cells were subsequently excited with wavelengths of 340 and 380 nm and emission was collected at a wavelength of 510 nm. Albumin (1 mg/ml) diluted in basic medium was added to the cells 60 seconds after the commencement of excitation. In addition, N9 microglia were treated with albumin (1 mg/ml) in the presence of pertussis toxin (2 μg/ml), U73122 (2 μM), PP2 (500 nM) or UO126 (20 μM). Microglia were also treated with the inhibitors alone. Control microglia were treated with basic medium in the absence of any other stimulus. Calcium responses were recorded from ten cells and the results were averaged and expressed as 340/380 fluorescence ratios.

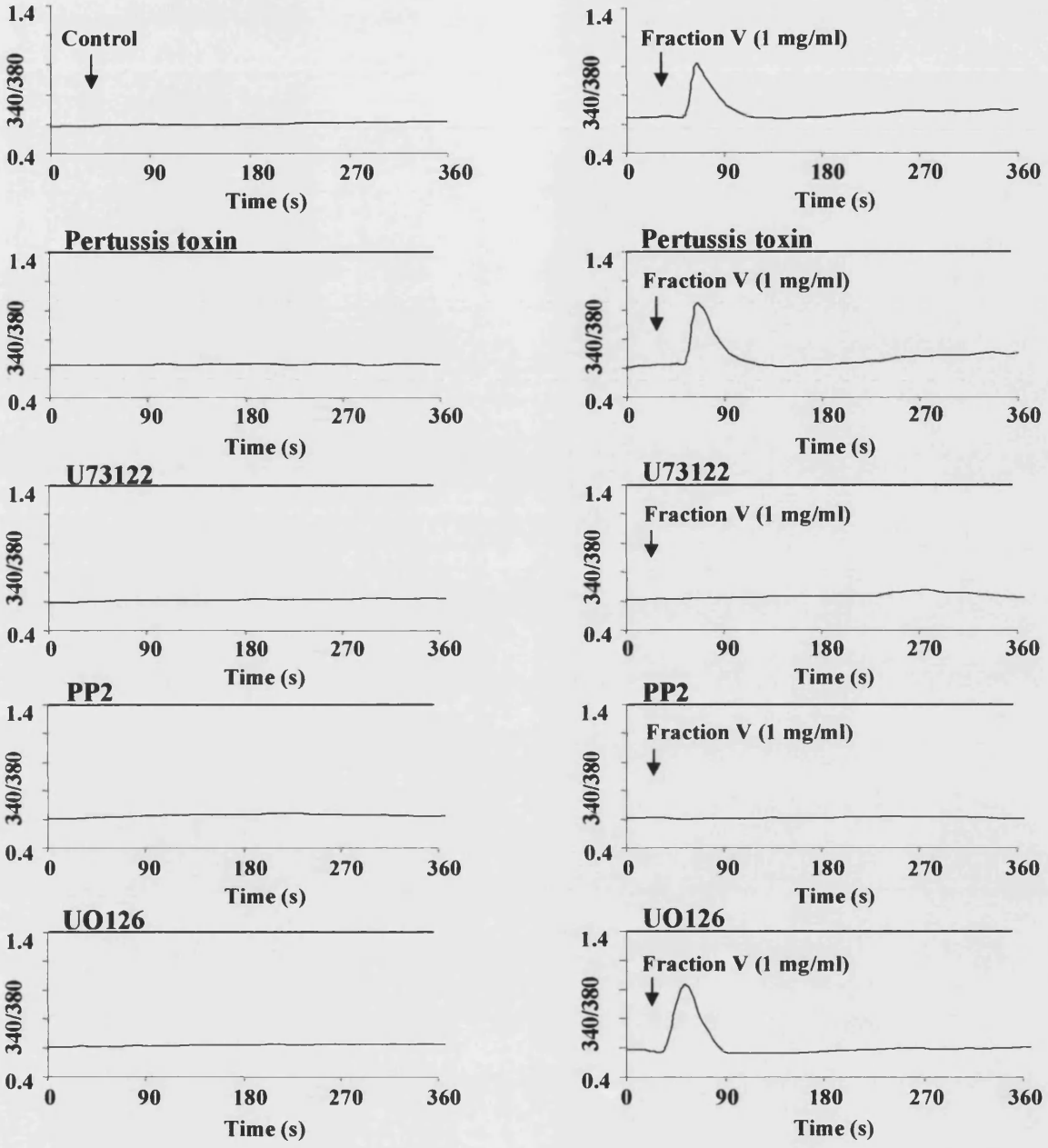

Figure 4.18 Modulation of fraction V induced calcium transients in N9 cells

Representative traces depicting the effects of various inhibitors on intracellular calcium transients evoked by fraction V in N9 microglia. N9 microglia were loaded with fura-2 (5 μM) in basic medium for 45 minutes at 37 °C. Cells were subsequently excited with wavelengths of 340 and 380 nm and emission was collected at a wavelength of 510 nm. Fraction V (1 mg/ml) diluted in basic medium was added to the cells 60 seconds after the commencement of excitation. In addition, N9 microglia were treated with fraction V (1 mg/ml) in the presence of pertussis toxin (2 μg/ml), U73122 (2 μM), PP2 (500 nM) or UO126 (20 μM). Microglia were also treated with the inhibitors alone. Control microglia were treated with basic medium in the absence of any other stimulus. Calcium responses were recorded from ten cells and the results were averaged and expressed as 340/380 fluorescence ratios.

The ability of albumin or fraction V to induce proliferation in macrophages isolated from neonatal or adult rats was subsequently investigated. Counting the number of macrophages present per field of view revealed that exposure to albumin (1, 2 or 12 mg/ml) or fraction V (1, 2 or 12 mg/ml) did not increase cell numbers above control levels after 24 hours in culture ('basal' or 'SFM') (Table. 4.7A). These findings were mirrored using the cell titer assay (Table. 4.7B). Furthermore, LPS (2 μg/ml) did not induce macrophage proliferation after 24 hours in culture as assessed using either assay (Table. 4.7A,B). Interestingly, macrophages adopted a bipolar morphology in the presence of high concentrations of albumin (12 mg/ml) or fraction V (12 mg/ml), whereas macrophages treated with LPS (2 μg/ml) or lower concentrations of albumin or fraction V were amoeboid in appearance as were control macrophages ('basal' or 'SFM') (Fig. 4.19). Moreover, albumin (1-12 mg/ml) or fraction V (1-12 mg/ml) did not induce calcium transients in macrophages isolated from either neonatal (Fig. 4.20) or adult rats (Fig. 4.21). In contrast, thapsigargin (1 μM) evoked the release of calcium from intracellular stores in macrophages isolated from either age rat, which confirms that the stores are full and capable of mounting a response. Macrophages were more sensitive than microglia to thapsigargin treatment; thapsigargin led to a sustained enhancement of intracellular calcium, which did not return to baseline even after 1200 seconds (20 minutes) (Fig. 4.20, Fig. 4.21: insets). To determine whether calcium release from intracellular stores was sufficient to initiate proliferation, microglia and macrophages were treated with thapsigargin (1-1000 nM) for 8, 24, or 48 hours. However, thapsigargin treatment did not induce a proliferative response in either of the cell types at any of the time points studied (Table. 4.8).

A

	Cell number per field	
Treatment	**Adult**	**Neonate**
Basal	6.3 ± 3.7	6.3 ± 1.6
SFM	6.4 ± 8.2	6.4 ± 0.4
1 mg/ml albumin	6.5 ± 0.1	6.1 ± 0.2
1 mg/ml fraction V	6.0 ± 0.5	6.2 ± 0.0
2 mg/ml albumin	6.2 ± 6.1	6.4 ± 7.4
2 mg/ml fraction V	6.0 ± 4.9	6.4 ± 4.9
12 mg/ml albumin	6.1 ± 1.2	6.2 ± 2.9
12 mg/ml fraction V	6.2 ± 2.9	6.1 ± 0.4
LPS (2 μg/ml)	6.3 ± 2.0	6.2 ± 0.6

B

	Optical density (492 nm)	
Treatment	**Adult**	**Neonate**
Basal	0.23 ± 0.1	0.22 ± 0.1
SFM	0.24 ± 0.1	0.23 ± 0.1
1 mg/ml albumin	0.25 ± 0.1	0.20 ± 0.1
1 mg/ml fraction V	0.25 ± 0.1	0.26 ± 0.2
2 mg/ml albumin	0.24 ± 0.1	0.22 ± 0.1
2 mg/ml fraction V	0.24 ± 0.1	0.23 ± 0.1
12 mg/ml albumin	0.22 ± 0.1	0.23 ± 0.1
12 mg/ml fraction V	0.25 ± 0.1	0.22 ± 0.1
LPS (2 μg/ml)	0.23 ± 0.2	0.2 ± 0.3

Table 4.7 Assessment of peritoneal macrophage proliferation

Macrophage proliferation was assessed by counting the number of cells present per field (**A**) or the cell titer assay (**B**). Peritoneal macrophages isolated from neonatal or adult rats were treated with increasing concentrations of albumin (1, 2 or 12 mg/ml) or fraction V (1, 2 or 12 mg/ml) in SFM for 2 hours. The SFM was then replaced with SCM for 22 hours before proliferation was assessed. In addition, macrophages treated with LPS (2 μg/ml) in SCM for 24 hours were assessed for proliferation. Control macrophages were left untreated for 24 hours (basal) or were exposed to SFM for 2 hours then SCM for 22 hours (SFM). The values shown represent the mean ± SEM of data from experiments performed in triplicate. Statistical analysis was performed using ANOVA followed by the Tukey post test. There was no statistical difference between treatments.

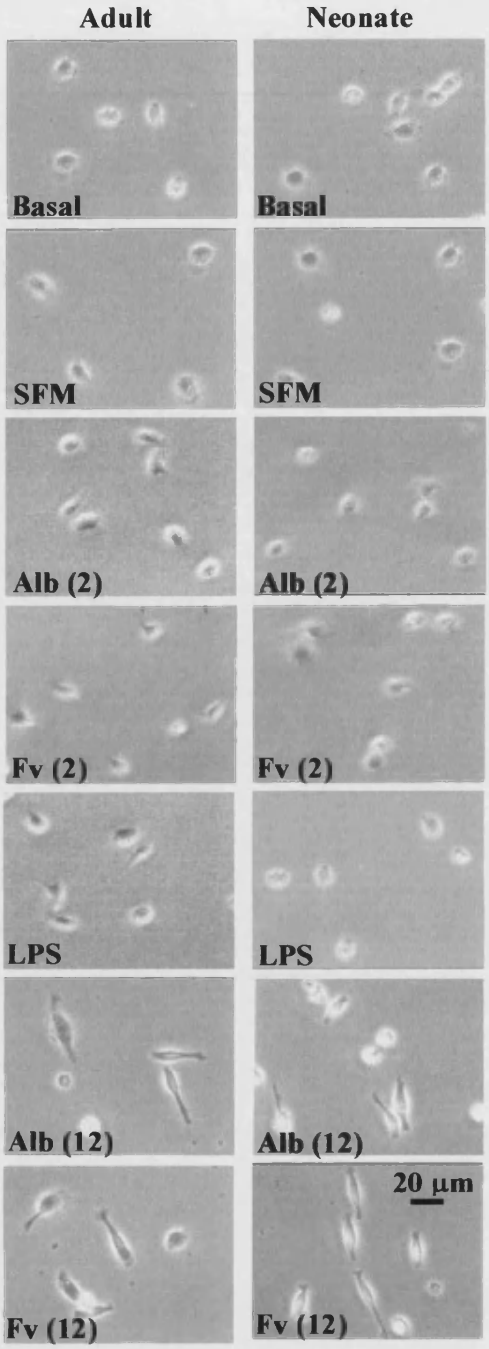

Figure 4.19 Peritoneal macrophage morphology

The photographs represent control macrophages ('basal' or 'SFM') or macrophages treated with albumin, fraction V or LPS. Peritoneal macrophages isolated from neonatal or adult rats were treated with albumin (Alb: 2 or 12 mg/ml) or fraction V (Fv: 2 or 12 mg/ml) in SFM for 2 hours. The SFM was then replaced with SCM for 22 hours before photographs were taken. In addition, macrophages were treated with LPS in SCM for 24 hours. Control macrophages were left untreated for 24 hours (basal) or were exposed to SFM for 2 hours then SCM for 22 hours (SFM).

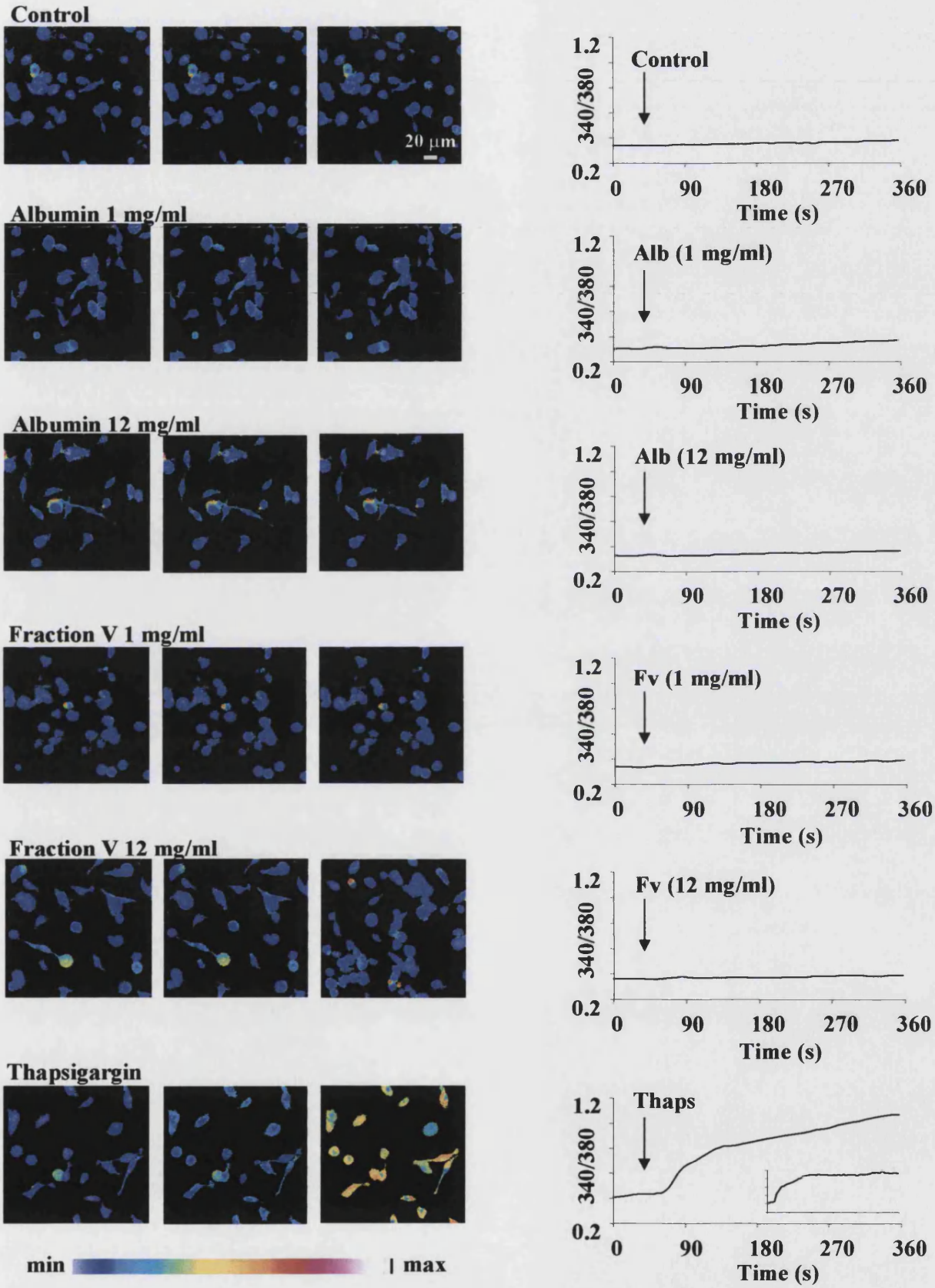

Figure 4.20 (see overleaf for figure legend)

Figure 4.20 Calcium transients elicited in peritoneal macrophages from neonatal rats
Representative false colour images and traces depicting intracellular calcium levels in albumin, fraction V or thapsigargin treated peritoneal macrophages (isolated from neonatal rats). Peritoneal macrophages isolated from neonatal rats were loaded with fura-2 (5 μM) in basic medium for 45 minutes at 37 °C. Cells were subsequently excited with wavelengths of 340 and 380 nm and emission was collected at a wavelength of 510 nm. Albumin (Alb: 1 or 12 mg/ml), fraction V (Fv: 1 or 12 mg/ml) or thapsigargin (Thaps: 1 μM) diluted in basic medium was added to the cells 60 seconds after the commencement of excitation. Control cells were treated with basic medium in the absence of any other stimulus at the same time point. Calcium responses were recorded from ten cells and the results were expressed as 340/380 fluorescence ratios. False colour images corresponding to each treatment are also displayed. Images were captured at 0, 70 and 300 seconds (from left to right) and the scale bar provides an indication of intracellular calcium levels. **Inset**: Trace depicting the effects of thapsigargin (1 μM) over a 1200 second period.

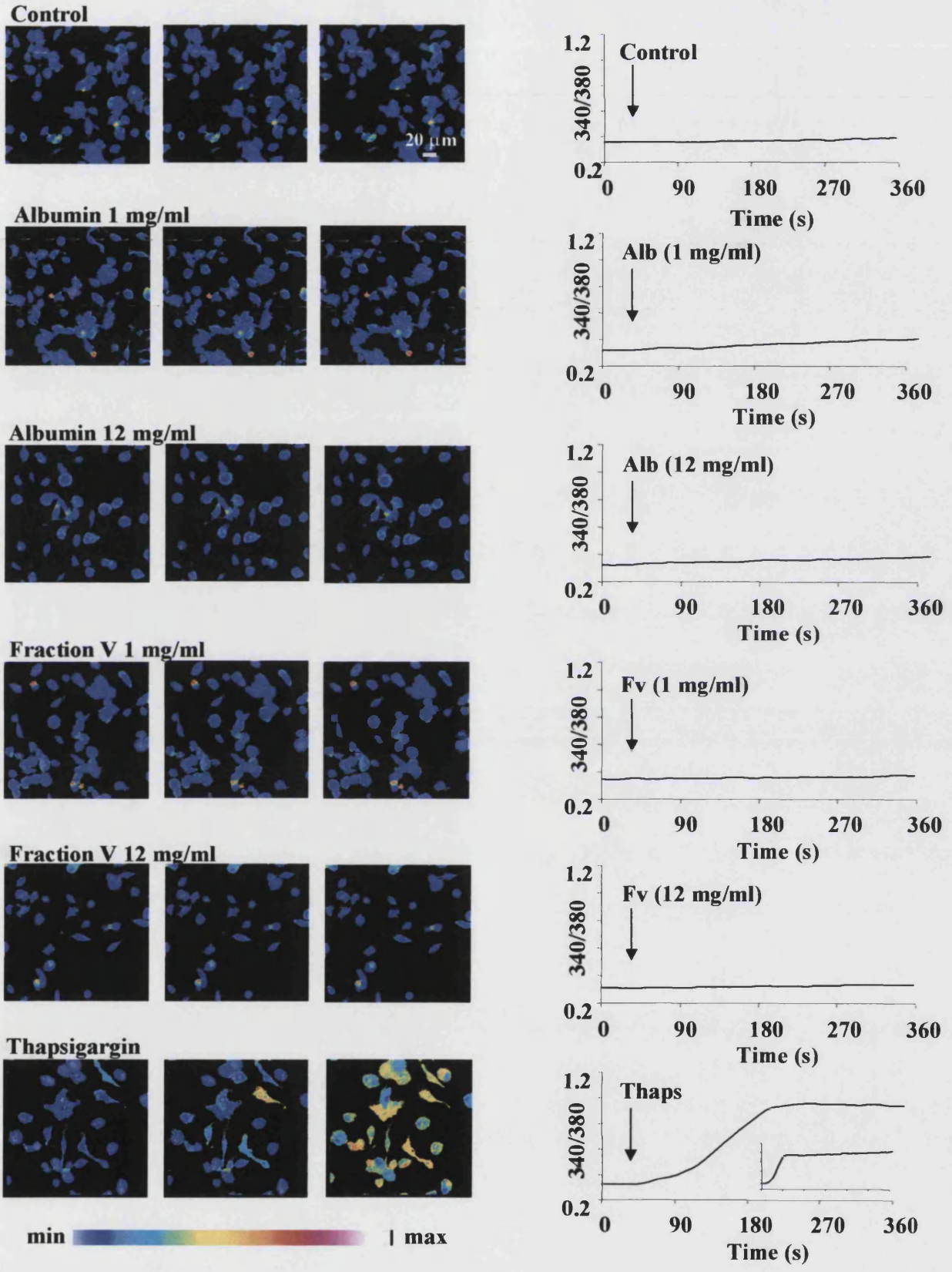

Figure 4.21 (see overleaf for figure legend)

Figure 4.21 Calcium transients elicited in peritoneal macrophages from adult rats

Representative false colour images and traces depicting intracellular calcium levels in albumin, fraction V or thapsigargin treated peritoneal macrophages (isolated from adult rats). Peritoneal macrophages isolated from adult rats were loaded with fura-2 (5 μM) in basic medium for 45 minutes at 37 °C. Cells were subsequently excited with wavelengths of 340 and 380 nm and emission was collected at a wavelength of 510 nm. Albumin (Alb: 1 or 12 mg/ml), fraction V (Fv: 1 or 12 mg/ml) or thapsigargin (Thaps: 1 μM) diluted in basic medium was added to the cells 60 seconds after the commencement of excitation. Control cells were treated with basic medium in the absence of any other stimulus at the same time point. Calcium responses were recorded from ten cells and the results were expressed as 340/380 fluorescence ratios. False colour images corresponding to each treatment are also displayed. Images were captured at 0, 70 and 300 seconds (from left to right) and the scale bar provides an indication of intracellular calcium levels. **Inset**: Trace depicting the effects of thapsigargin (1 μM) over a 1200 second period.

A

[Thapsigargin]	Macrophage (adult)	Macrophage (neonate)	Microglia
0 (basal)	0.21 ± 0.06	0.16 ± 0.01	0.1 ± 0.01
1 nM	0.16 ± 0.02	0.19 ± 0.04	0.09 ± 0.02
10 nM	0.18 ± 0.06	0.13 ± 0.03	0.08 ± 0.01
100 nM	0.17 ± 0.06	0.18 ± 0.04	0.09 ± 0.01
1000 nM	0.17 ± 0.04	0.19 ± 0.01	0.1 ± 0.01

B

[Thapsigargin]	Macrophage (adult)	Macrophage (neonate)	Microglia
0 (basal)	0.2 ± 0.05	0.18 ± 0.06	0.17 ± 0.03
1 nM	0.23 ± 0.02	0.2 ± 0.07	0.18 ± 0.02
10 nM	0.17 ± 0.06	0.18 ± 0.05	0.18 ± 0.02
100 nM	0.16 ± 0.02	0.24 ± 0.06	0.17 ± 0.01
1000 nM	0.2 ± 0.03	0.2 ± 0.02	0.2 ± 0.01

C

[Thapsigargin]	Macrophage (adult)	Macrophage (neonate)	Microglia
0 (basal)	0.16 ± 0.01	0.15 ± 0.01	0.16 ± 0.01
1 nM	0.22 ± 0.01	0.15 ± 0.01	0.17 ± 0.02
10 nM	0.21 ± 0.01	0.13 ± 0.01	0.16 ± 0.01
100 nM	0.24 ± 0.02	0.14 ± 0.02	0.15 ± 0.01
1000 nM	0.17 ± 0.01	0.13 ± 0.01	0.15 ± 0.02

Table 4.8 Effects of thapsigargin on microglial or peritoneal macrophage proliferation
Proliferation was assessed using the cell titer assay. Microglia or peritoneal macrophages isolated from neonatal or adult rats were treated with increasing concentrations of thapsigargin (1-1000 nM) in SCM for 8 (**A**), 24 (**B**), or 48 (**C**) hours. Control cells were left untreated for 8, 24 or 48 hours respectively (0: basal). The values shown represent the mean ± SEM of data from experiments performed in triplicate. Statistical analysis was performed using ANOVA followed by the Tukey post test. According to this test there was no statistical difference between the treatments.

Next the effects of albumin or fraction V on intracellular free calcium in astrocytes were studied. Fraction V (serum albumin) has previously been shown to evoke calcium waves in astrocytes (Nadal et al., 1995), whilst at low concentrations fraction V causes the uptake of calcium into intracellular stores. The calcium mobilizing action of fraction V is due to the presence of an unidentified protein bound polar lipid, whereas calcium uptake is mediated by the protein component of albumin (Nadal et al., 1996).

In this experiment the TSA-3 astrocyte cell line was used, these cells exhibit similar responses to primary astrocytes and are 100 % pure as determined by GFAP staining (Personal communication: Gareth Pryce). Fraction V was found to trigger calcium transients in TSA-3 astrocytes, whereas lower concentrations of fraction V caused the uptake of calcium into intracellular stores (Fig. 4.22). However, in contrast to the findings reported by Nadal et al., (1995) albumin did not evoke calcium uptake into intracellular stores in TSA-3 astrocytes (Fig. 4.23). In fact albumin did not exert any discernable effects on calcium transients in these cells, which is consistent with findings reported by Tabernero et al., (1999). Collectively, these findings illustrate that albumin triggers different signalling pathways in microglia, macrophages and astrocytes. In particular albumin induces calcium transients in microglia but not macrophages or astrocytes.

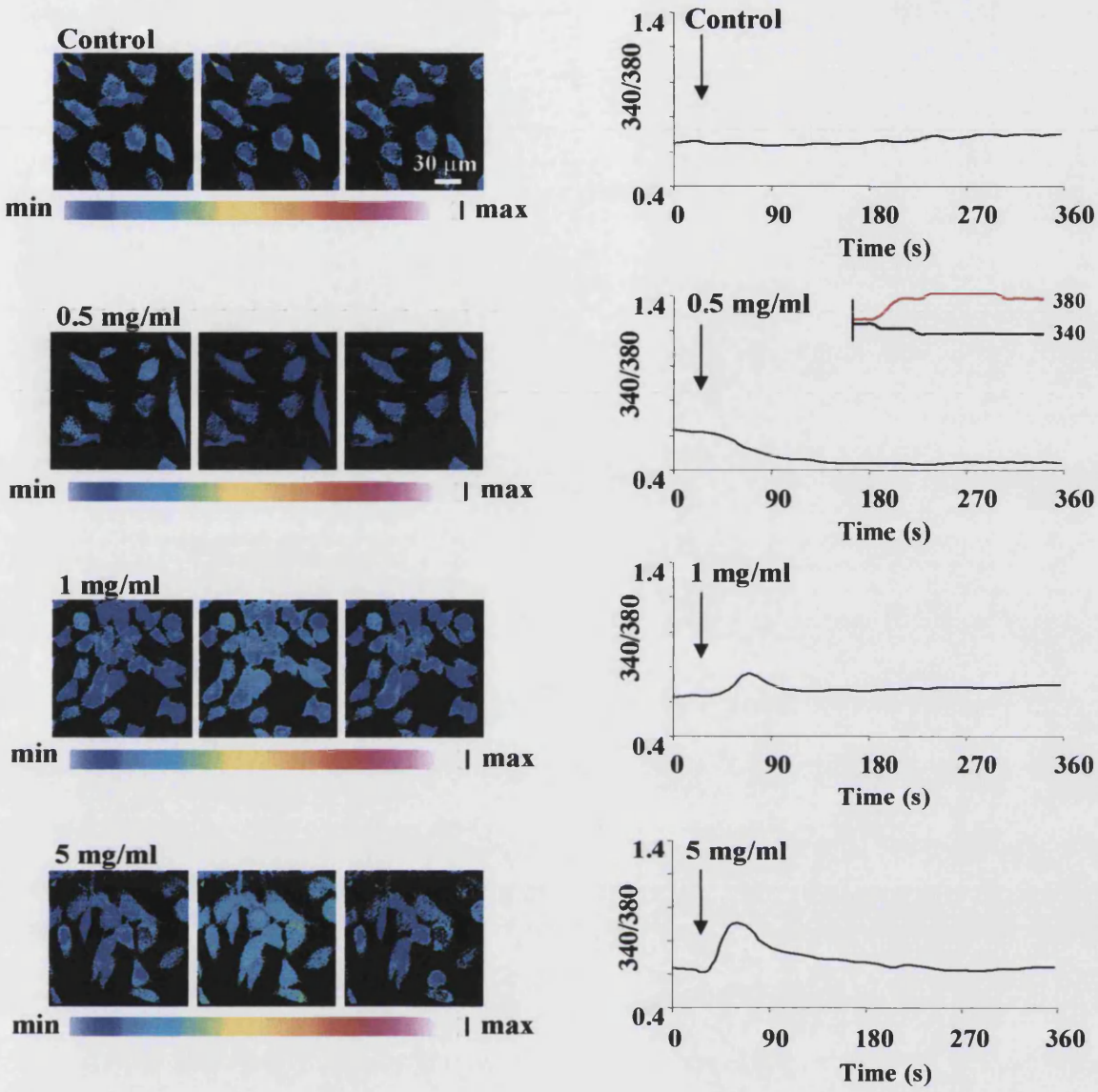

Figure 4.22 Effects of fraction V on intracellular calcium transients in TSA-3 astrocytes
Representative false colour images and traces depicting intracellular calcium transients evoked in fraction V treated TSA-3 astrocytes. TSA-3 astrocytes were loaded with fura-2 (5 µM) in basic medium for 45 minutes at 37 °C. Cells were excited with wavelengths of 340 and 380 nm and emission was collected at a wavelength of 510 nm. Fraction V (0.5, 1 or 5 mg/ml) diluted in basic medium was added to the cells 60 seconds after the commencement of excitation. Control cells were treated with basic medium in the absence of fraction V at the same time point. Calcium responses were recorded from ten cells and the results were expressed as 340/380 fluorescence ratios. False colour images corresponding to each treatment are also displayed. Images were captured at 0, 70 and 300 seconds (from left to right) and the scale bar provides an indication of intracellular calcium levels. **Inset**: In the presence of fraction V (0.5 mg/ml) the intensity of the excitation maxima for fura-2 shifts creating a higher reference point at 380 nm (red line), whereas a reduction occurs at 340 nm (black line). This is indicative of a decrease in intracellular calcium.

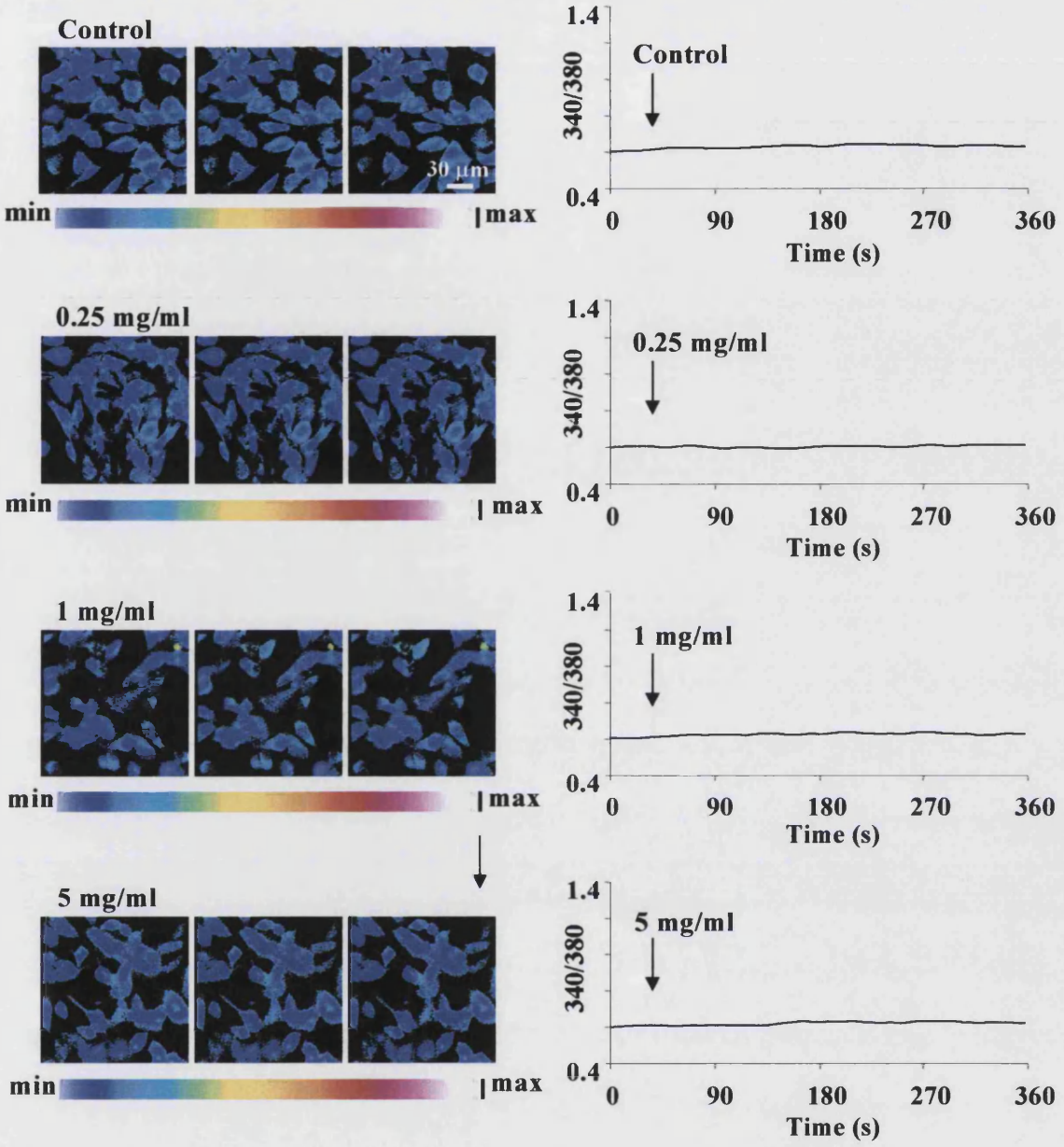

Figure 4.23 Effects of albumin on intracellular calcium transients in TSA-3 astrocytes
Representative false colour images and traces depicting intracellular calcium levels in albumin treated TSA-3 astrocytes. TSA-3 astrocytes were loaded with fura-2 (5 µM) in basic medium for 45 minutes at 37 °C. Cells were subsequently excited with wavelengths of 340 and 380 nm and emission was collected at a wavelength of 510 nm. Albumin (0.25, 1 or 5 mg/ml) diluted in basic medium was added to the cells 60 seconds after the commencement of excitation. Control cells were treated with basic medium in the absence of albumin at the same time point. Calcium responses were recorded from ten cells and the results were expressed as 340/380 fluorescence ratios. False colour images corresponding to each treatment are also displayed. Images were captured at 0, 70 and 300 seconds (from left to right) and the scale bar provides an indication of intracellular calcium levels.

4.6 Albumin treated microglia induce neuronal death

Activated microglia (Thery et al., 1991; Kingham et al., 1999; Combs et al 1999) and peripheral macrophages (Flavin et al., 1997) that invade the CNS in stroke and other disease states have been demonstrated to trigger neuronal apoptosis. Therefore, the effects of albumin or fraction V treated microglia on neuronal death was assessed. Microglia were treated with albumin or fraction V in SFM for 2 hours. The SFM was then replaced with SCM for 22 hours before the medium was collected. Medium was subsequently applied to cultures of cerebellar granule neurones for 24 hours before neuronal apoptosis was appraised using Hoescht 33342. Medium collected from microglia treated with albumin (1 mg/ml) (Fig. 4.24A) or fraction V (1 mg/ml) (Fig. 4.24B) was found to induce a significant increase in neuronal apoptosis. Conversely, untreated cerebellar granule neurones ('basal') contained few apoptotic cells after 24 hours in culture. Neuronal cultures exposed to medium collected from microglia left untreated for 24 hours (control) or microglia treated with SFM for 2 hours then SCM for 22 hours (SFM) also contained low levels of apoptosis. The increase in apoptosis was not attributable to the presence of albumin (1 mg/ml) or fraction V (1 mg/ml) in the medium; since the direct application of these agents to neuronal cultures did not increase apoptosis above control levels ('basal' or 'SFM'). Furthermore, the addition of control microglial conditioned medium to neurones in the presence of albumin (1 mg/ml) or fraction V (1 mg/ml) did not increase neuronal death above controls ('basal' or 'SFM').

To ascertain whether microglial derived NO or glutamate contribute to neuronal apoptosis, the effect of AMT-HCl or a cocktail of glutamate receptor antagonists on cell death was appraised. AMT-HCl (0.3 μM) was pre-incubated with microglia before the addition of albumin of fraction V, medium was then collected after 24 hours and applied to cultures of cerebellar granule neurones. In contrast, the glutamate antagonist cocktail (CNQX, 20

μM; MK801, 10 μM; MSPG, 200 μM) was pre-incubated with the neurones before the addition of microglial conditioned medium. Neither AMT-HCl nor the glutamate antagonists attenuated neuronal death induced by microglia treated with albumin (1 mg/ml) or fraction V (1 mg/ml). Furthermore, neuronal cultures treated with AMT-HCl or the glutamate receptor antagonists directly did not contain significantly different levels of apoptosis from control cultures. These findings suggest that neuronal apoptosis induced by albumin or fraction V treated microglia is NO and glutamate independent. In contrast, boiling the microglial conditioned medium afforded neuroprotection, which suggest that the neurotoxic agent(s) are heat labile (Zhao and Eghbali-Webb 2001).

To determine at which time point microglia release the neurotoxic agent (s), microglia were treated with albumin (1 mg/ml) or fraction V (1 mg/ml) in SFM for 2 hours. The SFM was then replaced with SCM for 1, 4, 6, 14 or 22 hours. Microglia conditioned medium was subsequently incubated with cerebellar granule cells for a further 24 hours before apoptosis was assessed. Using this approach, neurotoxin release was demonstrated to occur 6 hours after the addition of albumin (1 mg/ml) or fraction V (1 mg/ml) and the neurotoxicity of the conditioned medium increased with time (Fig. 4.25). Furthermore, medium collected from albumin (1 mg/ml) or fraction V (1 mg/ml) treated microglia induced similar profiles of neuronal death temporally.

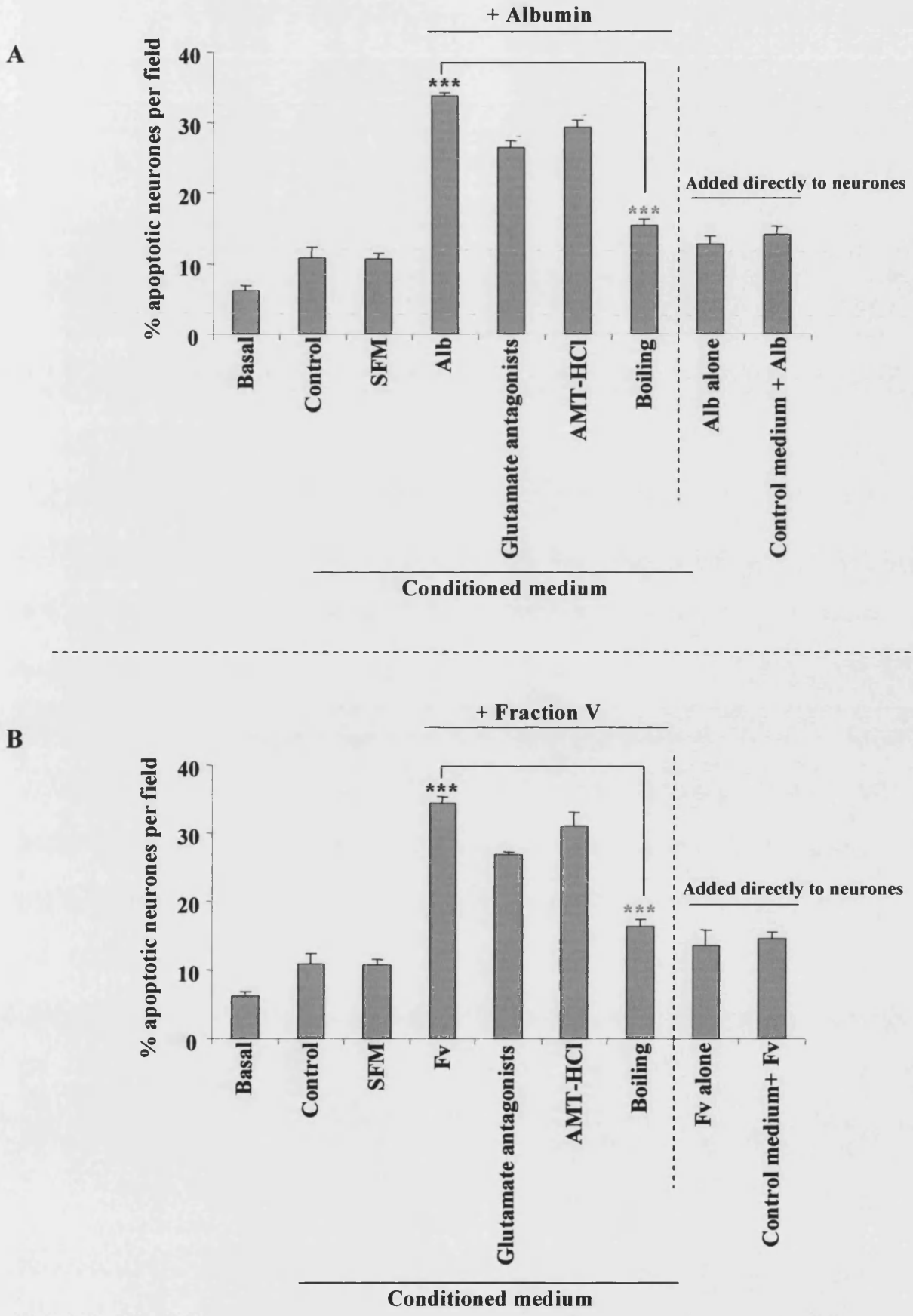

Figure 4.24 (see overleaf for figure legend)

Figure 4.24 Albumin or fraction V treated microglia induce neuronal death

Neuronal apoptosis induced by medium obtained from albumin or fraction V treated microglia was assessed using Hoescht 33342. Microglia were treated with albumin (Alb: 1 mg/ml) (**A**) or fraction V (Fv: 1mg/ml) (**B**) in SFM for 2 hours. The SFM was then replaced with SCM for 22 hours before the medium was collected. In addition, microglia were treated with albumin (Alb: 1 mg/ml) or fraction V (Fv: 1 mg/ml) in SFM in the presence of AMT-HCl (0.3 μM). At 2 hours the SFM was replaced with SCM supplemented with AMT-HCl (0.3 μM) for a further 22 hours before the medium was collected. Control medium was collected from microglia left untreated for 24 hours (control) or microglia exposed to SFM for 2 hours then SCM for 22 hours (SFM). Microglial conditioned medium was subsequently applied to cultures of cerebellar granule neurones for 24 hours then the neurones were fixed. To assess the effect of glutamate on neuronal death, glutamate receptor antagonists (CNQX, 20 μM; MK801, 10 μM; MSPG, 200 μM) were pre-incubated with the neurones for 1 hour before the addition of medium collected from albumin (1 mg/ml) or fraction V (1 mg/ml) treated microglia ('glutamate antagonists'). In addition, medium obtained from albumin or fraction V treated microglia was boiled before being applied to cultures of neurones ('boiling'). Neurones were also left untreated for 24 hours (basal) or were treated with albumin (Alb alone: 1 mg/ml) or fraction V (Fv alone: 1 mg/ml) in the presence or absence of control microglial conditioned medium (control medium + Alb or Fv respectively) for 24 hours before being fixed (to the right of dashed line). Following fixation, neurones were stained with Hoescht 33342. Non-apoptotic cells possessed large brightly stained nuclei, whereas apoptotic cells possessed brightly stained pyknotic nuclei. Neurones displaying pyknotic nuclei were counted and the degree of apoptosis was expressed as a percentage of the total number of cells counted. The values shown represent the mean ± SEM of data from experiments performed in triplicate. Experiments consisted of 3 coverslips per treatment, comprising ten fields of view. Statistical analysis was performed using ANOVA followed by the Tukey post test. *** $P < 0.001$ vs 'control' or 'SFM'. *** $P < 0.001$ vs neurones treated with conditioned medium collected from albumin (Alb) or fraction V (Fv) treated microglia respectively.

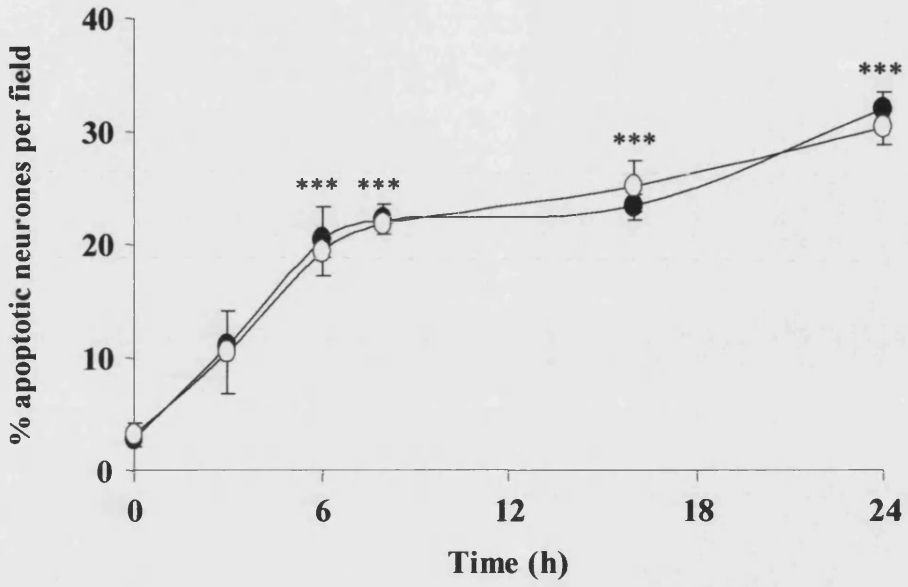

Figure 4.25 Time course of neuronal death

The time course of neuronal apoptosis induced by medium collected from albumin or fraction V treated microglia was assessed using Hoescht 33342. Microglia were treated with albumin (Alb: 1 mg/ml; open circles) or fraction V (Fv: 1 mg/ml; closed circles) in SFM for 2 hours. The SFM was then replaced with SCM for 1, 4, 6 14 or 22 hours before the medium was collected. Microglial conditioned medium was subsequently applied to cultures of cerebellar granule neurones for 24 hours then the neurones were fixed. Following fixation, neurones were stained with Hoescht 33342. Non-apoptotic cells possessed large brightly stained nuclei, whereas apoptotic cells possessed brightly stained pyknotic nuclei. Neurones displaying brightly stained pyknotic nuclei were counted and the degree of apoptosis was expressed as a percentage of the total number of cells counted. The values shown represent the mean ± SEM of data from experiments performed in triplicate. Experiments consisted of 3 coverslips per treatment, comprising ten fields of view. Statistical analysis was performed using ANOVA followed by the Tukey post test. *** $P < 0.001$ vs control (control describes time 0).

The effects of albumin or fraction V treated macrophages on neuronal apoptosis were subsequently studied. Macrophages isolated from neonatal or adult rats were treated with albumin (12 mg/ml) or fraction V (12 mg/ml) in SFM for 2 hours. The SFM was then replaced with SCM for 22 hours before the medium was collected. Medium was subsequently applied to cultures of cerebellar granule neurones for 24 hours before neuronal apoptosis was appraised using Hoescht 33342. Medium collected from macrophages treated with albumin (12 mg/ml) or fraction V (12 mg/ml) induced neuronal apoptosis (Fig. 4.26). Conversely, untreated cerebellar granule neurones ('basal') contained few apoptotic cells after 24 hours in culture. Neuronal cultures exposed to medium collected from macrophages left untreated for 24 hours (control) or macrophages treated with SFM for 2 hours then SCM for 22 hours (SFM) also induced similar levels of neuronal apoptosis as those macrophages treated with albumin (12 mg/ml) or fraction V (12 mg/ml). Moreover, there were no differences between the results obtained with macrophages isolated from neonatal or adult rats.

The increase in apoptosis was not attributable to the presence of high concentrations of albumin (12 mg/ml) or fraction V (12 mg/ml) in the medium; since the direct application of these proteins to neuronal cultures did not increase apoptosis above control levels ('basal'). Furthermore, the addition of control macrophage conditioned medium to neurones in the presence of albumin (12 mg/ml) or fraction V (12 mg/ml) did not significantly increase neuronal death above controls ('basal').

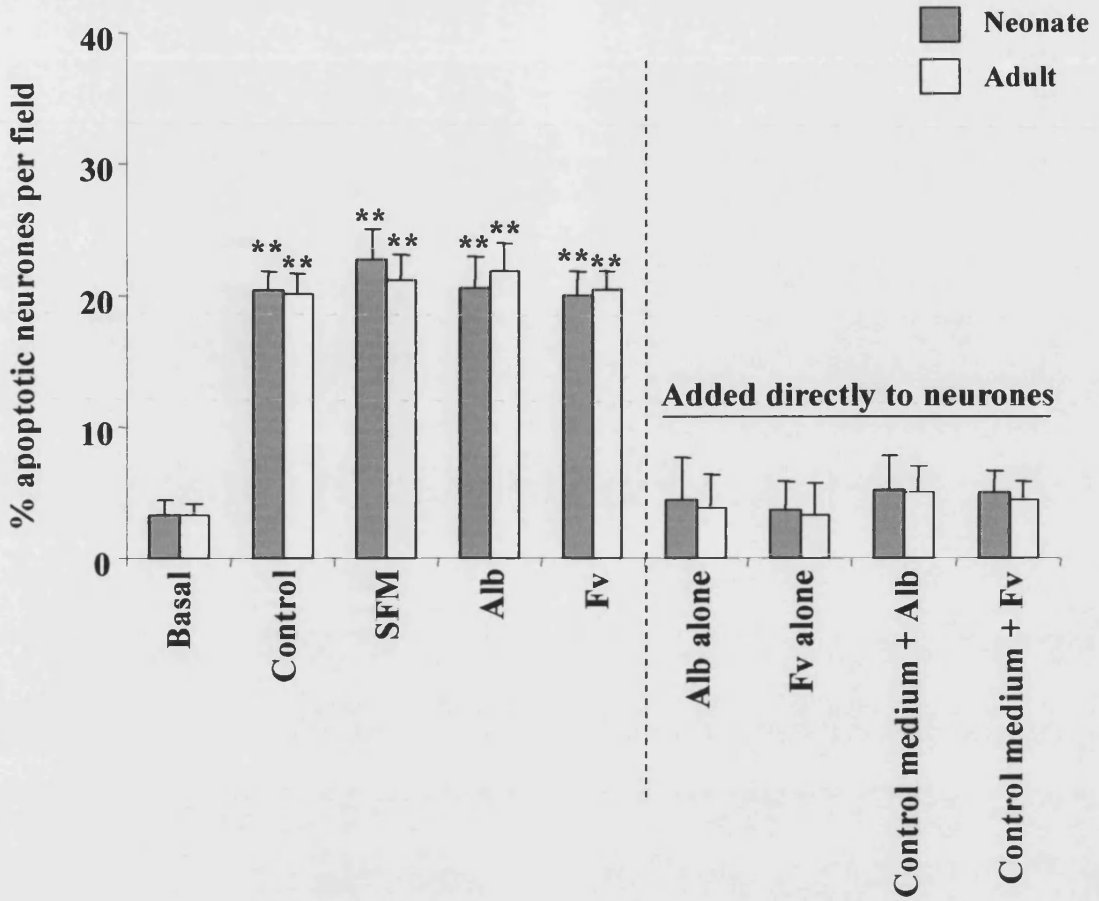

Figure 4.26 Effects of albumin or fraction V treated macrophages on neuronal death

Neuronal apoptosis induced by medium obtained from albumin or fraction V treated macrophages was assessed using Hoescht 33342. Peritoneal macrophages isolated from neonatal (grey bars) or adult rats (open bars) were treated with albumin (Alb: 12 mg/ml) or fraction V (Fv: 12 mg/ml) in SFM for 2 hours. The SFM was then replaced with SCM for 22 hours before the medium was collected. Control medium was collected from macrophages left untreated for 24 hours (control) or macrophages exposed to SFM for 2 hours then SCM for 22 hours (SFM). Conditioned medium was subsequently applied to cultures of cerebellar granule neurones for 24 hours then the neurones were fixed. Control neurones were either left untreated for 24 hours (basal) or were treated with albumin (Alb alone: 12 mg/ml) or fraction V (Fv alone: 12 mg/ml) in the presence or absence of control macrophage conditioned medium (control medium + Alb or Fv respectively) for 24 hours before being fixed (to the right of dashed line). Following fixation, neurones were stained with Hoescht 33342. Non-apoptotic cells possessed large brightly stained nuclei, whereas apoptotic cells possessed brightly stained pyknotic nuclei. Neurones displaying pyknotic nuclei were counted and the degree of apoptosis was expressed as a percentage of the total number of cells counted. The values shown represent the mean ± SEM of data from experiments performed in triplicate. Experiments consisted of 3 coverslips per treatment, comprising ten fields of view. Statistical analysis was performed using ANOVA followed by the Tukey post test. ** $P < 0.01$ vs 'basal' (basal describes untreated neurones).

4.7 Isolation of the putative albumin 'binding protein'

The putative albumin 'binding protein' was isolated from a preparation of N9 microglial cell lysates using albumin conjugated to agarose beads as 'bait'. The N9 microglial cell line (N9) was used in these experiments because a very large amount of cellular protein was required. Using this approach a single protein was precipitated that exhibited a molecular mass of approximately 225 kDa, which corresponds to a protein that is predicted to be 1875 amino acids in length (Fig. 4.27). The putative albumin 'binding protein' was also present in lysates prepared from TSA-3 astrocytes (TSA-3) and cerebellar granule neurones (CGC). Furthermore, a prominent band was detectable at approximately 45 kDa in lysates prepared from TSA-3 astrocytes. Conversely, no discernable bands were detectable in lysates prepared from peritoneal macrophages (Mac) isolated from adult rats. Peritoneal macrophages isolated from adult rats were used in these experiments because adult rats yield approximately 10 times more macrophages then neonates. Moreover, the results in this chapter suggest that peritoneal macrophages isolated from adult or neonatal rats behave similarly. As a control 'neat' albumin agarose complex, which had not been incubated with cell lysates was resolved on a Tris-HCl pre-cast gel (Beads). This resulted in the visualisation of a band at approximately 66 kDa, which corresponds to the molecular weight of albumin. Therefore, the observed results are not merely due to the presence of the albumin agarose complex.

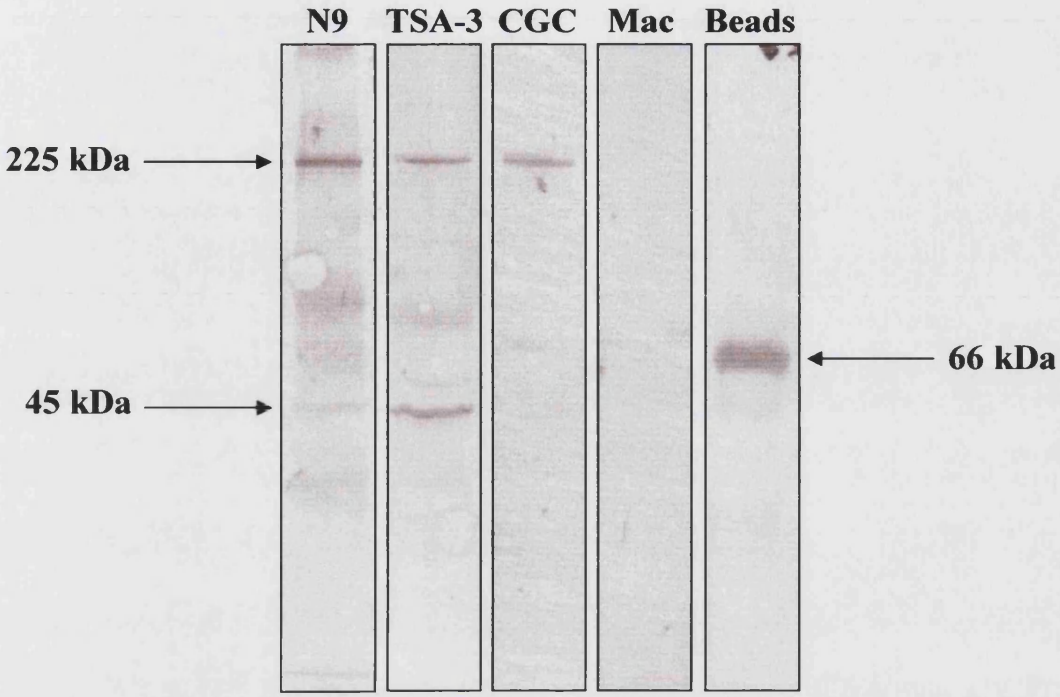

Figure 4.27 Expression patterns of the putative albumin 'binding protein'

Representative PVDF membrane stained with coumassie blue demonstrating the presence of the putative 225 kDa albumin 'binding protein'. N9 microglia (N9), TSA-3 astrocytes (TSA-3), cerebellar granule neurones (CGC) and peritoneal macrophages isolated from adult rats (Mac) were lysed after 24 hours in culture. The lysates were incubated with albumin conjugated to agarose beads for 3 hours at 4 °C with end over end mixing. The albumin-bead complex was pelleted by centrifugation then washed in three changes of lysis buffer. The samples were subsequently mixed with laemelli buffer, boiled then resolved by SDS-page electrophoresis. The albumin-bead complex was mixed with laemelli buffer, boiled then ran on a gel as a control (Beads). After which the proteins were transferred on to a PVDF membrane before being stained with coumassie blue.

4.8 Characterisation of the putative albumin 'binding protein'

To identify the 225 kDa 'binding protein' the protein was subjected to N-terminal sequencing by Dr Fox (Alta Bioscience, Birmingham, UK). Edmun degradation was used to sequentially remove the amino acids from the N-terminus. The amino acids were subsequently identified using HPLC against standards. However, this approach was unsuccessful due to the presence of an 'N-terminal block'. This suggests that the putative 'binding protein' possesses a post-translational modification such as an acetyl, formyl or myristyl group, which prevents the amino acids situated at the N-terminus from being sequenced.

MALDI fingerprinting was employed in a further attempt to identify the putative 'binding protein'. Fingerprinting was performed by Dr Packman (PNAC facility, Cambridge University, UK). Using this approach the putative 'binding protein' was determined to be myosin heavy chain IX (accession number: NP_071855), which exhibits a precise molecular mass of 227 kDa.

The functions of myosin IX have received little attention; however it has been proposed to mediate phagocytosis of bacteria (Graf et al., 2000). Subsequently the ability of microglia or macrophages to internalise FITC labeled albumin was explored. Microglia or macrophages (isolated from neonatal or adults rats) were incubated with FITC tagged albumin for 1 hour in SFM at 37 °C. Fluorescence microscopy revealed that microglia but not peritoneal macrophages internalise albumin (Fig. 4.28). Microglial staining was punctate indicative of a vesicular location and uptake was inhibited at 4 °C, which suggest that the process is active and dynamic.

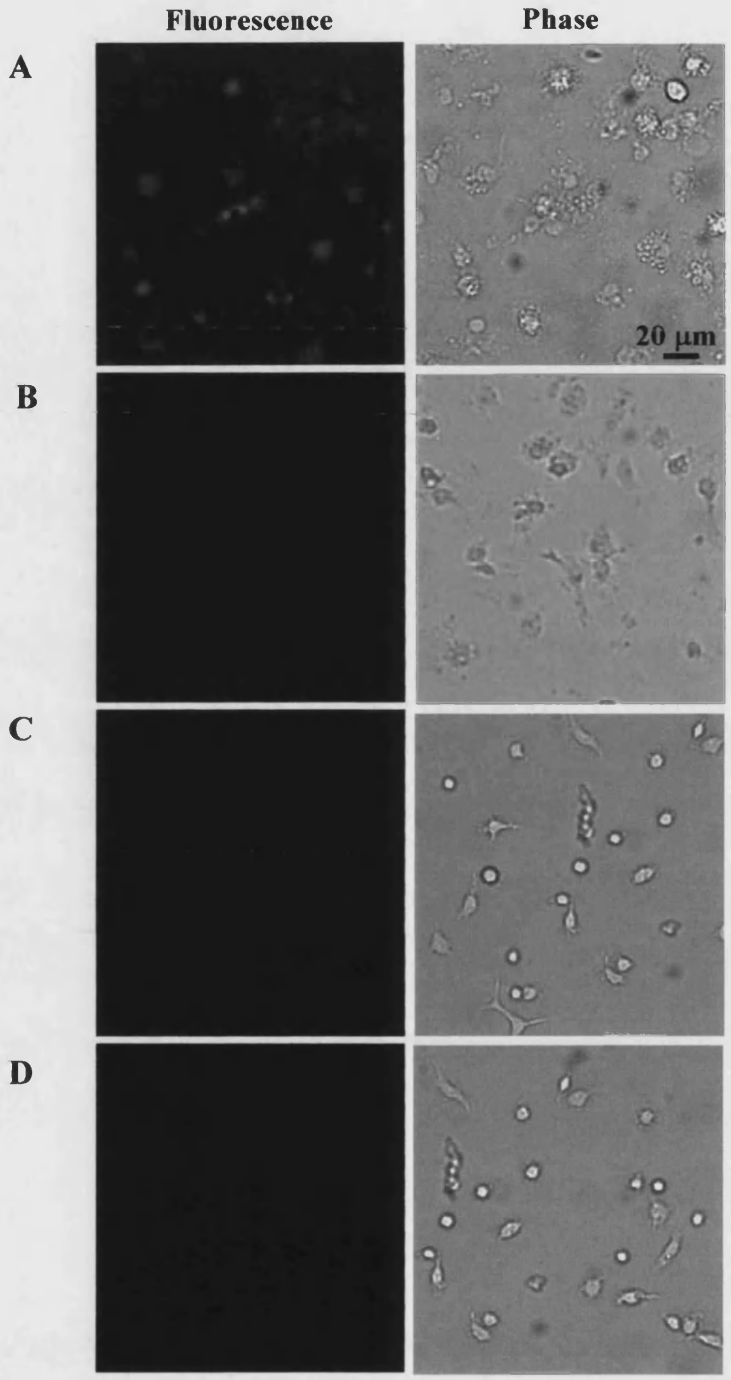

Figure 4.28 Internalisation of FITC labelled albumin by microglia or peritoneal macrophages Images representing FITC labelled albumin uptake in microglia and peritoneal macrophages. Microglia were treated with FITC labelled albumin (0.25 mg/ml) in SFM for 1 hour at 37 ºC (**A**) or 4 ºC (**B**). Peritoneal macrophages isolated from neonatal (**C**) or adult rats (**D**) were also incubated with FITC-albumin for 1 hour at 37 ºC. Phase contrast and fluorescent images were subsequently photographed with an exposure time of 30 seconds.

4.9 Discussion

Albumin was found to induce microglial iNOS expression, glutamate release and proliferation possibly by binding and activating myosin heavy chain IX. The concentrations of albumin that were found to elicit microglial signalling (0.25-2 mg/ml) are likely to fall in the range associated with BBB damage. Conversely, albumin did not appear to bind to myosin heavy chain IX in peritoneal macrophages; which may account for the inability of albumin to induce signalling in these cells. Similar results were obtained with macrophages isolated from neonatal or adult rats; consequently in the following discussion the 'age' of macrophage is not mentioned. Experimental data revealed that albumin and fraction V were equi-potent and induced similar signalling events. This suggests that albumin bound fatty acids, lipids or immunoglobulins do not contribute to the cell signalling cascades described here. Therefore, in the following discussion the term 'albumin' is used to describe the results obtained with both albumin and fraction V.

4.9.1 Myosin IX the putative albumin 'binding protein' in microglia

Putative albumin 'binding proteins' have been described in various cell types. The 60 kDa glycoprotein (gp60) or albondin mediates transcellular albumin transport across endothelial cells, which is critical for the maintenance of normal oncotic pressure across microvessels (Minshall et al., 2000). ^{125}I-albumin has also been demonstrated to bind specifically, saturably, and reversibly to hepatocytes, a process that may mediate the hepatic extraction of fatty acids and other substances that tightly bind to albumin (Weisiger et al., 1981). Furthermore, maleylated albumin has been shown to function as a scavenger receptor ligand (Alford et al., 1998). In this study albumin was demonstrated to induce microglial cell signalling, which appeared to be mediated at least in part by an interaction with myosin heavy chain IX (isolated from murine N9 microglia). The most

extensively characterised class IX myosins include Myr 5 and Myr 7 in the rat and myosin IXa and IXb in humans. Class IX myosins are unconventional non-muscle forms of myosin. Class II myosins are defined as conventional myosins, the best studied example of which is the skeletal muscle isoform. In contrast, unconventional myosins play a role in many diverse functions including cell locomotion, phagocytosis, organelle transport and signal transduction (Mermall et al., 1998). All members of the myosin family share a common structure. They are typically composed of two heavy chains that are approximately 2000 amino acids in length (Alberts et al., 2002). The amino terminal of the heavy chain forms the actin binding motor head domain, which converts chemical energy liberated by ATP hydrolysis into mechanical force, whilst the carboxyl terminal domain of the heavy chain forms an extended α helix. Two heavy chains generally associate by twisting their α helical tail domains together into a coiled-coil conformation, which forms a stable dimer comprising two head domains and a single rodlike tail (Alberts et al., 2002). The rodlike tail is responsible for binding to specific proteins and cargo and therefore determines the function and cellular location of a particular myosin isoform (Soldati 2003). Each myosin heavy chain is also associated with up to 3 myosin light chains, which co-localise with the head domain. Myosin light chains function to stabilize the head domain and regulate motor activities (Bahler 2000).

Class IX myosins are associated with the cytoskeleton, which underlies the plasma membrane (Wirth et al., 1996; Müller et al., 1997). In particular, myosin IX (myr 5) associates with dynamic regions of the cell periphery including membrane ruffles and laemellipodia (Müller et al., 1997). In support of this, myosin heavy chain IX was only precipitated with an albumin-agarose conjugate when cell lysates were incubated on ice for long periods of time, a process which serves to fully solubilise membranes. This

therefore provides evidence that myosin heavy chain IX is indeed membrane anchored. Furthermore, N-terminal sequencing of myosin heavy chain IX proved unsuccessful, which suggests that the N-terminus of myosin heavy chain IX is post-translationally modified. Candidate modifications include membrane anchors such as myristyl groups.

Considering myosin I (Allen and Aderem 1995), IIV (Titus 1999) and X (Cox et al., 2002) are involved in phagocytosis, it seems plausible that myosin IX may mediate albumin uptake into microglia, which in turn triggers intracellular signalling. Indeed microglia but not macrophages were demonstrated to take up FITC labelled albumin in a temperature sensitive manner. Moreover, the labelled albumin appeared to be located in vesicles, which is consistent with the notion that albumin is phagocytosed in a receptor-dependent regulated manner. To date little has been published regarding the precise roles of myosin IX in cells, although myr 5 has been reported to mediate the uptake of the bacterium Shigella flexneri into epithelial cells (Graf et al., 2000). Since it is unlikely that albumin comes into direct contact with myosin heavy chain IX at the plasma membrane, it is conceivable that albumin interacts with a transmembranous adapter/receptor, which couples to myosin IX. Collectively, these components may constitute an 'albumin entry complex' in the plasma membrane. Nevertheless, such an 'adaptor' was not isolated using albumin-agarose precipitation; it is possible that the concentration of this putative 'adaptor' was below the sensitivity range for coumassie staining and therefore eluded detection, alternatively the adaptor may not be proteinaceous.

Recently, astrocytes (Tabernero et al., 2002a) and neurones (Tabernero et al., 2002b) have also been reported to internalize albumin *in vitro*. Moreover, a protein that migrates to the same position as myosin heavy chain IX was isolated from both of these cell types using an albumin-agarose conjugate. These findings suggest that myosin heavy chain IX may

mediate the effects of albumin in astrocytes and neurones as well as microglia. Interestingly, N9 microglia express more myosin heavy chain IX than astrocytes or neurones, which may reflect the highly phagocytic nature of microglia. Therefore, it would be interesting to investigate whether microglial activators which induce phagocytosis also trigger the up-regulation of myosin IX.

In agreement with previous findings albumin did not induce any discernible effects on intracellular calcium transients in TSA-3 astrocytes (Tabernero et al., 1999), however this conflicts with data published by Nadal et al., (1995) who demonstrated that albumin evokes calcium uptake into stores in primary astrocytes. In a parallel experiment, fraction V was found to induce calcium release from stores in TSA-3 astrocytes, which is consistent with previous reports (Nadal et al., 1995). The calcium mobilizing effects of fraction V have been attributed to the presence of a protein bound lipid other than LPA (Nadal et al., 1995) and are therefore probably mediated by a different receptor. In support of this, a protein with an approximate molecular weight of 45 kDa was also precipitated from TSA-3 astrocyte lysates using an albumin-agarose conjugate, which suggests that the albumin used in the conjugate contains attached lipid groups (information unavailable from the supplier). Putative candidates for the 45 kDa protein include the G_i protein coupled receptors Edg-1 (Zondag et al., 1998), Edg-3 or H218 (An et al., 1999), which bind shingosine-1-phosphate (SIP) a lysophospholipid lipid that is known to associate with fraction V serum albumin (Nadal 2001). Nadal et al., (1995) demonstrated that calcium transients induced by the albumin bound lipid were pertussis toxin sensitive as was the proliferative response. In support of this, SIP induces calcium transients in activated monocytes (Fueller et al., 2003) and cells transfected with Edg-3 or H218 proliferate when stimulated with SIP (An et al., 2000). Regardless of the identity of the albumin bound lipid, these results highlight that albumin induces different signalling

cascades in microglia and astrocytes, which seems plausible considering that these cells exhibit different embryological origins (Ling et al., 1980; Kitamura et al., 1984; Hickey and Kimura 1988).

Interestingly, albumin did not induce intracellular signalling in peritoneal macrophages. Myosin IX (human IXb) has been demonstrated to move to a cytoplasmic location in differentiated macrophages, which may subsequently preclude signal transduction (Wirth et al., 1996). However, the results presented in this chapter reveal that myosin heavy chain IX is undetectable in peritoneal macrophages using the albumin-agarose precipitation method. This suggests that either myosin heavy chain IX does not bind albumin in macrophages, or that myosin heavy chain IX is not expressed by peritoneal macrophages. Nevertheless, macrophages adopted a bipolar morphology in the presence of high concentrations of albumin, whereas at lower concentrations macrophages were amoeboid in appearance. This suggests that albumin promotes cytoskeletal reorganisation in macrophages, possibly via an interaction with a different isoform of myosin.

In contrast to the typical structure of other myosin heavy chains, myosin heavy chain IX functions as a monomer (Wirth et al., 1996). Moreover, the rodlike tail domains of IXb and myr 5 contain a GTPase activating domain (GAP) for Rho GTPases (Reinhard et al., 1995; Post et al., 1998). Interestingly, the expression of myr 5 in insect or mammalian cells induces the formation of long cellular processes, which is dependent on GAP activity (Muller et al., 1997). Thus, it seems likely that myosin IX may be involved in the formation of microglial ramifications. In support of this, albumin increases the number of branches emanating from microglial cell bodies, which corroborates the theory that albumin modulates the function of myosin IX.

In addition to a GAP domain, myosin IXb comprises a diacylglycerol binding domain, which is similar to those found in PKC (Wirth et al., 1996). The presence of such a domain is consistent with the finding that albumin induces phospholipase c activity, which subsequently leads to the generation of IP_3 and DAG. Thus, DAG may regulate the activity of myosin heavy chain IX by relaying feedback signals to the DAG binding domain. Indeed PIP_2 (IP_3 precursor) and DAG (Botelho et al., 2000) have recently been implicated in actin reorganization during phagocytosis in RAW macrophages.

The motor domain of myosin IX (myr 5) has been also been reported to play a role in cell signalling. Myr 5 comprises an N terminal extension that is structurally homologous to a RAS binding domain, although an expressed N-terminal truncation of myosin IX (amino acids 2-117) has been demonstrated to lack intrinsic RAS binding activity (Kalhammer et al., 1997). This however may be an experimental artifact since albumin induces ERK activation in microglia, which implies that the RAS binding domain is active in native myosin IX. A prerequisite for RAS binding is the presence of basic residues. The RAS binding domain of myosin IX is uncharged; therefore it is possible that RAS binding requires the presence of basic amino acids in other regions of the heavy chain (amino acids 118-1875), which would explain why RAS binding was not observed in experiments using N-terminal truncations.

4.9.2 Downstream pathways: iNOS expression

This study provides evidence that albumin treated microglia upregulate the expression of iNOS but not COX-2. iNOS expression was found to be ERK dependent. Accordingly, other microglial activators including LPS (Bhat et al., 1998; Pyo et al, 1998), thrombin (Ryu et al., 2000) and adenovirus infection (Bhat and Fan 2002) induce iNOS expression via ERK-dependent mechanisms. This is consistent with the fact that the iNOS promoter

contains an AP-1 binding site, which is a transcription factor that is produced by activated ERK (Kristof et al., 2001). Interestingly, nitrite was undetectable in the culture medium collected from albumin treated microglia. This discrepancy could be attributed to a lack of essential enzymatic co-factors such as tetrahydrobiopterine (BH_4) (Ding et al., 1997; Barker et al., 1998) or NADPH (Shin et al., 2002), without which NO cannot be generated even in the presence of iNOS. This may be an advantageous mechanism in the CNS, which serves to safeguard neurones against free radical damage. Another possible explanation for the absence of nitrite in the culture medium is that NO rapidly reacts with superoxide to form peroxynitrite which in turn nitrates tyrosine residues therefore rendering NO (nitrite) undetectable. Alternatively, iNOS may fulfill other functions in microglia, which are distinct from the canonical NO producing role.

Macrophages were resistant to the concentrations of albumin that stimulated iNOS expression in microglia. In contrast, macrophages and microglia expressed iNOS in response to LPS, which suggests that macrophages and microglia do share common signalling pathways. However, it should be noted that exposure of macrophages to 12 mg/ml of albumin triggered iNOS expression and NO production (as indicated by the presence of nitrite in the culture medium). In this instance iNOS expression and nitrite production may be a consequence of non-specific receptor binding, considering that receptor mediated events are evoked by low concentrations of agonist. Moreover, phosphorylated ERK was not detectable in macrophages treated with 12 mg/ml of albumin or fraction V, which provides further evidence that iNOS expression, occurs via an alternate route in this case. Similarly, phosphorylated ERK was undetectable in macrophage lysates treated with LPS, which conflicts with a previous report (Chen and Wang 1999). Moreover, phosphorylated ERK has been implicated in LPS induced iNOS expression in RAW macrophages (Ajizian and English 1999). Although, Ajizian and

English (1999) co-stimulated their macrophages with LPS and IFNγ, whereas in this study LPS was used in isolation.

4.9.3 Downstream pathways: glutamate release

Albumin was demonstrated to induce microglial glutamate release via the Xc^- transporter, which mediates the exchange of glutamate for cystine (Piani and Fontana 1994). This transport system is important in regulating glutathione concentrations, since the availability of cystine is a rate limiting step in synthesis (Piani and Fontana 1994). Interestingly, albumin also increases the synthesis and release of glutamate from neurones (Tabernero et al., 2002b). This phenomenon was attributed to the increased production of acetyl Co A, which in turn augments α-ketoglutarate efflux from the citric acid cycle, a bio-synthetic intermediate from which glutamate is synthesized (Tabernero et al., 2002b) (Fig. 4.29). Therefore, it seems plausible that albumin stimulates microglial metabolism resulting in the increased production of glutamate. This is turn may trigger glutamate exchange for cystine, from which glutathione and other enzymes involved in the management of oxidative stress can be synthesized. Therefore, glutamate release by activated microglia may be an intrinsic survival mechanism designed to protect microglia from the reactive nitrogen and oxygen species they produced during inflammatory reactions. However, as a consequence microglia may inadvertently contribute to excitotoxic damage in neurodegenerative diseases.

Macrophages did not release glutamate into the culture medium in response to albumin (1-12 mg/ml). This is consistent with the finding that albumin does not appear to bind to myosin heavy chain IX in macrophages. Interestingly, LPS did not induce glutamate release from macrophages either, although the same concentration of LPS triggered

glutamate release from microglia. Similarly, Klegaris and McGeer (1997) reported that LPS, PMA and Aβ only slightly increased glutamate release from peritoneal macrophages. This might be because resting macrophages are actively synthesizing a number of enzymes, which concomitantly enhances the basal glutamate cystine exchange rate so that stimulation by LPS or other inflammatory stimuli cannot increase glutamate release further. In support of this, untreated macrophages released very high levels of glutamate into the culture medium, which is in accord with previous findings (Klegaris and McGeer 1997). The concentration of glutamate released from untreated macrophages was approximately 5 fold higher than the concentrations found in culture medium harvested from untreated microglia. Therefore, it would appear that resting macrophages are in a higher activational state then resting microglia, which corroborates FACS data presented in chapter 3. Moreover, ramified microglia are known to down regulate macrophage associated properties including non-specific esterase activity, the ability to perform phagocytosis and to bind acetylated low density lipo-protein, which is indicative of their resting phenotype (Giulian and Baker 1986). Consequently, microglia are exquisitely sensitive to subtle changes in the brain's microenvironment (Kreutzberg 1996).

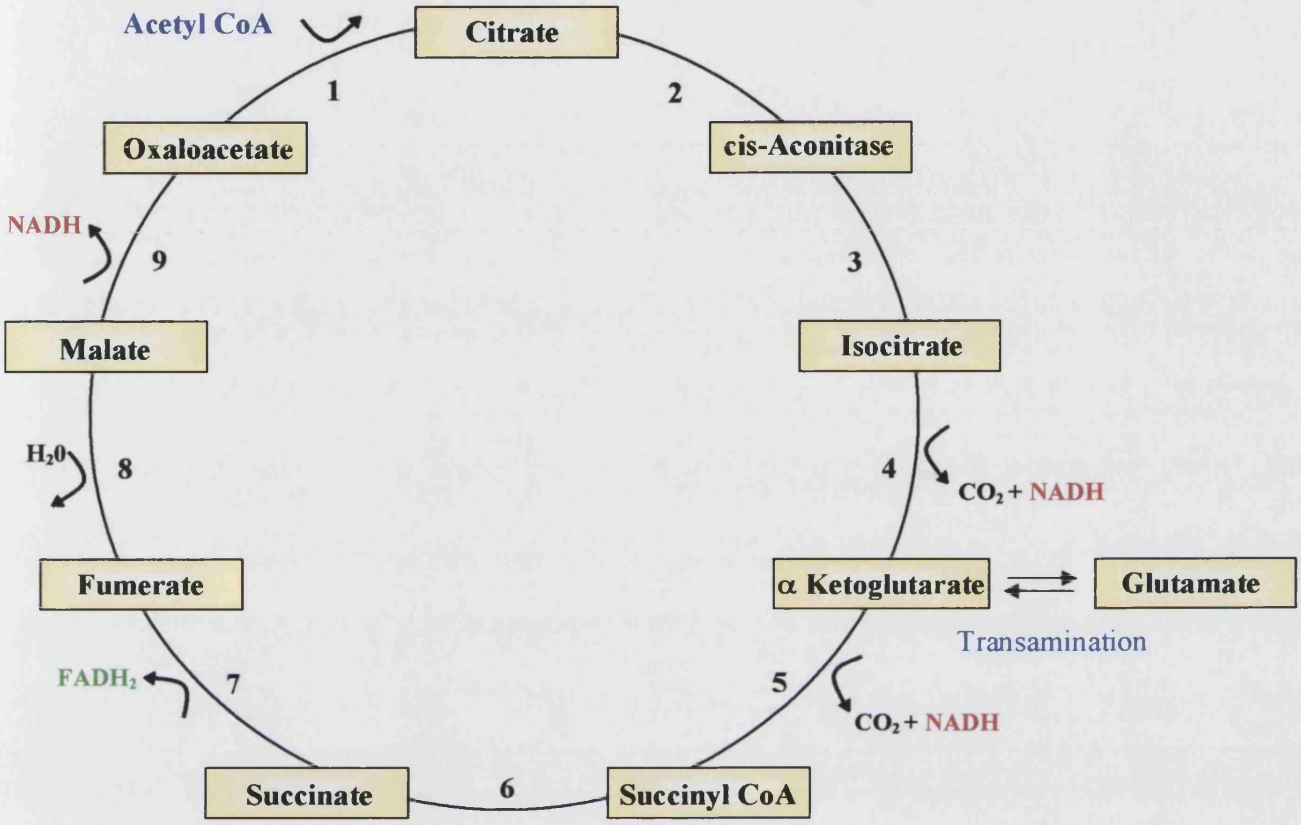

Figure 4.29 Synthesis of glutamate from the citric acid cycle intermediate α-ketoglutarate
The citric acid cycle begins with the condensation of acetyl co-enzyme A with oxaloacetate. The cycle ultimately results in the regeneration of oxaloacetate and the production of two molecules of carbon dioxide. The cycle also produces three NADH, one $FADH_2$ and one ATP per pyruvate molecule. In addition, glutamate and other amino acids can be sythesised from α-ketoglutarate. The reactions of the citric acid cycle are catalysed by the following enzymes (as numbered in the diagram): 1, Citrate synthase; 2, Aconitase; 3, Aconitase; 4, Isocitrate dehydrogenase; 5, α Ketoglutarate dehydrogenase complex; 6, Succinyl CoA synthase; 7, Succinate dehydrogenase; 8, Fumerate; 9, Malate dehydrogenase (adapted from Berg et al., 2002).

4.9.4 Downstream pathways: proliferation

In vivo microglia proliferate in response to pathogen invasion or injury (Graeber et al., 1988c; Streit and Graeber 1993). The results presented here show that albumin-treated primary microglia or N9 microglia proliferate, whereas albumin-treated peritoneal macrophages do not. Albumin-induced proliferation may be an intrinsic host immune response. Expansion of the local microglial population would be an advantageous response to BBB damage in terms of minimising tissue damage and infection. Similarly, albumin with attached lipids may be involved in the formation of astrocytic scars following BBB damage, since fraction V induces astrocyte proliferation *in vitro* (Nadal et al., 1995). Moreover, thrombin has been reported to induce microglial proliferation and activation (Möller et al., 2000a), which suggests that a number of plasma proteins may act in synergy following BBB breakdown. Conversely, LPS did not induce microglial or macrophage proliferation, the former is consistent with previous reports (Suzumura et al., 1991; Liu et al., 2001).

Albumin-induced proliferation in primary microglia was mediated by a Src kinase, phospholipase c and was calcium-dependent. In support of this, albumin triggered calcium release from thapsigargin-sensitive intracellular stores in N9 microglia but not macrophages. Albumin-induced calcium transients were also Src kinase and phospholipase c dependent, which is consistent with the proliferation data obtained in primary microglia. Phospholipase c γ is known to comprise SH2 domains and is activated by receptor tyrosine kinases or non receptor tyrosine kinases which include members of the Src family (Berridge 1993; Carpenter and Ji 1999; Kim et al., 2000). Therefore, it is likely that a Src kinase lies upstream of phospholipase c activation and subsequent IP_3 sensitive calcium release. Moreover, Src kinases (Stzelecka-Kiliszek et al., 2002) have

been implicated in FcγRIII dependent phagocytosis, which indicates that these kinases may also be involved in the internalization of FITC albumin in microglia. It is worth noting that the albumin used in this study was essentially immunoglobulin free, which rules out the possibility that albumin interacts with an Fc receptor to mediate myosin heavy chain IX activation and intracellular signalling. Interestingly, proliferation was not instigated by the application of thapsigargin to microglia or macrophages, which implies that calcium *per se* is not sufficient to initiate cell division. It may be that the amplitude and/or the duration of a calcium transient encodes a particular response.

4.9.5 Albumin treated microglia exhibit a neurotoxic phenotype

Medium harvested from albumin treated microglia induced neuronal apoptosis. These findings provide evidence that albumin activated microglia may aggravate neurodegeneration in disorders involving loss of BBB integrity. Neuronal death was not attenuated by the iNOS inhibitor AMT-HCl or a cocktail of glutamate receptor antagonists (MK801, CNQX and MSPG). These results suggest that neuronal death is NO and glutamate independent. The former is not surprising given that the half life of NO in biological systems is approximately 5 seconds (Kulkarni and Sharma 1993; Alberts et al., 2002; Berg et al., 2002). In contrast, boiling the microglial conditioned medium afforded neuroprotection, which suggests that the neurotoxic agent(s) are heat labile (Zhao and Eghbali-Webb 2001). The increase in neuronal apoptosis was not attributed to the presence of albumin (or fraction V) in the medium since the direct application of albumin to neurones did not induce death. Neuronal death was not induced by the addition of albumin (or fraction V) in the presence of control microglial conditioned medium either. Taken together, these findings imply that the neurotoxins are secreted by albumin treated microglia. Candidate neurotoxins may include cytokines (Combs et al., 2002) or proteases

(Flavin et al., 1997; Flavin et al., 2000; Kingham and Pocock 2001), which have previously been demonstrated to induce neuronal death *in vitro*.

Interestingly, untreated macrophages ('basal' or 'SFM') triggered neuronal apoptosis, which is in accord with previous findings (Flavin et al., 1997). This suggests that peripheral monocytes, which invade the CNS during injury, may contribute to neuronal degeneration. These findings also support the hypothesis that peripheral macrophages are more 'activated' than microglia. Furthermore, neuronal death was not augmented by treating macrophages with albumin, which is consistent with other results presented in this chapter and corroborates the notion that albumin does not bind and activate myosin IX signalling in these cells.

4.9.6 Conclusion

Here it is shown that albumin induces iNOS expression, glutamate release, proliferation and the release of neurotoxins possibly via an interaction with myosin heavy chain IX in microglia. Signalling is mediated intracellularly by a number of second messengers including ERK, a Src kinase and IP_3 induced calcium release (Fig. 4.30). In contrast, albumin does not induce signalling in peritoneal macrophages. These findings are interesting considering that both microglia and macrophages are of the same lineage. Thus, it may be that microglia represent a distinct subset of macrophages that are destined for the CNS during development (Perry 2001) and therefore possess intrinsically different biochemical properties to peripheral macrophages.

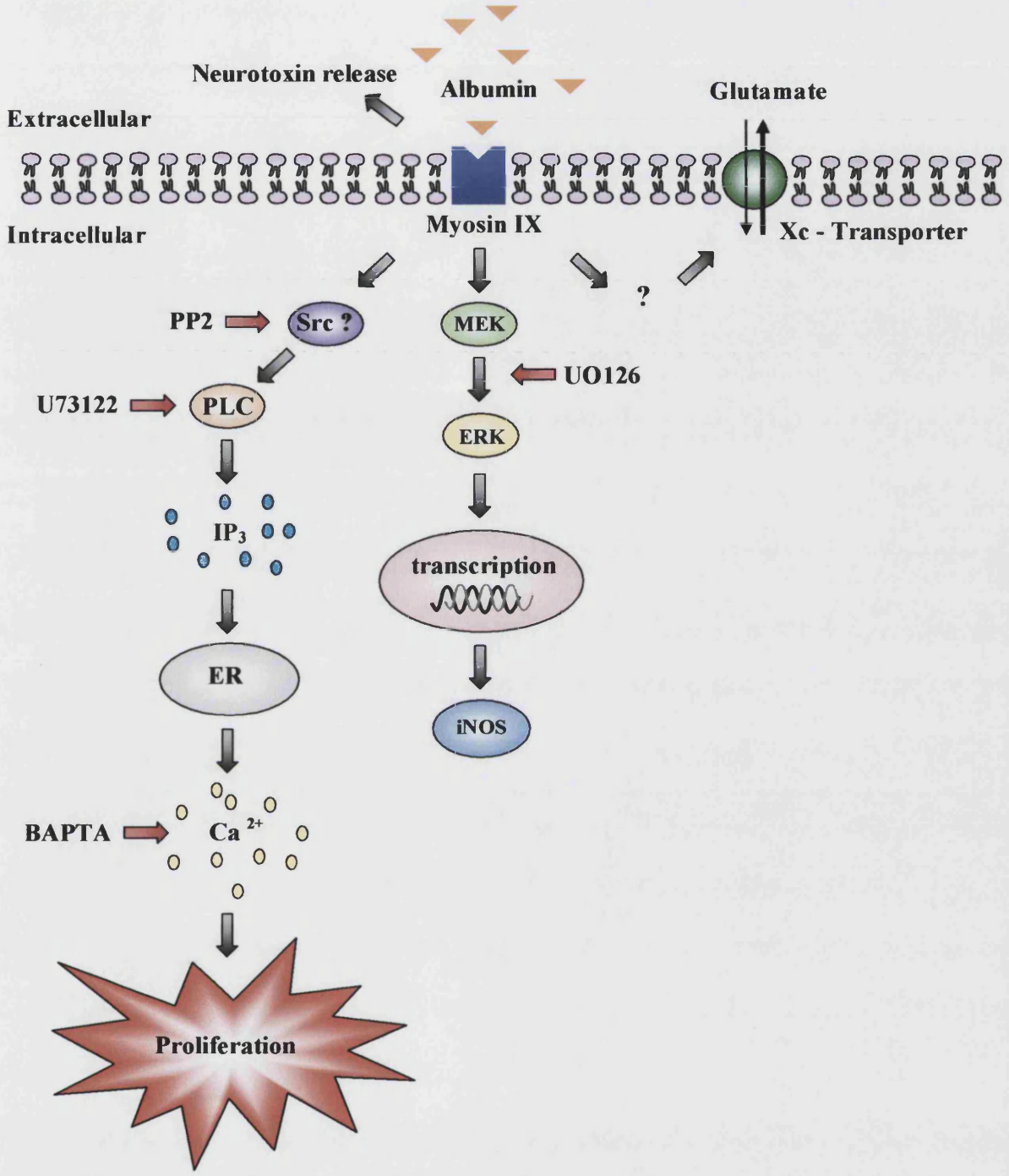

Figure 4.30 Signalling cascades elicited in albumin treated microglia

Albumin interacts with myosin IX to induce iNOS expression, glutamate release, proliferation and the release of as yet undetermined neurotoxins. iNOS expression is mediated intracellularly by ERK. The pathway leading to glutamate release is currently undetermined; however secretion involves the Xc^- transporter. Proliferation is calcium dependent, the source of which is the endoplasmic reticulum. The release of calcium is mediated by PLC and therefore involves IP_3. A Src kinase, probably lying upstream of PLC, is also involved in calcium release and subsequent proliferation.

5.0 Investigation of microglial signalling elicited by CgA or Aβ

5.1 Introduction

This chapter explores the intracellular signalling cascades elicited in microglia treated with chromogranin A (CgA) or $A\beta_{(25-35)}$ (see below for a description of CgA and section 1.6 for a description of Aβ); two proteins that are associated with the pathology of AD.

5.1.1 Physiological roles of chromogranin A

CgA consists of 457 amino acids and is a member of the Granin family of acidic glycoproteins. CgA was originally identified in the secretory granules of chromaffin cells. However, it is now known that CgA is widely distributed in the secretory granules of nervous tissue (Volknandt et al., 1987) as well as endocrine tissue (Fischer-Colbrie et al., 1987).

The exact functions of CgA in the brain are currently under investigation, although CgA has been demonstrated to act as a calcium binding protein within secretory vesicles (Reiffen and Gratzl 1986). CgA has also been reported to possess neuromodulatory properties, exemplified by its ability to attenuate the effect of dopaminergic transmission in the nucleus accumbens (Brudzynski et al., 1994). In the periphery, CgA is proteolytically processed leading to the formation of pancreastatin, parastatin, catestatin, and vasostatin. These peptides mediate the regulation of pancreatic (Ishizuka et al., 1989) and parathyroid secretions (Fasciotto et al., 1993), the control of catecholamine release from chromaffin cells (Mahata et al., 1997) and vasoinhibition respectively (Angeletti 1994). Thus, it is conceivable that derivatives of CgA may also play functional roles in the CNS.

5.1.2 Pathological roles of chromogranin A

CgA is implicated in a number of neurodegenerative disorders including AD, stroke, Parkinson's disease and Pick's disease. In AD, CgA accumulates in granular deposits, which are associated with senile plaques (Rangon et al., 2003) and in the surrounding dystrophic neurites (Munoz 1991; Yasuhara et al., 1994; Rangon et al., 2003). Furthermore, the CgA gene maps to a chromosomal locus associated with APP, which indicates that CgA and APP may act synergistically in pathology (Modi et al., 1989). Following a stroke CgA is upregulated in axonal swellings located at the infarct periphery (Yasuhara et al., 1994). CgA also accumulates in the Lewy bodies present in the substantia nigra in Parkinson's disease (Nishimura et al., 1994). Similarly, CgA is upregulated in the Pick bodies and swollen neuronal processes in Pick's disease (Yasuhara et al., 1994). Pertinent to this study, CgA is a potent microglial activator inducing microglia to switch from a resting ramified phenotype into a reactive neurotoxic state (Ciesielski-Treska et al., 1998; Kingham et al., 1999; Ciesielski-Treska et al., 2001). Taken together these findings suggest that common pathways involving CgA may underlie pathological processes in neurodegenerative disorders.

5.1.3 Summary of results

Previously it has been reported that CgA treated microglia assume an activated amoeboid morphology characterised by ED-1 immunoreactivity, iNOS expression, NO production and glutamate release (Kingham et al., 1999). The continuous synthesis of NO in CgA activated microglia subsequently leads to mitochondrial depolarisation and apoptosis (Kingham and Pocock 2000). Work in this chapter revealed that iNOS expression, glutamate release, mitochondrial depolarisation and apoptosis are inhibited by poly I, which suggests that signalling is mediated by the

scavenger receptor. These events with the exception of glutamate release were also attenuated by pre-treatment with UO126 or PP2, implying that signalling is mediated intracellularly by a Src kinase and ERK. Consistent with this, the phosphorylated forms of ERK 1 and 2 were detectable 30 minutes after the addition of CgA and reached maximal levels 3 hours after treatment. Furthermore, PP2 inhibited CgA induced ERK phosphorylation, which suggests that a Src kinase lies upstream of ERK activation.

$A\beta_{(25-35)}$ (hereafter referred to as Aβ) was also demonstrated to trigger microglia to apoptose and cell death was mediated by mitochondrial depolarisation. Furthermore, apoptosis and mitochondrial depolarisation were attenuated by poly I, which suggests that these signalling events are also scavenger receptor-dependent. In contrast to CgA treatment, apoptosis and mitochondrial depolarisation were iNOS and ERK independent. Although, Aβ induced apoptosis and mitochondrial depolarisation were abrogated by pertussis toxin and PP2, implicating $G_{i/o}$ proteins and Src kinases in signalling.

In a parallel series of experiments, conditioned medium harvested from CgA or Aβ treated microglia was found to induce neuronal apoptosis. Microglial derived neurotoxin(s) were heat labile. Appearance of the neurotoxin(s) in microglial conditioned medium became apparent 16 hours after CgA or Aβ treatment, which suggests that the neurotoxin(s) are synthesised *de novo*.

5.2 CgA but not Aβ induces iNOS expression in microglia

Microglia treated with CgA or Aβ in SCM were analysed for iNOS expression after 24 hours in culture. It should be noted that microglia were treated with CgA or Aβ in SCM in all subsequent experiments described in this chapter. Western blot analyses revealed that CgA (50-1000 nM) induced a dose dependent increase in iNOS expression (Fig. 5.1A), whereas Aβ (15-55 μM) did not evoke the expression of this inflammatory mediator (Fig. 5.1B). iNOS was also undetectable in untreated microglia after 24 hours in culture (basal). (Fig 5.1A,B). Analysis of β-actin levels demonstrated that the observed changes were not due to differences in protein loading. The concentrations of Aβ used in this study may seem very high, however the aim was to replicate the high concentrations of Aβ found in senile plaques in an *in vitro* system.

Time course analysis revealed that iNOS was initially detectable 6 hours after the addition of CgA (100 nM) and that iNOS expression increased with time (Fig. 5.1C). Conversely, Aβ (55 μM) did not induce microglial iNOS expression at any point over the same time course. In a parallel experiment, nitrite, a stable breakdown product of NO was measured in microglial conditioned medium. However, nitrite was not detectable above control levels (basal) in medium collected 24 hours after CgA (100 nM) or Aβ (55 μM) treatment (table 5.1). These findings were not attributed to assay failure since nitrite was detectable in medium collected from LPS (2 μg/ml) treated peritoneal macrophages.

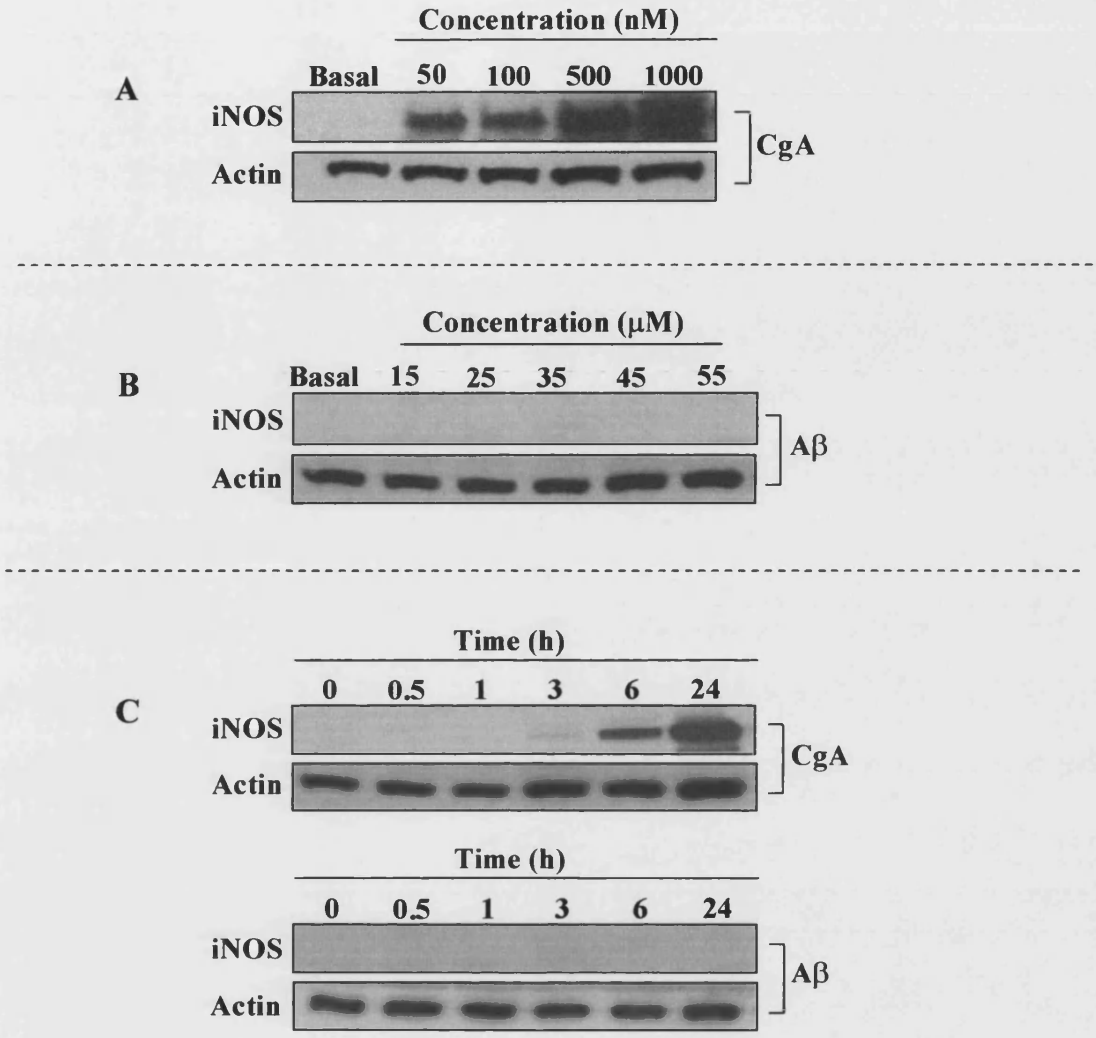

Figure 5.1 CgA but not Aβ induces iNOS expression

Representative Western blots of iNOS expression in microglial cell lysates. **A**: Microglia were treated with increasing concentrations of CgA (50-1000 nM) for 24 hours before lysates were prepared. Control lysates were prepared from microglia left untreated for 24 hours (basal) **B**: Microglia were treated with increasing concentrations of Aβ (15-55 μM) for 24 hours before lysates were prepared. Control lysates were prepared from microglia treated as described in A **C**: Microglia were treated with CgA (100 nM) or Aβ (55 μM) for 0.5, 1, 3, 6 or 24 hours before lysis. Lysates were subjected to Western blot analyses using an antibody raised against iNOS (1:5000), which in turn was detected by goat anti-rabbit IgG (HRP) (1:500). To ensure equal protein loading blots were reprobed with an antibody recognising β-actin (1:1000) followed by exposure to goat anti-mouse IgG (HRP) (1:1000).

Treatment	[Nitrite](nM/μg protein)
Basal	1.04 ± 0.03
CgA (100 nM)	0.97 ± 0.08
Aβ (55 μM)	0.82 ± 0.06
Macrophage (LPS: 2 μg/ml)	493.1 ± 0.9 ***

Table 5.1 Nitrite release from microglia

Nitrite concentrations (nM/μg of protein) were measured in microglial conditioned medium using Griess reagent. Microglia were treated with CgA (100 nM) or Aβ (55 μM) for 24 hours before medium was collected. Medium was also collected from peritoneal macrophages (isolated from adult rats) treated with LPS (2 μg/ml) for 24 hours. Control medium was collected from microglia left untreated for 24 hours (basal). The values shown represent the mean concentration in nM/μg of protein ± SEM of data from experiments performed in triplicate. Statistical analysis was performed using an ANOVA followed by the Tukey post test. *** $P < 0.001$, vs 'basal'.

The signalling pathways that mediate CgA-induced iNOS expression were subsequently studied using a number of inhibitors. Western blot analyses revealed that pre-treatment with poly I (i: 0.1 μg/ml; ii: 0.5 μg/ml), a scavenger receptor antagonist, entirely abated CgA-induced iNOS expression (Fig. 5.2A,B). Pre-treatment with pertussis toxin (Ptx; i: 1 μg/ml; ii: 2 μg/ml), a $G_{i/O}$ protein inhibitor or BAPTA-AM (i: 1 μM; ii: 10 μM), a membrane permeable calcium chelator did not exert an inhibitory effect on iNOS expression. Furthermore, microglia treated with the inhibitors alone did not express significantly different levels of iNOS from control (basal). In contrast, pre-treatment with PP2 (i: 50 nM; ii: 100 nM), a Src kinase inhibitor or UO126 (i: 1 μM; ii: 5 μM) an ERK inhibitor significantly attenuated CgA-induced iNOS expression. Maximal inhibition was obtained with PP2 or UO126 at concentrations of 100 nM and 5 μM respectively. Densitometry revealed that at these concentrations the inhibitors caused a five fold reduction in iNOS expression (Fig. 5.2B). Furthermore, microglia treated with PP2 (100 nM) or UO126 (5 μM) alone contained similar levels of iNOS as control microglia (basal).

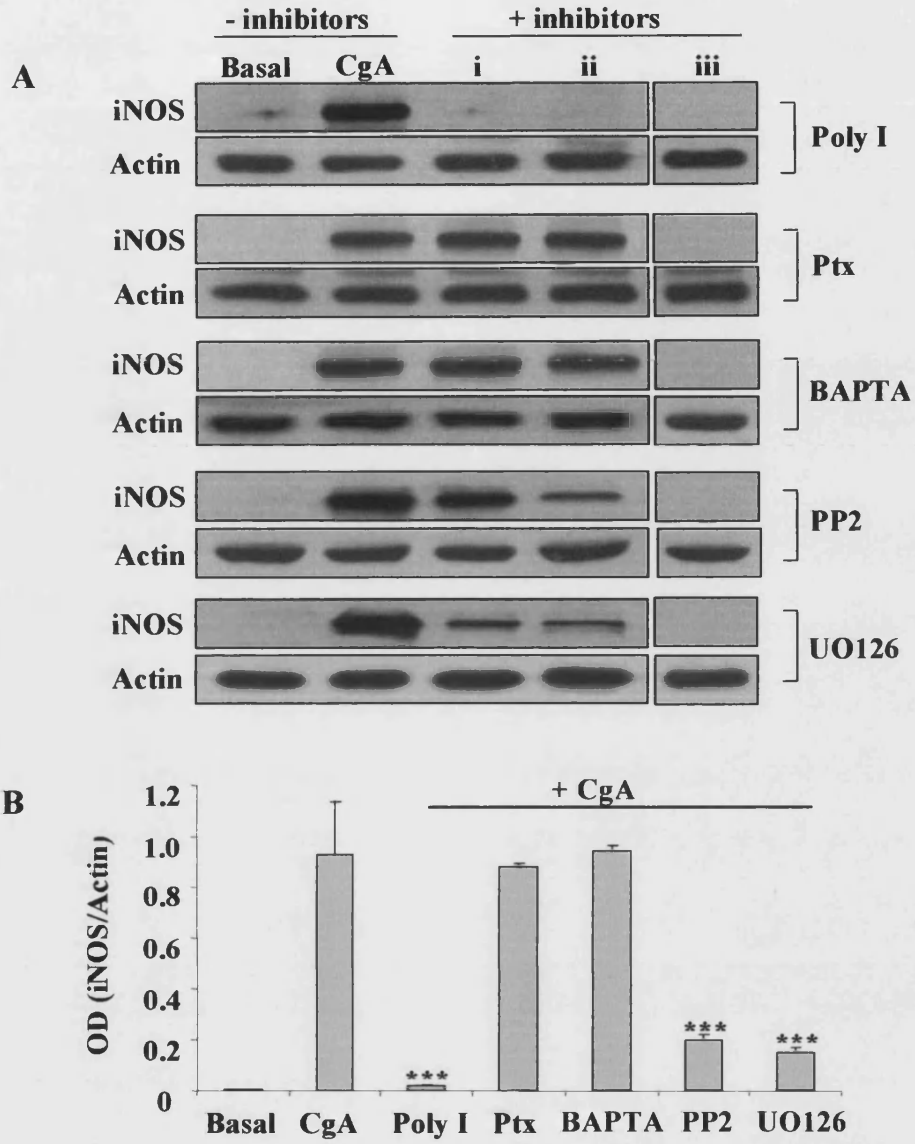

Figure 5.2 Modulation of CgA-induced iNOS expression

Representative Western blots of iNOS expression in microglial cell lysates. **A**: Microglia were treated with CgA (100 nM) for 24 hours before lysates were prepared. In addition, lysates were prepared from microglia treated with CgA (100 nM) in the presence of poly I (0.1 μg/ml; ii: 0.5 μg/ml), pertussis toxin (Ptx, i: 1 μg/ml; ii: 2 μg/ml), BAPTA (i: 1 μM; ii: 10 μM), PP2 (i: 50 nM; ii: 100 nM) or UO126 (i: 1 μM; ii: 5 μM). Lysates were also prepared from microglia treated with the inhibitors (iii: poly I; 0.5 μg/ml, Ptx; 2 μg/ml, BAPTA; 10 μM, PP2; 100 nM, UO126; 5 μM) alone. Control lysates were prepared from microglia left untreated for 24 hours (basal). Lysates were subjected to Western blot analyses using an antibody raised against iNOS (1:5000). To ensure equal loading blots were re-probed using an antibody recognising β-actin (1:1000). **B**: Densitometric analysis of iNOS bands (in the presence of the highest concentration of inhibitor where applicable) and β-actin bands was performed and levels of iNOS were normalised with respect to β-actin. Statistical analysis was performed using ANOVA followed by the Tukey post test. *** $P < 0.001$ vs 'CgA'.

Since UO126 inhibited CgA-induced iNOS expression, the presence of phospho-ERK was assessed in microglial lysates. CgA (100 nM) but not Aβ (55 μM) elicited a rapid phosphorylation of ERK 1 and 2 (Fig. 5.3A). Phospho-ERK was initially detectable 30 minutes after the addition of CgA (100 nM) and expression increased with time. Maximal phosphorylation was reached by 3 hours, followed by a decline in phosphorylation reaching lower levels by 24 hours post CgA treatment. Analysis of total ERK levels indicated that these results were not due to differences in protein loading. Furthermore, parallel time courses using untreated microglial cells demonstrated that ERK phosphorylation did not significantly increase over the experimental period (Fig. 5.3B). This suggests that the increases in ERK phosphorylation are due to the addition of CgA.

The order of second messenger activation leading to iNOS expression was subsequently investigated. Src kinases are involved in membrane proximal signalling events (Alberts et al., 2002), therefore the effects of PP2 pre-treatment on CgA (100 nM) induced ERK phosphorylation were assessed. Western blot analyses demonstrated that, pre-treatment with PP2 (50 nM; 100 nM) caused the complete inhibition of CgA-induced ERK phosphorylation in microglia (Fig. 5.3C). Furthermore, pre-treatment with Poly I (0.1 μg/ml; 0.5 μg/ml) completely abolished the phosphorylation of ERK. Analysis of total ERK expression demonstrated that these results were not a consequence of unequal protein loading.

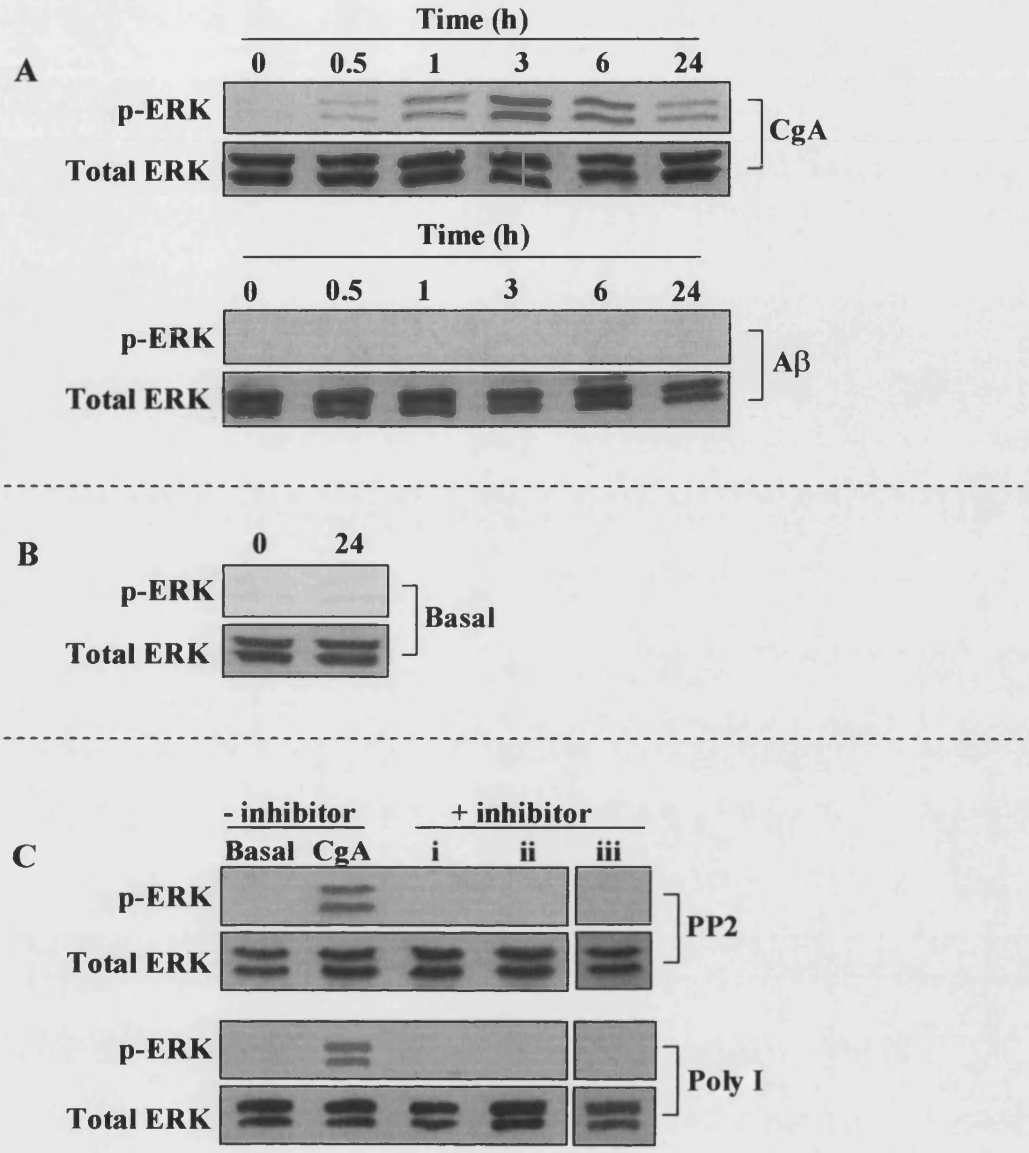

Figure 5.3 CgA but not Aβ induces the phosphorylation of ERK

Representative Western blots of ERK phosphorylation in microglial cell lysates. **A**: Microglia were treated with CgA (100 nM) or Aβ (55 μM) and lysates were prepared after 0, 0.5, 1, 3, 6 or 24 hours. **B**: Control lysates were prepared from untreated microglia after 0 and 24 hours in culture. **C**: Microglia were treated with CgA (100 nM) for 24 hours before lysates were prepared. In addition, microglia were treated with CgA (100 nM) in the presence of PP2 (i: 50 nM; ii: 100 nM) or poly I (0.1 μg/ml; ii: 0.5 μg/ml). Lysates were also prepared from microglia treated with the inhibitors (iii: PP2; 100 nM, poly I; 0.5 μg/ml) alone. Control lysates were prepared from microglia left untreated for 24 hours (basal). Lysates were subjected to Western blot analyses using an antibody raised against phospho-ERK (1:750), which in turn was detected by goat anti-mouse IgG (HRP) (1:1000). To ensure equal loading blots were re-probed using an antibody recognising total ERK (1:500) followed by exposure to goat anti-rabbit IgG (HRP) (1:500).

5.3 Neither CgA nor Aβ induce COX-2 expression in microglia

Microglia were analysed for COX-2 expression following exposure to CgA or Aβ for 24 hours. COX-2 was undetectable in CgA (50-1000 nM) or Aβ (15-55 μM) treated microglia as demonstrated by Western blotting (Fig. 5.4A,B). In contrast, microglia treated with LPS (2 μg/ml) for 24 hours expressed COX-2, whereas COX-2 was absent in microglia left untreated for 24 hours (basal). Furthermore, time course analyses demonstrated that COX-2 was undetectable in microglial lysates 1, 3, 8 or 48 hours after CgA (100 nM) or Aβ (55 μM) treatment (Fig. 5.4C).

5.4 CgA but not Aβ induces glutamate release from microglia

Microglia exposed to CgA (50-1000 nM) for 24 hours released glutamate in a dose dependent fashion (Fig. 5.5A). Glutamate concentrations ranged from 244-598 nM/μg of protein. Microglia left untreated for 24 hours (basal) secreted very low concentrations of glutamate, giving a basal reading of approximately 40 nM/μg of protein. Time course analysis revealed that glutamate was initially detectable 3 hours after the addition of CgA (100 nM) and that the levels of released glutamate increased with time (Fig. 5.5B). Conversely, Aβ (55 μM) did not stimulate the release of glutamate above control levels (basal). The signalling pathways that mediate CgA-induced glutamate release were subsequently studied. Pre-treatment with poly I (0.5 μg/ml) reduced CgA-induced glutamate secretion to control levels (Fig. 5.5C). In contrast, pre-treatment with pertussis toxin (Ptx; 2 μg/ml), BAPTA-AM (10 μM), PP2 (100 nM) or UO126 (5 μM) did not modulate CgA-induced glutamate release. Furthermore, medium collected from microglia treated with the inhibitors alone did not contain significantly different levels of glutamate from control medium (basal).

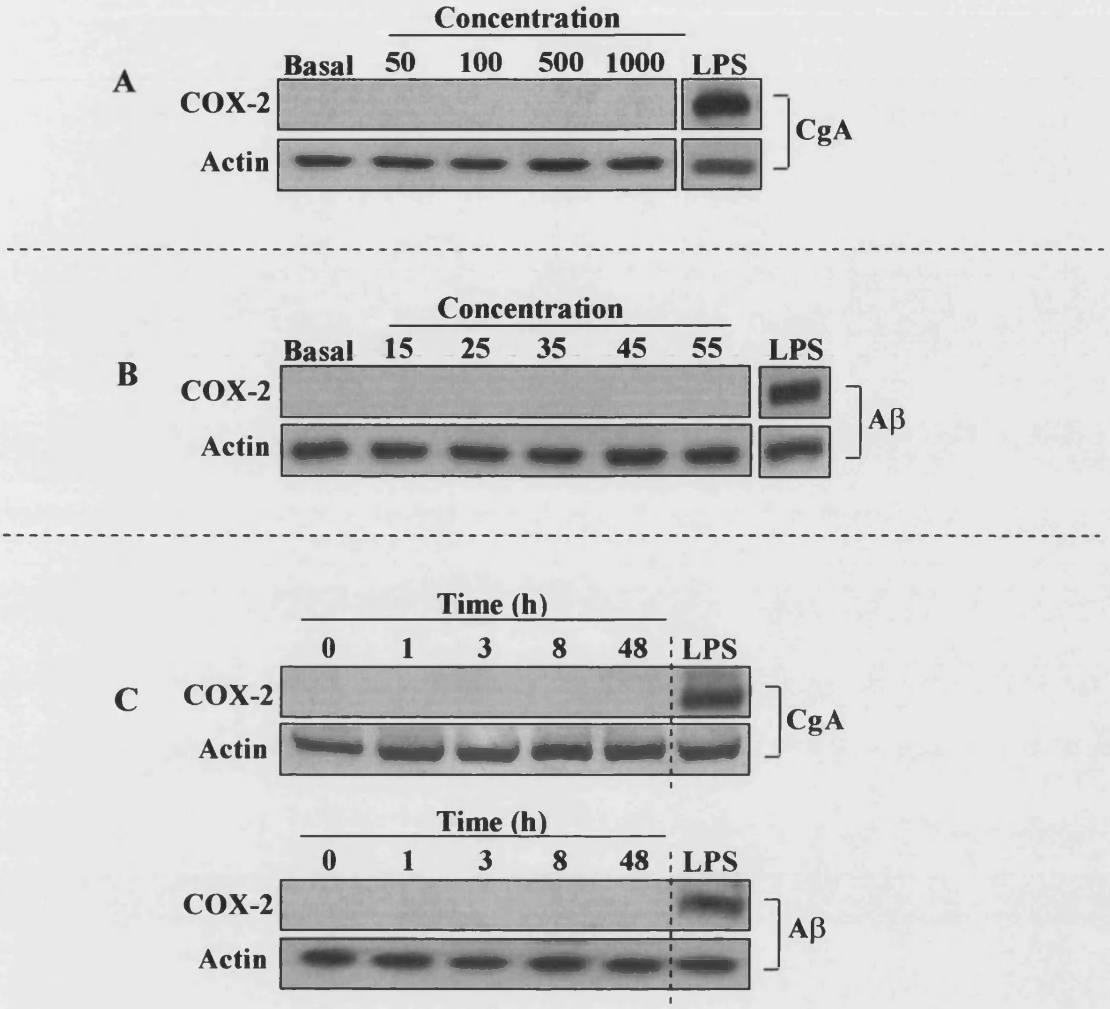

Figure 5.4 Neither CgA nor Aβ induce COX-2 expression

Representative Western blots of COX-2 expression in microglial cell lysates. **A**: Microglia were treated with increasing concentrations of CgA (50-1000 nM) for 24 hours before lysates were prepared. Lysates were also prepared from microglia treated with LPS (2 μg/ml) for 24 hours. Control lysates were prepared from microglia left untreated for 24 hours (basal) **B:** Microglia were treated with increasing concentrations of Aβ (15-55 μM) for 24 hours before lysates were prepared. Lysates were also prepared from microglia treated with LPS (2 μg/ml) for 24 hours. Control lysates were prepared from microglia treated as described in A. **C**: Microglia were treated with CgA (100 nM) or Aβ (55 μM) for 0, 1, 3, 8 or 48 hours before lysis. As a positive control microglia were treated with LPS (2 μg/ml) for 24 hours. Lysates were subjected to Western blot analysis using an antibody raised against COX-2 (1:750), which in turn was detected by donkey anti-goat IgG (HRP) (1:1000). To ensure equal protein loading blots were reprobed with an antibody recognising β-actin (1:1000) followed by exposure to goat anti-mouse IgG (HRP) (1:1000).

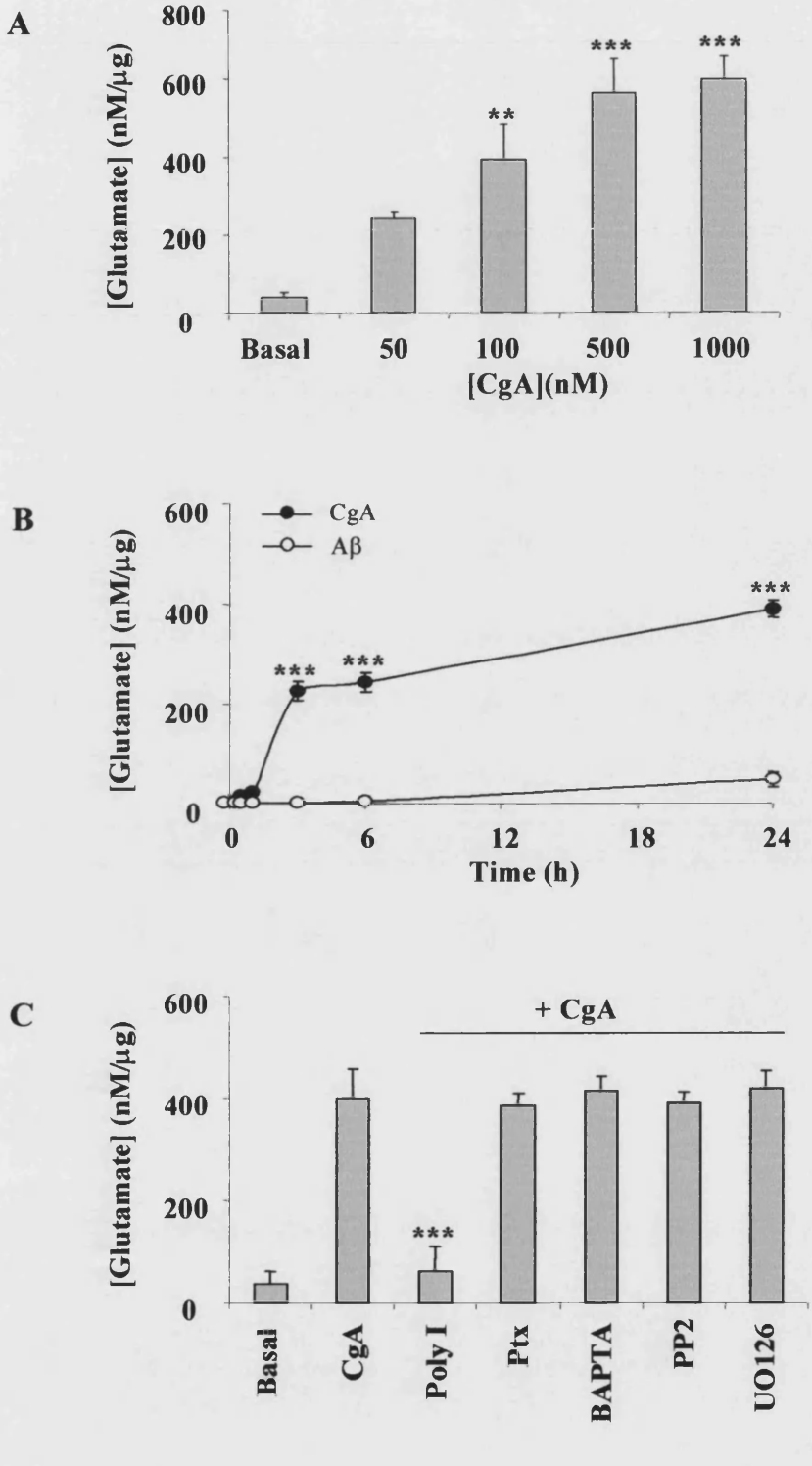

Figure 5.5 (see overleaf for figure legend)

Figure 5.5 CgA but not Aβ stimulates glutamate release

Glutamate concentrations (nM/μg of protein) were measured in microglial conditioned medium using a fluorometric assay. **A**: Microglia were treated with increasing concentrations of CgA (50-1000 nM) for 24 hours before the medium was collected. Control medium was collected from microglia left untreated for 24 hours (basal). **B**: Microglia were treated with CgA (100 nM; closed circles) or Aβ (55 μM; open circles) for 0, 0.25, 0.5, 1, 3, 6 or 24 hours before medium was collected. **C**: Medium was collected from microglia treated with CgA (100 nM) for 24 hours. In addition, medium was collected from microglia treated with CgA (100 nM) in the presence of poly I (0.5 μg/ml), pertussis toxin (Ptx: 2 μg/ml), BAPTA-AM (10 μM), PP2 (100 nM) or UO126 (5 μM). Control medium was collected from microglia treated as described in A. The values shown represent the mean (nM/μg of protein) ± SEM of data from experiments performed in triplicate. Statistical analysis was performed using ANOVA followed by the Tukey post test. * $P < 0.05$, ** $P < 0.01$, *** $P < 0.001$ vs control. (A: control describes basal. B: control describes 0 hours. C: control describes CgA treated).

To verify that glutamate release was not due to cell membrane disruption, CgA (1000 nM) treated microglia were stained with propidium iodide and fluoroscein diacetate. Staining revealed that microglial cultures exposed to CgA for 24 hours (1000 nM) contained few cells exhibiting propidium iodide staining (table 5.2). Similarly, microglial cultures left untreated for 24 hours contained few cells that stained with propidium iodide. This suggests that CgA induced glutamate release occurs via a regulated pathway and is not due to loss of cell membrane integrity.

	Basal	CgA (1000 nM)
% propidium iodide stained cells	2.8 ± 1.2	2.7 ± 2.2

Table 5.2 Analysis of microglial membrane integrity following exposure to CgA
Microglia treated with CgA were stained with propidium iodide and fluoroscein diacetate to provide an estimation of cell membrane integrity. Microglia were treated with CgA (1000 nM) for 24 hours before staining was performed. Control microglia were left untreated for 24 hours before staining (basal). Cells possessing propidium iodide staining were expressed as a percentage of the total number of cells counted (cells possessing propidium iodide staining or fluoroscein diacetate staining). The values shown represent the mean ± SEM of data from experiments performed in triplicate. Statistical analysis was performed using a two sided unpaired students T-Test. According to this test there was no difference between the treatments.

5.5 CgA or Aβ induces microglia to apoptose

Following CgA or Aβ treatment, microglia ultimately adopt a shrunken conformation that is characteristic of dying cells. This phenomenon was investigated further using the fluorescent dyes JC-1 and Hoechst 33342, which enable the identification of depolarised mitochondria and pyknotic nuclei respectively. Staining revealed that exposure of microglia to CgA (50-1000 nM) for 48 hours resulted in a dose dependent increase in the number of cells displaying depolarised mitochondria or nuclear pyknosis (Fig. 5.6A). In contrast, the vast majority of untreated microglia possessed polarised mitochondria and large healthy nuclei at the same time point (basal). Time course analyses demonstrated that mitochondrial depolarisation induced by CgA preceded apoptosis temporally (Fig. 5.6B). Microglia displaying depolarised mitochondria were initially detectable 24 hours after the addition of CgA (100 nM), whereas microglia exhibiting significant levels of nuclear pyknosis were not detectable until 32 hours post treatment.

Exposure of microglia to Aβ (15-55 μM) for 48 hours also induced in a dose dependent increase in mitochondrial depolarisation and nuclear pyknosis (Fig. 5.6C). Conversely, microglia treated with the reverse peptide, $A\beta_{(35\text{-}25)}$ (55 μM) for 48 hours, possessed polarised mitochondria and large healthy nuclei. This indicates that apoptosis and mitochondrial depolarisation are a specific response to Aβ treatment. As with CgA treatment, Aβ induced mitochondrial depolarisation preceded apoptosis temporally. Microglia displaying depolarised mitochondria were initially detectable 32 hours after the addition of Aβ (55 μM), whereas apoptotic cells were not detectable until 40 hours after Aβ (55 μM) treatment (Fig. 5.6D).

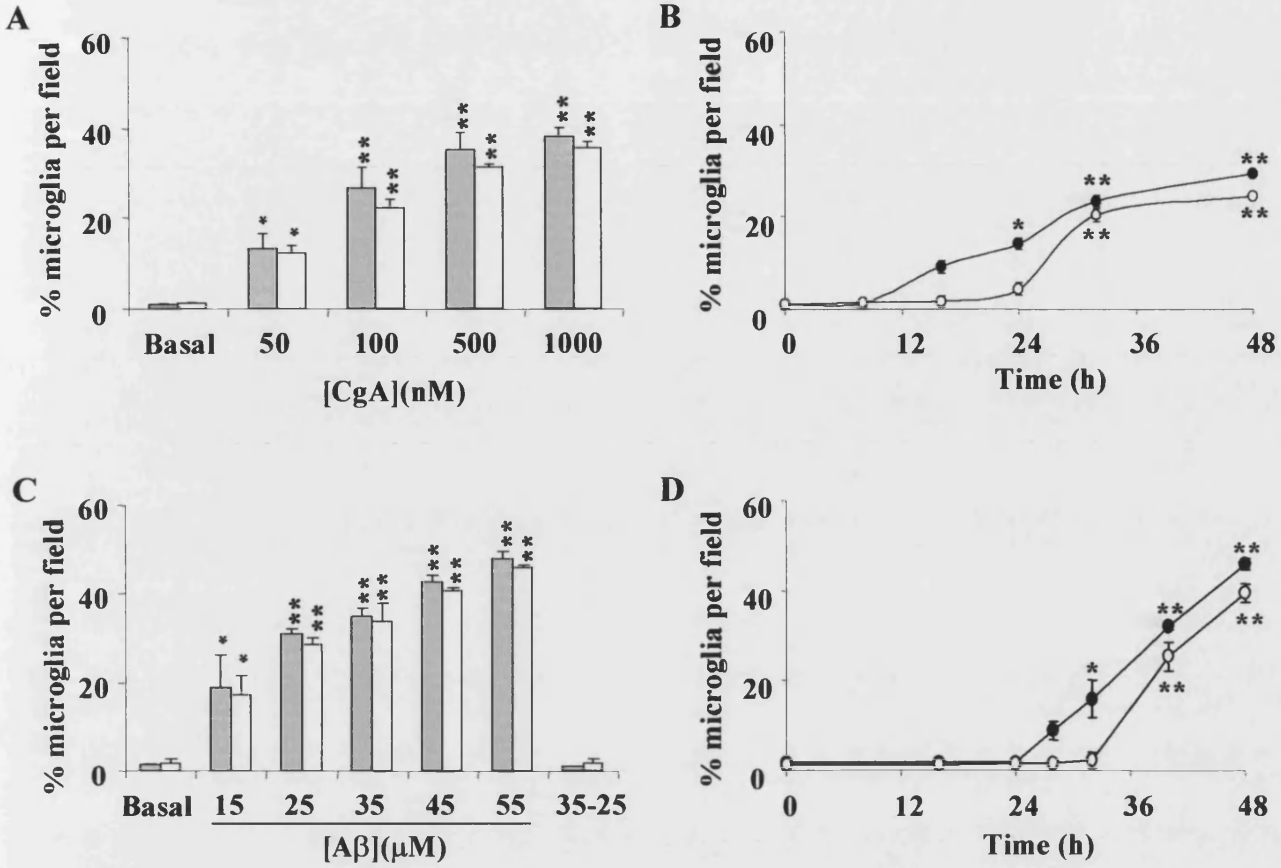

Figure 5.6 CgA or Aβ induces mitochondrial depolarisation and apoptosis

Microglia treated with CgA or Aβ were stained with JC-1 or Hoechst 33342 to provide an estimation of mitochondrial depolarisation and apoptosis respectively. **A**: Microglia were treated with increasing concentrations of CgA (50-1000 nM) for 48 hours then the cells were stained with JC-1 (grey bars) or Hoechst 33342 (open bars). Control microglia were left untreated for 48 hours before staining (basal). **B**: Microglia were treated with CgA (100 nM) for 0, 8, 16, 24, 32 or 48 hours before being stained with JC-1 (closed circles) or Hoechst 33342 (open circles). **C**: Microglia were treated with increasing concentrations of Aβ (15-55 μM) or the reverse peptide $A\beta_{(35-25)}$ (55 μM) for 48 hours before the cells were stained with JC-1 (grey bars) or Hoechst 33342 (open bars). Control microglia were treated as described in A (basal). **D**: Microglia were treated with Aβ (55 μM) for 0, 16, 24, 28, 32, 40 or 48 hours before being stained with JC-1 (closed circles) or Hoechst 33342 (open circles). Cells displaying depolarised mitochondria or brightly stained pyknotic nuclei were counted and the degree of mitochondrial depolarisation or apoptosis was expressed as a percentage of the total number of cells counted. The values shown represent the mean ± SEM of data from experiments performed in triplicate. Experiments consisted of 3 coverslips per treatment, each comprising 10 fields of view and experiments were performed on three independent occasions. Statistical analysis was performed using ANOVA followed by the Tukey post test. * $p < 0.05$ vs control; ** $p < 0.01$ vs control (A, C: control describes basal. B, D: control describes 0 hours).

Apoptosis is often preceded by a reduction in mitochondrial membrane potential ($\Delta\Psi$), which is caused by the opening of the PT pore (Zamzami et al., 1996). The involvement of the PT pore in CgA or Aβ induced apoptosis was subsequently assessed using the pore inhibitor cyclosporin A (CsA) (Zamzami et al., 1996; Seaton et al., 1998; Yang and Cortopassi 1998; Kingham and Pocock 2000). Pre-treatment with CsA (1 μM) significantly attenuated CgA (100 nM) or Aβ (55 μM) induced mitochondrial depolarisation and apoptosis after 48 hours in culture (Fig. 5.7A,B). This suggests that the PT pore is involved in both CgA or Aβ induced cell death.

The upstream signalling pathways involved in CgA or Aβ induced mitochondrial depolarisation and apoptosis were also studied using the same battery of inhibitors employed in previous experiments. Pre-treatment with poly I (0.5 μg/ml) reduced CgA (100 nM) induced mitochondrial depolarisation and apoptosis to control levels (Fig. 5.7A). Pre-treatment with pertussis toxin (Ptx; 2 μg/ml) or BAPTA-AM (10 μM) exerted no inhibitory effect on these parameters, whereas PP2 (100 nM) or UO126 (5 μM) pre-treatment significantly attenuated CgA-induced mitochondrial depolarisation and apoptosis. Furthermore, pre-treatment with poly I (0.5 mg/ml), pertussis toxin (Ptx; 2 μg/ml) or PP2 (100 nM) significantly attenuated Aβ (55 μM) induced mitochondrial depolarisation and apoptosis (Fig. 5.7B), whilst pre-treatment with neutralising RAGE antibody (200 μg/ml), BAPTA-AM (10 μM) or UO126 (5 μM) exerted no inhibitory effects. Moreover, microglial cultures treated with the inhibitors alone did not contain significantly different levels of mitochondrial depolarisation or apoptosis from control (basal).

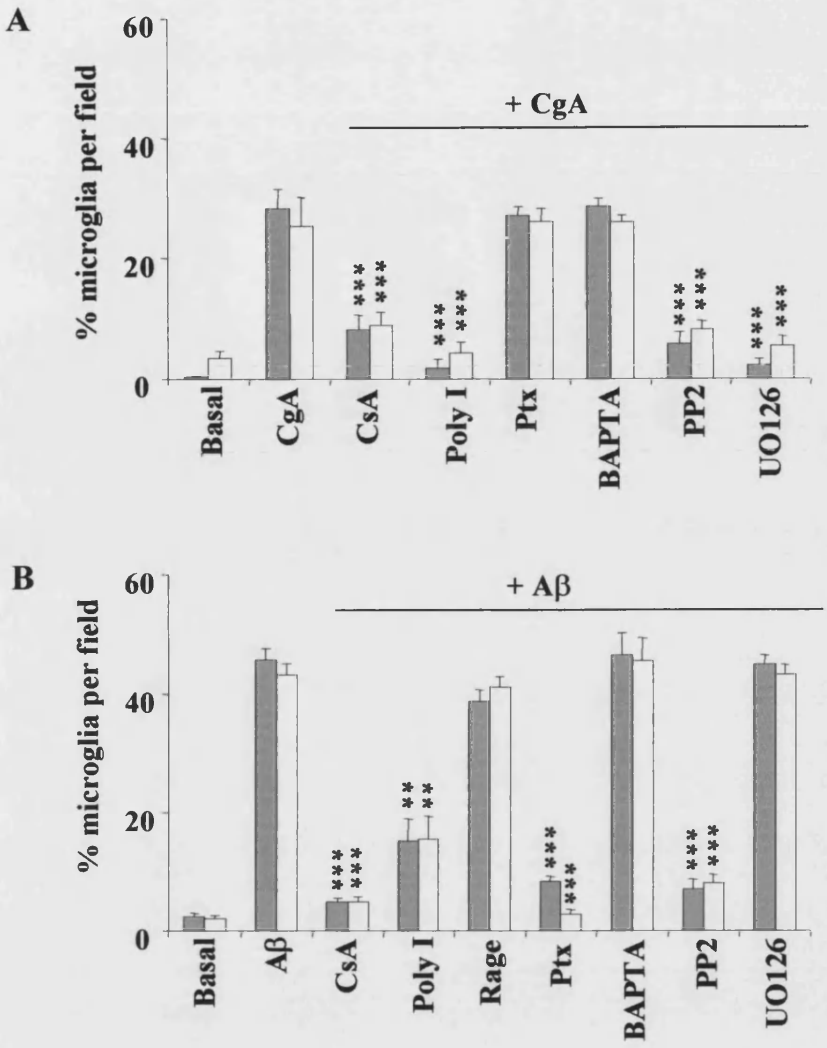

Figure 5.7 Modulation of mitochondrial depolarisation and apoptosis

Microglia treated with CgA or Aβ in the presence of inhibitors were stained with JC-1 or Hoechst 33342 to provide an estimation of mitochondrial depolarisation and apoptosis respectively. Microglia were treated with CgA (100 nM) (**A**) or Aβ (55 μM) (**B**) for 48 hours then the cells were stained with JC-1 (grey bars) or Hoechst 33342 (open bars). In addition, microglia treated with CgA (100 nM) or Aβ (55 mM) in the presence of CsA (1 μM), Poly I (0.5 μg/ml), neutralising RAGE antibody (200 μg/ml: Aβ treated microglia only), Ptx (2 μg/ml), BAPTA-AM (10 μM), PP2 (50 nM) or UO126 (5 μM) were stained with JC-1 (grey bars) or Hoechst 33342 (open bars) after 48 hours in culture. Control microglia were left untreated for 48 hours before staining (basal). Cells displaying depolarised mitochondria or brightly stained pyknotic nuclei were counted and the degree of mitochondrial depolarisation or apoptosis was expressed as a percentage of the total number of cells counted. The values shown represent the mean ± SEM of data from experiments performed in triplicate. Experiments consisted of 3 coverslips per treatment, each comprising 10 fields of view and experiments were performed on three independent occasions. Statistical analysis was performed using ANOVA followed by the Tukey post test. ** $p < 0.01$ vs control. *** $p < 0.001$ vs control. (A: control describes CgA treated microglia. B: control describes Aβ treated microglia).

5.6 Neither CgA nor Aβ induce calcium transients in N9 microglia

Despite the finding that BAPTA-AM did not inhibit the CgA or Aβ induced signalling events studied so far, the ability of these microglial activators to elicit intracellular calcium transients was tested in N9 microglia using fura-2. The N9 cell line is a well characterised microglial cell line, which exhibits similar responses to primary microglia (Corradin et al., 1993; Ferrari et al., 1996; Kingham et al., 1999). Accordingly, CgA (100 nM) induced iNOS expression in N9 microglia, whilst Aβ (55 μM) did not (Fig. 5.8).

Calcium transients were undetectable in untreated N9 microglia (Fig. 5.9). Similarly, application of CgA (100 nM) or Aβ (55 μM) did not evoke calcium transients in these cells (Fig. 5.9). In contrast, ATP (1 μM), a microglial activator known to induce calcium release from IP_3 regulated stores (Möller et al., 2000b; Nagai et al., 2001), evoked a rapid calcium response in N9 microglia. Furthermore, N9 cells were resistant to a wide range of CgA (100-10000 nM) (Fig. 5.10) or Aβ (0.1-55 μM) concentrations (Fig. 5.11).

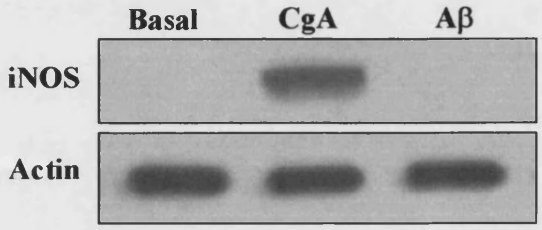

Figure 5.8 CgA but not Aβ induces iNOS expression in N9 microglia.
Representative Western blots of iNOS expression in N9 microglia cell lysates. N9 Microglia were exposed to CgA (100 nM) or Aβ (55 μM) for 24 hours before lysates were prepared. Control lysates were prepared from N9 microglia left untreated for 24 hours (basal). Lysates were subjected to Western blot analyses using an antibody raised against iNOS (1:5000). To ensure equal protein loading blots were reprobed with an antibody recognising β-actin (1:1000).

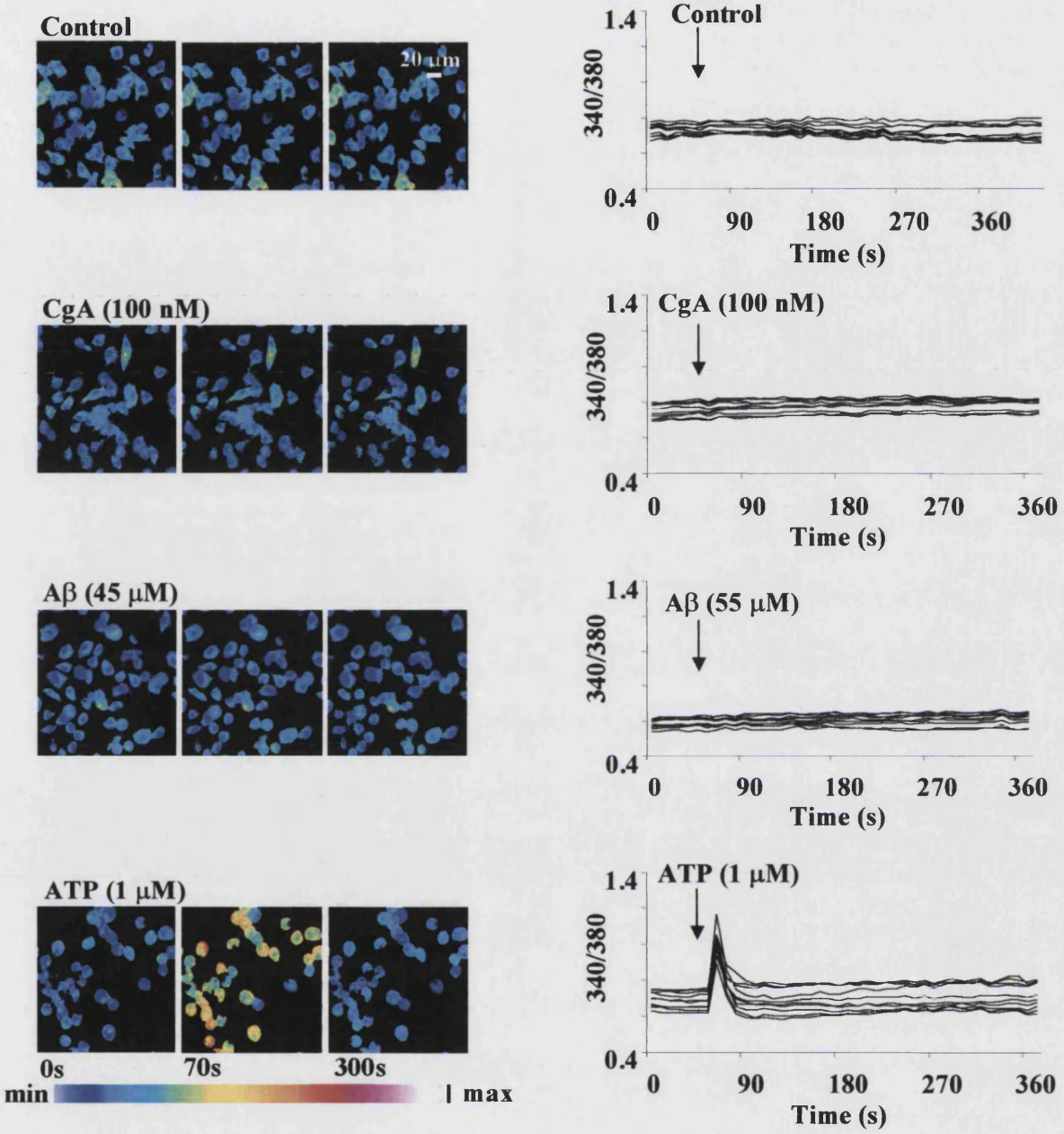

Figure 5.9 Effect of CgA or Aβ on intracellular calcium fluxes in N9 microglia

Representative false colour images and traces depicting the effects of CgA, Aβ or ATP on intracellular calcium in N9 microglia. N9 microglia were loaded with fura-2 (5 µM) in basic medium for 45 minutes at 37 °C. Cells were subsequently excited with wavelengths of 340 and 380 nm and emission was collected at a wavelength of 510 nm. CgA (100 nM), Aβ (55 µM) or ATP (1 µM) diluted in basic medium were added to the cells 60 seconds after the commencement of excitation. Control N9 cells were treated with basic medium alone at the same time point. Calcium responses were recorded from ten cells and the results were expressed as 340/380 fluorescence ratios. False colour images corresponding to each treatment are also displayed. Images were captured at 0, 70 and 300 seconds (from left to right) and the scale bar provides an indication of intracellular calcium levels.

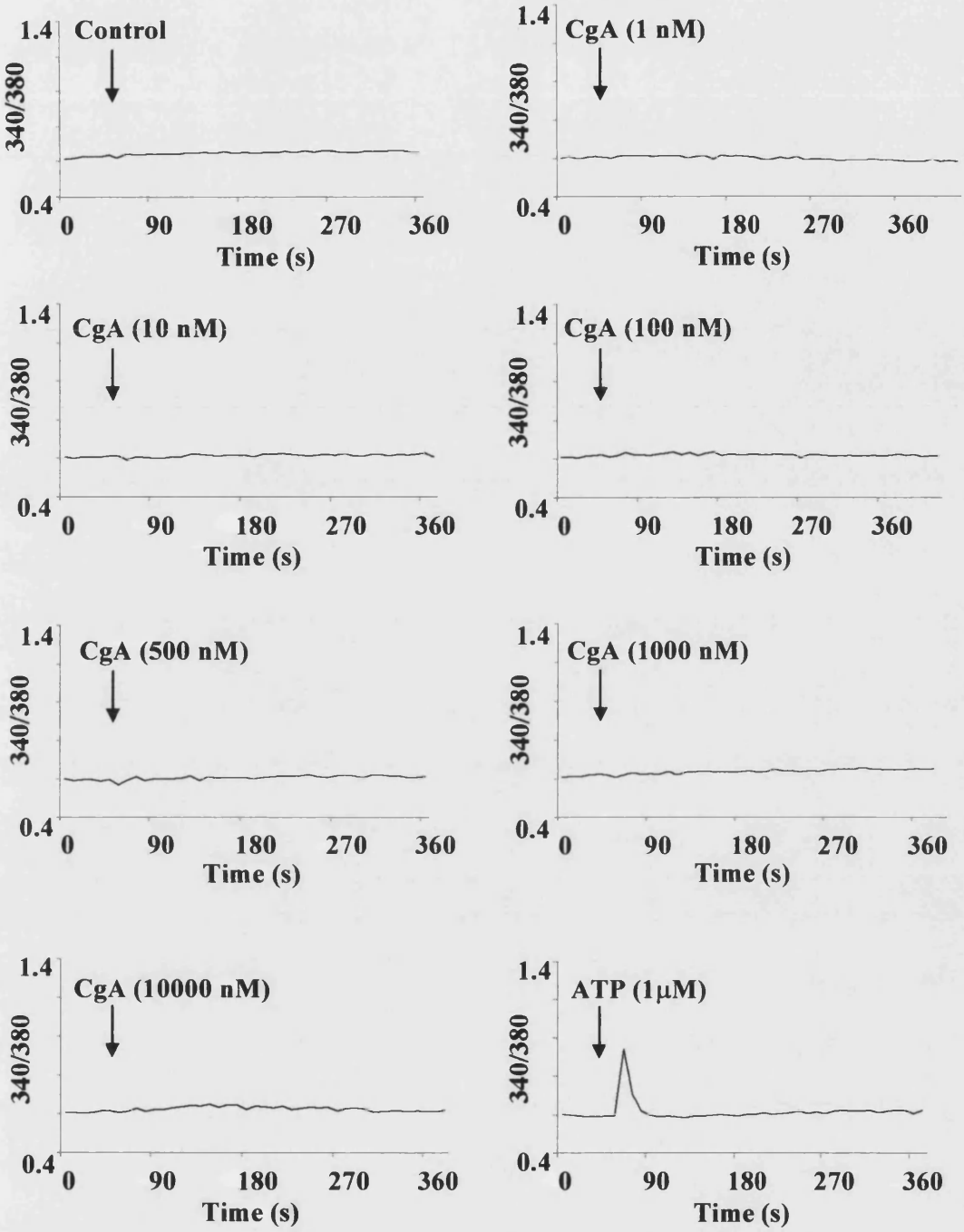

Figure 5.10 Dose dependent effects of CgA on intracellular calcium in N9 microglia
Representative traces depicting the effects of increasing concentrations of CgA on intracellular calcium in N9 microglia. N9 microglia were loaded with fura-2 (5 μM) in basic medium for 45 minutes at 37 °C. Cells were subsequently excited with wavelengths of 340 and 380 nm and emission was collected at a wavelength of 510 nm. CgA (1-10000 nM) diluted in basic medium was added to the cells 60 seconds after the commencement of excitation, as a positive control microglia were treated with ATP (1 μM). Control N9 cells were treated with basic medium alone at the same time point. Calcium responses were recorded from ten cells and the results were averaged and expressed as 340/380 fluorescence ratios.

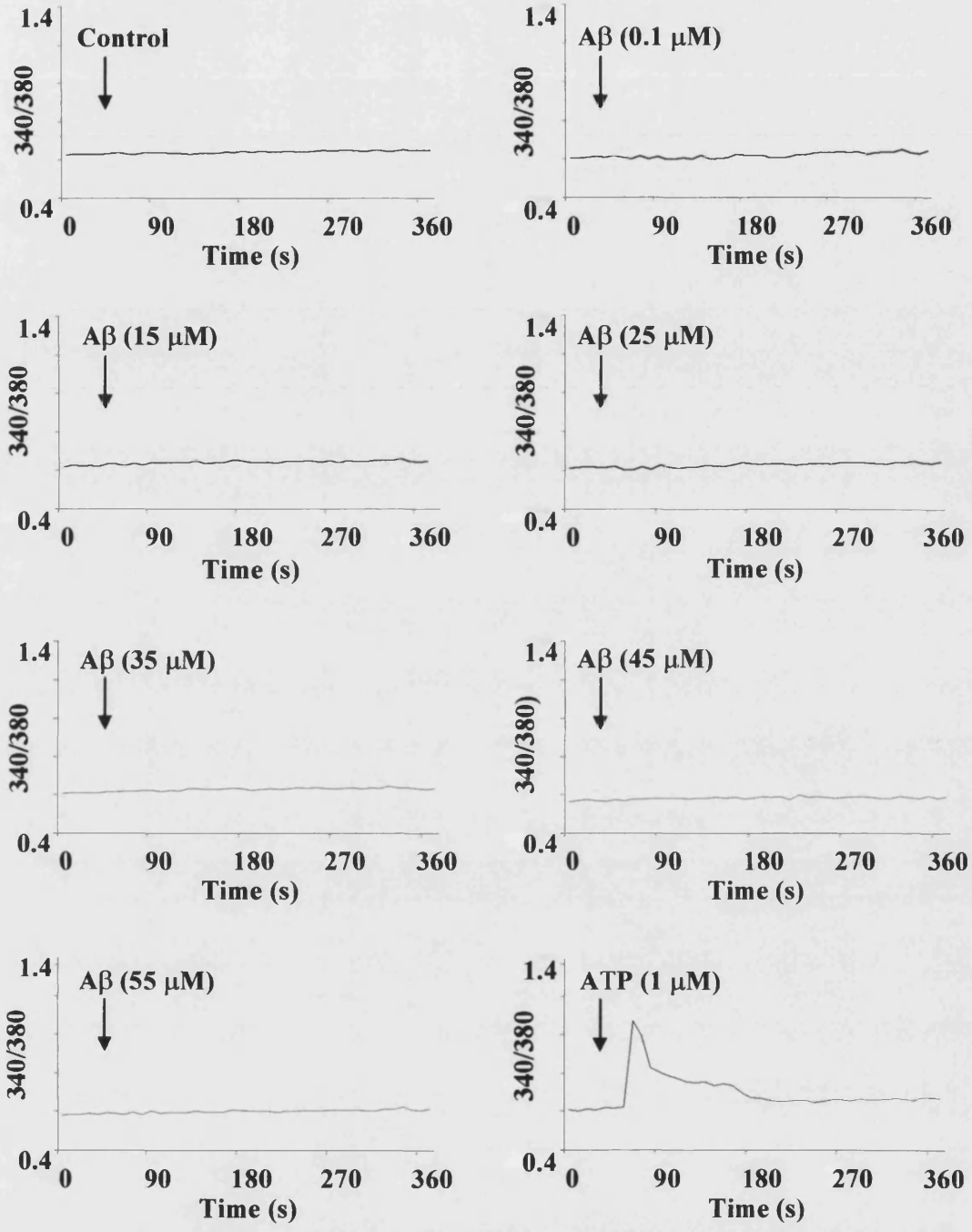

Figure 5.11 Dose dependent effects of Aβ on intracellular calcium in N9 microglia

Representative traces depicting the effects of increasing concentrations of Aβ on intracellular calcium in N9 microglia. N9 microglia were loaded with fura-2 (5 μM) in basic medium for 45 minutes at 37 °C. Cells were subsequently excited with wavelengths of 340 and 380 nm and emission was collected at a wavelength of 510 nm. Aβ (0.1-55 μM) diluted in basic medium was added to the cells 60 seconds after the commencement of excitation, as a positive control microglia were treated with ATP (1 μM). Control N9 cells were treated with basic medium alone at the same time point. Calcium responses were recorded from ten cells and the results were averaged and expressed as 340/380 fluorescence ratios.

5.7 CgA or Aβ treated microglia induce neuronal death

Inflammatory mediators released from activated microglia can exacerbate neurodegeneration (Thery et al,. 1991; Kingham et al., 1999; Combs et al., 1999). Subsequently, conditioned medium harvested from CgA (100 nM) or Aβ (55 μM) treated microglia was applied to cultures of cerebellar granule neurones and neuronal apoptosis was assessed using Hoescht 33342. Cerebellar granule neurones exhibited a dense network of cable like neurites after 8 days in culture, and contained few apoptotic nuclei (Basal) (Fig. 5.12A,C). Similarly, neurones exposed to conditioned medium collected from microglia left untreated for 24 hours also contained low levels of apoptotic cells after 24 hours in culture. In contrast, medium obtained from microglia treated with CgA (100 nM) or Aβ (55 μM) for 24 hours induced a significant increase in neuronal apoptosis (Fig. 5.12A,D). Neuronal death was reversed by boiling conditioned medium obtained from CgA (100 nM) or Aβ (55 μM) treated microglia, which suggests that the neurotoxic agent(s) are heat labile. The increase in apoptosis was not attributable to the presence of CgA (100 nM) or Aβ (55 μM) in the culture medium, since the direct application of these agents to neuronal cultures did not increase apoptosis above basal levels. Furthermore, the addition of control microglial conditioned medium to neurones in the presence of CgA (100 nM) or Aβ (55 μM) did not increase neuronal death above basal levels. To determine at which point neurotoxic agents were released, microglia were treated with CgA (100 nM) or Aβ (55 μM) and the conditioned medium was removed over a period of 0-24 hours. Medium was subsequently incubated with cerebellar granule cells for 24 hours before apoptosis was appraised. Using this approach, significant levels of neurotoxin release were found to occur 16 hours after the addition of CgA or Aβ and the neurotoxicity of the conditioned medium increase with time (Fig. 5.12B).

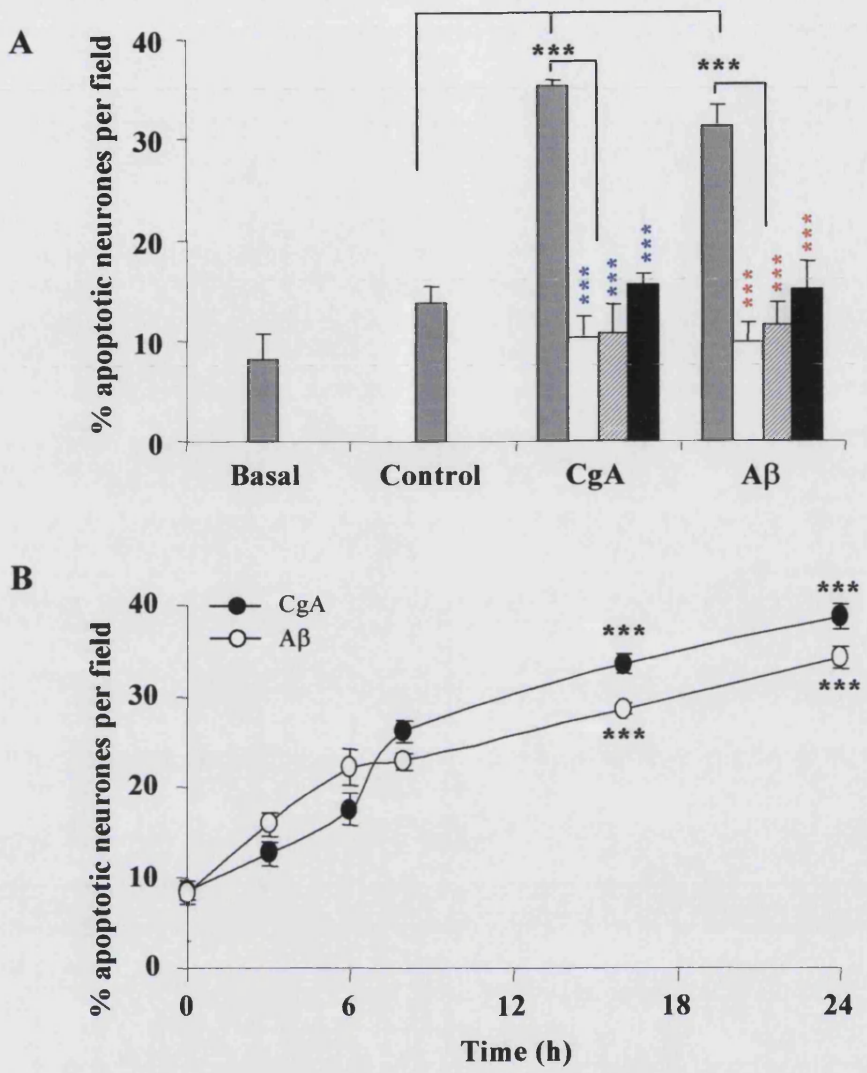

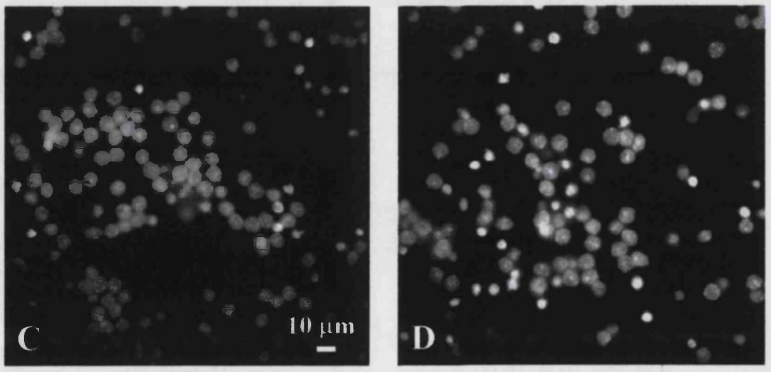

Figure 5.12 (see overleaf for figure legend)

Figure 5.12 CgA or Aβ treated microglia induce neuronal apoptosis

Neuronal apoptosis induced by medium obtained from CgA or Aβ treated microglia was assessed using Hoescht 33342. **A**: Microglia were treated with CgA (100 nM) or Aβ (55 μM) for 24 hours before medium was collected. Control medium was collected from microglia left untreated for 24 hours (control). Medium was then applied to cerebellar granule neurones for 24 hours before the neurones were fixed and stained with Hoescht 33342. In addition, medium collected from CgA (100 nM) or Aβ (55 μM) treated microglia was boiled before being applied to neuronal cultures (open bars). Neurones were also left untreated for 24 hours (basal) or were treated with CgA (100 nM) or Aβ (55 μM) in the presence (hatched bars) or absence (black bars) of control microglial conditioned medium for 24 hours. **B**: Medium was collected from microglia treated with CgA (100 nM) (closed circles) or Aβ (55 μM) (open circles) for 0, 3, 6, 8, 16 or 24 hours. Medium was then applied to cerebellar granule neurones for 24 hours. Neurones were subsequently stained with Hoescht 33342. Following staining, non-apoptotic cells possessed large brightly stained nuclei (**C**), whereas apoptotic cells possess brightly stained pyknotic nuclei (**D**). Neurones displaying brightly stained pyknotic nuclei were counted and the degree of apoptosis was expressed as a percentage of the total number of cells counted. The values shown represent the mean ± SEM of data from experiments performed in triplicate. Experiments consisted of 3 coverslips per treatment, comprising ten fields of view. Statistical analysis was performed using ANOVA followed by the Tukey post test. *** $p < 0.001$ vs control. (Control describes neuronal cultures treated with medium harvested from untreated microglia "Control"). *** $p < 0.001$ vs 'CgA treated'. *** $p < 0.001$ vs 'Aβ' treated.

5.8 Discussion

There is compelling evidence that inflammatory processes play a significant role in AD. Indeed in a number of studies NSAIDs have been shown to reduce the incidence of AD (McGeer et al., 1996; Stewart et al., 1997). The principle action of these drugs is to suppress the production of pro-inflammatory products that are primarily secreted by activated microglia. This implies that microglia play an important role in disease progression. Consequently, in this chapter the signalling cascades elicited in CgA or Aβ treated microglia were studied because both of these proteins are located at the inflammatory foci associated with senile plaques. Experimental data revealed that CgA and Aβ stimulated microglial signalling pathways via scavenger receptor dependent mechanisms. Scavenger receptors are upregulated on microglia in AD tissue in particular around senile plaques (Honda et al., 1998). This implies that CgA and Aβ may signal via scavenger receptors *in vivo*.

Ultimately, CgA or Aβ treated microglia underwent mitochondrial depolarisation, which precipitated apoptotic cell death. Dissection of the signalling cascades elicited in CgA or Aβ treated microglia revealed that these activators triggered different upstream signalling events. These findings suggest that CgA and Aβ bind to different scavenger receptor isoforms, although the identity of which remains to be delineated. CgA was found to induce iNOS expression, mitochondrial depolarisation and apoptosis via a Src kinase and ERK. CgA also evoked the release of high concentrations of glutamate into the culture medium. In contrast, Aβ did not induce iNOS expression or glutamate release. Aβ mediated signalling was found to involve a Src kinase and a G_i protein, but not ERK.

Previously, CD36 (a class B receptor) has been reported to induce the activation of ERK and Src kinases (Moore et al., 2002). Furthermore, class A scavenger receptors couple to Src kinases (Miki et al., 1996) and G_i proteins (Whitman et al., 2000; Post et al., 2002). This suggests that CgA may signal via CD36, whereas Aβ might signal through a class A scavenger receptor in the pathways described in this chapter. A recent study has also demonstrated that scavenger receptors induce NO production following ligand induced activation (Alford et al., 1998). However, this is the first report to show that scavenger receptors trigger glutamate release and ultimately mitochondrial depolarisation and apoptosis. These are exciting observation since until recently scavenger receptors were not known to instigate cell signalling.

5.8.1 CgA and Aβ act as scavenger receptor agonists

Additional evidence to suggest that CgA acts as a novel scavenger receptor agonist is provided by studying the proteins primary sequence. CgA comprises 457 amino acids a high proportion of which are consecutive negatively charged glutamic acid residues (Swiss Prot search) (Fig. 5.13). Negatively charged species are a recognised structural feature of scavenger receptor ligands. For example, native LDL does not function as a scavenger receptor ligand, whereas acetylated and oxidised LDL exhibit a high affinity for the receptor (Zhang et al., 1993). Other known scavenger receptor ligands include LPS (Hampton et al., 1991) and dextran sulphate (Pollaud-Cherion et al., 1998).

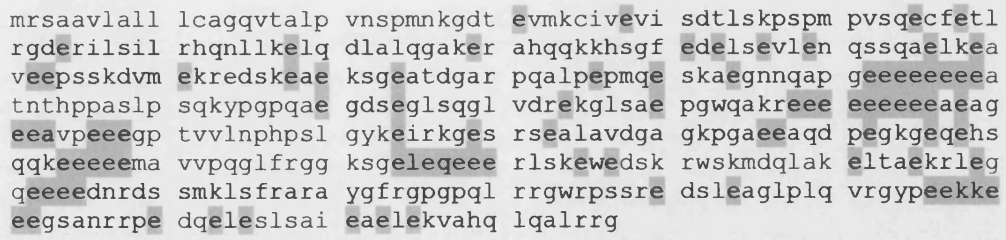

Figure 5.13 Sequence of CgA

CgA comprises 457 amino acids a high proportion of which are consecutive negatively charged glutamic acid residues (e) (Swiss Prot search).

Numerous reports have demonstrated that Aβ acts as an agonist for the scavenger receptor. In particular Aβ (1-42) has been shown to bind to a class A scavenger receptor (Paresce et al., 1996, 1997), CD36 (a class B receptor) (Moore et al., 2002; El Khoury et al., 2003) and SR-B1 (a class B receptor) (Husemann et al., 2001). A recent report extends these findings to demonstrate that a multi-protein assembly comprising of CD36, α6β1 integrin and CD47 mediates Aβ (1-42, 1-40 or 25-35) binding (Bamberger et al., 2003). Additionally, Aβ (1-42) has been reported to interact with formylpeptide receptors (Le et al., 2001; Tiffany et al., 2001) and Aβ (1-42, 1-40 or 25-35) can also bind RAGE (Yan et al., 1996; 1997), although this study reveals that RAGE is not involved in Aβ-induced apoptosis. Thus, it is likely that a multitude of receptors play complementary roles in the varying responses of microglia to Aβ *in vivo*.

5.8.2 Downstream pathways: iNOS and COX-2

Microglia treated with CgA upregulated the expression of iNOS, which is consistent with previous findings (Taupenot et al., 1996; Kingham et al., 1999). However, nitrite, the stable breakdown product of NO was undetectable in the culture medium (see section for 4.9.2 for theories to explain this discrepancy). CgA-induced iNOS expression was mediated intracellularly by the Src kinase-dependent phosphorylation of ERK. Furthermore, other microglial activators including LPS (Bhat et al., 1998; Pyo et al, 1998), thrombin (Ryu et al., 2000) and adenovirus infection (Bhat and Fan 2002) trigger iNOS expression via ERK-dependent mechanisms. Previous studies have also demonstrated that Src kinases mediate ERK phosphorylation (Combs et al., 1999; Moore et al., 2002), which corroborates the findings presented in this chapter. *In vivo*, microglia surrounding senile plaques display enhanced phosphotyrosine staining, which suggests that similar signalling events may occur in AD (Wood and Zinsmeister 1991). It should be noted that additional transcription factors must contribute to iNOS expression in CgA treated microglia, given that UO126 completely inhibited ERK phosphorylation but only partially attenuated iNOS expression. One potential candidate is NFκβ whose ability to evoke iNOS transcription has been documented (Nathan et al., 1994; Chao et al., 1997; Kim et al., 2003).

In contrast to CgA treatment, Aβ did not trigger the up-regulation of iNOS expression. There have been contradictory reports regarding the effects of Aβ on NO metabolism. Li et al., 1996 reported that Aβ(25-35) does not induce microglial NO production, whereas microglia treated with Aβ (1-40) or Aβ(1-42) do synthesis NO. Other reports have shown that neither Aβ(25-35) (Kopec and Carroll 1998; Casal et

al, 2002) nor Aβ(1-42) (Casal et al, 2002) induce iNOS expression or NO production in microglia. Moreover, some investigators have observed an increase in NO production only when microglia are treated with Aβ(25-35) (Goodwin et al., 1995; Meda et al., 1995), Aβ(1-42) (Meda et al., 1995) or Aβ(1-40) (Murphy et al., 1998; Gasic-Milenkovic et al., 2003) in combination with cytokines. These findings imply that Aβ may require the presence of a 'co-stimulator' to induce microglial activation. In support of this the extracellular environment surrounding senile plaques is rich in a variety of pro-inflammatory agents including cytokines and complement proteins (McGeer and McGeer 1997, 1999), which are likely to augment the effects of Aβ on microglia *in vivo*.

Aβ also failed to stimulate the phosphorylation of ERK in microglia. On the contrary, Aβ(25-35) (McDonald et al., 1998) or Aβ(1-42) (Moore et al., 2002) have previously been reported to induce ERK activation in cultured microglia. Aβ(25-35) also elicits the activation of p38 (McDonald et al., 1998; Pyo et al., 1998) and JNK, which are other members of the MAPK family. The variation in these results may reflect differences in the tissue culture models employed, since microglia were isolated by percoll gradients in this study, whereas McDonald et al., (1998), Pyo et al., (1998) and Moore et al., (2002) isolated microglia from mixed glial cultures after 7-14 days *in vitro*. Thus, their microglia may have been more activated and therefore 'primed' to Aβ activation (Slepko and Levi 1996).

CgA or Aβ did not induce COX-2 expression in microglia. As yet the effects of these activators on COX-2 synthesis by cultured microglia have not been reported in the literature. Nevertheless, epidemiological studies have demonstrated that NSAIDs reduce the risk of developing AD (McGeer et al., 1996; Stewart et al., 1997), which suggests that COX-2 does plays a central role in AD.

5.8.3 Downstream pathways: glutamate

Microglia treated with CgA released glutamate into the culture medium. Glutamate is a nonessential amino acid, which is generated in the mitochondria from α ketoglutarate (Berg et al., 2002). Thus, in response to cellular stress, microglial metabolism and subsequent glutamate synthesis may be enhanced to support the production of the anti-oxidant glutathione (see section 4.9.3). Previously it has been reported that CgA-induced glutamate release is mediate in part by the Xc^- transporter (Kingham et al., 1999). Other microglial activators including soluble APPα (Barger and Basile 2001), LPS (Piani and Fontana 1994), PMA (Nakamura et al., 2003) and albumin (chapter 4) also trigger glutamate secretion via this transporter. Furthermore, zymosan (stimulates phagocytosis), TNFα and various bacterial products including protein A and tuberculin induce microglial glutamate release, although the involvement of the Xc^- transporter has not been investigated (Piani and Fontana 1994). This suggests that glutamate secretion by activated microglia is a common phenomenon. However, it should be noted that Aβ did not evoke glutamate release from microglia. Consistent with this, cultured microglia treated with Aβ(1-42) or Aβ(1-42) plus IFNγ have previously been reported to release very low levels of glutamate (Barger and Basile 2001). Similarly, Aβ(25-35) does not induce glutamate release from peritoneal macrophages (Klegaris and McGeer 1997).

The signalling cascades involved in glutamate release from activated microglia have received little attention, although, PKC (Nakamura et al, 2003), NO (Kingham et al., 1999; Nakamura et al, 2003) and reactive oxygen species (Kingham et al., 1999) have recently been implicated. In this study, CgA induced glutamate release was deemed to be scavenger receptor-dependent but ERK and Src independent. Glutamate release preceded iNOS expression; therefore it would appear that release is NO independent, however this supposition conflicts with previous findings (Kingham et al., 1999; Nakamura et al, 2003). This inconsistency may be due to differences in assay sensitivities, since in this study glutamate was measured fluorometrically, whereas Kingham et al., (1999) and Nakamura et al, (2003) used a commercially available colorimetric kit. Considering glutamate is a potent neurotoxin, the elucidation of signalling pathways involved in microglia glutamate release may provide targets for therapeutic intervention.

5.8.4 Downstream pathways: apoptosis

Cell loss in AD was originally believed to be confined to specific neuronal populations, however apoptotic microglia have been detected around senile plaques in AD post-mortem tissue (Yang et al., 1998). Furthermore, fragmented DNA has been demonstrated to co-localise with microglia and oligodendrocytes as well as neurones in AD brains (Lassmann et al., 1995). Activation induced apoptosis may be an intrinsic self-regulatory mechanism; considering that activated microglia produce prodigious quantities of neurotoxic agents, a commitment to death may prevent bystander damage to neighbouring neurones. This theory is supported by the finding that activation induced microglial apoptosis *in vitro* is associated with LPS treatment (Liu et al., 2001).

Previously, it has been demonstrated that CgA treated microglia ultimately undergo apoptotic cell death, which is mediated by a NO dependent fall in mitochondrial membrane potential (Kingham and Pocock 2000). CgA-induced apoptosis is cytochrome *c* independent, although microglia exhibit other signatures of apoptosis including DNA fragmentation and caspase-1 activity (Kingham et al., 1999; Kingham and Pocock 2000). In this study nitrite was undetectable in the culture medium collected from CgA treated microglia, although inhibition of the scavenger receptor, Src kinases or ERK attenuated iNOS expression and subsequent death, implying that apoptosis is NO dependent. It is possible that NO reacts with superoxide to form peroxynitrite, which in turn nitrates tyrosine residues in susceptible proteins, therefore rendering NO (nitrite) undetectable in the culture medium. Activation of mGluRs are also involved in CgA-induced microglial apoptosis (Kingham et al., 1999; Taylor et al., 2002; 2003), which suggests that secreted glutamate feeds back on to membrane bound receptors to instigate a self perpetuating cycle of cell death.

In this investigation, apoptotic microglia were initially detectable 40 hours after the addition of CgA, whereas Kingham et al., (1999) detected apoptotic microglia 24 hours after CgA treatment; a discrepancy that was attributed to differences in culture conditions or batch to batch CgA variability. In accordance with previous findings CgA also induced mitochondrial depolarisation (Kingham and Pocock 2000; Taylor et al., 2002). Mitochondrial depolarisation preceded apoptosis temporally, but succeeded iNOS expression, whilst inhibition of the mitochondrial PT pore ameliorated apoptosis (Kingham and Pocock 2000). Moreover, inhibition of the scavenger receptor, Src kinases or ERK attenuated CgA-induced mitochondrial depolarisation as well as iNOS expression, which implies that mitochondrial dysfunction is indeed a result of NO production. Collectively, this data corroborates

previous findings, which illustrate that mitochondrial depolarisation is NO dependent and that apoptosis is mediated by mitochondrial depolarisation (Kingham and Pocock 2000). Increasing evidence is accumulating to suggest that NO plays a key role in cell death. NO has been reported to promote the activation of caspases and apoptosis in macrophage cell lines (Messmer et al., 1998). Furthermore, Complexes I, II and IV of the electron transport chain are readily nitrated by NO dependent mechanisms (Clementi et al., 1998; Murray et al., 2003). Oxidative damage subsequently results in mitochondrial dysfunction, which in turn may precipitate mitochondrial PT pore opening and downstream apoptosis (Hortleno et al., 1997; Heales and Bolãnos 2002).

Analogous to CgA treatment, Aβ was found to trigger microglial apoptosis, which is consistent with recent findings (Taylor et al., 2002, 2003). Korotzer et al., (1993) have also demonstrated that process bearing microglia show signs of degeneration after exposure to Aβ(25-35). In addition, it has been demonstrated that a low dose (5 μM) of Aβ(25-35) induces microglial cell rounding (Casal et al., 2002), which is a morphological transition that often precedes activation induced death in microglia. Aβ induced apoptosis was also mediated by mitochondrial depolarisation as demonstrated using the PT pore inhibitor cyclosporin A. Likewise, oligodendrocytes treated with Aβ(25-35) or Aβ(1-40) undergo apoptosis, which is accompanied by loss of mitochondrial function (Xu et al., 2001). Consistent with these findings Aβ(25-35) has been shown to selectively decrease complex IV (cytochrome oxidase) activity in isolated mitochondria (Canevari et al., 1999), therefore it is conceivable that internalised Aβ may trigger mitochondrial damage via this mechanism in microglia.

Microglial apoptosis and mitochondrial depolarisation induced by Aβ involved an upstream G_i protein and a Src kinase. Scavenger receptors do not exhibit the characteristic seven membrane spanning topology of receptors that signal through $G_{i/o}$ proteins (Peiser and Gordon 2001), although these results and others (Pollaud-Cherion et al., 1998; Whitman et al., 2000; Post et al., 2002) indicate that scavenger receptors can interact with $G_{i/o}$ proteins. Moreover, Aβ(1-42) has been demonstrated to induce G_i dependent signalling pathways in human monocytes (Le et al., 2001) and N9 microglia (Tiffany et al., 2001). With respect to Src kinases, Aβ(25-35) has been reported to activate Lyn (a Src kinase) in microglia (McDonald et al, 1997). The order of second messenger activation induced by Aβ was not delineated in this study. However, G_i proteins have been documented to directly evoke Src activity (Ma et al., 2000). Additionally, Src kinases participate in ERK activation through G_i protein dependent mechanisms (Igishi et al., 1998); although it should be emphasised that phospho-ERK was not detectable following Aβ treatment in this investigation. Nevertheless, it is conceivable that a Src kinase lies downstream of G protein activation in the Aβ-induced signalling cascades that are described in this chapter.

5.8.5 Downstream pathways: calcium

CgA did not elicit calcium transients in N9 microglia, which is consistent with previous findings (Personal communication: Dr Jennifer Pocock). However, this challenges a study by Taupenot et al (1996), which states that CgA induces a rapid rise in intracellular calcium in primary microglia. These authors postulated that calcium transients mediate actin re-organisation, which subsequently causes microglia to adopt an amoeboid morphology, although no direct evidence for this was reported (Taupenot et al., 1996). Similarly, Aβ(25-35) did not trigger calcium fluxes

in the N9 microglial cell line. Consistent with this, Tiffany et al., (2001) demonstrated that Aβ(1-42) does not elicit calcium transients in N9 microglia unless the cells are pre-treated with LPS, which serves to up-regulate microglial receptor expression. Conversely, Aβ(25-35) has been reported to evoke increases in intracellular free calcium in cultured microglia (Korotzer et al., 1995). Furthermore, Combs et al., (1999) demonstrated that Aβ(25-35) induces calcium transient in THP monocytes, which are often used to model microglial signalling (McDonald et al., 1997, 1998). However, the signalling events elicited by CgA or Aβ in this study were not modulated by BAPTA-AM, which supports the theory that CgA or Aβ-induced signalling cascades leading to cell death are calcium independent in microglia.

5.8.6 CgA or Aβ treated microglia exhibit a neurotoxic phenotype

Medium harvested from CgA or Aβ treated microglia was found to induce neuronal apoptosis, which is consistent with previous reports (Ciesielski-Treska et al., 1998; Kingham et al., 1999; Ciesielski-Treska et al., 2001; Combs et al., 1999, 2001). Neurotoxin release was found to occur approximately 16 hours after the addition of CgA or Aβ, which suggests that neurotoxins are synthesised *de novo*. Neuronal death evoked by CgA stimulated microglia is caspase 8 (Ciesielski-Treska et al., 2001) and 3 dependent (Kingham et al., 1999; Ciesielski-Treska et al., 2001). Furthermore, the Fas transmembrane receptor (Fas/Apo1/CD95), cytochrome *c* release and p38 are involved in the neuronal response to toxins derived from CgA stimulated microglia (Ciesielski-Treska et al., 2001). However, it should be emphasised that Ciesielski-Treska et al., (2001) used cortical neurones in their studies, whereas cerebellar granule neurones were employed in this investigation.

Results presented in this chapter revealed that boiling microglial conditioned medium derived from CgA or Aβ treated microglia conferred neuroprotection, which suggests that the neurotoxic agents are heat labile and therefore may be proteinaceaous. The increase in apoptosis was not attributed to the presence of CgA or Aβ in the medium since the direct application of these agents to neurones did not induce death. The former is consistent with previous findings (Ciesielski-Treska et al., 1998; Kingham et al., 1999). Neuronal death induced by CgA activated microglia is NO independent (Kingham et al., 1999; Ciesielski-Treska et al., 1998). This also appears to be the case for Aβ. Similarly, NO independent death has been observed for cultured hippocampal neurones exposed to peritoneal macrophage conditioned medium (Flavin et al,. 1997). These findings are not surprising considering the half life of NO is approximately 5 seconds (Kulkarni and Sharma 1993; Alberts et al., 2002; Berg et al., 2002). Consequently, NO should not be present in microglial conditioned medium by the time it is applied to neuronal cultures.

Recently, cathepsin B (Kingham and Pocock 2001) and glutamate (Kingham et al., 1999) have been implicated in neuronal death induced by CgA activated microglia. In contrast, the neurotoxic factors released by Aβ treated microglia have not been as extensively studied, although a recent report demonstrates that TNFα is implicated in neuronal death induced by Aβ (25-35) treated microglia (Combs et al., 2001). On the contrary TNFα is not involved in neuronal death induced by CgA activated microglia (Ciesielski-Treska et al., 1998). Therefore, it appears that a combination of different microglial derived neurotoxins act in concert to mediate neuronal death in response to specific stimuli.

The finding that Aβ did not induce neuronal death directly is intriguing because many reports have demonstrated that Aβ(25-35) (Loo et al., 1993; Pike et al., 1993; Watt et al., 1994; Abe and Saito 2000; Taylor et al., 2002, 2003), Aβ(1-42) (Loo et al., 1993; Troy et al., 2000) and Aβ(1-40) (Abe and Saito 2000) are neurotoxic. It is possible that cerebellar granule neurones can resist a 24 hour exposure to Aβ. In support of this, senile plaques are predominantly located in the hippocampus and the cortex in AD (Crowther 1990), which implies that the cerebellum is less susceptible to AD pathology. Moreover, Marin et al., (2000) reported that active caspase 3 was not detectable in cerebellar granule neurones until 48 hours after Aβ(25-35) treatment, whilst Allen et al., (2001) demonstrated that cerebellar granule neurones subjected to Aβ(25-35) did not undergo apoptosis until 120 hours post treatment. Neurones were found to die more rapidly when exposed to Aβ(25-35) in SFM, however this represent a 'double insult' (Allen et al., 2001).

5.8.7 Conclusion

Previously, it has been reported that CgA induces glutamate release and a NO dependent decrease in mitochondrial polarisation, which in turn triggers microglial apoptosis (Kingham et al., 1999; Kingham and Pocock 2000). The data presented in this chapter extends these findings by demonstrating that CgA induces microglial iNOS expression, glutamate release, mitochondrial depolarisation and apoptosis via an interaction with a scavenger receptor. These signalling events with the exception of glutamate release are subsequently mediated by the Src kinase dependent phosphorylation of ERK (Fig. 5.14). Similarly, Aβ was demonstrated to induce microglial apoptosis via a scavenger receptor-dependent mechanism. Aβ induced cell death was also mediated by mitochondrial depolarisation and involved a G_i protein

and a Src kinase (Fig. 5.15). Furthermore, microglia treated with either activator promoted neuronal apoptosis. In light of these findings, manipulation of scavenger receptor coupled signalling pathways may provide novel therapeutic strategies for the prevention of neurodegeneration in AD and possibly other neurological disorders.

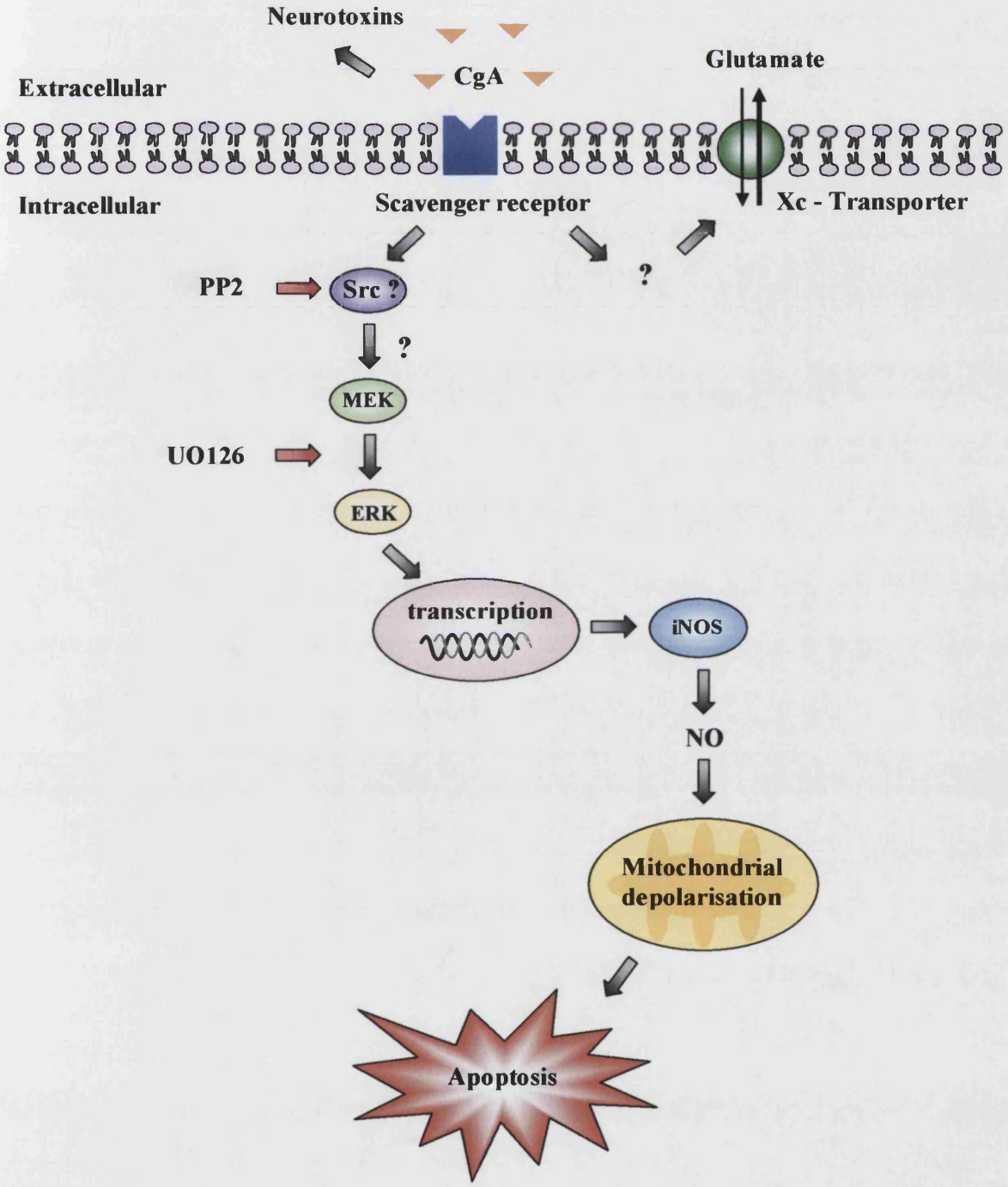

Figure 5.14 Signalling cascades elicited in CgA treated microglia

CgA induces iNOS expression, glutamate release, mitochondrial depolarisation and apoptosis via the scavenger receptor. These signalling events with the exception of glutamate release were subsequently mediated intracellularly by the Src kinase dependent phosphorylation of ERK. The pathways leading to glutamate release are currently undetermined; however secretion is known to be mediated by the Xc^- transporter (Kingham et al., 1999). CgA treated microglia were also found to release neurotoxins.

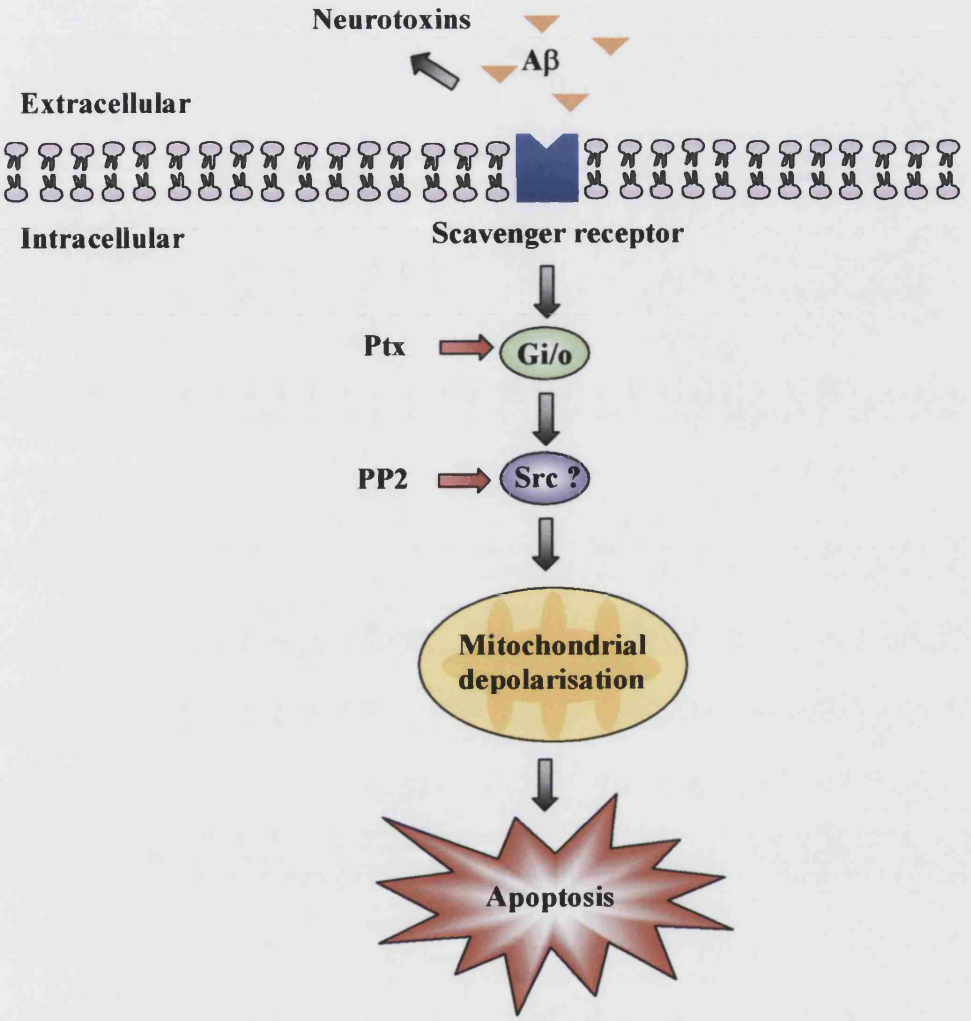

Figure 5.15 Signalling cascades elicited in Aβ treated microglia

Aβ induces mitochondrial depolarisation, which in turn triggers apoptosis; events that are mediated via the scavenger receptor. Signalling also involves a Gi/o protein and a Src kinase. Although, the precise order of second messenger activation remains to be determined. Hence in reality the depicted sequence may be reversed: ie a Src kinase upstream of a Gi/o protein. Aβ treated microglia were also found to release neurotoxins.

6.0 Effects of ischaemia on microglial signalling

6.1 Introduction

In this chapter the effects of an ischaemic insult on microglial signalling were explored. In addition, the effects of ischaemia followed by fraction V or $A\beta_{(25-35)}$ (hereafter referred to as Aβ) treatment were studied; the rationale being that stroke is a known risk factor for AD (Tatemichi et al., 1994; Kokmen et al., 1996; Moroney et al., 1996; Desmond et al., 2000; Madureira et al., 2001). Pure albumin was not used in these experiments because fraction V and albumin were found to elicit identical effects in chapter 4.

6.1.1 Models of ischaemia

Ischaemia can be modelled using a number of paradigms, which are briefly outlined below.

6.1.1.1 *In vitro* models of ischaemia

Brain slices or cultured cells are frequently used in *in vitro* models of ischaemia, although the three dimensional architecture of the brain is not replicated in these models they are useful because they enable the signalling pathways in isolated cell types to be studied. Ischaemia can be modelled *in vitro* by exposing cells to 95 % N_2 and 5 % CO_2 in the presence of medium lacking glucose or other metabolic substrates (Yenari and Giffard 2001), and this was the method employed in this chapter. Alternatively, ischaemia can be modelled by inhibiting glycolysis and the electron transport chain (Pocock and Nicholls 1998). 2-deoxy-glucose is commonly used to inhibit glycolysis (Lyons and Kettenmann 1998; Pocock and Nicholls 1998), whilst the electron transport chain can be inhibited by agents such as antimycin A (Swanson 1992; Swanson et al., 1995), cyanide (Pocock and Nicholls 1998) or azide (Swanson 1992; Swanson et al., 1995, 1997).

6.1.1.2 *In vivo* models of ischaemia

The anterior and posterior parts of the brain receive blood from the two internal carotid and the two vertebral arteries respectively. The internal carotid and vertebral arteries branch and divide many times thereby perfusing all areas of the brain (Snell 1997; Young and Young 1997; Kiernan 1998). The middle cerebral artery (MCA) is the largest branch of the internal carotid artery and is often used to model focal ischaemia (Abe and Hayashi 1997; Hayashi et al., 1999; Zhu D et al., 2002). Occlusion of the MCA is commonly achieved by inserting a thread into the carotid artery, which is then advanced to block the vessel (Abe and Hayashi 1997; Sharp et al., 1998; Hayashi et al., 1999). Other models of focal ischaemia include photochemical induced infarction, which is a non-invasive procedure. In this paradigm a photosensitive dye such as Rose Bengal is administered intravenously, the brain is then irradiated with laser light. The reaction between the dye and the light induces platelet aggregation and thrombi formation, which subsequently produces a focal infarct (Yan et al., 1998; Sharp et al., 1998; Takamatsu et al., 2000; Eichenbaum et al., 2002).

As outlined above, focal ischaemia is produced by occlusion of specific cerebral blood vessels; therefore the brain suffers damage to select regions. In contrast, global ischaemia is caused by cardiac arrest or severe hypotension and produces widespread ischaemic damage (Sharp et al., 1998). Common models of global ischaemia include bilateral carotid artery occlusion (Braun et al., 1998; Horner et al., 1998; Sharp et al., 1998) or four vessel (carotid and vertebral) occlusion (Pulsinelli and Brierley 1979; Clemens et al., 1997; Schmidt-Kastner et al., 1997; Sharp et al., 1998;).

6.1.3 Summary of results

Microglial signalling was investigated after exposure to ischaemia for 3 hours followed by 'reperfusion' for 24 hours. In addition, the effects of ischaemia followed by fraction V or Aβ treatment were studied. Experimental data revealed that ischaemia *per se* did not induce iNOS expression or nitrite production. Moreover, microglia exposed to ischaemia followed by fraction V or Aβ treatment expressed similar levels of iNOS as those cells treated with the fraction V or Aβ alone. Ischaemia did not elicit the phosphorylation of ERK or induce glutamate release either. Nor did ischaemia followed by fraction V or Aβ treatment affect the levels of p-ERK expression or glutamate release induced by fraction V or Aβ treatment alone. Analysis of microglial conditioned medium revealed that microglia subjected to ischaemia or Aβ did not secrete TNFα or TGFβ. Conversely, fraction V was a potent stimulus for TNFα but not TGFβ release. Furthermore, microglia subjected to ischaemia then fraction V or Aβ secreted identical levels of TNFα as those cells treated with either activator alone, whereas ischaemia potentiated TGFβ release induced by Aβ but not fraction V.

Assessment of cellular viability demonstrated that ischaemia *per se* did not adversely effect cell survival. However, ischaemia followed by fraction V treatment triggered microglia to undergo apoptosis, which was mediated by mitochondrial depolarisation. Cell death was found to be iNOS and calcium independent. Moreover, G_i proteins, Src kinases or ERK were not implicated in apoptosis or mitochondrial depolarisation induced by the combined insult. To recapitulate, fraction V induces a calcium-dependent proliferative response in microglia (see chapter 4). Interestingly, ischaemia did not induce any appreciable effects on calcium transients induced by fraction V as measured immediately after the ischaemic insult or 24 hours later, although proliferation was precluded.

Moreover, ischaemia treatment alone did not modulate intracellular free calcium levels at the time points studied.

Ischaemia followed by Aβ treatment potentiated the levels of microglial apoptosis and mitochondrial depolarisation induced by Aβ alone. Mitochondrial depolarisation mediated apoptosis in microglia exposed to Aβ alone or microglia subjected to ischaemia then Aβ. Poly I, PP2 and pertussis toxin were found to attenuate apoptosis and mitochondrial depolarisation induced by the combined insult. This suggests the involvement of scavenger receptors, Src kinases and G_i proteins in signalling; the very same second messengers that mediate Aβ-induced mitochondrial depolarisation and apoptosis. Furthermore, ischaemia did not induce any discernable effects on intracellular calcium levels associated with Aβ treatment as measured immediately after the ischaemic insult or 24 hours later.

In a parallel series of experiments, conditioned medium harvested from microglia subjected to ischaemia was found to be neurotoxic. Appearance of neurotoxins in conditioned medium became evident 6 hours after the ischaemic insult. Neuronal death was NO, glutamate and ATP independent. Moreover, depleting the microglia conditioned medium of TNFα or TGFβ did not protect against neuronal death. This is in keeping with the finding that ischaemia did not induce the release of these cytokines from microglia. Boiling the conditioned medium conferred neuro-protection, which indicates that the neurotoxin(s) are heat labile, although the identity of which remains to be delineated. Finally, it was revealed that ischaemia did not potentiate neuronal apoptosis induced by microglia treated with fraction V or Aβ. The combined insults induced essentially the same levels of neuronal death as microglia treated with fraction V or Aβ alone.

6.2 Effects of ischaemia on iNOS and p-ERK expression

Microglia were analysed for iNOS expression after exposure to ischaemia. In addition, microglial iNOS levels were appraised after exposure to ischaemia followed by fraction V or Aβ treatment. An ischaemic episode was modelled by exposing microglia to 95 % N_2 in 5 % CO_2 for 3 hours in the presence of DMEM lacking glucose, pyruvate or foetal calf serum at 37 °C. Thus, the microglia were deprived of metabolic substrates that could be used for respiration under anaerobic conditions. Control microglia were maintained in an atmosphere of 5 % CO_2 in air (normoxic) at a temperature of 37 °C for the same time period. Following the ischaemic episode some microglia were treated with fraction V (1 mg/ml) in SFM for 2 hours. The SFM was then replaced with SCM for the remainder of the experimental period. Microglia were also exposed to Aβ (45 μM) in SCM following the initial ischaemic insult. These activation protocols were used in all experiments described in this chapter. A 3 hour ischaemic insult was chosen because in pilot experiments this time period did not cause the microglia to detach from the coverslips, which is a phenomenon that has been reported with longer periods of ischaemia (Yu et al., 1989; Personal communication: Ms Susan Griffin, Department of Molecular Pathogenesis, Institute of Neurology, UCL; Dr Amanda Liddle, Department of Neuroinflammation, Institute of Neurology, UCL).

Western blot analyses revealed that microglia subjected to ischaemia for 3 hours followed by either SCM for 24 hours (ischaemia SCM) or SFM for 2 hours then SCM for 22 hours (ischaemia SFM) did not express iNOS (Fig. 6.1A). In contrast, fraction V (1 mg/ml) induced an increase in iNOS expression after 24 hours in culture, whilst iNOS was undetectable in microglia treated with Aβ for 24 hours. Ischaemia prior to the addition of fraction V or Aβ did not modulate the levels of iNOS expression induced by either

activator alone. Moreover, control microglia that were left untreated for 27 hours (basal) or were treated with SFM for 2 hours then SCM for 22 hours (SFM) did not express iNOS. Analysis of β-actin levels demonstrated that the observed changes in iNOS expression were not due to differences in protein loading.

In a parallel experiment, nitrite, a stable breakdown product of NO was measured in the culture medium. Nitrite was not detectable in medium collected from microglia subjected to ischaemia for 3 hours followed by either SCM for 24 hours (ischaemia SCM) or SFM for 2 hours then SCM for 22 hours (ischaemia SFM) (Fig. 6.1B). Similarly, nitrite was undetectable in medium collected from fraction V (1 mg/ml) or Aβ (45 μM) treated microglia, which is consistent with findings presented previously (see chapter 4 and 5 respectively). An ischaemic insult prior to the addition of fraction V or Aβ did not modulate the levels of nitrite induced by either activator alone. Furthermore, medium collected from control microglia, which were either left untreated for 27 hours (basal) or were treated with SFM for 2 hours then SCM for 22 hours (SFM) contained negligible amounts of nitrite. These findings were not attributed to assay failure since nitrite was detectable in culture medium collected from LPS (2 μg/ml) treated peritoneal macrophages.

A

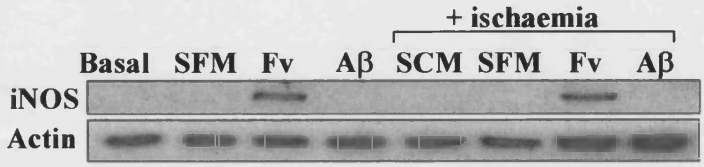

B

Treatment	[Nitrite](nM/mg of protein)
Basal	1.1 ± 0.02
SFM	1.3 ± 0.05
Fv (1 mg/ml)	1.0 ± 0.03
Aβ (45 μM)	1.1 ± 0.04
Ischaemia (SCM)	1.2 ± 0.02
Ischaemia (SFM)	1.1 ± 0.4
Ischaemia +Fv (1 mg/ml)	1.2 ± 0.02
Ischaemia + Aβ (45 μM)	1.0 ± 0.03
Macrophage (LPS: 2 μg/ml)	487.3 ± 4.5 ***

Figure 6.1 (see overleaf for figure legend)

Figure 6.1 Modulation of iNOS expression and nitrite production by ischaemia

Representative Western blots of iNOS expression in microglial cell lysates. **A**: Lysates were prepared from microglia exposed to ischaemia for 3 hours followed by either SCM for 24 hours (ischaemia SCM) or SFM for 2 hours then SCM for 22 hours (ischaemia SFM). Microglia were also treated with fraction V (Fv: 1mg/ml) in SFM for 2 hours. The SFM was then replaced with SCM for 22 hours before lysates were prepared. Furthermore, lysates were prepared from microglia treated with Aβ (45 μM) in SCM for 24 hours. To assess the effects of ischaemia on subsequent microglial signalling, microglia were exposed to a 3 hour period of ischaemia before being treated with fraction V (Fv: 1 mg/ml) or Aβ (45 μM) then lysates were prepared. Control lysates were prepared from microglia left untreated for 27 hours (basal) or microglia exposed to SFM for 2 hours then SCM for 22 hours (SFM). Lysates were subjected to Western blot analyses using an antibody raised against iNOS (1:5000), which in turn was detected by goat anti-rabbit IgG (HRP) (1:500). To ensure equal loading blots were re-probed using an antibody recognising β-actin followed by exposure to goat anti-mouse IgG (HRP) (1:1000). Nitrite concentrations were also measured in microglial conditioned medium **B**: Medium was collected from microglia treated as above. Medium was also collected from peritoneal macrophages (isolated from adult rats) treated with LPS (2 μg/ml) in SCM for 24 hours. Medium was subsequently appraised for nitrite using Griess reagent. The values shown represent the mean concentration in nM/mg of protein ± SEM of data from experiments performed in triplicate. Statistical analysis was performed using ANOVA followed by the Tukey post test. *** $P < 0.001$, vs 'basal' or 'SFM'.

The effects of ischaemia on ERK phosphorylation were subsequently explored. Western blot analyses revealed that microglia subjected to ischaemia for 3 hours followed by either SCM (ischaemia SCM) or SFM (ischaemia SFM) for 1 hour did not express p-ERK (Fig. 6.2A). In contrast, fraction V (1 mg/ml) evoked an increase in p-ERK levels after 1 hour in culture, whilst p-ERK was undetectable in microglia treated with Aβ for 1 hour. A 3 hour ischaemic insult prior to the addition of fraction V or Aβ did not modulate the levels of p-ERK observed with either activator alone. Moreover, control microglia that were left untreated for 4 hours (basal) or were treated with SFM for 1 hour (SFM) did not express p-ERK either. Analysis of total ERK illustrated that the observed changes in ERK phosphorylation were not due to differences in protein loading.

Experimental data in chapter 4 demonstrated that ERK mediated iNOS expression in fraction V treated microglia. To determine whether ERK was responsible for mediating iNOS expression in microglia subjected to ischaemia then fraction V, the effects of UO126 on iNOS expression were investigated. Microglia were incubated with UO126 (5 μM) during the ischaemic insult and also during fraction V exposure. Following these successive treatments the medium was replaced with SCM supplemented with UO126 for a further 22 hours before lysates were prepared. Western blotting revealed that UO126 prevented iNOS expression in microglia subjected to ischaemia followed by fraction V treatment (Fig. 6.2B). This suggests that iNOS expression is also mediated by ERK under these conditions.

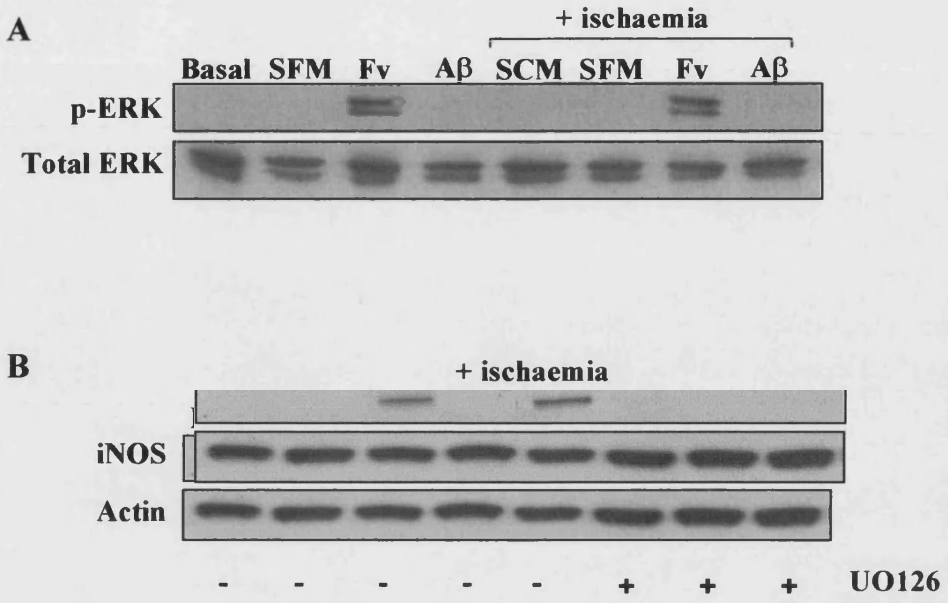

Figure 6.2 Modulation of p-ERK expression by ischaemia

Representative Western blots of p-ERK and iNOS expression in microglial cell lysates. **A**: Lysates were prepared from microglia exposed to ischaemia for 3 hours followed by either SCM (ischaemia SCM) or SFM for 1 hour (ischaemia SFM). Microglia were also treated with fraction V (1 mg/ml) in SFM for 1 hour or Aβ (45 μM) in SCM for 1 hour before lysates were prepared. In addition, lysates were prepared from microglia that were exposed to a 3 hour period of ischaemia before being treated with fraction V (Fv: 1 mg/ml) or Aβ (45 μM) for 1 hour. Control lysates were prepared from microglia left untreated for 4 hours (basal) or microglia exposed to SFM for 1 hour (SFM). Lysates were subjected to Western blot analyses using an antibody raised against p-ERK (1:750), which in turn was detected by goat anti-mouse IgG (HRP) (1:1000). To ensure equal loading blots were re-probed using an antibody recognising total ERK (1:500) followed by exposure to goat anti-rabbit IgG (HRP) (1:500). **B**: Lysates were prepared from microglia exposed to ischaemia for 3 hours followed by SFM for 2 hours then SCM for 22 hours (ischaemia SFM). Microglia were also treated with fraction V (Fv: 1mg/ml) in SFM for 2 hours. The SFM was then replaced with SCM for 22 hours before lysates were prepared. Furthermore, microglia were exposed to ischaemia for 3 hours before being treated with fraction V (Fv: 1 mg/ml) then lysates were prepared. To determine the involvement of ERK in signalling, lysates were prepared from microglia exposed to fraction V alone or in combination with ischaemia in the presence of UO126 (5 μM). Microglia were incubated with UO126 during the ischaemic insult and also during fraction V exposure. Following these successive treatments the medium was replaced with SCM supplemented with UO126 for a further 22 hours before lysates were prepared. Lysates were also prepared from microglia treated with UO126 alone (U). Control lysates were prepared from microglia left untreated for 27 hours (basal) or microglia exposed to SFM for 2 hours then SCM for 22 hours (SFM). Lysates were subjected to Western blot analyses using an antibody raised against iNOS. To ensure equal loading blots were re-probed using an antibody recognising β-actin.

6.3 Effects of ischaemia on glutamate and cytokine release

The effects of an ischaemic insult on glutamate and TNFα release were subsequently explored. Microglia subjected to ischaemia for 3 hours followed by either SCM for 24 hours (ischaemia SCM) or SFM for 2 hours then SCM for 22 hours (ischaemia SFM) released very low levels of glutamate (Fig. 6.3A) or TNFα (Fig. 6.3B) into the culture medium. In contrast, microglia treated with fraction V (1 mg/ml) released large amounts of glutamate and TNFα after 24 hours in culture, whilst these mediators were present in very low concentrations in medium collected from microglia treated with Aβ for 24 hours. An ischaemic insult prior to the addition of fraction V or Aβ did not modulate levels of glutamate or TNFα release induced by either activator alone. Moreover, control microglia that were left untreated for 27 hours (basal) or were treated with SFM for 2 hours then SCM for 22 hours (SFM) released very low levels of glutamate or TNFα.

Next the effects of ischaemia on TGFβ release were studied. Very low levels of TGFβ were detectable in culture medium collected from microglia subjected to ischaemia for 3 hours followed by either SCM for 24 hours (ischaemia SCM) or SFM for 2 hours then SCM for 22 hours (ischaemia SFM) (Fig. 6.3C). Similarly, low levels of TGFβ were present in medium collected from microglia treated with fraction V (1 mg/ml) or Aβ after 24 hours in culture. An ischaemic insult prior to the addition of fraction V or Aβ did not modulate fraction V induced TGFβ levels, whereas Aβ induced TGFβ levels were significantly augmented. Moreover, control microglia that were left untreated for 27 hours (basal) or were treated with SFM for 2 hours then SCM for 22 hours (SFM) released very low levels of this cytokine

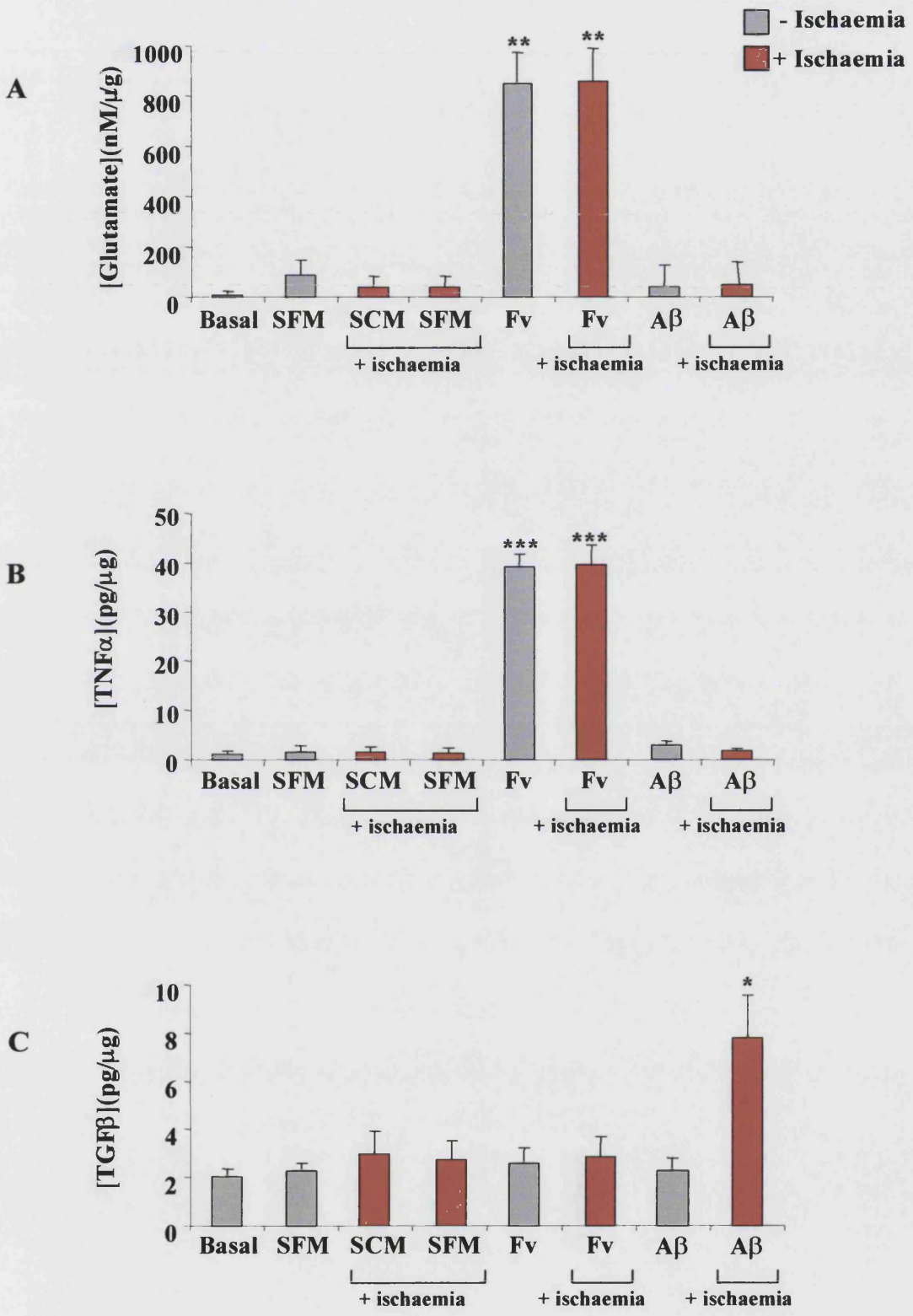

Figure 6.3 (see overleaf for figure legend)

Figure 6.3 Modulation of glutamate and cytokine release by ischaemia

Glutamate (nM/μg of protein), TNFα (pg/μg of protein) and TGFβ concentrations (pg/μg of protein) measured in microglial conditioned medium. Medium was harvested from microglia exposed to ischaemia for 3 hours followed by either SCM for 24 hours (ischaemia SCM: red bars) or SFM for 2 hours then SCM for 22 hours (ischaemia SFM: red bars). Microglia were also treated with fraction V (Fv: 1 mg/ml) in SFM for 2 hours. The SFM was then replaced with SCM for 22 hours before medium was collected. Furthermore, medium was collected from microglia treated with Aβ (45 μM) in SCM for 24 hours. To assess the effects of ischaemia on subsequent microglial signalling, microglia were exposed to a 3 hour period of ischaemia before being treated with fraction V (Fv: 1 mg/ml) or Aβ (45 μM) then medium was collected (red bars). Control medium was obtained from microglia left untreated for 27 hours (basal) or microglia exposed to SFM for 2 hours then SCM for 22 hours (SFM). Medium was subsequently appraised for the presence of glutamate (**A**), TNFα (**B**) or TGFβ (**C**). The values shown represent the mean (nM/μg or pg/μg of protein respectively) ± SEM of data from experiments performed in triplicate. Statistical analysis was performed using ANOVA followed by the Tukey post test. * $P < 0.05$, ** $P < 0.01$, *** $P < 0.001$ vs control (A, B: control describes 'basal' or 'SFM'. C: control describes Aβ treated)

To verify that the observed changes in glutamate and cytokine release were not due to cell membrane disruption, microglia were stained with propidium iodide and fluoroscein diacetate after 24 hours in culture. Staining revealed that microglial cultures exposed to ischaemia ('ischaemia SCM' or 'ischaemia SFM'), fraction V (1 mg/ml) or Aβ (45 μM) contained very few cells that stained with propidium iodide after 24 hours in culture (table 6.1). Furthermore, microglial cultures subjected to ischaemia followed by fraction V or Aβ contained negligible numbers of cells exhibiting propidium iodide staining as did control cultures. This suggests that the observed increases in glutamate and cytokine release occur via regulated pathways and that the changes are not due to loss of cell membrane integrity.

Treatment	% Propidium iodide positive microglia
Basal	0.6 ± 0.3
SFM	1.0 ± 0.6
Ischaemia (SCM)	1.5 ± 0.5
Ischaemia (SFM)	1.4 ± 0.4
Fv (1 mg/ml)	0.7 ± 0.4
Aβ (45 μM)	1.1 ± 0.3
Ischaemia + Fv (1 mg/ml)	1.2 ± 0.6
Ischaemia + Aβ (45 μM)	1.3 ± 1.5

Table 6.1 Analysis of microglial membrane integrity

Microglia were stained with propidium iodide and fluoroscein diacetate to provide an estimation of cell membrane integrity. Microglia exposed to ischaemia for 3 hours followed by either SCM for 24 hours (ischaemia SCM) or SFM for 2 hours then SCM for 22 hours (ischaemia SFM) were stained. Microglia were also treated with fraction V (Fv: 1mg/ml) in SFM for 2 hours. The SFM was then replaced with SCM for 22 hours before staining. Furthermore, microglia were treated with Aβ (45 μM) in SCM for 24 hours before staining. To assess the effects of the combined insults on cell membrane integrity, microglia were exposed to ischaemia for 3 hours before being treated with fraction V (Fv: 1 mg/ml) or Aβ (45 μM) then the cells were stained. Control microglia were left untreated for 27 hours (basal) or were exposed to SFM for 2 hours then SCM for 22 hours (SFM) before staining. Cells possessing propidium iodide staining were expressed as a percentage of the total number of cells counted (cells possessing propidium iodide staining or fluoroscein diacetate staining). The values shown represent the mean ± SEM of data from experiments performed in triplicate. Statistical analysis was performed using an ANOVA followed by the Tukey post test. According to this test there was no significant difference between the treatments.

6.4 Effects of ischaemia on cellular viability and mitochondrial status

The effects of ischaemia on cellular viability were subsequently assessed. Microglial cultures subjected to ischaemia for 3 hours followed by either SCM for 48 hours (ischaemia SCM) or SFM for 2 hours then SCM for 46 hours (ischaemia SFM) contained very few cells showing signs of apoptosis, necrosis or mitochondrial depolarisation (Fig. 6.4A). Similarly, microglial cultures treated with fraction V (1 mg/ml) contained very few cells exhibiting signs of apoptosis, necrosis or mitochondrial depolarisation after 48 hours in culture. Microglial cultures treated with Aβ (45 μM) also contained few necrotic cells after 48 hours in culture, whereas a large proportion of the cells were apoptotic and exhibited depolarised mitochondria. An ischaemic insult prior to the addition of fraction V or Aβ augmented the levels of apoptosis and mitochondrial depolarisation but not necrosis induced by either activator alone. Control cultures that were left untreated for 51 hours (basal) or were treated with SFM for 2 hours then SCM for 46 hours (SFM) contained very few microglia exhibiting signs of apoptosis, necrosis or mitochondrial depolarisation. Since none of the treatments caused a significant increase in microglial necrosis, the cells were only analysed for apoptosis in subsequent experiments.

Analysis of the total number of microglia per field of view revealed that microglial cultures treated with fraction V contained considerably more cells than cultures exposed to other treatments (Fig 6.4B), which is consistent with previous findings. Interestingly, fraction V treated microglial cultures that were pre-exposed to an ischaemic insult contained the same number of cells as control cultures ('basal' or 'SFM').

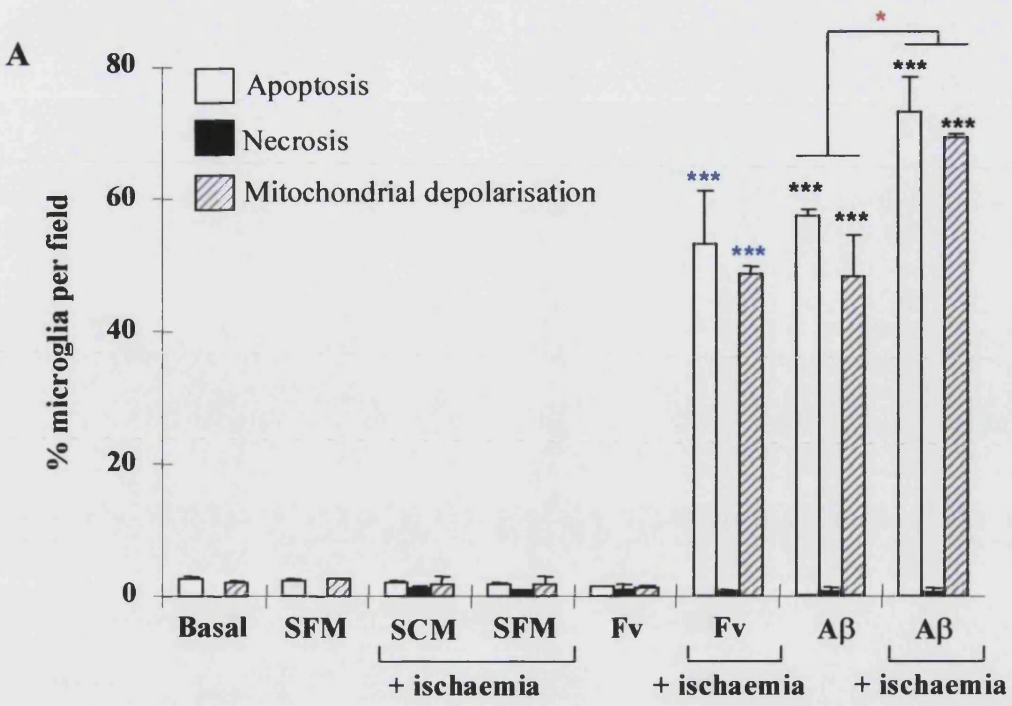

B

		+ ischaemia			+ ischaemia		+ ischaemia
Basal	SFM	SCM	SFM	Fv	Fv	Aβ	Aβ
6.1 ± 0.4	6.3 ± 0.6	6.1 ± 0.5	6.0 ± 0.8	15.2 ± 1.1	6.3 ± 0.5	6.3 ± 0.6	6.1 ± 0.5

Figure 6.4 Modulation of cellular viability by ischaemia

Amounts of apoptosis, necrosis and mitochondrial depolarisation were assessed in microglial cultures. **A**: Microglia were exposed to ischaemia for 3 hours followed by either SCM for 48 hours (ischaemia SCM) or SFM for 2 hours then SCM for 46 hours (ischaemia SFM). Microglia were also treated with fraction V (Fv: 1mg/ml) in SFM for 2 hours. The SFM was then replaced with SCM for 46 hours. Furthermore, microglia were treated with Aβ (45 μM) in SCM for 48 hours. To assess the effects of ischaemia on subsequent microglial signalling, microglia were exposed to a 3 hour period of ischaemia before being treated with fraction V (Fv: 1 mg/ml) or Aβ (45 μM). Control microglia were either left untreated for 51 hours (basal) or were exposed to SFM for 2 hours then SCM for 46 hours (SFM). Microglia were subsequently appraised for apoptosis using Hoechst 33342 (open bars), necrosis using a combination of Hoechst 33342 and propidium iodide (black bars) and mitochondrial depolarisation using JC-1 (hatched bars). Cells displaying brightly stained pyknotic nuclei, signs of necrosis or depolarised mitochondria were counted and values were expressed as a percentage of the total number of cells counted. **B**: Proliferation was assessed by counting the number of microglia present per field of view. The values shown represent the mean ± SEM of data from experiments performed in triplicate. Experiments consisted of 3 coverslips per treatment, each comprising 10 fields of view and experiments were performed on three independent occasions. Statistical analysis was performed using ANOVA followed by the Tukey post test. * $p < 0.05$ vs 'Aβ'. *** $p < 0.01$ vs 'basal' or 'SFM'. *** $p < 0.001$ vs 'Fv'.

Next the time courses of apoptosis and mitochondrial depolarisation induced by the combined insults (ischaemia followed by fraction V or Aβ treatment) were appraised. An ischaemic insult prior to the addition of fraction V (1 mg/ml) increased the levels of mitochondrial depolarisation and apoptosis (Fig. 6.5A). Microglia displaying depolarised mitochondrial were initially detectable between 24-32 hours after the addition of fraction V, whilst pyknotic nuclei were detectable between 32-42 hours. Therefore, mitochondrial depolarisation preceded apoptosis temporally. Conversely, microglial cultures treated with fraction V (1 mg/ml) alone contained very few cells displaying depolarised mitochondria and apoptosis over the 48 hour period studied.

Microglia subjected to an ischaemic insult prior to the addition of Aβ (45 μM) followed the same time course of mitochondrial depolarisation and apoptosis as those microglia treated with Aβ (45 μM) alone, although levels were augmented at each time point (Fig. 6.5B). Here again mitochondrial depolarisation was found to precede apoptosis temporally. As a reference the results obtained from microglial cultures subjected to ischaemia for 3 hours then SCM for 48 hours were plotted. These cultures contained negligible numbers of cells displaying depolarised mitochondria (Fig. 6.5B: black triangle) or pyknotic nuclei over the 48 hour period studied (Fig. 6.5B: black square).

A

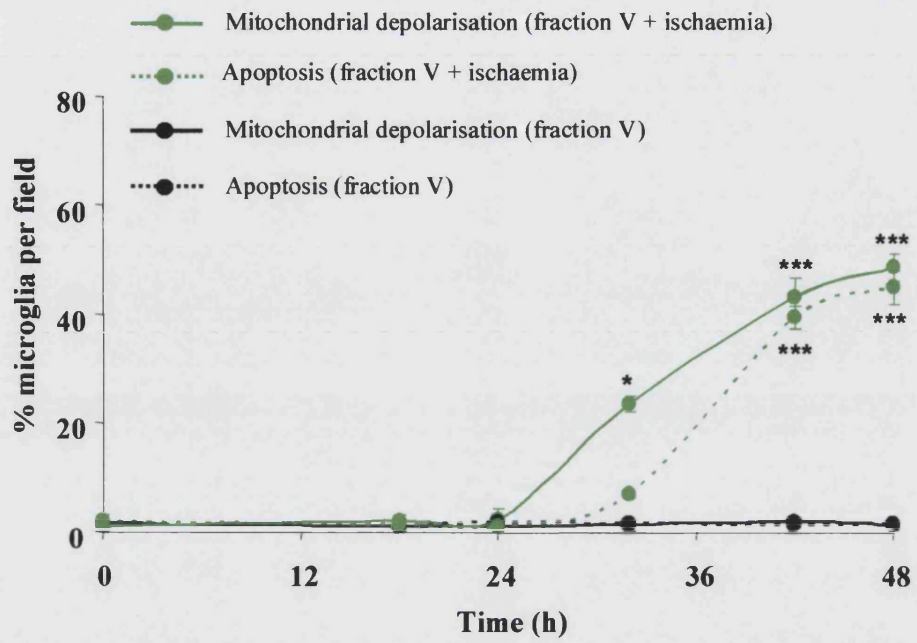

B

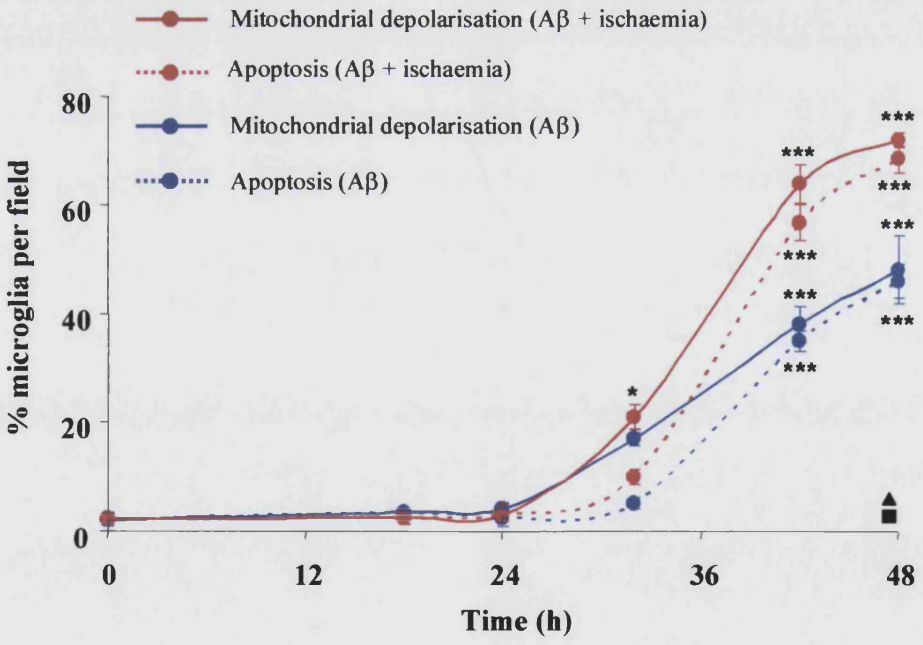

Figure 6.5 (see overleaf for figure legend)

Figure 6.5 Time axes of mitochondrial depolarisation and apoptosis

Time courses of mitochondrial depolarisation and apoptosis were assessed using JC-1 (bold lines) and Hoescht 33342 (dashed lines). **A**: Microglia were treated with fraction V (1 mg/ml) in SFM for 2 hours. The SFM was then replaced with SCM for 16, 22, 30, 40 or 46 hours before staining (black lines). In addition, microglia were exposed to ischaemia for 3 hours then fraction V (1 mg/ml) (green lines) for 16, 22, 30, 40 or 46 hours before staining. **B**: Microglia were stained following treatment with Aβ (45 μM) in SCM for 18, 24, 32, 42 or 48 hours (blue lines). Microglia were also exposed to ischaemia for 3 hours then treated with Aβ (45 μM) (red lines) for 18, 24, 32, 42 or 48 hours before staining. As a reference, microglia subjected to ischaemia for 3 hours then SCM for 48 hours were stained (Hoescht 3342: black triangle and JC-1: black square). Microglia were stained for apoptosis using Hoechst 33342 (dashed lines) or mitochondrial depolarisation using JC-1 (bold lines). Cells displaying brightly stained pyknotic nuclei or depolarised mitochondria were counted and values were expressed as a percentage of the total number of cells counted. The values shown represent the mean ± SEM of data from experiments performed in triplicate. Experiments consisted of 3 coverslips per treatment, each comprising 10 fields of view and experiments were performed on three independent occasions. Statistical analysis was performed using ANOVA followed by the Tukey post test. * $p < 0.05$, *** $p < 0.01$ vs control (control describes time 0).

To determine whether mitochondrial depolarisation was responsible for initiating microglial apoptosis the effect of the PT inhibitor cyclosporin A (CsA) (Zamzami et al., 1996; Seaton et al., 1998; Yang and Cortopassi 1998; Kingham and Pocock 2000) on these parameters was investigated. Ischaemia or fraction V treatment alone did not elicit cell death and results presented in chapter 5 revealed that Aβ induced apoptosis is mediated by mitochondrial depolarisation, therefore the effects of CsA on mitochondrial depolarisation and apoptosis induced by the combined insults were studied in isolation. Pre-treatment with CsA (1 μM) was found to significantly attenuate mitochondrial depolarisation and apoptosis induced by ischaemia followed by fraction V (Fig. 6.6A) or Aβ (Fig. 6.6B) treatment. This suggests that the PT pore is involved in cell death associated with both insults. Next the upstream signalling pathways involved in mitochondrial depolarisation and apoptosis were studied. In these experiments the same range of inhibitors that were used in previous experiments were employed. In this way the signalling cascades induced by ischaemia followed by fraction V or Aβ treatment could be compared with the second messenger pathways induced by each activator alone. Pre-treatment with AMT-HCl (0.3 μM), pertussis toxin (Ptx: 2 μg/ml), BAPTA-AM (10 μM), U73122 (2 μM), PP2 (100 nM) or UO126 (5 μM) did not exert an inhibitory effect on mitochondrial depolarisation and apoptosis induced by an ischaemic insult followed by fraction V (1 mg/ml) treatment (Fig. 6.6A). In contrast, pre-treatment with poly I (0.5 μg/ml) significantly attenuated mitochondrial depolarisation and apoptosis induced by ischaemia followed by Aβ (45 μM) treatment (Fig. 6.6B). Pertussis toxin (Ptx: 2 μg/ml) or PP2 (100 nM) also significantly attenuated mitochondrial depolarisation and apoptosis induced by ischaemia then Aβ treatment (Fig. 6.6B), whilst pre-treatment with neutralising RAGE antibody (200 μg/ml), AMT-HCl (0.3 μM), BAPTA-AM (10 μM), U73122 (2 μM) or UO126 (5 μM) exerted no inhibitory effects.

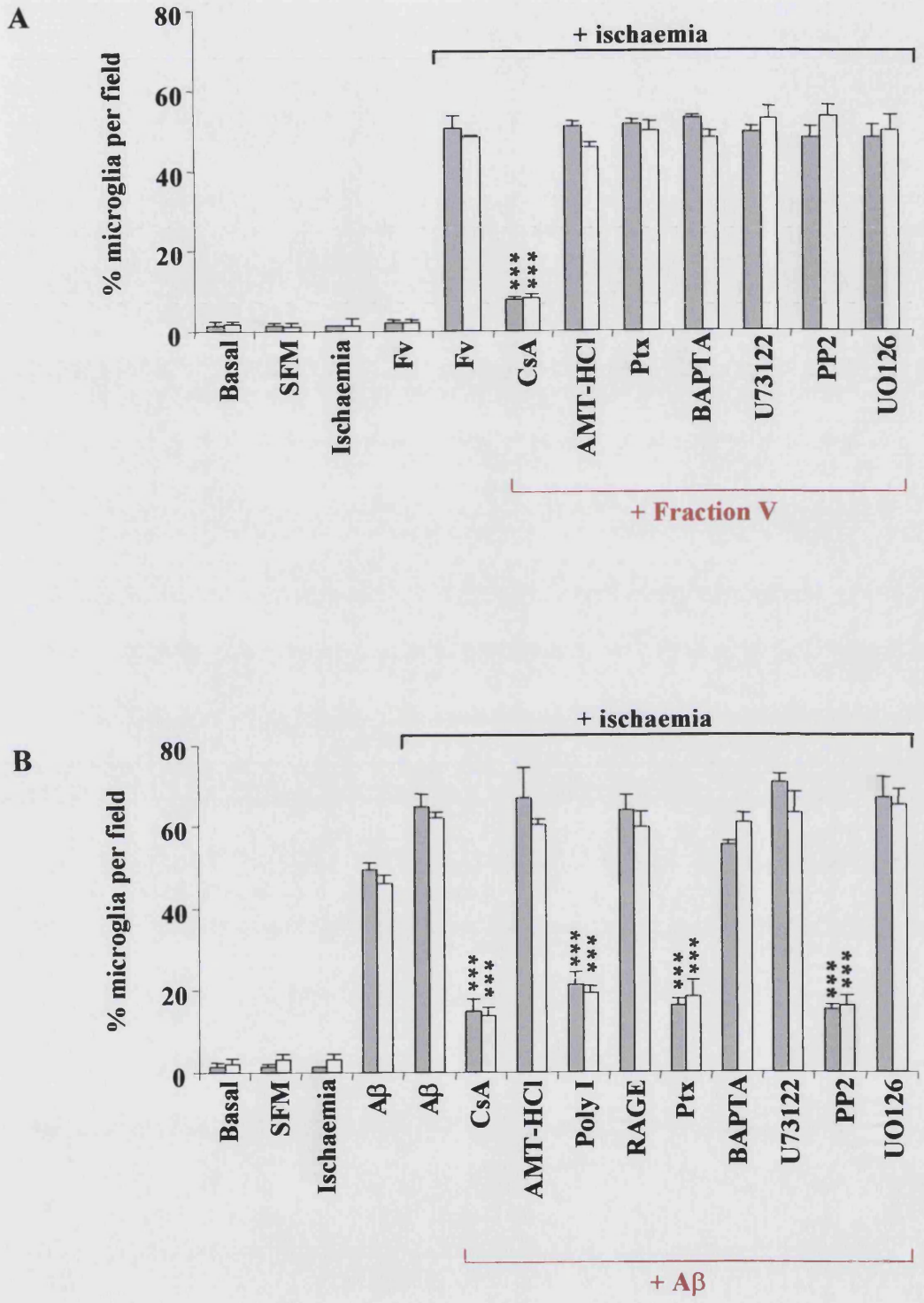

Figure 6.6 (see overleaf for figure legend)

Figure 6.6 Signalling mechanisms involved in mitochondrial depolarisation and apoptosis
Apoptosis and mitochondrial depolarisation was assessed using JC-1 and Hoescht 33342 respectively. **A**: Microglia were exposed to ischaemia for 3 hours followed by SFM for 2 hours then SCM for 46 hours (ischaemia) before staining. Microglia were also exposed to a 3 hour period of ischaemia, after which the cells were treated with fraction V (Fv: 1mg/ml) in SFM for 2 hours. The SFM was then replaced with SCM for 46 hours before staining was performed. In addition, microglia were exposed to ischaemia for 3 hours then treated with fraction V (Fv: 1 mg/ml) in SFM in the presence of cyclosporin A (CsA: 1 μM), AMT-HCl (0.3 μM), pertussis toxin (Ptx: 2 μg/ml), BAPTA-AM (10 μM), U73122 (2 μM), PP2 (100 nM) or UO126 (5 μM). At 2 hours the SFM was replaced with SCM supplemented with the appropriate concentration of inhibitor for a further 46 hours before staining. Microglia were also treated with fraction V (1 mg/ml) alone in SFM for 2 hours, after which the SFM was replaced with SCM for 46 hours before staining. Control microglia were left untreated for 51 hours (basal) or were exposed to SFM for 2 hours then SCM for 46 hours (SFM) before staining. **B**: Microglia were exposed to ischaemia for 3 hours followed by SCM for 48 hours (ischaemia) then the cells were stained. Microglia were also exposed to a 3 hour period of ischaemia then treated with Aβ (45 μM) in SCM for 48 hours before staining. In addition, microglia were exposed to ischaemia for 3 hours then treated with Aβ (45 μM) in SCM in the presence of cyclosporin A (CsA: 1 μM), AMT-HCl (0.3 μM), poly I (0.5 μg/ml), neutralising RAGE antibody (200 μg/ml), pertussis toxin (Ptx: 2 μg/ml), BAPTA-AM (10 μM), U73122 (2 μM), PP2 (100 nM) or UO126 (5 μM) before staining. Furthermore, microglia were also treated with Aβ (45 μM) alone in SCM for 48 hours alone before staining. Control microglia were treated as described in A. Microglia were subsequently appraised for apoptosis using Hoechst 33342 (open bars) or mitochondrial depolarisation using JC-1 (grey bars). Cells displaying brightly stained pyknotic nuclei or depolarised mitochondria were counted and values were expressed as a percentage of the total number of cells counted. The values shown represent the mean ± SEM of data from experiments performed in triplicate. Experiments consisted of 3 coverslips per treatment, each comprising 10 fields of view and experiments were performed on three independent occasions. Statistical analysis was performed using ANOVA followed by the Tukey post test. *** $p < 0.01$ vs control (A: control describes fraction V + ischaemia. B: control describes Aβ + ischaemia).

6.5 Effects of ischaemia on intracellular free calcium

In this section the effects of an ischaemic insult on intracellular calcium levels in N9 microglia were explored. N9 microglia were subjected to ischaemia for 3 hours then loaded with Fura-2 for 45 minutes at 37 °C, after which recordings were made (Smith et al., 2003). Changes in calcium levels were undetectable in N9 microglia subjected to ischaemia alone as measured immediately after the insult (Fig. 6.7) or 24 hours later (Fig. 6.8). Consistent with previous findings, fraction V (1 mg/ml) induced a mono-phasic increase in intracellular calcium, whereas Aβ (45 μM) did not induce changes in intracellular free calcium. A 3 hour period of ischaemic did not alter the effects of fraction V (1 mg/ml) or Aβ (45 μM) on calcium levels in N9 microglia as measured immediately after the insult (Fig. 6.7) or 24 hours later (Fig. 6.8). Furthermore, calcium fluxes were undetectable in control N9 microglia at each time point.

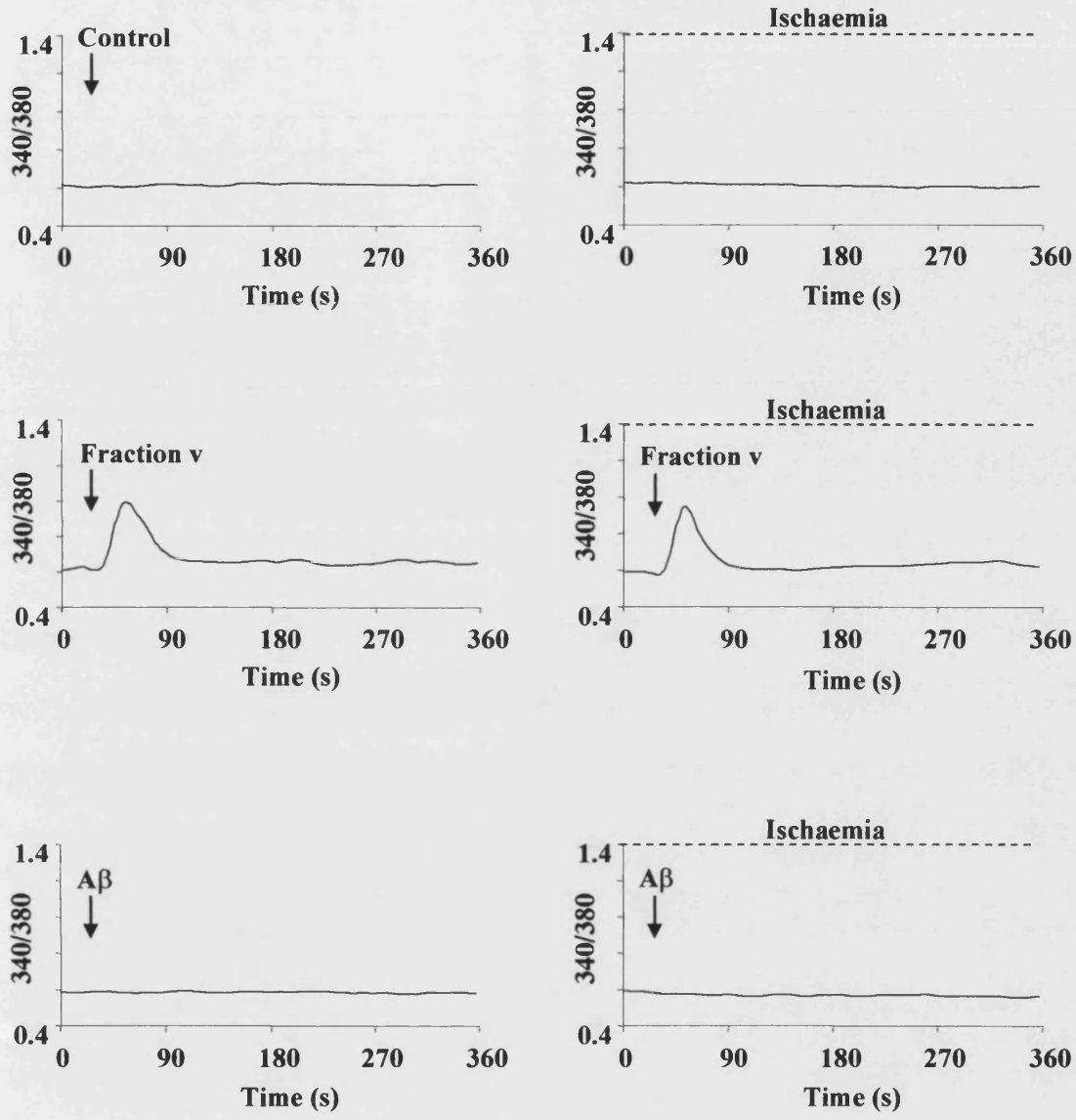

Figure 6.7 Modulation of calcium transients immediately after ischaemia

Representative traces depicting the immediate effects of ischaemia on intracellular free calcium associated with fraction V or Aβ treatment in N9 microglia. N9 microglia were subjected to ischaemia for 3 hours then the cells were loaded with fura-2 (5 μM) in basic medium for 45 minutes at 37 °C. Cells were subsequently excited with wavelengths of 340 and 380 nm and emission was collected at a wavelength of 510 nm. Recordings were made from microglia subjected to ischaemia in the absence of any other stimulus. In addition, fraction V (Fv: 1 mg/ml) or Aβ (45 μM) were added to ischaemia pre-treated N9 cells 60 seconds after the commencement of recording. Control N9 cells were treated with basic medium, fraction V (Fv: 1 mg/ml) or Aβ (45 μM) after 60 seconds of recording (without pre-exposure to ischaemia). Calcium responses were recorded from ten cells and the results were averaged and expressed as 340/380 fluorescence ratios.

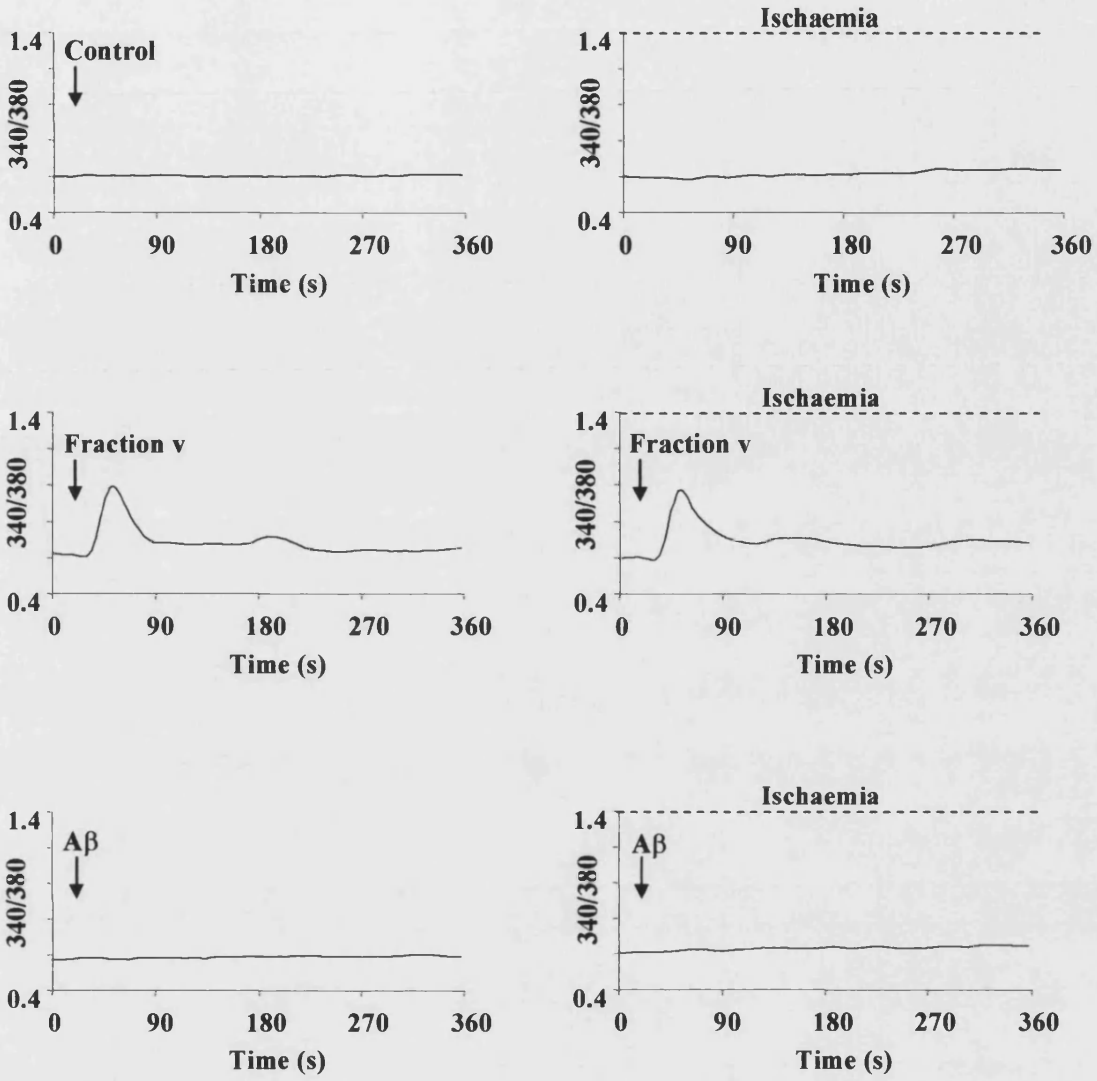

Figure 6.8 Modulation of calcium transients 24 hours after ischaemia

Representative traces depicting the effects of ischaemia on intracellular free calcium associated with fraction V or Aβ treatment in N9 microglia 24 hours post insult. N9 microglia were subjected to ischaemia for 3 hours, the cells were then returned to normoxic conditions for 24 hours before the cells were loaded with fura-2 (5 μM) in basic medium for 45 minutes at 37 °C. Cells were subsequently excited with wavelengths of 340 and 380 nm and emission was collected at a wavelength of 510 nm. Recordings were made from microglia subjected to ischaemia alone. In addition, fraction V (Fv: 1 mg/ml) or Aβ (45 μM) were added to ischaemia pre-treated N9 cells 60 seconds after the commencement of recording. Control N9 cells were treated with basic medium, fraction V (1 mg/ml) or Aβ (45 μM) after 60 seconds of recording (without pre-exposure to ischaemia). Calcium responses were recorded from ten cells and the results were averaged and expressed as 340/380 fluorescence ratios.

6.6 Effects of ischaemia treated microglia on neuronal apoptosis

The effect of microglial conditioned culture medium on neuronal death was subsequently assessed. Microglial conditioned medium was applied to cultures of cerebellar granule neurones for 24 hours then neuronal apoptosis was appraised using Hoescht 33342. Medium collected from microglia subjected to ischaemia for 3 hours followed by either SCM for 24 hours (ischaemia SCM) or SFM for 2 hours then SCM for 22 hours (ischaemia SFM) was found to induce neuronal apoptosis (Fig. 6.9A). Similarly, conditioned medium collected from microglia treated with fraction V (1 mg/ml) or Aβ (45 μM) for 24 hours induced a significant increase in neuronal death. An ischaemic insult prior to the addition of fraction V or Aβ did not potentiate the levels of neuronal death induced by microglia treated with fraction V or Aβ alone. Untreated cerebellar granule neurones ('control') contained few apoptotic cells after 24 hours in culture. Moreover, neuronal cultures that were exposed to medium collected from microglia left untreated for 27 hours (control) or microglia treated with SFM for 2 hours then SCM for 22 hours (SFM) contained low levels of apoptosis.

To determine at which time point microglia subjected to ischaemia release the neurotoxic agent(s), microglia were exposed to ischaemia for 3 hours then the medium was replaced with SCM (since the results obtained with both SFM and SCM were essentially identical in all experiments described in this chapter) for 1, 4, 6, 14 or 22 hours. Microglia conditioned medium was subsequently incubated with cerebellar granule cells for a further 24 hours before apoptosis was assessed. Using this approach, neurotoxin release was demonstrated to occur 6 hours after the ischaemic insult and the neurotoxicity of the conditioned medium increased with time (Fig. 6.9B).

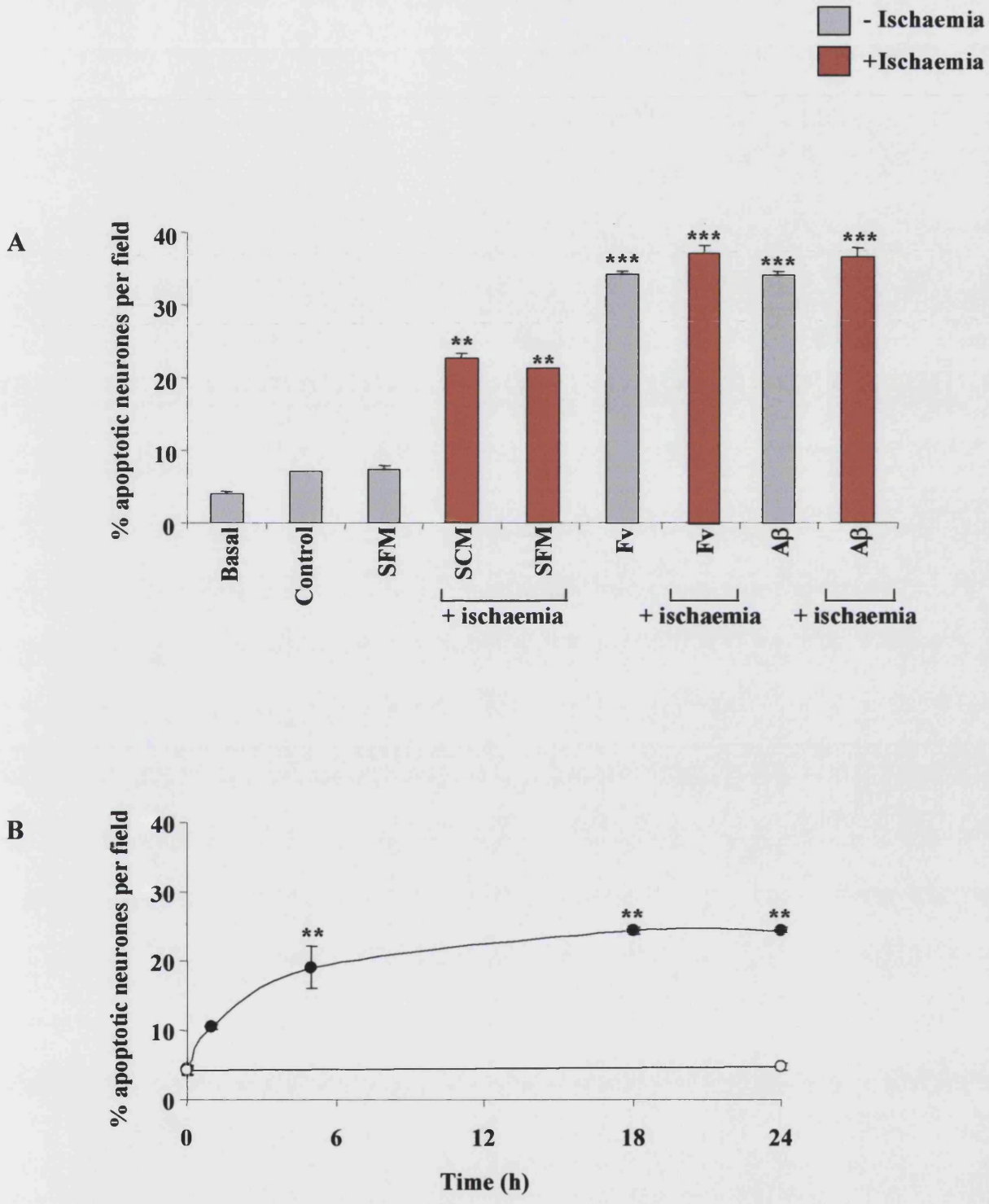

Figure 6.9 (see overleaf for figure legend)

Figure 6.9 Effects of ischaemia treated microglia on neuronal apoptosis

Neuronal apoptosis induced by medium obtained from microglia was assessed using Hoescht 33342. **A**: Medium was collected from microglia exposed to ischaemia for 3 hours followed by either SCM for 24 hours (ischaemia SCM: red bars) or SFM for 2 hours then SCM for 22 hours (ischaemia SFM: red bars). Microglia were also treated with fraction V (Fv: 1 mg/ml) in SFM for 2 hours. The SFM was then replaced with SCM for 22 hours before medium was collected. In addition, microglia were treated with Aβ (45 μM) in SCM for 24 hours then medium was collected. To assess the effects of combined insults on neuronal death, microglia were exposed to ischaemia for 3 hours before being treated with fraction V (Fv: 1 mg/ml) or Aβ (45 μM) then medium was collected (red bars). Control medium was obtained from microglia that were left untreated for 27 hours (control) or were exposed to SFM for 2 hours then SCM for 22 hours (SFM). Medium was subsequently added to cultures of cerebellar granule neurones then the neurones were fixed. Control neurones were left untreated for 24 hours (basal) before being fixed **B**: Microglia were subjected to ischaemia for 3 hours, then medium was collected at 0, 3, 6, 18 or 24 hours post insult (closed circles). Control medium was collected from untreated microglia at the same time points (open circles). Medium was subsequently applied to cerebellar granule neurones for 24 hours then the cells were fixed. Neurones were stained with Hoescht 33342. Following staining, non-apoptotic cells possessed large brightly stained nuclei, whereas apoptotic cells possess brightly stained pyknotic nuclei. Neurones displaying brightly stained pyknotic nuclei were counted and the degree of apoptosis was expressed as a percentage of the total number of cells counted. The values shown represent the mean ± SEM of data from experiments performed in triplicate. Experiments consisted of 3 coverslips per treatment, comprising ten fields of view. Statistical analysis was performed using ANOVA followed by the Tukey post test. ** $p < 0.01$, *** $p < 0.001$ vs control. (A: Control describes neuronal cultures treated with medium harvested from untreated microglia "Control". B: control describes time 0).

Next the identity of the neurotoxic agent(s) released by microglia subjected to ischaemia was investigated. To recap, ischaemia *per se* did not induce iNOS expression or NO production; neither did it induce glutamate release from microglia. Therefore, neuronal apoptosis was deemed to be NO and glutamate independent. This supposition was confirmed using the iNOS inhibitor AMT-HCl and a cocktail of glutamate receptor antagonists (CNQX, 20 μM; MK801, 10 μM; MSPG, 200 μM). AMT-HCl (0.3 μM) was pre-incubated with microglia before they were exposed to ischaemia and medium was collected after 24 hours then applied to cultures of cerebellar granule neurones for a further 24 hours. In contrast, the glutamate antagonist cocktail (CNQX, 20 μM; MK801, 10 μM; MSPG, 200 μM) was pre-incubated with the neurones before the addition of microglial conditioned medium. As postulated neither AMT-HCl nor the glutamate antagonists attenuated neuronal apoptosis induced by ischaemia (Fig. 6.10). Furthermore, neuronal cultures treated with AMT-HCl or the glutamate receptor antagonists alone did not contain significantly different levels of apoptosis from control cultures.

The effect of the broad spectrum purinergic antagonist PPADS (North and Barnard 1997; Troadec et al., 1999; von Kügelgen and Wetter 2000) on neuronal apoptosis induced by ischaemia treated microglia was subsequently assessed. In this way the role of microglial derived ATP in neurotoxicity could be ascertained. PPADS (100 μM) was pre-incubated with the neurones before the addition of microglial conditioned medium. PPADS did not protect the neurones against apoptosis, which suggests that apoptosis is ATP independent (Fig. 6.10). In support of this, the addition of ATPase (0.5 U/ml) to medium collected from microglia subjected to ischaemia did not attenuate neuronal apoptosis. Moreover, PPADS or ATPase did not adversely affect cell survival when incubated with the neurones alone.

Boiling the microglial conditioned medium was found to afford neuroprotection, which suggests that the neurotoxic agent(s) are heat labile. However, depleting the microglia conditioned medium of TNFα or TGFβ did not protect against neuronal apoptosis. This is consistent with the findings that ischaemia did not induce the release of these cytokines from microglia. Similarly, conditioned medium that was obtained from microglia treated with fraction V (1 mg/ml) alone and was depleted of TNFα did not attenuate neuronal apoptosis. In support of this, the direct addition of TNFα (100 pg/well) to neuronal cultures did not bring about apoptosis (Fig. 6.11), which is consistent with previous findings (Thery et al., 1991). Approximately 40 pg of TNFα was measured in microglial conditioned medium obtained from fraction V treated microglia, however 100 pg of TNFα was applied to neuronal cultures, in this way the effects of TNFα on neuronal apoptosis were not underestimated.

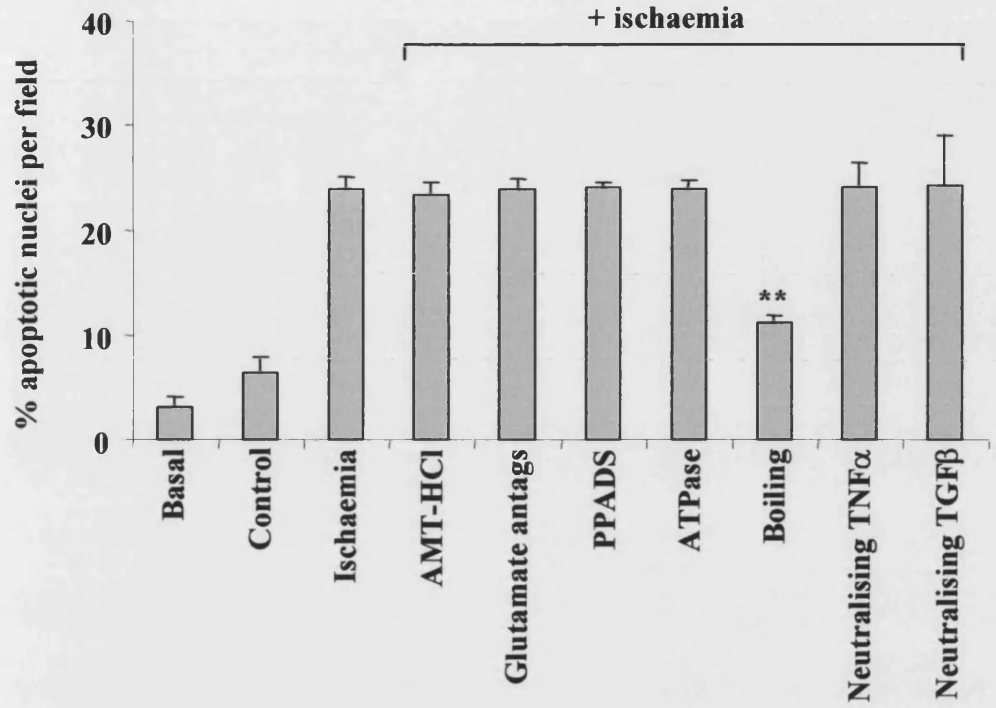

Figure 6.10 Analysis of neurotoxins released from microglia subjected to ischaemia

Neuronal apoptosis induced by medium obtained from microglia subjected to ischaemia was assessed using Hoescht 33342. Microglia were exposed to ischaemia for 3 hours then the cells were incubated in SCM for a further 24 hours in the presence or absence of AMT-HCl (0.3 μM) before medium was collected. Microglial conditioned medium was subsequently applied to cultures of cerebellar granule neurones for 24 hours. To assess the effects of glutamate or ATP on neuronal death, glutamate receptor antagonists (CNQX, 20 μM; MK801, 10 μM; MSPG, 200 μM) ('glutamate antags') or PPADS (100 μM) were pre-incubated with the neurones for 1 hour before conditioned medium was applied to the neurones for a further 24 hours. In addition, ATPase (0.5 U/ml) was added to microglial conditioned medium for 1 hour before the medium was applied to neuronal cultures for 24 hours. Conditioned medium was also boiled before being applied to cultures of neurones ('boiling') for 24 hours. Furthermore, microglial conditioned medium was immuno-depleted of TNFα or TGFβ before being applied to neurones. Control microglia were left untreated for 27 hours (control) then medium was collected and added to neurones fro 24 hours, whilst control neurones were left untreated for 24 hours (basal). Neurones were subsequently fixed then stained with Hoescht 33342. Neurones displaying brightly stained pyknotic nuclei were counted and the degree of apoptosis was expressed as a percentage of the total number of cells counted. The values shown represent the mean ± SEM of data from experiments performed in triplicate. Experiments consisted of 3 coverslips per treatment, comprising ten fields of view. Statistical analysis was performed using ANOVA followed by the Tukey post test. ** $p < 0.01$ vs 'ischaemia'.

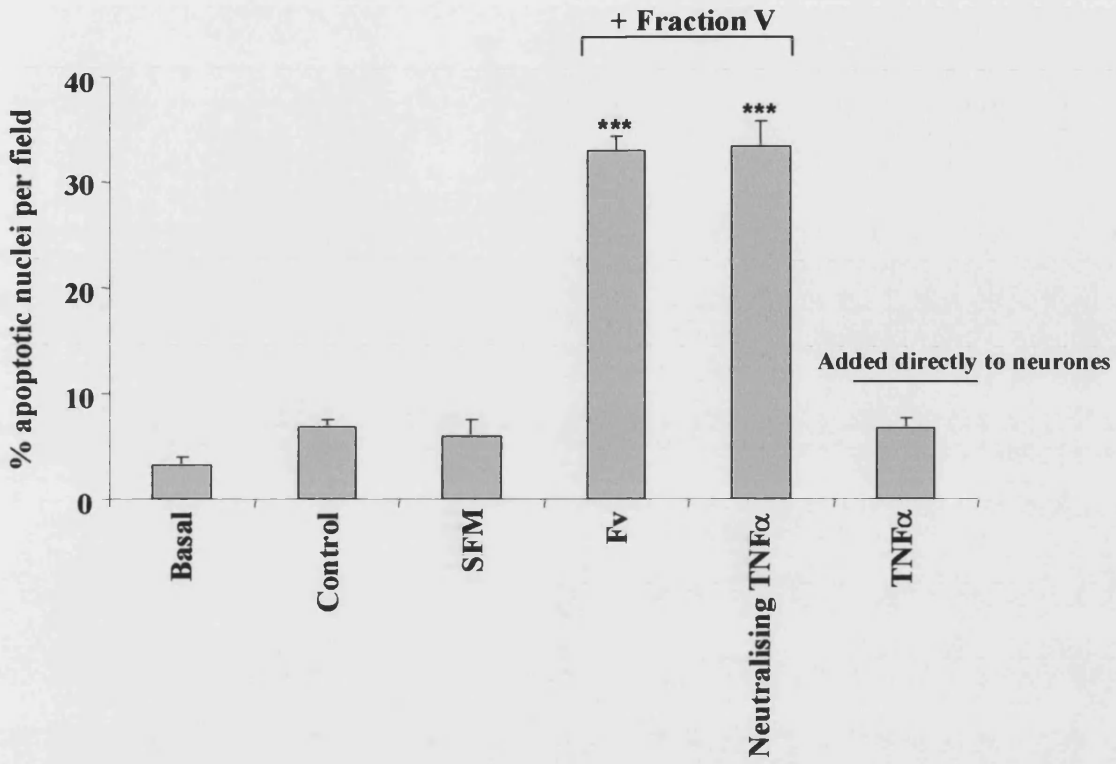

Figure 6.11 Assessment of fraction V induced neurotoxicity with respect to TNFα

Neuronal apoptosis induced by medium obtained from fraction V treated microglia was assessed using Hoescht 33342. Microglia were treated with fraction V (Fv: 1 mg/ml) in SFM for 2 hours. The SFM was then replaced with SCM for 22 hours before the medium was collected. Control medium was collected from microglia left untreated for 24 hours (control) or microglia exposed to SFM for 2 hours then SCM for 22 hours (SFM). Microglial conditioned medium was subsequently applied to cultures of cerebellar granule neurones for 24 hours then the neurones were fixed. To assess the effect of TNFα on neuronal death, fraction V (1 mg/ml) conditioned medium was neutralised with anti-TNFα antibody. Neutralised medium was subsequently applied to cultures of neurones for 24 hours before the neurones were fixed. TNFα (100 pg/well) was also added directly to neuronal culture for 24 hours then the cells were fixed. Control neurones were left untreated for 24 hours (basal) before being fixed. Following fixation, neurones were stained with Hoescht 33342. Non-apoptotic cells possessed large brightly stained nuclei, whereas apoptotic cells possessed brightly stained pyknotic nuclei. Neurones displaying pyknotic nuclei were counted and the degree of apoptosis was expressed as a percentage of the total number of cells counted. The values shown represent the mean ± SEM of data from experiments performed in triplicate. Experiments consisted of 3 coverslips per treatment, comprising ten fields of view. Statistical analysis was performed using ANOVA followed by the Tukey post test. *** $P < 0.001$ vs control (Control describes neuronal cultures treated with medium harvested from untreated microglia 'control').

6.7 Discussion

Research has mainly focussed on the effects of ischaemia on neurones (Goldsburg and Choi 1993; Strasser and Fischer 1995; Pringle et al., 1997; Pocock and Nicholls 1998). However, the results presented in this chapter clearly demonstrate that ischaemia can modulate microglial signalling. In light of the close proximity of microglia to neurones and the emerging awareness of microglial-neuronal interactions this area of research deserves further investigation. Experimental data presented in this chapter revealed that microglia exposed to ischaemia followed by fraction V or Aβ treatment underwent mitochondrial depolarisation, which gave rise to apoptotic cell death. In contrast, microglia subjected to ischaemia alone remained viable. Examination of the signalling cascades elicited in microglia by ischaemia alone or in combination with fraction V or Aβ demonstrated that these treatments triggered different upstream signalling events, which are discussed below.

6.7.1 Ischaemia and iNOS

In vivo, iNOS expression in microglia has been reported in post-natal rats subjected to hypoxia (You and Kaur 2000). iNOS and nitrite are also detectable in the penumbra after transient focal ischaemia and may be involved in the conversion of penumbra into infarction (Zhu D et al., 2002). Furthermore, inhibition of iNOS reduces infarct volume by 30-40 % (Parmentier et al., 1999; Zhu D et al., 2002). *In vitro*, cultured microglia subjected to hypoxia up-regulate the expression of iNOS, which is accompanied by the concomitant production of NO (Park et al., 2002). Re-oxygenation was required for NO production but not iNOS expression, which is not surprising considering oxygen is essential for the oxidation of L-arginine. In support of these findings the iNOS gene has recently been demonstrated to contain a functional hypoxia response element (Melillo et

al., 1995). However, the results presented in this chapter revealed that a 3 hour period of ischaemia did not induce iNOS expression or nitrite production in microglia following reoxygenation. The variations in these results and those published by Park et al., (2002) may reflect differences in the experimental methodologies employed. Firstly, Park et al., (2002) subjected microglia to hypoxia and not ischaemia and secondly these authors prepared their microglia by agitating mixed glial cultures after 10 days *in vitro*, which is known to cause a graded activation of microglial cells (Slepko and Levi 1996). As a result, their microglia may have exhibited a heightened activation state, rendering the cells more susceptible to hypoxic insults. An alternative explanation might be that ischaemia is not a suitable stimulus to promote iNOS expression, whereas hypoxia is. It could be that glucose is a requirement for iNOS expression in microglia (Shin et al., 2002). The data presented in this chapter also demonstrated that ischaemia followed by fraction V or Aβ treatment did not potentiate the levels of iNOS or nitrite production associated with fraction V or Aβ treatment alone. Consistent with this, a synergistic effect of LPS or IFNγ on hypoxia induced iNOS expression was not observed by Park et al, (2002).

6.7.2 Ischaemia and ERK

Ischaemia did not induce the phosphorylation of ERK in microglia. In keeping with this, hypoxic (Park et al., 2002) or ischaemic (Walton et al., 1998) insults have been demonstrated to induce the activation of p38 but not ERK or JNK in microglia. It may be that phosphorylation events are reduced following ischaemia due to the depletion of ATP, which is an essential molecule required for phosphorylation (Berg et al., 2002). However, it is possible that the peak of ERK phosphorylation may have occurred during the ischaemic period; therefore the presence of phospho-ERK may have eluded detection by Western blot analyses. This seems unlikely however, considering ERK remained

phosphorylated for long periods of time after albumin or CgA treatment (see chapters 4 and 5 respectively). Importantly, UO126 (ERK inhibitor) was found to abate iNOS expression in microglia subjected to ischaemia then fraction V treatment. This suggests that ischaemia does not affect the ability of fraction V to elicit ERK activation and subsequent iNOS expression. However, a synergistic effect of ischaemia on fraction V or Aβ associated p-ERK levels was not found.

6.7.3 Ischaemia and glutamate

There is no enzyme to terminate the action of glutamate; hence the synaptic action of glutamate is terminated by the removal of glutamate from the extracellular space by a family of uptake transporters. These Na^+ symporters transport glutamate by exploiting transmembrane ion gradients, which are ultimately set up by the Na^+/K^+ ATPase. Consequently, plasma membrane depolarisation occurring as a result of ischaemia causes glial and neuronal glutamate uptake carriers to operate in reverse, which in turn exacerbates the accumulation of extracellular glutamate (Szatkowski and Atwell 1994; Takahashi et al, 1997; Katsumori et al., 1999; Rossi et al., 2000). However, the results presented in this thesis demonstrate that ischaemia did not induce microglia to secrete glutamate into the culture medium. This might be because ramified microglia express very low levels of glutamate transporters, therefore glutamate is not pumped out of the cells when ion gradients are run down. In accordance with earlier findings fraction V but not Aβ induced microglial glutamate release. Furthermore, ischaemia did not potentiate glutamate release associated with either activator alone. Collectively, these data provide evidence that microglia are probably not the main cell type involved in glutamate release and ensuing excitotoxic damage in response to ischaemia.

6.7.4 Ischaemia and cytokine secretion

TNFα has recently been show to play a central role in ischaemic injury. *In vivo*, TNFα potentiates damage following transient or permanent focal ischaemia (Barone et al., 1997). Moreover, administration of the soluble TNFα receptor or anti-TNFα antibody ameliorates ischaemic damage (Barone et al., 1997; Nawashiro et al., 1997). This suggests that TNFα contributes to pathological inflammatory processes in ischaemia. Microglia are the main source of TNFα in the brain, therefore microglial activation is most likely to underlie TNFα dependent neuronal injury. Accordingly, cultured microglia subjected to hypoxia have been reported to secrete TNFα (Park et al., 2002). However, the results presented here revealed that ischaemia did not evoke the release of TNFα from microglia. Aβ treatment did not induce microglia to release TNFα either. There have been mixed reports regarding the effects of Aβ on TNFα secretion from microglia. Many investigators have demonstrated that microglia treated with Aβ(1-42) (Nagai et al., 2001; Casal et al., 2002) or Aβ(25-35) (Meda et al., 1995; Pyo et al 1998; Nagai et al., 2001) do secrete this cytokine. Conversely, a few studies have demonstrated that microglia treated with Aβ(25-35) (Forloni et al., 1997; Casal et al., 2002), Aβ(1-40) (Gasic-Milenkovic et al., 2003) or Aβ(1-42) (Kopec and Carroll 1998) do not secrete TNFα. One report has also shown that Aβ(1-40) fails to instigate TNFα release from THP monocytes (Klegaris et al., 1997), a cell type that is often used to model microglia. Furthermore, some studies have shown that Aβ(1-40) requires the presence of a co-stimulator such as M-CSF (Murphy et al., 1998) or LPS (Yates et al., 2000) to induce cytokine production. In line with this, the extracellular environment surrounding senile plaques is rich in pro-inflammatory agents including proteases and complement proteins (McGeer and McGeer 1997, 1999), which are likely to augment the effects of Aβ on microglia *in vivo*.

In contrast to ischaemia and Aβ treatment, fraction V was found to evoke a dramatic increase in TNFα secretion. Other blood borne factors have been demonstrated to potentiate LPS induced TNFα secretion (Si et al., 2000), which implies that TNFα may play a vital role in inflammatory processes following BBB damage. Results presented in this chapter also revealed that ischaemia followed by fraction V or Aβ treatment did not potentiate the levels of secreted TNFα associated with fraction V or Aβ treatment alone. This suggests that additional transcriptional factors are not activated in response to the 'combined' insult and therefore a synergistic effect on TNFα release is not observed.

The ability of activated microglia to release TGFβ *in vitro* has not been extensively researched. Data presented in this chapter revealed that ischaemia did not induce microglia to secrete TGFβ. Fraction V or Aβ did not evoke TGFβ release from microglia either. The latter is consistent with previous findings in human monocytes (Meda et al., 1999). Interestingly, microglia subjected to ischaemia followed by Aβ treatment secreted TGFβ, whereas microglia treated with ischaemia followed by fraction V did not release this cytokine. Previously it has been reported that microglia synthesise TGFβ following ischaemic insults *in vivo* (Gehrmann et al., 1995; Lehrmann et al., 1998). TGFβ is known to reduce neuronal damage (Justica et al., 2001) and suppresses astrocytic scar formation (Hunter et al., 1993; Lindholm et al., 1993). Furthermore, TGFβ is a classical wound healing factor, which acts through the enhancement of extracellular matrix deposition and the promotion of angiogenesis to instigate repair (Ling and Robinson 2002). Therefore, the up-regulation of TGFβ expression may represent a beneficial response to injury. Indeed, it may be the balance between cytotoxic and neuro-protective cytokines that determines the extent of ischaemic injury *in vivo*.

6.7.5 Ischaemia and microglial viability

Cultured microglia were resistant to a 3 hour period of ischaemia, after which the cells appeared healthy and did not exhibit morphological characteristics of necrosis, apoptosis or mitochondrial perturbations. Similarly, it has been reported that microglial cultures exposed to ischaemia for 3 or 6 hours followed by reoxygenation exhibit very low levels of death (Yenari and Giffard 2001). Lyons and Kettenmann (1998) also found that microglia are extremely resistant to 6 hours of hypoxia. In contrast, the vast majority of microglia died when subjected to chemical ischaemia involving 6 hours of hypoxia in the presence of 2-deoxyglucose (a non-hydrolysable analogue of glucose) (Lyons and Kettenmann 1998). Interestingly, if microglia were subjected to hypoxia in the presence of mannitol (a non-metabolizable sugar) considerably less microglia died (Lyons and Kettenmann 1998). Mannitol acts as a free radical scavenger and therefore may protect the microglia from reactive oxygen or nitrogen species these cells produce during ischaemic episodes. Together these findings demonstrate that microglia can tolerate ischaemic conditions for a few hours, after which the cells endure death, which is probably due to saturation of survival mechanisms.

Cultured astrocytes also exhibit a similar susceptibility to ischaemic-like insults as microglia (Yu et al., 1989; Goldsberg and Choi 1993; Smith et al., 2003). Conversely, other CNS cell populations appear to be more vulnerable to such insults. The majority of cultured neurones (Goldsburg and Choi 1993; Strasser and Fischer 1995; Pringle et al., 1997) and oligodendrocytes (Lyons and Kettenmann 1998; Fern and Möller 2000) succumb to ischaemic insults after 25-60 minutes of exposure. The ability of microglia and also astrocytes to withstand ischaemia may reflect the fact that they possess large intracellular glycogen stores, which are depleted to fuel respiration under anaerobic conditions (Swanson and Choi 1993).

Despite the finding that microglia are extremely tolerant of a 3 hour period of ischaemia, microglia underwent mitochondrial depolarisation, which in turn precipitated apoptosis when subjected to ischaemia followed by fraction V treatment. Microglial cultures subjected to ischaemia then fraction V contained the same number of cells per field as control cultures. This suggests that such an insult 'overrides' fraction V induced signalling, which would normally lead to proliferation. Although it should be noted that microglia subjected to ischaemia still react to fraction V with a robust calcium response. This suggests that a different signalling cascade is elicited in microglia subjected to ischaemia then fraction V treatment; however the involvement of G_i proteins, Src kinases, ERK or calcium was eliminated.

Microglial cultures subjected to ischaemia then Aβ contained more cells displaying depolarised mitochondria and pyknotic nuclei than those cultures treated with Aβ alone. Moreover, the pathway leading to cell death was the same with or without the initial ischaemic insult and involved scavenger receptor ligation coupled to the activation of a Src kinase and a G_i protein. Ischaemia may potentiate the signalling cascade induced by Aβ by increasing the number of scavenger receptors on the cell surface, alternatively ischaemia may prime the intracellular pathway leading to apoptosis thereby heightening the response upon the application of Aβ. Collectively, these findings illustrate that microglia are relatively resistant to ischaemia *per se*, although the cells are unable to withstand a double insult, which inevitably culminates in apoptosis.

6.7.6 Ischaemia and calcium transients

Ischaemia did not modulate calcium fluxes in N9 microglia as measured immediately after the insult or 24 hours later. This is consistent with results obtained in astrocytes subjected to chronic hypoxia (24 hours) (Smith et al, 2003). Results in this chapter also demonstrated that ischaemia did not change the calcium response profiles obtained with fraction V or Aβ. In contrast, Smith et al. (2003) reported that hypoxia augments the effects of the calcium mobilizing agonist bradykinin, a response that was store mediated. This phenomenon was attributed to the enlargement of store capacity by hypoxia or perhaps the reduced clearance of calcium from the cytoplasm (Smith et al, 2003).

6.7.7 Ischaemia and microglial induced neuronal apoptosis

Ischaemia treated microglia were demonstrated to induce neuronal apoptosis. In support of this, the appearance of activated microglia coincides with delayed neuronal death in the hippocampus (Morioka et al., 1991). Moreover, CNS injury can be reduced by inhibiting macrophage recruitment in spinal cord ischaemia (Giulian and Robertson 1990). *In vivo*, it is conceivable that microglia would induce more neuronal death because neurones would also be compromised by the ischaemic insult rendering them more vulnerable to subsequent damage.

Neuronal apoptosis induced by ischaemia treated microglia was glutamate, TNFα and TGFβ independent, which is in accord with previous findings (Flavin et al., 1997; 2000). It has been proposed that macrophage-like cells induce neurotoxicity through the release of large proteins such as proteases and lipases (Flavin et al., 1997; 2000). In line with this, the neurotoxin(s) released by ischaemia treated microglia were heat labile indicative of a proteinaceous nature, although the precise identity of the neurotoxin(s) remains to be

elucidated. Interestingly, ischaemia followed by fraction V or Aβ treatment did not potentiate the levels of neuronal apoptosis induced by microglia subjected to fraction V or Aβ alone. In light of these results, it would appear that neurotoxin release cannot be elevated beyond a certain threshold even in the presence of a combination of insults probably because 'activation' and subsequent 'secretion' pathways are saturated.

6.7.8 Conclusions

Cultured microglia appear to be relatively resistant to ischaemia. Nevertheless, microglia were extremely sensitive to ischaemia followed by another insult. This suggests that a stroke may shape subsequent microglial responses. To summarise, microglia subjected to ischaemia then fraction V expressed similar levels of iNOS as those cells treated with fraction V alone. Furthermore, microglia subjected to ischaemia then fraction V expressed iNOS via an ERK dependent mechanism. Microglia exposed to ischaemia then fraction V also secreted similar levels of glutamate, TNFα, TGFβ and neurotoxins as those cells treated with fraction V alone. Interestingly, there was no significant difference in the calcium responses detectable in microglia exposed to ischaemia then fraction V or fraction V alone. However, microglia subjected to ischaemia then fraction V did not proliferate. In contrast, the cells underwent mitochondrial depolarisation, which in turn induced apoptosis (Fig. 6.12).

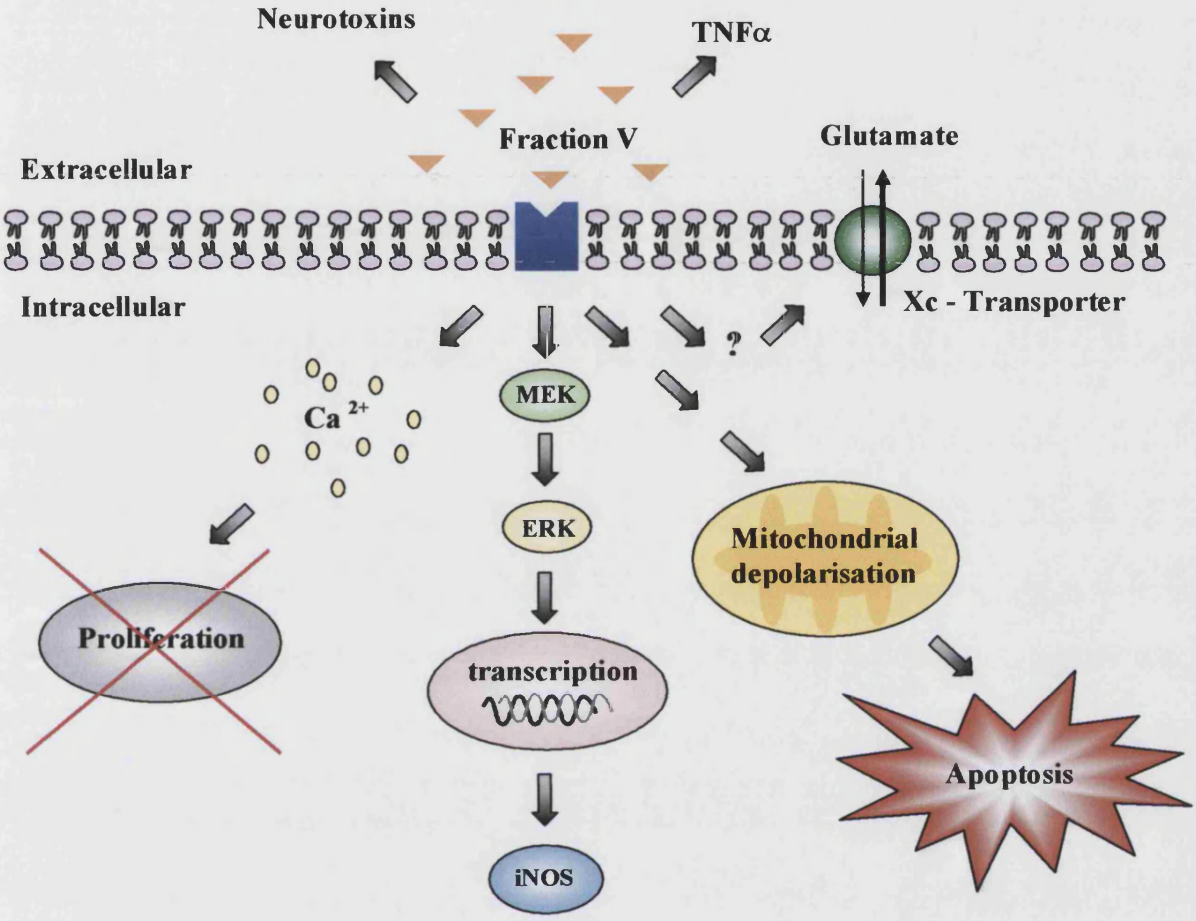

Figure. 6.12 Signalling elicited in microglia subjected to ischaemia then fraction V

Microglia subjected to ischaemia then fraction V expressed similar levels of iNOS as microglia treated with fraction V alone. Furthermore, microglia subjected to ischaemia then fraction V expressed iNOS via an ERK dependent mechanism. Microglia exposed to ischaemia then fraction V also secreted similar levels of glutamate, TNFα, TGFβ and neurotoxins as those cells treated with fraction V alone. There was no significant difference in the calcium responses detectable in microglia exposed to ischaemia then fraction V or fraction V alone. However, microglia subjected to ischaemia then fraction V did not proliferate. In contrast, the cells underwent mitochondrial depolarisation, which in turn precipitated apoptotic cell death.

Microglia subjected to ischaemia then Aβ secreted essentially identical quantities of neurotoxins as microglia treated with Aβ alone. Furthermore, microglia underwent mitochondrial depolarisation, which precipitated apoptosis. However, microglial cultures subjected to ischaemia then Aβ displayed greater levels of mitochondrial depolarisation and apoptosis than those cultures exposed to Aβ alone. Importantly, upstream signalling was mediated via the scavenger receptor, a Src kinase and a Gi/o protein in response to either treatment. Microglia subjected to the combined insult were also found to secrete the anti-inflammatory cytokine TGFβ, whereas TGFβ was not secreted by microglia subjected to ischaemia or Aβ alone (Fig. 6.13).

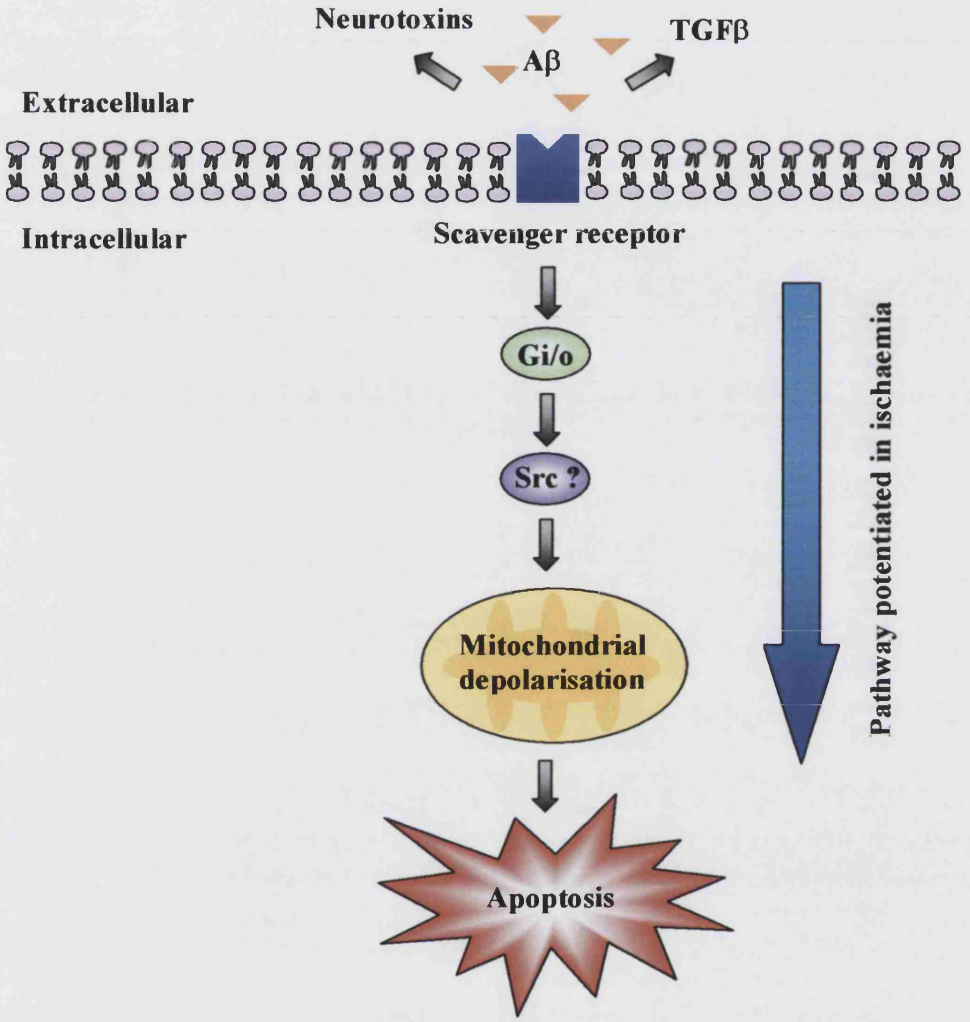

Figure 6.13 Signalling elicited in microglia subjected to ischaemia then Aβ

Microglia subjected to ischaemia then Aβ secreted essentially identical quantities of neurotoxins as microglia treated with Aβ alone. Furthermore, microglia underwent mitochondrial depolarisation, which precipitated apoptosis. However, cultures subjected to ischaemia then Aβ displayed greater levels of mitochondrial depolarisation and apoptosis than those cultures exposed to Aβ alone. Upstream signalling was mediated via the scavenger receptor, a Src kinase and a Gi/o protein in response to either treatment. Microglia subjected to the combined insult were also found to secrete the anti-inflammatory cytokine TGFβ, whereas TGFβ was not secreted by microglia subjected to ischaemia or Aβ alone.

7.0 General discussion

7.1 Evaluation of tissue culture models

Nowadays, *in vitro* models are widely used to study cell signalling. In this thesis, the effects of a number of activators on microglial signalling and subsequent neuronal survival have been explored using tissue culture models. The main advantages of *in vitro* systems over *in vivo* models are that they enable responses of individual cells type to be delineated. However, there is some concern that *in vitro* systems do not reflect the true properties of an individual cell type, since the 3-dimensional architecture of the brain is disrupted during isolation, therefore neighbouring cells cannot contribute to signalling as would occur *in vivo*. Nevertheless, cell culture models provide useful tools to explore cell signalling in ways that would not be feasible *in vivo*.

In this study microglia were isolated using percoll density gradients, a method that was validated according to the findings of Ford et al., (1995) (see chapter 3). Using percoll density gradients extremely pure cultures of microglia can be obtained. Furthermore, when prepared in this way microglia are less activated and more akin to their naturally occurring state *in vivo* because the cells are not cultured for long periods of time, which is a requirement when isolating microglia from mixed glial cultures (Nolte et al., 1996; McDonald et al., 1997; Möller et al., 2000a, b; Casal et al., 2002). Thus, microglia isolated by percoll density gradient provide a good model of the *in vivo* situation. An alternative '*in vitro*' approach would have been to use post mortem tissue to isolate primary microglia. However, such an approach is problematic since it takes a considerable length of time to collect and prepare post mortem tissue during which time a number of cellular changes can occur. In addition, a frequent supply of post-mortem tissue is difficult to obtain. Slice cultures are another model that could have been used in this study, although responses from individual cells are difficult to dissect in such preparations.

A major point that is thrown into light by this investigation is that macrophages, which are frequently used to study microglial signalling (Klegaris and McGeer 1997; Shalit et al., 1997; Smits et al., 2001a, b), may not actually provide a suitable microglial model. Macrophages were demonstrated to possess different signalling properties to microglia. Macrophages also expressed more cell surface receptors than microglia, which suggests that macrophages are more activated than their CNS counterparts. Taken together these results indicate that macrophages may not provide an accurate representation of microglial responses.

The other major cell type utilised in this thesis were cerebellar granule neurones. Preparing neurones from the cerebellum leaves the rest of the brain spare from which microglia can be isolated, thereby minimising wastage. Moreover, the cerebellum develops post-natally (Jacobson 1991), which means that neurones can be prepared from neonatal animals. Hippocampal or cortical neurones may have provided better neuronal models, considering these regions are predominantly involved in the pathology of AD. However, lower yields are obtained from these preparations because cells have to be isolated from embryonic tissue.

7.2 Microglial signalling: common and divergent routes

In this thesis albumin, CgA, or Aβ were demonstrated to trigger diverse signalling cascades in microglia. In contrast, ischaemia *per se* did not appear to exert any effects on microglial signalling, although ischaemia followed by albumin (fraction V) or Aβ treatment altered the microglial responses observed with albumin or Aβ treatment alone. These findings suggest that microglia are more sensitive to receptor mediated events as opposed to 'physical' stimuli such as ischaemia. Nevertheless, ischaemia was found to

manipulate/prime receptor mediated signalling, which suggests that a stroke may condition subsequent microglial responses implying that microglia possess some form of 'molecular memory'. Thus, a stroke may alter the course of AD possibly by exacerbating inflammatory processes. Indeed microglia subjected to ischaemia followed by Aβ treatment released more TGFβ than cells exposed to either stimulus alone.

The 'end point' of microglial activation is a field of research that has not been extensively studied. In this investigation activated microglia were found to proliferate or apoptose. Proliferation may represent a beneficial response instigated to combat injury and minimise tissue damage. *In vitro,* cultured microglia that undergo proliferation do inevitably die. However, *in vivo* activated microglia may proliferate, then revert back to a ramified quiescent phenotype after the damaging event has subsided (Jordon and Thomas 1988). Activation induced apoptosis of microglia may also be an advantageous mechanism, which serves to terminate inflammatory reactions thereby limiting bystander damage to neighbouring neurones. Experimental data revealed that microglial apoptosis was mediated by mitochondrial depolarisation in response to CgA, Aβ or combined insults involving ischaemia then a subsequent treatment (fraction V or Aβ). This suggests that mitochondria are exquisitely sensitive to pathological changes and act as a common executioner of cell death in microglia. These findings provide a very small insight into the ultimate fate of activated microglia, but also highlight that this is an area of research that warrants further investigation.

Investigation of microglial signalling pathways revealed that these cells utilise a multitude of second messengers including calcium, G proteins, ERK and Src kinases. Interestingly, ERK and Src kinases are activated by different microglial activators and mediated both

divergent and common responses. For example, Src kinases mediate albumin-induced proliferation as well as CgA or Aβ-dependent apoptosis. Moreover, ERK is involved in LPS-induced iNOS expression (Bhat et al., 1998) and the expression of iNOS in response to albumin or CgA treatment. COX-2 was not induced by albumin, CgA or Aβ treatment, which implies that prostaglandins synthesis is not upregulated in response to these stimuli. However, LPS triggered the expression of this inflammatory mediator; therefore COX-2 expression can be induced in microglia by independent signalling pathways. A complex interplay between iNOS and COX-2 signalling is emerging (Patel et al., 1999; Clancy et al., 2000), which may account for suppression of COX-2 expression in CgA or albumin activated microglia. Glutamate was another common mediator secreted by activated microglia. This amino acid is known to play a central role in neurodegeneration in particular following ischaemic damage. However, the results presented in this thesis, revealed that ischaemia *per se* did not evoke the release of glutamate from microglia, therefore it is conceivable that other activators associated with ischaemic injury such as leaked blood borne factors (i.e. albumin) or agents associated with dystrophic neurites (i.e. CgA) trigger microglia to release glutamate. Accordingly, activated microglia may be an important secondary source of glutamate in pathological states.

Collectively, the results presented in this thesis demonstrate that the outcome of microglial signalling is a conglomerate of a number of second messenger pathways, which act synergistically to instigate a coordinated response. *In vivo*, microglial signalling is likely to be influenced by a myriad of factors, which act via different receptors to initiate a complex response mediated by overlapping and divergent signalling pathways. Moreover, the finding that albumin may induce signalling via an interaction with myosin heavy chain IX suggests that microglia may also signal through non-conventional receptor types.

7.3 Suggestions for future work

This project has opened a number of avenues for future work. It would be of interest to analyse the involvement of other second messengers including p38 and SAPKs in the signalling cascades induced by CgA, Aβ, albumin or ischaemia. Investigation of respiratory burst activity or phagocytic capability following microglial activation would also be interesting. Perhaps inhibition of phagocytosis may provide a unifying approach to inhibit microglial activation and subsequent local inflammatory responses in disease states. Indeed albumin is internalized by microglia and Aβ is also taken up by these cells (Paresce et al., 1996, 1997; Kopec and Carroll 1998). Moreover, scavenger receptors have recently been demonstrated to mediate phagocytosis (Platt et al., 1996; Paresce et al., 1996), therefore it is conceivable that CgA is internalised too.

An in depth study of the cytokine profiles released by microglia activated by albumin, CgA, Aβ or ischaemia would be a valuable exercise. To follow on from this, the signalling pathways leading to cytokine secretion could be investigated. An expansion of this project could include the exploration of astrocyte signalling induced by CgA, Aβ, albumin or ischaemia. Therefore, a wider picture of glial signalling in pathological situations could be portrayed. Furthermore, a comparison of the signalling cascades elicited by Aβ(25-35), Aβ(1-40) or Aβ(1-42) would be useful because the results presented in this thesis and by other investigators (Forloni et al., 1997; Kopec and Carroll 1998; Casal et al., 2002; Gasic-Milenkovic et al., 2003) have highlighted that these species of Aβ elicit different signalling cascades. If it turns out that all Aβ fragments fail to induce microglia inflammatory responses then the ability of CgA or albumin to act as co-stimuli could be explored.

Finally, the use of peripheral monocytes as tools to deliver drugs into the CNS following ischaemia (peripheral blood cells are not recruited into the CNS in AD) could be explored. Circulating monocytes are inevitably recruited to the ischaemic core (Kato and Walz 2000), therefore these cells could be exploited to directly target agents to damaged areas. Moreover, problems associated with crossing the BBB would be circumvented.

7.4 General conclusions

Under physiological conditions resident microglia are quiescent and are randomly scattered throughout the CNS (Thomas 1992). Occasionally microglia become activated to play a classical role as 'scavenging cells' for the maintenance and restoration of proper CNS homeostasis. Microglia proliferate, change morphology then phagocytose debris or cells that have become pathologically damaged or developmentally unnecessary. These functions however are strictly regulated and do not elicit secondary neuronal damage. In contrast, chronic microglial activation may be a cause of neurodegeneration. In this study the signalling pathways triggered in microglia treated with albumin, CgA, Aβ, ischaemia or a combination of insults were explored in an attempt to model pathological conditions associated with stroke and Alzheimer's disease. A common property shared by microglia subjected to these insults was the ability to induce neuronal death. Extrapolation of these findings implies that *in vivo* microglia are very sensitive to BBB injury, ischaemia or the presence of foreign bodies such as CgA or β-amyloid plaques. Thus, in neurodegenerative diseases the accumulation of numerous pathologies may lead to the development of a chronic inflammatory response, which in turn may exacerbate neuronal death and contribute to cognitive decline (Fig. 7.1). In light of this, selective modulation of microglial signalling pathways may provide avenues for therapeutic strategies to alleviate the symptoms of neurological disorders.

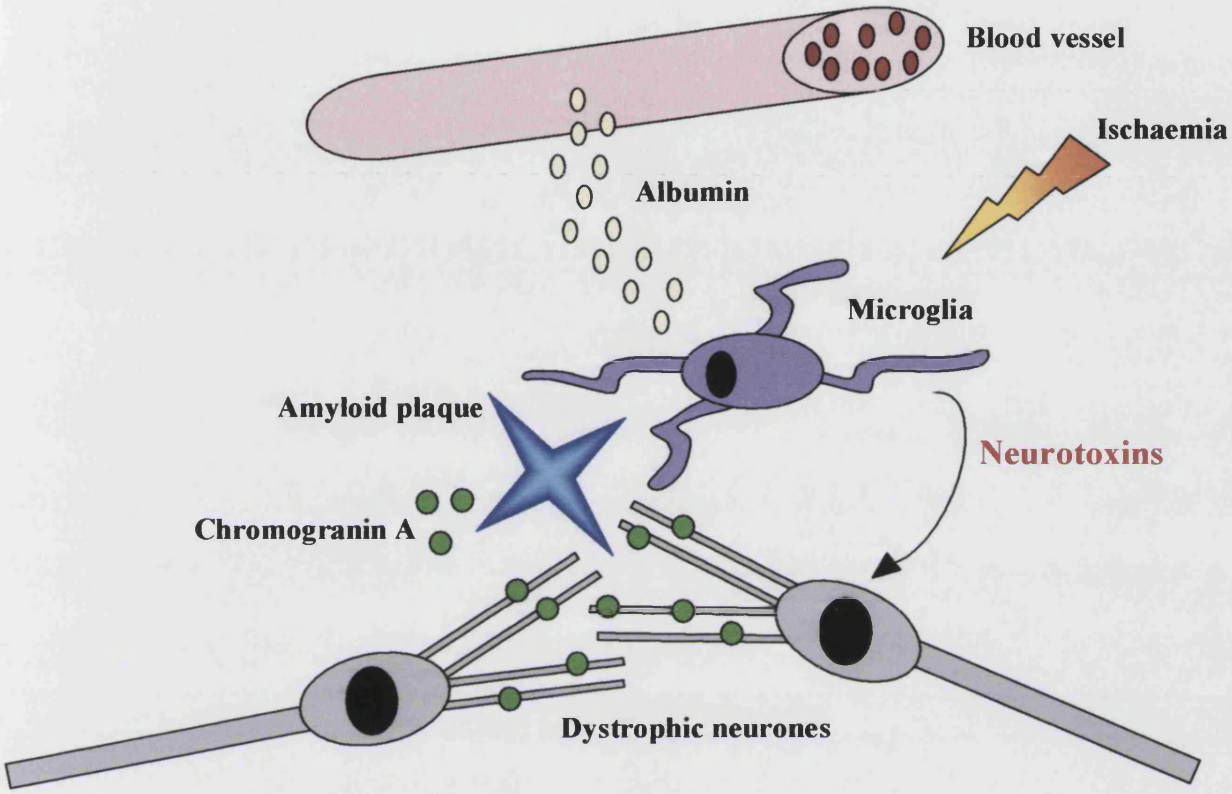

Figure 7.1 Microglial activation in stroke and Alzheimer's disease

A combination of pathological processes contribute to microglial activation in Alzheimer's disease and stroke including the presence of amyloid plaques, the accumulation of extracellular and intra-neuronal deposits of CgA, BBB damage and ischaemic injury. Activated microglia subsequently release neurotoxins, which fuel neuronal damage thereby augmenting cognitive impairment.

8.0 References

Abe K., Hayashi T. (1997) Expression of the glial cell line derived neurotrophic factor gene in the rat brain after transient MCA occlusion. *Brain Res.* 776, 230-234.

Abe K., Saito H. (2000) Amyloid β neurotoxicity is not mediated by the mitogen activated protein kinase cascade in cultured rat hippocampal and cortical neurons. *Neurosci. Lett.* 292, 1-4.

Abo A., Boyhan A., Wcst I., Thrasher A. J., Segal A. W. (1992) Reconstitution of neutrophil NAPDH oxidase activity in the cell free system by four components: p67 phox, p47 phox, p21Racl and cytochrome b_{245}. *J. Biol. Chem.* 267, 16767-16770.

Adams J. P., Sweatt J. D. (2002) Molecular psychology: role for the ERK MAP kinase cascade in memory. *Ann. Rev. Pharmacol. Tox.* 42, 135-163.

Aggarwal B. B., Eessalu T. E., Hass P. E. (1985) Characterisation of receptors for human tumour necrosis factor and their regulation by γ-interferon. *Nature.* 318, 665-667.

Ajizian S. J., English K. (1999) Specific inhibitors of p38 and extracellular signal related kinase mitogen activated protein kinase pathways block inducible nitric oxide synthase and tumour necrosis factor accumulation in murine macrophages stimulated with lipopolysaccharide and interferon γ. *J Infect. Dis.* 179, 939-944.

Alafuzoff I., Adolfsson R., Bucht G., Winbald B. (1983) Albumin and immunoglobulin in plasma and cerebrospinal fluid and blood cerebrospinal fluid barrier function in patients with dementia of Alzheimer's type and multi-infarct dementia. *J. Neurosci.* 60, 465-472.

Alberts B., Johnson A., Lewis J., Raff M., Roberts K., Walter K. (2002) *Molecular Biology of the Cell.* Fourth Edition. Garland publishing Inc. New York. USA.

Alessi D. R., Cuenda A., Cohen P., Dudley D. T., Saltiel A. R. (1995) PD98059 is a specific inhibitor of the activation of mitogen activated protein kinase kinase *in vitro* and *in vivo*. *J. Biol. Chem.* 270, 27459-27494.

Alford P. B., Xue Y., Thai S. F., Shackelford R. E. (1998) Maleylated BSA enhances production of nitric oxide from macrophages. *Biochem. Biophys. Res. Comm.* 245, 185-189.

Allen J. W., Eldadah B. A., Huang X., Knoblach S. M., Faden A. I. (2001) Multiple caspases are involved in β amyloid induced neuronal apoptosis. *J. Neurosci. Res.* 65, 45-53.

Allen L. H., Aderem A. (1995) A role for MARCKS, the alpha isozyme of protein kinase C and myosin I in zymosan phagocytosis by macrophages. *J. Exp. Med.* 182, 829-840.

An S., Zheng Y., Bleu T. (2000) Sphingosine 1- phosphate induced cell proliferation, survival, and related signalling events mediated by G protein coupled receptors Edg-3 and Edg-5. *J. Biol. Chem.* 275, 288-296.

An S., Bleu T., Huang W., Hallmark O. G., Coughlin S. R., Goetzl E. J. (1999) Identification of cDNAs encoding two G protein coupled receptors for lysoshingolipids. *FEBS Lett.* 417, 279-282.

Anderson B. B., Korbo L., Pakkenberg B. (1992) A quantitative study of the human cerebellum with unbiased stereological techniques. *J. Comp. Neurol.* 326, 549-560.

Angeletti R. H., Aardal S., Serk-Hanssen S., Gee P., Helle K. B. (1994) Vasoinhibitory activity of synthetic peptides from amino terminus of chromogranin A. *Acta. Physiol. Scand.* 152, 11-19.

Archibald K., Perry M. J., Molnar E., Henley J. H. (1998) Surface expression and metabolic half life of AMPA receptors in cultured rat cerebellar granule cells. *Neuropharmacol.* 37, 1345-1353.

Aronica E., Condorelli D. F., Nicoletti F., Dell Albani P., Amico C., Balazs R. (1993) Metabotropic glutamate receptors in cultured cerebellar granule cells: developmental profile. *J. Neurochem.* 60, 559-565.

Bahler M (2000) Are class III and class IX myosins motorized signalling molecules. *Biochem. Biophys. Acta.* 1496, 52-59.

Bamberger M. E., Harris M. E., McDonald D. R., Husemann J., Landreth G. E. (2003) A cell surface receptor complex for fibrillar β-amyloid mediates microglial activation. *J. Neurosci.* 23, 2665-2674.

Banati R. (2003) Neuropathological imaging: *in vivo* detection of glial activation as a measure of disease and adaptive change in the brain. *Brit. Med. Bul.* 65, 121-131.

Banati R., Gehrmann J., Schubert P., Kreutzberg G. W. (1993a) Cytotoxicity of microglia. *Glia.* 7, 111-118.

Banati R., Gehrmann J., Czech C., Monning U., Jones L. L., Konig G., Beyreuther K., Kreutzberg G. W. (1993b) Early and rapid *de novo* synthesis of Alzheimer's beta A4 amyloid precursor protein (APP) in activated microglia. *Glia.* 9, 199-210.

Barber B. J., Schultz T. J., Randlett D. L. (1990) Comparative analysis of protein content in rat mesenteric tissue, peritoneal fluid and plasma. *Am J. Physiol.* 258, 714-718.

Barger S. W., Basile A. S. (2001) Activation of microglia by secreted amyloid precursor protein evokes release of glutamate by cysteine exchange and attenuates synaptic function. *J. Neurochem.* 76, 846-854.

Barinaga M. (1998) Stroke damaged neurones may commit cellular suicide. *Science.* 281, 1302-1303.

Barker J. E., Strangward H. M., Brand M. P., Hurst R. D., Land J. M., Clark J. B., Heales S. J. R. (1998) Increased inducible nitric oxide synthase protein but limited nitric oxide formation occurs in astrocytes of the *hph-1* (tetrahydroptcrin) deficient mouse. *Brain Res.* 804, 1-6.

Baron M., Gallego A. (1972) The relation of the microglia with the pericytes in the cat cerebral cortex. *Z. Zellforsch.* 128, 42-57.

Barone F. C., Arvin B., White R. F., Miller A., Webb C. L., Wilette R. N., Lysko P. G., Feuerstein G. Z. (1997) Tumour necrosis factor α a mediator of focal ischaemic brain injury. *Stroke.* 28, 1233-1244.

Bastian A. J., Mugnaini E., Thach W. (1999) Cerebellum in *'Fundamental Neuroscience'*. Edited by Zigmond M. J., Bloom F. E., Londis S. C., Squire L. R. Academic Press, San Diego. USA.

Bauxbaum J. D. Choi E. K., Luo Y., Lilliehook C., Crowley A. C., Merriam D. E., Wasco W. (1998a) Calsenilin: a calcium binding protein that interacts with the presenilins and regulates the levels of a presenilin fragment. *Nat. Med.* 4, 1177-1181.

Bauxbaum J. D., Liu K. L., Luo Y., Slack J. L., Stocking K. L., Peschon J. J., Johnson R. S., Castner B. J., Cerretti D. P., Black R. A. (1998b) Evidence that tumour necrosis factor α converting enzyme is involved in the regulated α-secretase cleavage of the Alzheimer's amyloid precursor protein. *J. Biol. Chem.* 273, 27765-27767.

Becher B., Antel J. P. (1996) Comparison of phenotypic and functional properties of immediately *ex vivo* and cultured human adult microglia. *Glia.* 18, 1-10.

Benveniste E. N., Nguyen V. T., O'Keefe G. M. (2001) Immunological aspects of microglia: relevance to Alzheimer's disease. *Neurochem. Internat.* 39, 381-391.

Berg J. M., Tymoczko J. L., Stryer L. (2002) *Biochemistry.* Fifth Edition. W. H Freeman and Company. New York, USA.

Berridge M. (1993) Inositol triphosphate and calcium signalling. *Nature.* 361, 315-325.

Bhat N. R., Fan F. (2002) Adenovirus infection induces microglial activation: involvement of mitogen activated protein kinase pathways. *Brain Res.* 948, 93-101.

Bhat N. R., Zhang P., Lee J. C., Hogan E. L. (1998) Extracellular signal-regulated kinase and p38 subgroups of mitogen-activated protein kinases regulate inducible nitric oxide synthase and tumor necrosis factor-alpha gene expression in endotoxin-stimulated primary glial cultures. *J. Neurosci.*18, 1633-1641.

Biber K., Laurie D. J., Berthele A., Sommer B., Tölle T. R., Gebicke-Härter P. J., van Calker D., Boddeke H. W. (1999) Expression and signalling of group I metabotropic glutamate receptors in astrocytes and microglia. *J. Neurochem.* 72, 1671-1680.

Biting L., Naidu A., Cordel B., Murphy Jr. G. M. (1996) β-amyloid peptide secretion by a microglial cell line is induced by β-amyloid (25-35) and lipopolysaccharide. *J. Biol. Chem.* 271, 16084-16089.

Black R. A., Rauch C. T., Kozlosky C. J., Peschon J. J., Slack J. L., Wolfson M. F., Castner B. J., Stocking K. L., Reddy P., Srinivasan S., Nelson N., Boiani N., Schooley K. A., Gerhart M., Davis R., Fitzner J. N., Johnson R. S., Paxton R. J., March C. J., Cerretti D. P. (1997) A metalloproteinase disintegrin that releases tumour necrosis factor-alpha from cells. *Nature.* 385, 729-733.

Booth P. L., Thomas W. E. (1991) Evidence for motility and pinocytosis in ramified microglia in tissue culture. *Brain Res.* 548, 163-171.

Botelho R. J., Teruel M., Dierckman R., Anderson R., Wells A., York J. D., Meyer T., Grinstein S. (2000) Localised biphasic changes in phosphatidylinositol 4-5 bis-phosphate at sites of phagocytosis. *J. Cell Biol.* 151, 1353-1367.

Boya J., Calvo J., Prado A. (1979) The origin of microglial cells. *J. Anat.* 129, 177-186.

Boyles J. K., Pita R., Wilson E., Mahley R. W., Taylor J. M. (1985) Apolipoprotein E associated with astrocytic glia of the central nervous system and with nonmyelinating glia of the peripheral nervous system. *J. Clin. Invest.* 76, 1501-1513.

Braak H., Braak E. (1991) Neuropathological stageing of Alzheimer related changes. *Acta. Neuropathol.* 82, 239-259.

Bradford M. M. (1976) A rapid and sensitive method for the quantitation of microgram quantities of protein utilizing the principle of protein dye binding. *Anal. Biochem.* 72, 248-254.

Braun N., Zhu Y., Krieglstein J., Culmsee C., Zimmermann H. (1998) Upregulation of the enzyme chain hydrolyzing extracellular ATP after transient forebrain ischaemia in the rat. *J. Neurosci.* 18, 4891-4900.

Bredt D. S., Snyder S. H. (1990) Isolation of nitric oxide synthase a calmodulin requiring enzyme. *Proc. Natl. Acad. Sci.* 87, 682-685.

Brion J. P. (1992) The pathology of the neuronal cytoskeleton in Alzhiemer's disease. *Biochem. Biophys. Acta.* 1160, 134-142.

Brownlee M. (1995) Advanced protein glycosylation in diabetes and aging. *Ann. Rev.* 46, 223-234.

Brudzynski S. M., Munoz D. G. (1994) Chromogranin A applied to the nucleus accumbens decreases locomotor activity induced by activation of the mesolimbic dopaminergic system in the rat. *Brain Res. Bull.* 35, 211-216.

Bruno V., Battaglia G., Casabona G., Copani A., Caciali F., Nicoletti F. (1998) Neuroprotection by glial metabotropic glutamate receptors is mediated by transforming growth factor β. *J. Neurosci.* 18, 9594-9600.

Budd S. L., Nicholls D. G. (1996) Mitochondria, calcium regulation and acute glutamate excitotoxicity in cultured cerebellar granule cells. *J. Neurochem.* 67, 2282-2291.

Café C., Torri C., Marzatico F. (1993) Cellular and molecular events of ischaemic brain damage. *Funct. Neurol.* 8, 121-133.

Cagnin A., Brooks D. J., Kennedy A. M., Gunn R. N., Myers R., Turkheimer F. E., Jones T., Banati R. B. (2001) *In vivo* measurement of activated microglia in dementia. *Lancet.* 358, 461-467.

Calvo C. F., Yoshimura T., Gelman M., Mallat M. (1996) Production of monocyte chemotactic protein 1 by rat brain macrophages. *Eur. J. Neurosci.* 8, 1725-1734.

Canevari L., Clark J. B., Bates T. E. (1999) β-amyloid fragment 25-35 selectively decreases complex IV activity in isolated mitochondria. *FEBS Lett.* 457, 131-134.

Carpenter G., Ji Q. (1999) Phospholipase C γ as a signal transducing element. *Exp. Cell Res.* 253, 15-24.

Carruth L. M., Demczuk S., Mizel S. B. (1991) Involvement of a calpain-like protease in the processing of the murine interleukin 1 alpha precursor. *J. Biol. Chem.* 266, 12162-12167.

Casal C., Serratosa J., Tusell J. M. (2002) Relationship between β-AP peptide aggregation and microglial activation. *Brain Res.* 928, 76-84.

Chao C. C., Lokensgard J. R., Sheng W. S., Peterson P. K. (1997) IL1 induces iNOS expression in human astrocytes via NF kappa B. *Neuroreport.* 8, 3163-3166.

Checler F. (1995) Processing of β-amyloid precursor protein and its regulation in Alzheimer's disease. *J. Neurochem.* 65, 1431-1444.

Chen B. C., Chen Y. H., Lin W. W. (1999) Involvement of p38 mitogen activated protein kinase in lipopolysaccharide induced iNOS and COX-2 expression in J774 macrophages. *Immunol.* 97, 124-129.

Chen C. C., Wang J. K. (1999) p38 but not p44/42 mitogen activated protein kinase is required for nitric oxide synthase induction mediated by lipopolysaccharide in RAW 264.7 macrophages. *Mol. Pharmacol.* 55, 481-488.

Choi D. W. (1988) Calcium mediated neurotoxicity: relationship to specific channel types and role in ischaemic damage. *Trends Neurosci.* 11, 465-469.

Choi D. W. (1992) Excitotoxic cell death. *J. Neurobiol.* 23, 1261-1276.

Choi H., Khoo C., Ryo J. K., Breemen E. V., Kim S. U., McLarnon J. G. (2002) Inhibition of lipopolysaccharide induced cyclooxygenase 2, tumour necrosis factor α and [Ca^{2+}] responses in human microglia by the peripheral benzodiazepine receptor ligand PK1195. *J. Neurochem.* 83, 546-555.

Chow S. C., Kass G. E. N., Orrenius S. (1997) Purines and their role in apoptosis. *Neuropharmacol.* 36, 1149-1156.

Ciesielski-Treska J., Ulrich G., Taupenot L., Chasserot-Golaz S., Corti A., Aunis D., Bader M. F. (1998) Chromogranin A induces a neurotoxic phenotype in brain microglial cells. *J. Biol. Chem.* 273, 14339-14346.

Ciesielski-Treska J., Ulrich G., Taupenot L., Chasserot-Golaz S., Zwiller J., Revel M. O., Aunis D., Bader M. F. (2001) Mechanisms underlying neuronal death induced by chromogranin activated microglia. *J. Biol. Chem.* 276, 13113-13120.

Citron M., Oltersdorf T., Haass C., McConologue L., Hung A. Y., Selbert P., Vigo-Pelfrey C., Lieberburg I., Selkoe D. J. (1992) Mutation of the β amyloid precursor protein in familial Alzheimer's disease increases β-protein production. *Nature.* 360, 672-674.

Clancy R., Varenika B., Huang W., Ballou L., Attur M., Amin A. R., Abramson S., B. (2000) Nitric oxide synthase/COX cross-talk: nitric oxide activates COX-1 but inhibits COX-2-derived prostaglandin production. *J. Immunol.* 165, 1582-1587.

Clark D. A., Coker R. (1998) Transforming growth factor beta (TGFβ). *Int. J. Biochem. Cell Biol.* 30, 293-298.

Clemens J. A., Stephenson D. T., Smalstig B., Dixon E. P., Little S. P. (1997) Global ischaemia activates nuclear factor κB in forebrain neurones of rats. *Stroke.* 28, 1073-1081.

Clementi E., Brown G. C., Feelisch M., Moncada S. (1998) Persistent inhibition of cell respiration by nitric oxide: crucial role of *s*-nitrosylation of mitochondrial complex I and protective action of glutathione. *Proc. Natl. Acad. Sci.* 95, 7631-7636.

Colton C. A., Gilbert D. L. (1987) Production of superoxide anions by a CNS macrophage, the microglia. *FEBS Lett.* 223, 284-288.

Combs C. K., Johnson D. E., Cannady S. B., Lehman T. M., Landreth G. E. (1999) Identification of microglial signal transduction pathways mediating a neurotoxic response to amyloidogenic fragments of beta-amyloid and prion proteins. *J. Neurosci.* 19, 928-939.

Combs C. K., Karlo C., Kao S., Landreth G. E. (2001) Beta-amyloid stimulation of microglia and monocytes results in TNFα dependent expression of inducible nitric oxide synthase and neuronal apoptosis. *J. Neurosci.* 21, 1179-1188.

Corder E. H., Saunders A. M., Strittmatter W. J., Schmechel D. E., Gaskell P. C., Small G. W., Roses A. D., Haines J. L., Pericak-Vance M. A. (1993) Gene dose of apolipoprotein E type 4 allele and the risk of Alzheimer's disease in late onset families. *Science.* 261, 921-923.

Corradin S. B., Mauel J., Donini S. D., Quattrocchi E., Ricciardi-Castagnoli P. (1993) Inducible nitric oxide synthase activity of cloned murine microglial cells. *Glia.* 7, 255-262.

Coughlin C. M., Breen K. C. (2000) Factors influencing the processing and function of the amyloid β precursor protein – a potential therapeutic target in Alzheimer's disease. *Pharmacol. Therapeut.* 86, 111-144.

Cox D., Berg J. S., Cammer M., Chinegwundoh J. O., Dale B. M., Cheney R. E., Greenberg S. (2002) Myosin X is a downstream effector of PI(3)K during phagocytosis. *Nat. Cell Biol.* 4, 469-477.

Coyle J. T., Schwarcz R. (2000) Implications of glial cell biology for psychiatry. *Arch. Gen. Psychiatry.* 57, 90-93.

Crawford S. E., Stellmach V., Murphy-Ullrich J. E., Ribeiro M. F., Lawler J., Hynes R. O., Boivin G. P., Bouck N. (1998) Thrombospondin 1 is a major activator of TGFβ1 *in vivo*. *Cell.* 93, 1159-1170.

Crowther R. A. (1990) Structural aspects of pathology in Alzheimer's disease. *Biochim. Biophys. Acta.* 1096, 1-9.

Dai X., Qu P., Dreyfus C. F. (2001) Neuronal signals regulate neurotrophin expression in oligodendrocytes in the basal forebrain. *Glia.* 34, 234-239.

Damoiseaux J. G., Dopp E. A., Calame W., Chao D., MacPherson G. G., Dijkstra C. D. (1994) Rat macrophage lysosomal membrane antigen recognised by monoclonal antibody ED-1. *Immunol.* 83, 140-147.

Dana N., Fathallah D. M., Arnaout A. (1991) Expression of a soluble and functional form of the human β2 integrin Cd11b/CD18. *Proc. Natl. Acad. Sci.* 88, 3106-3110.

Daum G., Eisenmann-Tappe I., Fries H., Troppmair J., Rapp U. R. (1994) The ins and outs of RAF kinases. *Trends Biochem. Sci.* 19, 474-480.

De Strooper B. (2003) Aph-1, Pen-2 and nicastrin with Presenilin generate an active gamma secretase complex. *Neuron.* 38, 9-12.

Dean J. L. E., Brook M., Clark A. R., Saklatvala J. (1999) p38 mitogen activated protein kinase regulates cyclooxygenase 2 mRNA stability and transcription in lipopolysaccharide treated human monocytes. *J. Biol. Chem.* 27, 264-269.

Del Bigio M. (1995) The ependyma: a protective barrier between brain and cerebrospinal fluid. *Glia.* 14, 1-13.

Delaere P., Duyckaerts C., He Y., Piette F., Hauw J. J. (1991) Subtypes and differential laminar distribution of βA4 deposits in Alzheimer's disease: relationship with the intellectual status of 26 cases. *Acta Neuropathol.* 81, 328-335.

Desmond D. W., Moroney J. T., Paik M. C., Sano M., Mohr J. P., Aboumatar S., Tseng C. L., Chan S., Williams J. B. W., Reimen R. H., Hauser W. A., Stern Y. (2000) Frequency and clinical determinants of dementia after ischaemic stroke. *Neurol.* 54, 1124-1131.

Diem K. (1962) *Scientific Tables.* Sixth Edition. Geigy Pharmaceutical Company Limited. Manchester, UK.

Ding M., St-Pierre B. A., Parkinson J. F., Medberry P., Wong J. L., Rogers N. E., Ignarro L. J., Merrill J. E. (1997) Inducible nitric oxide synthase and nitric oxide production in human fetal astrocytes and microglia. *J. Biol. Chem.* 272, 11327-11335.

Dirnagl U., Iadecola C., Moskowitz M. A. (1999) Pathobiology of ischaemic stroke: an integrated review. *Trends Neurol.* 22, 391-397.

Dopp J. M., Mackenzie-Graham A., Otero G. C., Merrill J. E. (1997) Differential expression, cytokine modulation and specific functions of type-1 and type-2 tumour necrosis factor receptors in rat glia. *J. Neuroimmunol.* 75, 104-112.

Dubois R., Aramson S. B., Crofford L., Gupta R. A., Simon L. S., Van de Putte L. B. A., Lipsky P. E. (1998) Cyclooxygenase in biology and disease. *FASEB J.* 12, 1063-1073.

Dukic-Stefanovic S., Gasic-Milenkovic J., Deuther-Conrad W., Munch G. (2003) Signal transduction pathways in mouse microglia N-11 cells activated by advanced glycation endproducts (AGEs). *J. Neurochem.* 87, 44-55.

Duta D. (2000) Mechanism of store operated calcium entry. *J. Biosci.* 25, 397-404.

Earnshaw W. C. (1999) A Cellular poison cupboard. *Nature.* 397, 387-389.

Eichenbaum J. W., Pevsner P. H., Pivawer G., Kleinman G. M., Chiriboga L., Stern A., Rosenbach A., Iannuzzi K., Miller D. C. (2002) A murine photochemical stroke model with histologic correlates of apoptotic and nonapoptotic mechanisms. *J. Pharmacol. Tox. Meth.* 47, 67-71.

Eickelberg O. (2001) Endless healing: TGFβ Smads and fibrosis. *FEBS Lett.* 506, 11-14.

Eikelenboom P., Bate C., Van Gool W. A., Hoozemans J. J. M., Rozemuller J. M., Veerhuis R., Williams A. (2002) Neuroinflammation in Alzheimer's disease and prion disease. *Glia.* 40, 232-239.

El Khoury J. B., Moore K. J., Means T. K., Leung J. L., Terada K., Toft M., Freeman M. W., Luster A. D. (2003) CD36 mediates the innate host response to β-amyloid. *J. Exp. Med.* 97, 1657-1666.

Eliasson C., Sahlgren C., Berthold C., Stakeberg J., Celis J. E., Betsholtz C., Eriksson J. E., Pekny M. (1999) Intermediate filament protein partnership in astrocytes. *J. Biol. Chem.* 274, 23996-24006.

Endres M., Namura S., Shimizu-Sasamata M., Waeber C., Zhang L., Gomez-Isla T., Hyman B. T., Moskowitz M. A. (1998) Attenuation of delayed neuronal death after mild focal ischemia in mice by inhibition of the caspase family. *J. Cereb. Blood Flow Metab.* 18, 238-2247.

Fasciotto B. H., Trauss C. A., Greeley G. H., Cohn D. V. (1993) Parastatin (porcine chromogranin A347-419), a novel chromogranin A-derived peptide, inhibits parathyroid cell secretion. *Endocrinol.* 133, 461-466.

Favata M. F., Horiuchi K. Y., Manos E. J., Daulerio A. J., Stradley D. A., Feeser W. S., Van Dyk D. E., Pitts W. J., Earl R. A., Hobbs F., Copeland R. A., Magolda R. L., Scherle P. A., Trzaskos J. M. (1998) Identification of a novel inhibitor of mitogen activated protein kinase kinase. *J. Biol. Chem.* 273, 18623-18632.

Feldman R. S., Jerrold S. M., Quenzer L. F. (1997) Parkinson's and Alzheimer's disease. In '*Neurophyschopharmacology.*' Sinauer Associates Inc. Massachusetts, USA.

Fern R., Möller T. (2000) Rapid ischaemic cell death in immature oligodendrocytes: a fatal glutamate release feedback loop. *J. Neurosci.* 20, 34-42.

Ferrari D., Villalba M., Chiozzi P., Falzoni S., Riccardi-Castagnoli P., Di Virgilio F. (1996) Mouse microglial cells express a plasma membrane pore gated by extracellular ATP. *J. Immunol.* 156, 1531-1539.

Fields T. A., Casey P. J. (1997) Signalling functions and biochemical properties of pertussis toxin sensitive G proteins. *Biochem. J.* 321, 561-571.

Fischer-Colbrie R., Hagn C., Schober M. (1987) Chromogranins A, B, and C: widespread constituents of secretory vesicles. *Ann. N. Y. Acad. Sci.* 493, 120-134.

Flavin M. P., Coughlin K., Ho L. T. (1997) Soluble macrophage factors trigger apoptosis in cultured hippocampal neurones. *Neurosci.* 80, 437-448.

Flavin M. P., Zhao G., Ho L. T. (2000) Microglia tissue plasminogen activator (tPA) triggers neuronal apoptosis *in vitro*. *Glia.* 29, 347-354.

Fontana A., Fierz W., Wekerle H. (1984) Astrocytes present myelin basic protein to encephalitogenic T-cell lines. *Nature.* 307, 273-276.

Ford A. L., Goodsall A. L., Hickey W. F., Sedgwick J. D. (1995) Normal ramified microglia separated from other central nervous system macrophages by flow cytometric sorting. *J. Immunol.* 154, 4309-4321.

Forloni G., Mangiarotti F., Angeretti N., Lucca E., De Simoni M. G. (1997) β-amyloid fragment potentiates IL-6 and TNFα secretion by LPS in astrocytes but not microglia. *Cytokine.* 9, 759-762.

Frackowiak J., Wisniewski H. M., Wegiel J., Merz G. S., Iqbal K., Wang K. C. (1992) Ultrastructure of the microglia that phagocytose amyloid and the microglia that produce β-amyloid fibrils. *Acta Neuropathol.* 84, 225-233.

Frei K., Bodmer S., Schwerdel C., Fontana A. (1986) Astrocyte derived interleukin 3 as a growth factor for microglial cells and peritoneal macrophages. *J. Immunol.* 137, 3521-3527.

Fueller M., Wang D. A., Tigyi G., Seiss W. (2003) Activation of human monocytic cells by lysophosphatidic acid and sphingosine-1-phosphate. *Cell. Sig.* 15, 367-375.

Gallo V., Kingsbury A., Balazs R., Jorgensen O. S. (1987) The role of depolarisation in the survival and differentiation of cerebellar granule cells in culture. *J. Neurosci.* 7, 2203-2213.

Gallo V., Ciotti M. T., Coletti A., Aloisi F., Levi G. (1982) Selective release of glutamate from cerebellar granule cells differentiating in culture. *Proc. Natl. Acad. Sci.* 79, 7919-7923.

Gasic-Milenkovic J., Dukic-Stefanovic S., Deuther-Conrad W., Gartner U., Munch G. (2003) β-amyloid peptide potentiates inflammatory responses induced by lipopolysaccharide, interferon-γ and 'advanced glycation endproducts' in a murine microglial cell line. *Eur. J. Neurosci.* 17, 813-821.

Gay D., Esiri M. (1991) Blood-brain barrier damage in acute multiple sclerosis plaques. An immunocytological study. *Brain.* 114, 557-572.

Gehrmann J., Banati R. B., Wiessner C., Hossmann K. A., Kreutzberg G. W. (1995) Reactive microglia in cerebral ischaemia: an earlier mediator of tissue damage. *Neuropathol. Appl. Neurobiol.* 21, 277-289.

Ghiso J., Frangione B. (2001) Cerebral amyloidosis, amyloid angiopathy and their relationship to stroke and dementia. *J. Alzheim. Dis.* 3, 65-73.

Goate A., Chartier-Harlin M., Mullan M., Brown J., Crawford F., Fidani L., Giuffra L., Haynes A., Irving N., James L., Mant R., Newton P., Rooke K., Roques P., Talbot C., Pericak-Vance M., Roses A., Williamson A., Rossor M., Owen M., Hardy J. (1991) Segregation of a missense mutation in the amyloid precursor protein gene with familal Alzheimer's disease. *Nature.* 349, 704-706.

Goedart M. (1993) Tau protein and the neurofibrillary pathology of Alzheimer's disease. *Trends Neurol. Sci.* 16, 460-465.

Goldberg M. P., Choi D. W. (1993) Combined oxygen and glucose deprivation in cortical cell culture: calcium dependent and calcium independent mechanisms of neuronal injury. *J. Neurosci.* 13, 3510-3524.

Goldsby R. A., Kindt T. J., Osborne B. A. (2001) Immunology. Fourth Edition. W. H. Freeman and Company. New York. USA.

Goldstein J. L., Ho Y. K., Basu S. K., Brown M. S. (1979) Binding site on macrophages that mediates uptake and degradation of acetylated low density lipoprotein, producing massive cholesterol deposition. *Proc. Natl. Acad. Sci.* 76, 333-337.

Goodwin J. L., Uemura E., Cunnick J. E. (1995) Microglial release of nitric oxide by the synergistic action of β-amyloid and IFN-γ. *Brain Res.* 692, 207-214.

Graeber M. B., Streit W. J., Kreutzberg G. W. (1988a) The microglial cytoskeleton: vimentin is localised within activated cells *in situ*. *J. Neurocytol.* 17, 573-580.

Graeber M. B., Streit W. J., Kreutzberg G. W. (1988b) Axotomy of the rat facial nerve leads to increased CR3 complement receptor expression by activated microglial cells *J. Neurosci. Res.* 21, 18-24.

Graeber M. B., Tetzlaff W., Streit W. J., Kreutzberg G. W. (1988c) Microglial cells but not astrocytes undergo mitosis following rat facial nerve axotomy. *Neurosci. Lett.* 85, 317-321.

Graeber M. B., Banati R. B., Streit W. J., Kreutzberg G. W. (1989) Immunophenotypic characterisation of rat brain macrophages in culture. *Neurosci. Lett.* 103, 241-246.

Graeber M. B., Streit W. J., Kiefer R., Schoen S. W., Kreutzberg G. W. (1990) New expression of myelomonocytic antigens by microglia and perivascular cells following lethal motor neurone injury. *J. Neuroimmunol.* 27, 121-131.

Graf B., Bahler M., Hilpela P., Bowe C., Adam T. (2000) Functional role for the class IX myosin myr 5 in epithelial cell infection by *Shigella flexneri*. *Cell. Microbiol.* 2, 601-616.

Green D. R., Reed J. C. (1998) Mitochondria and apoptosis. *Science.* 281, 1309-1312.

Grell M., Douni E., Wajant H., Lohden M., Clauss M., Maxeiner B., Georgopoulos S., Lesslauer W., Kollias G., Pfizenmaier K. (1995) The transmembrane from of tumour necrosis factor is the prime activating ligand of the 80 kDa tumour necrosis factor receptor. *Cell.* 83, 793-802.

Guilian D. (1987) Amoeboid microglia as effectors of inflammation in the central nervous system. *J. Neurosci. Res.* 18, 155-171.

Guilian D., Baker T. J (1986) Characterisation of amoeboid microglia isolated from developing mammalian brain. *J. Neurosci.* 6, 2163-2178.

Guilian D., Robertson C. (1990) Inhibition of mononuclear phagocytes reduces ischaemic injury in the spinal cord. *Ann Neurol.* 27, 33-42.

Gurr M. (1993) Fats. In *'Human Nutrition and Dietetics (Ninth Edition)'*. Edited by Garrow J. S. James W. P. T. Churchill and Livingstone. Singapore.

Guyton A. C., Hall J. E. (1996) *Text Book of Medical Physiology.* W. B. Saunders Company. Philadelphia, USA.

Haga S., Akai K., Ishii T. (1989) Demonstration of microglial cells in and around senile (neuritic) plaques in Alzheimer's brain. *Acta. Neuropathol.* 77, 569-575.

Hagemann C., Blank J. L. (2001) The ups and downs of MEK kinase interactions. *Cell. Sig.* 13, 863-875.

Hallet M. B., Hodges R., Cadman M., Blanchfield H., Dewitt S., Pettit E., Laffafian I., Davies E. V. (1999) Techniques for measuring and manipulating free Ca^{2+} in the cytosol and organelles of neutrophils. *J. Immunol. Meth.* 232, 77-88.

Hampton R. Y., Golenbock D. T., Penman M., Krieger M., Raetz C. R. (1991) Recognition and plasma clearance of endotoxin by scavenger receptors. *Nature.* 352, 342-344.

Hanke J. H., Gardner J. P., Dow R. L., Changelian P. S., Brissette W. H., Weringer E. J., Pollok B. A., Connelly P. A. (1996) Discovery of a novel, potent, and Src family selective tyrosine kinase inhibitor. *J. Biol. Chem.* 271, 695-701.

Hara H., Friedlander R. M., Gagliardini V., Ayata C., Fink K., Huang Z., Shimizu-Sasamata M., Yuan J., Moskowitz M. A. (1997) Inhibition of interleukin 1β converting enzyme family proteases reduces ischaemic and excitotoxic neuronal damage. *Proc. Natl. Acad. Sci.* 94, 2007-2012.

Hardy J. (1992) An 'anatomical cascade hypothesis' for Alzheimer's disease. *Trends Neurol. Sci.* 15, 200-201.

Hardy J., Allsop D. (1991) Amyloid deposition as the central event in the aetiology of Alzheimer's disease. *Trends Pharmacol. Sci.* 10, 383-388.

Hardy J. A., Higgins G. A. (1992) Alzheimer's disease the amyloid cascade hypothesis. *Science.* 256, 184-185.

Havenith C. E. G., Askew D., Walker W. S. (1998) Mouse resident microglia: Isolation and characterisation of immunoregulatory properties with naïve $CD4^+$ and $CD8^+$ T-cells. *Glia.* 22, 348-359.

Hayashi T., Sakurai M., Itoyama Y., Abe K. (1999) Oxidative damage and breakage of DNA in rat brain after transient MCA occlusion. *Brain Res.* 832, 159-163.

Head J. R., Griffin W. S. (1985) Functional capacity of solid tissue transplants in the brain: evidence for immunological privilege. *Proc. R. Soc. Lond. B. Biol. Sci.* 224, 375-387.

Heales S. J. R., Bolãnos J. P. (2002) Impairment of brain mitochondrial function by reactive nitrogen species: the role of glutathione in dictating susceptibility. *Neurochem. Intern.* 40, 469-474.

Heemskerk J. W. M., Farndale R. W., Sage S. O. (1997) Effects of U73122 on human platelet calcium signalling and protein tyrosine phosphorylation. *Biochem. Biophys. Acta.* 1355, 81-88.

Hellendall R. P., Ting J. P. Y. (1997) Differential regulation of cytokine induced major histocompatibility complex class II expression and nitric oxide release in rat microglia and astrocytes by effectors of tyrosine kinase, protein kinase c, and cAMP. *J. Neuroimmunol.* 74, 19-29.

Hendriks L., van Duijn C. M., Cras P., Cruts W., van Hul W., van Harskamp F., Warren A., McInnis M., Antonarakis S. E., Martin J. J., Hofman A., van Broeckhoven C. (1992) Presenile dementia and cerebral haemorrhage linked to a mutation at codon 692 of the β amyloid precursor protein gene. *Nat. Genet.* 1, 218-221.

Hengartner M. O. (2000) The biochemistry of apoptosis. *Nature.* 407, 770-776.

Henzi V., MacDermott A. B. (1992) Characteristics and functions of Ca^{2+} and inositol 1, 4, 5 triphosphate releasable stores of calcium in neurones. *Neurosci.* 46, 251-273.

Heron A., Pollard F., Dessi J., Moreau F., lasbennes Y., Ben-Ari Y., Charriaut-Marlangue C. (1993) Regional variability in DNA fragmentation after global ischaemia evidence by combined histological and gel electrophoresis observations in the rat brain. *J. Neurochem.* 61, 1973-1976.

Hickey W. F., Kimura H. (1988) Perivascular microglial cells of the CNS are bone marrow derived and present antigen *in vivo*. *Science.* 239, 290-292.

Hide I., Tanaka M., Inoue A., Nakajima K., Kohsaka S., Inoue K., Nakata Y. (2000) Extracellular ATP triggers tumour necrosis factor α release from rat microglia. *J. Neurochem.* 75, 965-972.

Hinz B., Brune K. (2001) Cyclooxygenase 2-10 years later. *J. Pharmacol. Exp. Therap.* 300, 367-375.

Hoffmann A., Kann O., Ohlemeyer C., Hanisch U. K., Kettenmann H. (2003) Elevation of basal intracellular calcium as a central element in the activation of brain macrophages (microglia): suppression of receptor evoked calcium signalling and control of release function. *J. Neurosci.* 23, 4410-4419.

Holgate S. T., Church M. K. (1995) Allergy. Mosby-Wolf. London, UK.

Hollmann M., Hartley M., Heinemann S. (1991) Ca^{2+} permeability of KA/AMPA gated glutamate receptor channels depends on subunit composition. *Science*. 252, 851-853.

Honda M., Akiyama H., Yamada Y., Kondo H., Kawabe Y., Takeya M., Takahashi K., Suzuki H., Doi T., Sakamoto A., Ookawara S., Mato M., Gough P. J., Greaves D. R., Gordon S., Kodama T., Matsushita M. (1998) Immunohistochemical evidence for a macrophage scavenger receptor in Mato cells and reactive microglia of ischaemia and Alzheimer's disease. *Biochem. Biophys. Res. Comm.* 245, 734-740.

Honda S., Sasaki Y., Ohsawa K., Imai Y., Nakamura Y., Inoue K., Kohsaka S. (2001) Extracellular ATP or ADP induce chemotaxis of cultured microglia through $G_{i/o}$ coupled P2Y receptors. *J. Neurosci.* 21, 1975-1982.

Honig L. S., Rosenberg R. N. (2000) Apoptosis and neurologic disease. *Am. J. Med.* 108, 317-330.

Horner C. H., Davies H. A., Stewart M. G. (1998) Hippocampal synaptic density and glutamate immunoreactivity following transient cerebral ischaemia in the chick. *Eur. J. Neurosci.* 10, 3913-3917.

Hornig C. R., Busse O., Domdorf W., Kaps M. (1983) Changes in CSF blood brain barrier parameters in ischaemic cerebral infarction. *J. Neurol.* 229, 11-16.

Hortleno S., Dallaporta B., Zamzami N., Hirsch T., Susin S. A., Marzo I., Bosca L., Kroemer G. (1997) Nitric oxide induces apoptosis via triggering mitochondrial permeability transition. *FEBS Lett.* 410, 373-377.

Hunter K. E., Sporn M. B., Davies A. M. (1993) Transforming growth factor-βs inhibit mitogen stimulated proliferation of astrocytes. *Glia*. 7, 203-211.

Husemann J., Loike J. D., Kodama T., Siverstein S. C. (2001) Scavenger receptor class B type 1 (SR-B1) mediates adhesion of neonatal murine microglia to fibrillar β-amyloid. *J. Neuroimmunol.* 114, 142-150.

Igishi T., Gutkind J. S. (1998) Tyrosine kinases of the Src family participate in signalling to MAP kinase from both G_q and G_i coupled receptors. *Biochem. Biophys. Res. Com.* 244, 5-10.

Imagawa T., Smith J. S., Coronado R., Campbell K. P. (1987) Purified ryanodine receptor from skeletal muscle sarcoplasmic reticulum is the Ca^{2+} permeable pore of the calcium release channel. *J. Biol. Chem.* 262, 16636-16643.

Innocenti G. M., Clarke S., Koppell H. (1983) Transitory macrophages in the white matter of the developing visual cortex. II. Development and relations with axonal pathways. *Dev. Brain Res.* 11, 55-66.

Iqbal K., Zaidi T., Bancher C., Grundke-Iqbal I. (1994) Alzheimer's paired helical filaments. *FEBS Lett.* 349, 104-108.

Irvins K. J., Thornton P. L., Troy T. T. (1999) Neuronal apoptosis induce by β amyloid is mediated by caspase 8. *Neurobiol. Dis.* 6, 440-449

Ischiropoulos H., Zhu L., Beckman J. S. (1992) Peroxynitrite formation from macrophage derived nitric oxide. *Arch. Biochem. Biophys.* 298, 446-451.

Ishizuka J., Asada I., Poston G. J., Luis F., Tatemoto K., Greeley G. H., Thompson J. C. (1989) Effect of pancreastatin on pancreatic endocrine and exocrine secretion. *Pancreas.* 4, 277-281.

Itagaki S., McGeer P. L., Akiyama H., Zhu S., Selkoe D. (1989). Relationship of microglia and astrocytes to amyloid deposits of Alzheimer's disease. *J. Neuroimmunol.* 24, 173-182.

Jacobson M. (1991) Developmental Neurobiology. Third Edition. Plenum Press. New York, USA.

Jones K. H., Senft J. A. (1985) An improved method to determine cell viability by simultaneous staining with fluorescein diacetate and propidium iodide. *J. Histochem. Cytochem.* 33, 77-79.

Jones L. L., Kreutzberg G. W., Raivich G. (1998) Transforming growth factor β 1, 2, and 3 inhibit proliferation of ramified microglia on an astrocyte monolayer. *Brain Res.* 795, 301-306.

Jones L. L., Banati R. B., Graeber M. B., Bonfanti L., Raivich G., Kreutzberg G. W. (1997) Population control of microglia: does apoptosis play a role. *J. Neurocytol.* 26, 755-770.

Jordon F. L., Thomas E. W. (1988) Brain macrophages: questions of origin and interrelationship. *Brain Res. Rev.* 13, 165-178.

Justica C., Perez-Asensio F. J., Burguete M. C., Salom J. B., Planas A, M. (2001) Administration of transforming growth factor-α reduces infarct volume after transient focal ischaemia in the rat. *J. Cereb. Blood Flow Metab.* 21, 1097-1104.

Kalaria R. N. (2002) Similarities between Alzheimer's disease and vascular dementia. *J. Neurol. Sci.* 203, 29-34.

Kalaria R. N., Premkumar D. R. D., Pax A. B., Cohen D. L., Lieberburg I. (1996) Production and increased detection of amyloid β protein and amyloidogenic fragments in brain microvessels, meningeal vessels and choroid plexus in Alzheimer's disease. *Mol. Brain Res.* 35, 58-68.

Kalhammer G., Bahler M., Schmitz F., Jockel J., Block C. (1997) Ras-binding domains: predicted function versus folding. *FEBS Lett.* 414, 599-602.

Kang J., Lemaire H. G., Unterbeck A., Salbaum J. M., Masters C. L., Grzeschik K. H., Multhaup G., Beyreuther K., Muller-Hill B. (1987) The precursor of Alzheimer's disease amyloid A4 protein resembles a cell surface receptor. *Nature.* 325, 733-736.

Kato H., Walz W. (2000) The initiation of the microglial response. ***Brain Pathol.*** 10, 137-143.

Kato H., Kogure K., Araki T., Itoyama Y. (1995) Graded expression of immunomolecues on activated microglia in the hippocampus following ischaemia in a rat model of ischaemic tolerance. *Brain Res.* 694, 85-93.

Kato H., Kogure K., Liu X., Araki T., Itoyama Y. (1996) Progressive expression of immunomolecules on activated microglia and invading leucocytes following focal cerebral ischaemia in the rat. *Brain Res.* 734, 203-212.

Katsumori H., Baldwin R. A., Wasterlain C. G. (1999) Reverse transport of glutamate during depolarisation in immature hippocampal slices. *Brain Res.* 819, 160-164.

Keflas P., Brown R. P., Brockell P. M. (1995) Signalling by $p60^{c\text{-}src}$ family of protein tyrosine kinases. *J. Biochem. Cell Biol.* 27, 551-563.

Kelton J. G., Stiller U. R., Holmes E. (1978) Comparison of chemical composition of peritoneal fluid and serum: a method for monitoring dialysis patients and a tool for assessing binding to serum proteins *in vivo*. *Ann. Intern. Med.* 89, 67-70.

Kiernan J. A. (1998) Barr's: *The Human Nervous System: An Anatomical Viewpoint (7th Edition).* Lippicott-Raven. Philadelphia, USA.

Kim H. S., Lee S. H., Kim S. S., Kim Y. K., Jeong S. J., Ma J., Han D. H., Cho B. K., Suh Y. H. (1998) Post-ischaemic changes in the expression of Alzheimer's APP isoforms in rat cerebral cortex. *Neuroreport.* 9, 533-537.

Kim J. M., Kim J. S., Jung H. C., Oh Y. K., Chung H. Y., Lee C. H., Song I. S. (2003) Helicobacter pylori infection activates NF kappa B signalling pathway to induce iNOS and protect human gastric epithelial cells from apoptosis. *Am. J. Physiol. Gastrointest. Liver Physiol.* (*Epub ahead of print*).

Kim M. J., Kim E., Ryu S. H., Suh P. (2000) The mechanism of phospholipase C γ1 regulation. *Exp. Mol. Med.* 32, 101-109.

Kimelberg H. K., Katz D. M. (1985) High-affinity uptake of serotonin into immunocytochemically identified astrocytes. *Science.* 228, 889-891.

Kimelberg H. K., Norenberg M. D. (1989) Astrocytes. *Sci. Am.* 260, 44-52.

Kingham P. J., Pocock J. M. (2000) Microglial apoptosis induced by chromogranin A is mediated by a mitochondrial depolarisation and the permeability transition but not by cytochrome c release. *J. Neurochem.* 74, 1452-1462.

Kingham P. J., Pocock J. M. (2001) Microglial secreted cathepsin B induces neuronal apoptosis. *J. Neurochem.* 76, 1475-1484.

Kingham P. J., Cuzner M. L., Pocock J. M. (1999) Apoptotic pathways mobilized in microglia and neurones as a consequence of chromogranin A-induced microglial activation. *J. Neurochem.* 73, 538-547.

Kitamura T., Miyake T., Fujita S. (1984) Genesis of resting microglia in the gray matter of mouse hippocampus. *J. Comp. Neurol.* 226, 421-433.

Klegaris A., McGeer P. L. (1997) β-amyloid protein enhances macrophage production of oxygen free radicals and glutamate. *J. Neurosci. Res.* 49, 229-235.

Klegaris A., Walker D. G., McGeer P. L. (1997) Interaction of Alzheimer's β-amyloid peptide with the human monocytic cell line THP-1 results in a protein kinase C dependent secretion of tumour necrosis factor α. *Brain Res.* 747, 114-121.

Koide M., Kawahara Y., Tsudda T., Yokoyama M. (1993) Cytokine induced expression of inducible type of nitric oxide synthase gene in cultured vascular smooth muscle cells. *FEBS Lett.* 318, 213-217.

Kokmen E., Whisnant J. P., O'Fallon W. M., Chu C. P., Beard C. M. (1996) Dementia after ischaemic stroke. *Neurol.* 46, 154-159.

Kolata G. (1985) Down-syndrome – Alzheimer's linked. *Science.* 230, 1152-1153.

Kontos H. A., Wei E. P., Povilishock J. T., Dalton W., Magiera C. J. (1980) Cerebral arteriolar damage by arachidonic acid and prostaglandin G_2. *Science*. 209, 1242-1244.

Kopec K. K., Carroll R. T. (1998) Alzheimer's β-amyloid peptide 1-42 induces a phagocytic response in murine microglia. *J. Neurochem*. 71, 2123-2131.

Korbo L., Anderson B. B., Ladefoged O., Möller A. (1993) Total numbers of various cell types in rat cerebellar cortex estimated using an unbiased steriological method. *Brain Res*. 609, 262-268.

Korotzer A. R., Pike C. J., Cotman C. W. (1993) β-Amyloid peptides induce degeneration of cultured rat microglia. *Brain Res*. 624, 121-125.

Korotzer A. R., Whittemore E. R., Cotman C. W. (1995) Differential regulation of beta-amyloid peptides of intracellular free Ca^{2+} concentration in cultured rat microglia. *Eur. J. Pharmacol*. 288, 125-130.

Kreutzberg G. W. (1996) Microglia: a sensor for pathological events in the CNS. *Trends Neurosci*. 19, 312-318.

Krieger M. (1992) Molecular flypaper and atherosclerosis: structure of the macrophage scavenger receptor. *Trends Biochem*. 17, 141-146.

Kristof A. S., Marks-Konczalik J., Moss J. (2001) Mitogen-activated protein kinases mediate activator protein-1-dependent human inducible nitric oxide synthase promoter activation. *J. Biol. Chem*. 11, 8445-8452.

Kroemer G., Dallaporta B., Resche-Rignon M. (1998) The mitochondrial death/life regulator in apoptosis and necrosis. *Ann. Rev. Physiol*. 60, 619-642.

Kulkarni A. B., Huh C. G., Becker D., Geiser A., Lyght M., Flanders K. C., Roberts A. B., Sporn M. B., Ward J. M., Kaelsson S. (1993) Transforming growth factor β1 null mutation in mice causes excessive inflammatory responses and early death. *Proc. Natl. Acad. Sci*. 90, 770-774.

Kulkarni S. K., Sharma A. C. (1993) Nitric oxide: a new generation of neurotransmitter. *Indian J. Pharmacol*. 25, 12-17.

Kumar K., Evans A T. (1997) Effect of hypothermia on microglial reaction in ischaemic brain. *Neuroreport*. 8, 947-950.

Ladner C., Lee J. M. (1998) Pharmacological drug treatment of Alzheimer's disease. The cholinergic hypothesis revisited. *J. Neuropathol. Exp. Neurol*. 57, 719-731.

Lammich S., Kojro E., Postina R., Gilbert S., Pfeiffer R., Jasionowski M., Haass C., Fahrenholz F. (1999) Constitutive and regulated alpha-secretase cleavage of Alzheimer's amyloid precursor protein by a disintegrin metalloprotease. *Proc. Natl. Acad. Sci.* 96, 3922-3927.

Lassmann H., Bancher C., Breitschopf H., Wegiel J., Bobinski M., Jellinger K., Wisniewski H. M. (1995) Cell death in Alzheimer's disease evaluated by DNA fragmentation *in situ*. *Acta. Neuropathol.* 89, 35-41.

Lavigne M. C., Malech H. L., Holland S. M., Leto T. L. (2001) Genetic requirement of p47*phox* for superoxide production by murine microglia. *FASEB J.* 15, 285-297.

Lawson L. J., Perry V. H., Gordon S. (1992) Turnover of resident microglia in the normal adult mouse brain. *Neurosci.* 48, 405-415.

Le Y., Gong W., Tiffany L., Tumanov A., Nedospasov S., Shen W., Dunlop N. M., Gao J. L., Murphy P. M., Oppenheim J. J., Wang J. M. (2001) Amyloid β42 activates a G protein coupled chemoattractant receptor, FPR-like 1. *J. Neurosci.* 21, 1-5.

Lees G. J. (1993) The possible contribution of microglia and macrophages to delayed neuronal death after ischaemia. *J. Neurol. Sci.* 114, 119-122.

Lehrmann E., Kiefer R., Christensen T., Tokya K. V., Zimmer J., Diemer N. H., Hartung H. P., Finsen B. (1998) Microglia and macrophages are major sources of locally produced transforming growth factor beta-1 after transient middle cerebral artery occlusion in rats. *Glia.* 24, 437-448.

Leuson J. H. W., Verhoeven A. J., Roos D. (1996) Interactions between the components of the human NADPH oxidase: a review about the intrigues in the *phox* family. *Front. Biosci.* 1, 72-90.

Levy E., Carman M. D., Fernandez-Madrid I. J., Power M. D., Lieberburg I., van Duinen S. G., Bots G. T A. M., Luyendijk W., Frangione B. (1990) Mutation of the Alzheimer's disease amyloid gene in hereditary cerebral haemorrhage, Dutch type. *Science.* 248, 1124-1126.

Li M., Sunamoto M., Ohnishi K., Ichimori Y. (1996) β-amyloid protein-dependent nitric oxide production from microglial cells and neurotoxicity. *Brain Res.* 720, 93-100.

Li Y. M., Tan A. X., Vlassara H. (1995) Antibacterial activity of lysozyme and lactoferrin is inhibited by binding of advanced glycation modified proteins to a conserved motif. *Nat. Med.* 1, 1057-1061.

Li T., Ma G., Cai H., Price D. L., Wong P. C. (2003) Nicastrin is required for assembly of presenilin/gamma secretase complexes to mediate notch signalling and for processing and trafficking of beta-amyloid precursor protein in mammals. *J. Neurosci.* 23, 3272-3277.

Lindholm D., Castren E., Kiefer R., Zafra F., Thoenen H. (1992) Transforming growth factor β in the rat brain: increases after injury and inhibition of astrocyte proliferation. *J. Cell Biol.* 117, 395-400.

Ling E. A. (1979) Transformation of monocytes into amoeboid microglia and into microglia in the corpus callosum of postnatal rats, as shown by labelling monocytes by carbon particles. *J. Anat.* 128, 847-858.

Ling E. A., Penney D., Lebond C. P. (1980) Use of carbon labelling to demonstrate the role of blood monocytes as precursors of the 'amoeboid cells' present in the corpus collosum of postnatal rats. *J. Comp. Neurol.* 193, 631-657.

Ling E. M., Robinson D. S. (2002) Transforming growth factor β1: its anti-inflammatory and pro-fibrotic effects. *Clin. Exp. All.* 32, 175-178.

Liu B., Wang K., Gao H. M., Mandavilli B., Wang J. Y., Hong J. S. (2001) Molecular consequences of activated microglia in the brain: overactivation induces apoptosis. *J. Neurochem.* 77, 182-189.

Loo D. T., Copani A., Pike C., Whittemore E. R., Walencewicz A. C., Cotman C. W. (1993) Apoptosis is induced by β amyloid in cultured central nervous system neurons. *Proc. Natl. Acad. Sci.* 90, 7951-7955.

Lu D. C., Rabizadeh S., Chandra S., Shayya R. F., Ellerby L. M., Ye X., Salvesen G. S., Koo E. H., Bredesen D. E. (2000) A second cytotoxic proteolytic peptide derived from amyloid β protein precursor. *Nat. Med.* 6, 397-404.

Luyendijk W., Bots G. T., Vegter-van der Vlis M., Went L. N., Frangione B. (1988) Hereditary cerebral haemorrhage caused by cortical amyloid angiopathy. *J. Neurol. Sci.* 85, 267-280.

Lynch D. R., Guttmann R. P. (2002) Excitotoxicity: Perspectives based on N-Methyl-D-Aspartate receptor subtypes. J. *Pharmacol. Exp. Therap.* 300, 717-723.

Lyons R. M., Gentry L. E., Purchio A. F., Moses H. L. (1990) Mechanism of activation of latent recombinant transforming growth factor beta by plasmin. *J. Cell Biol.* 110, 1361-1367.

Lyons S. A., Kettenmann H. (1998) Oligodendrocytes and microglia are selectively vulnerable to combined hypoxia and hypoglycemia injury *in vitro*. *J. Cereb. Blood Flow Met.* 18, 521-530.

McDonald D. R., Brunden K. R., Landreth G. E. (1997) Amyloid fibrils activate tyrosine kinase dependent signalling and superoxide production in microglia. *J. Neurosci.* 17, 2284-2294.

McDonald D. R., Bamberger M. E., Combs C. K., Landreth G. E. (1998) β-amyloid fibrils activate parallel mitogen activated protein kinase pathways in microglia and THP-1 monocytes. *J. Neurosci.* 18, 4451-4460.

McGeer E. G., McGeer P. L. (1997) Innate inflammatory reaction of the brain in Alzheimer disease. *McGill J. Med.* 3, 134-141.

McGeer E. G., McGeer P. L. (1999) Inflammation in the brain in Alzheimer's disease: implications for therapy. *J. Leukocyte Biol.* 65, 409-415.

McGeer P. L., Schulzer M., McGeer E. G. (1996) Arthritis and anti-inflammatory agents as possible protective factors for Alzheimer's disease: A review of 17 epidemiological studies. *Neurol.* 48, 1473-1474.

Ma C. Y., Huang J., Ali S., Lowry W., Huang W. Y. (2000) Src tyrosine kinase is a novel direct effector of G proteins. *Cell.* 102, 635-646.

Mackenzie I. R. A., Munoz D. G. (1998) Nonsteroidal anti-inflammatory drug use and Alzheimer type pathology in aging. *Neurol.* 50, 986-990.

Madureira S., Guerreiro M., Ferro J. M. (2001) Dementia and cognitive impairment three months after stroke. *Eur. J. Neurol.* 8, 621-627.

Magistretti P. J., Pellerin L., Rothman D. L., Shulman R. G. (1999) Energy on demand. *Science.* 283, 496-497.

Mahata S. K., O'Connor D. T., Mahata M., Yoo S. H., Taupenot L., Wu H., Gill B. M., Parmer R. J. (1997) Novel Autocrine Feedback Control of Catecholamine Release. A discrete chromogranin A fragment is a noncompetitive nicotinic cholinergic antagonist. *J. Clin. Invest.* 100, 1623-1633.

March C. J., Mosley B., Larsen A., Cerretti D. P., Braedt G., Price V., Gillis S., Henney C. S., Kronheim S. R., Grabstein K., Conlon P. J., Hopp T. P., Cosman D. (1985) Cloning, sequencing and expression of two distinct human interleukin 1 complementary DNAs. *Nature.* 315, 641-646.

Marin N., Romero B., Bosch-Morell F., Llansola M., Felipo V., Roma J., Romero F. J. (2000) β-amyloid induced activation of caspase 3 in primary cultures of rat neurones. *Mech. Ageing Develop.* 119, 63-67.

Marsden C. D., Fowler T. J. (1998) *Clinical Neurology.* Second Edition. Arnold Publishers. London, UK.

Marzolo M. P., Bernhardi R. V., Inestrosa N. C. (1999) Mannose receptor is present in a functional state in rat microglial cells. *J. Neurosci. Res.* 58, 387-395.

Matyszak M. K., Perry V. H. (1998) Bacillus Calmette-Guerin sequestered in the brain parenchyma escapes immune recognition. *J. Neuroimmunol.* 82, 73-80.

Meda L., Cassatella M. A., Szendrei G. I., Otvos Jr L., Baron P., Villalba M., Ferrari D., Rossi F. (1995) Activation of microglial cells by β-amyloid protein and interferon γ. *Nature.* 374, 647-650.

Meda L., Baron P., Prat E., Scarpini E., Scarlato G., Cassatella M. A., Rossi F. (1999) Proinflammatory profile of cytokine production by human monocytes and murine microglia stimulated with beta-amyloid [25-35]. *J. Neuroimmunol.* 93, 45-52.

Melillo G., Musso T., Sica A., Taylor L. S., Cox G. W., Varesio L. (1995) A hypoxia responsive element mediates a novel pathway of activation of the inducible nitric oxide synthase promoter. *J. Exp. Med.* 182, 1683-1693.

Mermall V., Post P. L., Mooseker M. S. (2000) Unconventional myosin in cell movement, membrane traffic and signal transduction. *Science.* 279, 527-533.

Messmer U. K., Reimer D. M., Brune B. (1998) Protease activation during nitric oxide induced apoptosis: comparison between poly ADP-ribose- polymerase and U1-70 kDa cleavage. *Eur. J. Pharmacol.* 349, 333-343.

Miguel-Hidalgo J. J., Alvarez X. A., Cacabelos R., Quack G. (2002) Neuroprotection by memantine against neurodegeneration induced by β amyloid (1-40). *Brain Res.* 958, 210-221.

Miki S., Tsukada S., Nakamura Y., Aimoto S., Hojo H., Sato B., Yamamoto M., Miki Y. (1996) Functional and possible physical association of scavenger receptors with cytoplasmic tyrosine kinase Lyn in monocytic THP-1-derived macrophages. *FEBS Lett.* 399, 241-244.

Ming Y., Mitsuhashi T., Wojciechowicz D., Shimizu N., Li J., Stito A., He C., Banerjee D., Vlassara H. (1996) Molecular identity and cellular distribution of advanced glycation endproduct receptors: Relationship of p60 to OST-48 and p90 to 80K-H membrane proteins. *Proc. Natl. Acad. Sci.* 93, 11047-11052.

Minghetti L., Levi G. (1995) Induction of prostanoid biosynthesis by bacterial lipopolysaccharide and isoproterenol in rat microglial cultures. *J. Neurochem.* 65, 2690-2698.

Minshall R D., Tiruppathi C., Vogel S. M., Niles W. D., Gilchrist A., Hamm H. E., Malik A. B. (2000) Endothelial cell surface gp60 activates vesicle formation and trafficking via G_i coupled Src kinase signalling pathway. *J. Cell Biol.* 150, 1057-1069.

Modi W. S., Levine M. A., Seuanez H. N., Dean M., O'Brien S. J. (1989) The human chromogranin A gene: chromosome assignment and RFLP analysis. *Am. J. Hum. Genet.* 45, 814-918.

Möller T, Nolte C., Burger R., Verhratsky A., Kettenmann H. (1997) Mechanisms of C5a and C3a complement fragment induced $[Ca^{2+}]_i$ signalling in mouse microglia. *J. Neurosci.* 17, 615-624.

Möller T., Hanisch U., Ransom B. R. (2000a) Thrombin induced activation of cultured rodent microglia. *J. Neurochem.* 75, 1539-1547.

Möller T., Kann O., Verkhratsky A., Kettenmann H. (2000b) Activation of mouse microglial cells affects P2 receptor signalling. *Brain Res.* 853, 49-59.

Möller T, Contos J. J., Musante D. B., Chun J., Ransom B. J. (2001) Expression and function of lysophosphatidic acid receptors in cultured rodent microglial cells. *J. Biol. Chem.* 276, 25946-25952.

Moncada S., Higgs A. (1993) Mechanisms of disease. *New Eng. J. Med.* 329, 2003-2012.

Moore K. J., El Khoury J., Medeiros L. A., Terada K., Geula C., Luster A. D., Freeman M. W. (2002) A CD36 initiated signalling cascade mediates inflammatory effects of β-amyloid. *J. Biol. Chem.* 277, 47373-47379.

Morioka T., Kalehua A. N., Streit W. J. (1991) The microglial reaction in the rat dorsal hippocampus following transient forebrain ischaemia. *J. Cereb. Blood Flow Metab.* 11, 966-973.

Moroney J. T., Bagiella E., Desmond D. W., Paik M. C., Stern Y., Tatemichi T. K. (1996) Risk factors for incident dementia after stroke. *Stroke.* 27, 1283-1289.

Moustakas A., Souchelnytskyi S., Heldin C. H. (2001) Smad regulation in TGFβ signal transduction. *J. Cell Sci.* 114, 4359-4369.

Mukaida N., Matsumoto T., Yokoi K., Matsushima K. (1998) Inhibition of neutrophil mediated acute inflammatory injury by an antibody against interleukin-8 (IL8) *Inflamm. Res.* 47, 151-157.

Mullan M., Crawford F., Axelam K., Houlden H., Lilius L., Winblad B., Lannfelt L. (1992) A pathogenic mutation for probable Alzheimer's disease in the APP gene at the N-terminus of β-amyloid. *Nat. Gen.* 1, 345-347.

Müller R. T., Honnert U., Reinhard J., Bähler M. (1997) The rat myr 5 is a GTPase activating protein for rho *in vivo*: Essential role of arginine 1695. *Mol. Biol. Cell.* 8, 2039-2053.

Munoz D. G. (1991) Chromogranin A like immunoreactive neurites are major constituents of senile plaques. *Lab. Invest.* 64, 826-832.

Murabe Y., Sano Y. (1981a) Morphological studies on neuroglia. *Cell Tissue Res.* 216, 569-580.

Murabe Y., Sano Y. (1981b) Thiaminepyrophosphatase activity in the plasma membrane of microglia. *Histochem.* 71, 45-52.

Murayama O., Tomita T., Nihonmatsu N., Murayama M., Sun X., Honda T., Iwatsubo T., Takashima A. (1999) Enhancement of amyloid β 42 secretion by 28 different presenilin 1 mutations of familial Alzheimer's disease. *Neurosci. Lett.* 265, 61-63.

Murphy Jr. G. M., Yang L., Cordell B. (1998) Macrophage colony stimulating factor augments β-amyloid induced interleukin 1, interleukin 6 and nitric oxide production by microglial cells. *J. Biol. Chem.* 273, 20967-20971.

Murphy S. (2000) Production of nitric oxide by glial cells: regulation and potential roles in the CNS. *Glia.* 29, 1-14.

Murray J., Taylor S. W., Zhang B., Ghosh S. S., Capaldi R. A. (2003) Oxidative damage to mitochondrial complex I due to peroxynitrite; identification of reactive tyrosines by mass spectrometry. *J. Biol. Chem. (E-pub ahead of print).*

Nadal A., Fuentes E., Pastor J., McNaughton P. A. (1995) Plasma albumin is a potent trigger of calcium signals and DNA synthesis in astrocytes. *Proc. Natl. Acad. Sci.* 92, 1426-1430.

Nadal A., Fuentes E., McNaughton P. A. (1996) Albumin stimulates the uptake of calcium into subcellular stores in rat cortical astrocytes. *J. Physiol.* 492, 737-750.

Nadal A., Fuentes E., Pastor J., McNaughton P. A. (1997) Plasma albumin induced calcium waves in rat cortical astrocytes. *Glia.* 19, 343-351.

Nadal A., Fuentes E., McNaughton P. A. (2001) Glial responses to lipids bound to albumin in serum and plasma. *In Glial Cell Function: Progress in Brain Research 132.* Edited by Castellano-Lopez B., Nieto-Sampedro M. Elsevier. The Netherlands.

Nagai A., Nakagawa E., Hatori K., Choi H. B., McLarnon J. G., Lee M. A., Kim S. U. (2001) Generation and characterisation of immortalised human microglial cell lines: Expression of cytokines and chemokines. *Neurobiol. Dis.* 8, 1057-1068.

Nagy Z (2000) Cell cycle regulatory failure in neurones: causes and consequences. *Neurobiol. Aging.* 21, 761-769.

Nakagawa T., Zhu H., Morishima N., Li E., Xu J., Yanker B. A., Yuan J. (2000) Caspase 12 mediates endoplasmic reticulum specific apoptosis and cytotoxicity by amyloid β. *Nature.* 403, 98-103.

Nakai M., Hojo K., Taniguchi T, Terashima A., Kawamata T., Hashimoto T., Maeda K., Tanaka C. (1998) PKC and tyrosine kinase involvement in amyloid β (25-35) induced chemotaxis of microglia. *Neuroreport.* 9, 3467-3470.

Nakajima K., Tohyama Y., Kohsaka S., Kurihara T. (2001) Ability of rat microglia to uptake extracellular glutamate. *Neurosci. Lett.* 307, 171-174.

Nakamura Y., Si Q. S., Takaku T., Kataoka K. (2000) Identification of a peptide sequence in albumin that potentiates superoxide production in microglia. *J. Neurochem.* 75, 2309-2315.

Nakamura Y., Ohmaki M., Murakami K., Yoneda Y. (2003) Involvement of protein kinase C in glutamate release from cultured microglia. *Brain Res.* 962, 122-128.

Namura S., Zhu J., Fink K., Endres M., Srinivasan A., Tomaselli K. J. Yuan J., Moskowitz M. A. (1998) Activation and cleavage of caspase 3 in apoptosis induced by experimental cerebral ischaemia. *J. Neurosci.* 18, 3659-3668.

Nathan C., Xie Q. W. (1994) Regulation of biosynthesis of nitric oxide. *J. Biol. Chem.* 269, 13725-13728.

Nawashiro H., Martin D., Hallenbach J. M. (1997) Neuroprotective effects of TNF binding protein in focal cerebral ischaemia. *Brain Res.* 778, 265-271.

Neeper M., Schmidt A. M., Brett J., Yan S. D., Wang F., Pan Y. C. E., Elliston K., Stern D., Shaw A. (1992) Cloning and expression of a cell surface receptor for advanced glycosylation end products of proteins. *J. Biol. Chem.* 267, 14998-15004.

Ni B., Wu X., Su Y., Stephenson D., Smalstig E. B., Clemens J., Paul S. M. (1998) Transient global forebrain ischaemia induces a prolonged expression of the caspase 3 mRNA in rat hippocampal CA1 pyramidal neurones. *J. Cereb. Blood Flow Metab.* 18, 248-256.

Nicholls D. G., Sihra T. S. (1986) Synaptosomes possess an excitatory pool of glutamate. *Nature*. 321, 772-723.

Nihashi T., Inao S., Kajita Y., Kawai T., Sugimoto T., Niwa M., Kabeya R., Hata N., Hayashi S., Yoshida J. (2001) Expression and distribution of beta amyloid precursor protein and beta amyloid peptide in reactive astrocytes after transient middle cerebral artery occlusion. *Acta. Neurochir*. 143, 287-295.

Nishimura M., Tomimoto H., Suenaga T., Nakamura S., Namba Y., Ikeda K., Akiguchi I., Kimura K. (1994) Synaptophysin and chromogranin A immunoreactivities of lewy bodies in Parkinson's disease brains. *Brain Res*. 634, 339-344.

Nolte C., Möller T., Walter T., Kettenmann H. (1996) Complement 5a controls motility of murine microglial cells *in vitro* via activation of an inhibitory G-protein and the rearrangement of the actin cytoskeleton. *Neuroscience*. 73, 1091-1107.

North R. A., Barnard E. A. (1997) Nucleotide receptors. *Curr. Opin. Neurobiol*. 7, 346-357.

Orlicek S. L., Hanke J. H., English B. K. (1999) The Src family selective tyrosine kinase inhibitor PP1 blocks LPS and IFN-gamma mediated TNF and iNOS production in murine macrophages. *Shock*. 5, 350-354.

Paresce D. M., Ghosh R. N., Maxfield F. R. (1996) Microglial cells internalise aggregates of the Alzheimer's disease amyloid β protein via a scavenger receptor. *Neuron*. 17, 553-565.

Paresce D. M., Chung H., Maxfield R. (1997) Slow degradation of aggregates of the Alzheimer's disease amyloid β protein by microglial cells. *J. Biol. Chem*. 272, 29390-29397.

Park S. Y., Lee H., Hur J., Kim S. Y., Kim H., Park J. H., Cha S., Kang S. S., Cho G. J., Choi W. S., Suk K. (2002) Hypoxia induces nitric oxide production in mouse microglia via p38 mitogen activated protein kinase pathway. *Mol. Brain Res*. 107, 9-16.

Parmentier S., Bohme G. A., Lerouet D., Damour D., Strutzmann J. M., Margaill I., Plotkine M. (1999) Selective inhibition of inducible nitric oxide synthase prevents ischaemic brain injury. *Brit. J. Pharmacol*. 1217, 546-552.

Patel R., Attur M. G., Dave M., Abramson S. B., Amin A. R. (1999) Regulation of cytosolic COX-2 and prostaglandin E2 production by nitric oxide in activate murine macrophages. *J. Immunol*. 162, 4191-4197.

Pawson T. (1995) Protein modules and signalling networks. *Nature*. 373, 573-580.

Pearce I. A., Cambray-Deakin M. A., Burgoyne R. D. (1987) Glutamate acting on NMDA receptors stimulates neurite outgrowth from cerebellar granule cells. *FEBS. Lett.* 223, 143-147.

Peiser L., Gordon S. (2001) The function of scavenger receptors expressed by macrophages and their role in the regulation of inflammation. *Microbes Infect.* 3, 149-159.

Pellegrini-Giampietro D. E., Zukin R. S., Bennett M. V. L., Cho S., Pulsinelli W. A. (1992) Switch in glutamate receptor gene expression in CA1 subfield of hippocampus following global ischaemia in rats. *Proc. Natl. Acad. Sci.* 89, 10499-10503.

Pennica D., Nedwin G. E., Hayflick J. S., Seeburg P. H., Derynck R., Palladino M. A., Kohr W. J., Aggarwal B. B., Goeddel D. V. (1984) Human tumour necrosis factor: precursor structure, expression and homology to lymphotoxin. *Nature.* 312, 724-728.

Perkinton M. S., Sihra T. S., Williams R. J. (1999) Ca^{2+} permeable AMPA receptors induce phosphorylation of cAMP response element-binding protein through a phosphatidylinositol 3-kinase dependent stimulation of the mitogen-activated protein kinase signalling cascade in neurones. *J. Neurosci.* 19, 5861-5874.

Perkinton M. S., James K. Ip., Wood G. L., Crossthwaite A. J., Williams R. J. (2002) Phosphatidylinositol 3-kinase signalling to MAP kinase (Erk1/2), Akt/PKB and CREB in striatal neurones. *J. Neurochem.* 80, 239-254.

Perry V. H. (1998) A revised view of the central nervous system microenvironment and major histocompatibility complex class 11 antigen presentation. *J. Neuroimmunol.* 90, 113-121.

Perry V. H. (2001) Microglia in the developing and mature central nervous system. In '*Glial cell development*'. Second edition. Edited by Jessen K. R., Richardson W. D. Oxford University Press, Oxford, UK.

Perry V. H., Gordon S. (1988) Macrophages and microglia in the nervous system. *Trends Neurosci.* 11, 273-277.

Perry V. H., Hume D. A., Gordon S. (1985) Immunohistochemical localization of macrophages and microglia in the adult and developing mouse brain. *Neurosci.* 15, 313-326.

Perry V. H., Anthony S. J., Brown H. C. (1997) The blood brain barrier and the inflammatory response. *Mol. Med. Tod.* 8, 335-341.

Piani D., Fontana A. (1994) Involvement of the cystine transport system xc in the macrophage induced glutamate dependent cytotoxicity to neurones. *J. Immunol.* 152, 3578-3585.

Pieser L., Gordon S. (2001) The function of scavenger receptors expressed by macrophages and their role in the regulation of inflammation. *Microb. Infect.* 3, 149-159.

Pike C. J., Burdick D., Walencewicz A. J., Glabe C. G., Cotman C. W. (1993) Neurodegeneration induced by β-amyloid peptide *in vitro*: the role of peptide assembly state. *J. Neurosci.* 13, 1676-1687.

Pinteaux E., Parker L. C., Rothwell N. J., Luheshi G. N. (2002) Expression of interleukin 1 receptors and their role in interleukin 1 actions in murine microglial cells. *J. Neurochem.* 83, 754-763.

Pitas R. E., Boyles J. K., Lee S. H., Foss D., Mahley R. W. (1987) Astrocytes synthesise apolipoprotein E containing lipoproteins. *Biochem. Biophys. Acta.* 917, 148-161.

Platt N., da Silva R. P., Gordon S. (1999) Class A scavenger receptors and the phagocytosis of apoptotic cells. *Immunol. Lett.* 65, 15-19.

Pocock J. M., Evans G. J. O. (2000) Single cell fluorescence imaging to investigate calcium signalling in primary cultured neurones. Calcium. In *'The Molecular Action of Calcium in Biology and Medicine'*. Edited by Pochet R., Donato R., Haiech J., Heizmann C., Gerke C. Kluwer Academic Publishers. The Netherlands.

Pocock J. M., Nicholls D. G. (1998) Exocytotic and nonexocytotic modes of glutamate release from cultured cerebellar granule cells during chemical ischaemia. *J. Neurochem.* 70, 806-813.

Pocock J. M., Cousin M. A., Parkin J., Nicholls D. G. (1995) Glutamate excytosis from cerebellar granule cells: the mechanism of a transition to an L-type Ca^{2+} channel coupling. *Neurosci.* 67, 595-607.

Pocock J.M., Liddle A. C., Hooper C., Taylor D. L., Davenport C. M., Morgan S. C. (2001). Activated microglia in Alzheimer's disease and stroke. Neuroinflammation – from bench to bedside. Ernst Schering Research Foundation. Edited by Kettenmann H., Burton G. A., Moenning U. J. Springer. Germany.

Pollaud-Cherion C., Vandaele J., Quartulli F., Seguelas M. H., Decerprit J., Pipy B. (1998) Involvement of calcium and arachidonate metabolism in acetylated low density lipoprotein stimulated tumour necrosis factor alpha production by rat peritoneal macrophages. *Eur. J. Biochem.* 253, 345-353.

Portugal J., Waring M. J. (1988) Assignment of DNA binding sites for 4,6-diamidine-2-phenylindole and bisbenzimide (Hoechst 33258). A comparative footprint study. *Biochim. Biophys. Acta.* 949, 158-168.

Possell H., Noack H., Putzke J., Wolf G., Sies H. (2000) Selective upregulation of inducible nitric oxide synthase (iNOS) by lipopolysaccharide (LPS) and cytokines in microglia: *in vitro* and *in vivo* studies. *Glia.* 32, 51-59.

Post P. L., Bokoch G. M., Mooseker M. S. (1998) Human myosin IXb is a mechanochemically active motor and a GAP for rho. *J. Cell. Sci.* 111, 941-950.

Post S. R., Gass C., Rice S., Nikolic D., Crump H., Post G. R. (2002) Class A scavenger receptors mediate cell adhesion via activation of $G_{i/o}$ and formation of focal adhesion complexes. *J. Lipid. Res.* 43, 1829-1836.

Pringle A. K., Iannotti F., Wilde G. J., Chad J. E., Seeley P. J., Sundstrom L. E. (1997) Neuroprotection by both NMDA and non-NMDA receptor antagonists in *in vitro* ischaemia. *Brain Res.* 755, 36-46.

Proetzel G., Pawlowski S. A., Wiles M. V., Yin M., Boivin G. P., Howles P. N., Ding J., Ferguson M. W., Doetschman T. (1995) Transforming growth factor beta 3 is required for secondary palate fusion. *Nat. Genet.* 11, 409-414.

Pulsinelli W. A., Brierley J. B. (1979) A new model of bilateral hemispheric ischaemia in the unanesthetized rat. *Stroke.* 10, 267-272.

Pyo H., Jou I., Jung S., Hong S., Joe E. (1998) Mitogen activated protein kinases activated by lipopolysaccharide and β-amyloid in cultured rat microglia. *Neuroreport.* 9, 871-874.

Pyo H., Joe E., Jung S., Lee S. H., Jou I. (1999) Gangliosides activate cultured rat brain microglia. *J. Biol. Chem.* 274, 34584-34589.

Raddassi K., Berthon B., Petit J. F., Lemaire G. (1994) Role of calcium in the activation of mouse peritoneal macrophages: induction of NO synthase by calcium ionophores and thapsigargin. *Cell. Immunol.* 153, 443-455.

Rang H. P., Dale M. M., Ritter J. M. (1999) *Pharamacology.* Fouth Edition. Churchill Livingstone New York. USA.

Rangon C. M., Haik S., Faucheux B. A., Metz-Boutigue M. H., Fierville F., Fuchs J. P., Hauw J. J., Aunis D. (2003) Different chromogranin immunoreactivity between prion and α-beta amyloid plaques. *Neuroreport.* 14, 755-758.

Ransom B. R., Sontheimer H. (1992) The neurophysiology of glial cells. *J. Clin. Neurophysiol.* 9, 224-251.

Reiffen F. U., Gratzl M. (1986) Chromogranins, widespread in endocrine and nervous tissue, bind Ca^{2+}. *FEBS. Lett.* 195, 327-330.

Reinhard J. Scheel A. A., Dickmann D., Hall A., Ruppert C., Bahler M. (1995) A novel type of myosin implicated in signalling by rho family GTPases. *EMBO J.* 14, 697-704.

Ritchie K., Lovestone S. (2002) The dementias. *The Lancet.* 360, 1759-1766.

Rivera S., Guillot S., Agassandian C., Ari Y. B., Khrestchatisky M. (1998) Serum deprivation induced apoptosis in cultured hippocampi is prevented by kainate. *Neuroreport.* 9, 3949-3953.

Roach T., Slater S., Koval M., White L., McFarland E. C., Okumara M., Thomas M., Brown E. (1997) CD45 regulates Src family member kinase activity associated with macrophage integrin mediated adhesion. *Curr. Biol.* 7, 408-417.

Robakis N. K., Ramakrishna N., Wolfe G., Wisniewski H. M. (1987) Molecular cloning and characterisation of a cDNA encoding the cerebrovascular and the neuritic plaque amyloid peptides. *Proc. Natl. Acad. Sci.* 84, 4190-4194.

Rogaev E. I., Sherrington R., Rogaeva E. A., Levesque G., Ikeda M., Linag Y., Chi H., Lin C., Holman K., Tsuda T., Mar L., Sorbi S., Nacmias B., Piacentini S., Amaducci L., Chumakov I., Coohen D., Lannfelt L., Fraser P. E., Rommens J. M., St George-Hyslop P. H. (1995) Familial Alzheimer's disease in kindreds with missense mutations in a gene on chromosome 1 related to Alzheimer's disease type 3 gene. *Nature.* 376, 775-778.

Rohn T. T., Ivins K. J., Bahr B. A., Cotman C. W., Cribbs D. H. (2000) A monoclonal antibody to amyloid precursor protein induces neuronal apoptosis. *J. Neurochem.* 74, 2331-2342.

Roit I., Brostoff J., Male D. (1987) Immunology. Second Edition. Churchill Livingstone, Edinburgh, UK.

Rossi D. J., Oshima T., Attwell D. (2000) Glutamate release in severe brain ischaemia is mainly by reversed uptake. *Nature.* 403, 316-321.

Rossjohn J., Cappai R., Feil C., Henry A., McKinstry W. J., Galatis D., Hesse L., Multhaup G., Beyreuther K., Masters C. L., Parker M. (1999) Crystal structure of the N-terminal, growth factor like domain of Alzheimer amyloid precursor protein. *Nature Struct. Biol.* 6, 327-331.

Rothwell N., Luheshi G. N. (2000) Interleukin 1 in the brain: biology, pathology and therapeutic target. *Trends. Neurol. Sci.* 23, 618-625.

Rothwell N., Allan S., Toulmond S. (1997) The role of interleukin 1 in acute neurodegeneration and stroke: pathological and therapeutic implications. *J. Clin. Invest.* 100, 2648-2652.

Rupalla K., Allegrini P. R., Sauer D., Wiessner C. (1998) Time course of microglia activation and apoptosis in various brain regions after permanent focal cerebral ischaemia in mice. *Acta Neuropathol.* 96, 172-178.

Ryu J., Pyo H., Jou I., Joe E. (2000) Thrombin induces NO release from cultured rat microglia via protein kinase C, mitogen activated protein kinase and NFκβ. *J. Biol. Chem.* 275, 29955-29959.

St George-Hyslop P. H., Tanzi R. E., Polinsky R. J., Haines J. L., Nee L., Watkins P. C., Myers R. H., Feldman R. G., Pollen D., Drachman D., Growdon J., Bruni A., Foncin J. F., Dalmon D., Frommelt P., Amaducci L., Sorbi S., Piancentini S., Stewart G. D., Hobbs W. J., Conneally M., Gusella J. F. (1987) The genetic defect causing familial Alzheimer's disease maps on chromosome 1. *Science.* 235, 885-890.

Salazar E. P., Rozengurt E. (1999) Bombesin and platelet derived growth factor induce association of endogenous focal adhesion kinase with Src in intact swiss 3T3 cells. *J. Biol. Chem.* 274, 28371-28378.

Saleh A., Srinivasula S., Acharya S., Fishel R., Alnemri E. S. (1999) Cytochrome c and dATP mediated oligomerization of APAF-1 is a prerequisite for pro-caspase 9 actiavtion. *J. Biol. Chem.* 274, 17941-17945.

Salvioli S., Ardizzoni A., Franceschi C., Cossarizza A. (1997) JC-1, but not $DiOC_6$ or rhodamine 123, is a reliable fluorescent probe to assess $\Delta\Psi$ changes in intact cells: implications for studies on mitochondrial functionality during apoptosis. *FEBS. Lett.* 411, 77-82.

Sanford L. P., Ormsby I., Gittengerger-de Groot A. C., Sariola H., Friedman R., Boivin G. P., Cardell E. L., Doetschman T. (1997) TGFβ2 knockout mice have multiple developmental defects that are non-overlapping with other TGFβ knockout phenotypes. *Develop.* 124, 2659-2670.

Sasaki T., Irie-Sasaki J., Penninger J. M. (2001) New insights into the transmembrane protein tyrosine phosphatase CD45. *Internat. J. Biochem. Cell Biol.* 33, 1041-1046.

Schellenberg G. D. (1995) Geneteic dissection of Alzheimer's disease, a heterogeneous disorder. *Proc. Natl. Acad. Sci.* 92, 8552-8559.

Schlichter L. C., Sakellaropoulous G., Ballyk B., Pennefather P. S., Phipps D. J. (1996) Properties of K^+ and Cl^- channels and their involvement in proliferation of rat microglial cells. *Glia.* 17, 225-226.

Schmidt A. M., Vianna M., Gerlach M., Brett J., Kao J., Esposito C., Hegarty H., Hurley W., Clauss M., Wang F., Pan Y. C. E., Tsang T. C., Stern D. (1992) Isolation and characterisation of two binding proteins for advanced glycosylation end products from bovine lung which are present on the endothelial cell surface. *J. Biol. Chem.* 267, 14987-14997.

Schmidt H. H. H. W., Pollock J. S., Nakane M., Gorsky L. D., Forstermann U., Murad F. (1991) Purification of a soluble isoform of guanylyl cyclase-activating factor synthase. *Proc. Natl. Acad. Sci.* 88, 365-369.

Schmidt-Kastner R., Fliss H., Hakim A. M. (1997) Subtle neuronal death in the striatum after short forebrain ischaemia in rats detected by *in situ* end-labelling for DNA damage. *Stroke.* 28, 163-170.

Schulz J. B., Weller M., Moskowitz M. A. (1999) Caspases as treatment targets in stroke and neurodegenerative disease. *Ann. Neurol.* 45, 421-429.

Schurr A. (2002) Lactate, glucoase and energy metabolism in the ischaemic brain. *Int. J. Mol. Med.* 10, 131-136.

Seaton T. A., Cooper J. M., Schapira A. H. V. (1998) Cyclosporin A inhibition of apoptosis induced by mitochondrial compex 1 toxins. *Brain Res.* 809, 12-17.

Segar R., Krebs E. G. (1995) The MAPK signalling cascade. *FASEB J.* 9, 726-735.

Selkoe D. J. (1994) Alzheimer's disease: a central role for amyloid. *J. Neuropathol. Exp. Neurol.* 53, 438-447.

Sessa W. C., Harrison J. K., Barber C. M., Zeng D., Durieux M. E., D'Angelo D. D., Lynch K. R., Peach M. (1992) Molecular cloning and expression of cDNA encoding endothelial cell nitric oxide synthase. *J. Biol. Chem.* 267, 15274-15276.

Shaffer L. M., Dority M. D., Gupta-Bansal R., Frederickson R. C. A., Younkin S. G., Brunden K. R. (1995) Amyloid β protein (Aβ) removal by neuroglial cells in culture. *Neurobiol. Aging.* 16, 737-745.

Shalit F., Sredni B., Rosenblatt-Bin H., Kazimirsky G., Brodie C., Huberman M. (1997) β-amyloid induces tumour necrosis factor α and nitric oxide production in murine macrophage cultures. *Neuroreport.* 8, 3577-3580.

Sharp F. R., Swanson R. A., Hokaniemi J., Kogure K., Massa S. M. (1998) Neurochemistry and molecular biology. In '*Stroke, pathophysiology, diagnosis and management.*' Third edition. Edited by Barnett H. J.M., Mohr J. P., Stein B. M., Yatsu F. M. Churchill and Livingstone. Philadelphia, USA.

Shaywitz A. J., Greenberg M. E. (1999) CREB: a stimulus-induced transcription factor activated by a diverse array of extracellular signals. *Ann. Rev. Biochem.* 68, 821-861.

Sherrington R., Rogaev E. I., Liang Y., Rogaeva E. A., Levesque G., Ikedda M., Chi H., Lin C., Li G., Holman K., Tsuda T., Mar L., Foncin J. F., Bruni A. C., Montesi M. P., Sorbi S., Rainero I., Pinessi L., Nee L., Chumkov I., Pollen D., Brookes A., Sanseau P., Polinsky R. J., Wasco W., Da Silva H. A. R., Haines J.L., Pericak-Vance M. A., Tanzi R. E., Roses A. D., Fraser P. E., Rommens J. M., St George-Hyslop P. H. (1995) Cloning of a gene bearing missense mutation in early onset familial Alzheimer's disease. *Nature.* 375, 754-760.

Sherwood L. (1993) *Human Physiology from Cells to Systems.* Third Edition. Brookes/Cole Publishing LTD. Minneapolis, USA,

Shigemoto-Mogami Y., Koizumi S., Tsuda M., Ohsawa K., Kohsaka S., Inoue K. (2001) Mechanisms underlying extracellular ATP evoked interleukin 6 release in mouse microglial cell line, MG-5. *J. Neurochem.* 78, 1339-1349.

Shin C. Y., Choi J. W., Ryu J. R., Ko K. H., Choi J. J., Kim H. S., Kim H. S., Lee J. C., Lee S. J., Kim H. C., Kim W. K. (2002) Glucose deprivation decreases nitric oxide production via NADPH depletion in immuno-stimulated rat primary astrocytes. *Glia.* 37, 268-274.

Si Q. S., Nakamura Y., Kataoka K. (1997) Albumin enhances superoxide production in cultured microglia *Glia.* 21, 413-418.

Si Q., Nakamura Y., Kataoka K. (2000) A serum factor enhances production of nitric oxide and tumour necrosis factor alpha from cultured microglia. *Exp. Neurol.* 162, 89-97.

Simon M. I., Strathmann M. P., Gautam N. (1991) Diversity of G proteins in signal transduction. *Science.* 252, 802-808.

Skoog I., Wallin A., Fredman P., Hesse C., Aevarsson O., Karlsson I., Gottfries C. G., Blennow K. (1998) A population study on blood-brain barrier function in 85-year-olds: relation to Alzheimer's disease and vascular dementia. *Neurol.* 50, 966-971.

Slepko N., Levi G. (1996) Progressive activation of adult microglial cells *in vitro*. *Glia.* 16, 241-246.

Smith I. F., Boyle J. P., Plant L. D., Pearson H.A., Peers C. (2003) Hypoxic remodelling of Ca^{2+} stores in type I cortical strocytes. *J. Biol. Chem.* 278, 4875-4881.

Smith M. A., Richey Harris P. L., Sayre L. M., Beckman J. S., Perry G. (1997) Widespread peroxynitrite mediated damage in Alzheimer's disease. *J. Neurosci.* 17, 2653-2657.

Smith R. A., Baglioni C. (1987) The active form of tumour necrosis factor is a trimer. *J. Biol. Chem.* 262, 6951-6954.

Smits H. A., Machiel de Vos N., Wat J. W. Y., van der Bruggen T., Verhoef J., Nottet H. S. L. M. (2001a) Intracellular pathways involved in TNFα and superoxide anion release by Aβ(1-42) stimulated primary human macrophages. *J. Neuroimmunol.* 115, 144-151.

Smits H. A., Beelen A. J., de Vos N. M., Rijsmus A., van der Bruggen T., Verhoef J., van Muiswinkel F., Nottet H. S. L. M. (2001b) Activation of human macrophages by amyloid-β is attenuated by astrocytes. *J. Immunol.* 166, 6869-6876.

Snell R. S. (1997) *Clinical neuroanatomy for medical students (4th Edition).* Lippicott-Raven. Philadelphia, USA.

Soares M. B. P., Titus R. G., Shoemaker C. B., David J. R., Bozza M. (1998) The vasoactive peptide maxadilan from sand fly saliva inhibits TNFα and induces IL-6 by mouse macrophages through interaction with the pituitary adenylate cyclase activating polypeptide (PACAP) receptor. *J. Immunol.* 160, 1811-1816.

Soldati T. (2003) Unconventional myosins, actin dynamics and endocytosis: A ménage a trois? *Traffic.* 4, 358-366.

Soledad M., Opazo C., Larrondo L. F., Munoz F. J., Ruiz F., Leighton F., Inestrosa N. C. (2000) The role of oxidative stress in the toxicity induced by amyloid β peptide in Alzheimer's disease. *Prog. Neurobiol.* 62, 633-648.

Soto C. (1999) Plaque busters: strategies to inhibit amyloid formation in Alzheimer's disease. *Mol. Med. Tod.* 77, 412-418.

Spector A. A., John K., Fletcher J. E. (1969) Binding of long chain fatty acids to bovine serum albumin. *J. Lipid. Res.* 10, 56-67.

Spranger M., Kiprianova I., Krempien S., Schwab S. (1998) Reoxygenation increases the release of reactive oxygen intermediates in murine microglia. *J. Cereb. Blood Flow Met.* 18, 670-674.

Spurti-Furga G. (1995) Regulation of the Src protein tyrosine kinase. *FEBS Lett.* 369, 62-66.

Stewart W. F., Kawas C., Corrada M., Metter E. J. (1997) Risk of Alzheimer's disease and duration of NSAID use. *Neurol.* 48, 626-632.

Strange P. (1992) Alzheimer's disease. In *'Brain Biochemistry and Brain Disorders'*. Oxford University Press. Oxford, UK.

Strasser U., Fischer G. (1995) Protection from neuronal damage induced by combined oxygen and glucose deprivation in organotypic hippocampal cultures by glutamate receptor antagonists. *Brain Res.* 687, 167-174.

Streit W J. (2002) Microglia as neuroprotecive immunocompetent cells of the CNS. *Glia.* 40, 133-139.

Streit W. J., Graeber M. B. (1993) Heterogeneity of microglial and perivascular cell populations: insights gained from the facial nucleus paradigm. *Glia.* 7, 68-74.

Streit W. J., Kreutzberg G. W. (1987) Lectin binding by resting and reactive microglia. *J. Neurocytol.* 16, 249-260.

Streit W. J., Graeber M. B., Kreutzberg W. (1989) Expression of Ia antigen on perivascular and microglial cells after sublethal and lethal motor neuron injury. *Exp. Neurol.* 105, 115-126.

Strittmatter W. J., Weisgraber K. H., Goedart M., Saunders A. M., Huang D., Corder E. H., Dong L. M., Jakes R., Alberts M. J., Gilbert J. R., Han S. H., Hulette C., Einstein G., Schmechel D. E., Pericak-Vance M. A., Roses A. D. (1994) Hypothesis: microtubule instability and paired helical filament formation in the Alzheimer's disease brain are related to apolipoprotein E genotype. *Exp. Neurol.* 125, 163-171.

Strzelecka-Kiliszek A., Kwiatkowska K., Sobota A. (2002) Lyn and Syk kinases are sequentially engaged in phagocytosis mediated by FcγR. *J. Immunol.* 169, 6787-6794.

Sturrock R. R. (1978) A developmental study of epiplexus cells and supraependymal cells and their possible relationship to microglia. *Neuropath. Appl. Neurobiol.* 4, 307-322.

Susin S. A., Lorenzo H. K., Zamzami N., Marzo I., Snow B. E., Brothers G. M., Mangion J., Jacotot E., Costantini P., Loeffler M., Larochette N., Goodlett D. R., Aebersold R., Siderovski D. P., Penninger J. M., Kroemer G. (1999) Molecular characterisation of mitochondrial apoptotic inducing factor. *Nature.* 397, 441-446.

Suzuki H., Franz H., Yamamoto T., Iwasaki Y., Konno H. (1988) Identification of the normal microglial population in human and rodent nervous tissue using lectin-histochemistry. *Neuropath. Appl. Neurobiol.* 14, 221-227.

Suzuki H., Kurihara Y., Takeya M., Kamada N., Kataoka M., Jishage K., Suzuki T., Takashima Y., Kawabe Y., Cynshi O., Wada Y., Honda M., Kurihara H., Aburatani H., Doi T., Matsumoto A., Azuma S., Noda T., Toyoda S., Takahashi K., Krujit J. K., van Berkel T. J. C. (1997) A role for macrophage scavenger receptors in atherosclerosis and susceptibility to infection. *Nature*. 386, 292-296.

Suzuki N., Cheung T. T., Cai X. D., Odaka A., Otvos L., Eckman C., Golde T. E., Younkin S. G. (1994) An increased percentage of long amyloid β protein secreted by familial amyloid β protein precursor (βAPP_{717}) mutants. *Science*. 264, 1336-1340.

Suzuki M., Tabuchi M., Ikeda M., Tomita T. (2002) Concurrent formation of peroxynitrite with the expression of inducible nitric oxide synthase in the brain during middle cerebral artery occlusion and reperfusion in rats. *Brain Res*. 951, 113-120.

Suzumura A., Marunouchi T., Yamamoto H. (1991) Morphological transformation of microglia *in vitro*. *Brain Res*. 545, 301-306.

Swanson R. A. (1992) Astrocyte glutamate uptake during chemical hypoxia *in vitro*. *Neurosci. Lett.* 147, 143-146.

Swanson R. A., Choi D. W. (1993) Glial glycogen stores affect neuronal survival during glucose deprivation *in vitro*. *J. Cereb. Blood Flow Metab*. 13, 162-169.

Swanson R. A., Farrell K., Simon R. P. (1995) Acidosis causes failure of astrocye glutamate uptake during hypoxia. *J. Cereb. Blood Flow Metab*. 15, 417-424.

Swanson R. A., Farrell K., Stein B. A. (1997) Astrocye energetics, function and death under conditions of incomplete ischaemia: a mechanism of glial death in the penumbra. *Glia*. 21, 142-153.

Szatkowski M., Atwell D. (1994) Triggering and execution of neuronal death in brain ischaemia: two phases of glutamate release by different mechanisms. *Trends. Neurosci.* 17, 359-365.

Tabernero A., Medina A., Sanchez-Abarca L. I., Lavado E., Medina J. M. (1999) The effect of albumin on astrocytes metabolism is not brought about through the control of cystolic calcium concentrations but by free fatty acid sequestration. *Glia*. 25, 1-9.

Tabernero A., Lavado E. M., Granda B., Velasco A., Medina J. M. (2001) Neuronal differentiation is triggered by oleic acid synthesised and released by astrocytes. *J. Neurochem*. 79, 606-616.

Tabernero A., Velasco A., Granda B., Lavado E. M., Medina J. M. (2002a) Transcytosis of albumin in astrocytes activates the sterol regulatory element binding protein 1, which promotes the synthesis of the neurotrophic factor oleic acid. *J. Biol. Chem.* 277, 4240, 4246.

Tabernero A., Granda B., Medina A., Sanchez-Abarca L. I., Lavado E., Medina J. M. (2002b) Albumin promotes neuronal survival by increasing the synthesis and release of glutamate. *J. Neurochem.* 81, 881-891.

Takahashi M., Billups B., Rossi D., Sarantis M., Hamann M., Attwell D. (1997) The role of glutamate transporters in glutamate homeostasis in the brain. *J. Exp. Biol.* 200, 401-409.

Takamatsu H., Tsukada H., Kakiuchi T., Tatsumi M., Umemra K. (2000) Changes in local cerebral blood flow in photochemically induced thrombotic occlusion model in rats. *Eur. J. Pharmacol.* 398, 375-379.

Tanzi R. E. (1998) Of calcium, caspases and cognitive decline. *Nat. Med.* 4, 1127-1128.
Tanzi R. E., Gusella J. F., Watkins P. C., Bruns G. A. P., St George-Hyslop P., van Keuren M. L., Patterson D., Pagan S., Kurnit D. M., Neve R. L. (1987) Amyloid β protein gene: cDNA, mRNA distribution, and genetic linkage near the Alzheimer's locus. *Science.* 235, 880-884.

Tatemichi T. K., Paik M., Bagiella E., Desmond D. W., Stern Y., Sano M., Hauser W. A., Mayeux R. (1994) Risk of dementia after stroke in hospitalized cohort. *Neurol.* 44, 1885-1891.

Taupenot L., Ciesielski-Treska J., Ulrich G., Chasserot-Golaz D., Bader M. F. (1996) Chromogranin A triggers a phenotypic transformation and the generation of nitric oxide in brain microglial cells. *Neurosci.* 72, 377-389.

Taylor D. L., Diemel L. T., Pocock J. M. (2003) Activation of microglial group III metabotropic glutamate receptors protects neurons against microglial neurotoxicity. *J. Neurosci.* 23, 2150-2160.

Taylor D. L., Diemel L. T., Cuzner M. L., Pocock J. M. (2002) Activation of group III metabotropic glutamate receptors underlies microglial reactivity and neurotoxicity following stimulation with chromogranin A, a peptide up-regulated in Alzheimer's disease. *J. Neurochem.* 82, 1179-1191.

Taylor-Kimberly W., LaVoie M. J., Ostaszewski B. L., Ye W., Wolfe M. S., Selkoe D. J. (2003) γ secretase is a membrane protein complex comprised of presenilin, nicastrin, aph-1 and pen-2. *Proc. Natl. Acad. Sci.* 100, 6382-6387.

Terzi E., Holzemann G., Seelig J. (1994a) Reversible random coil - β sheet transition of the Alzheimer's β-amyloid fragment (25-35). *Biochem.* 33, 1345-1350.

Terzi E., Holzemann G., Seelig J. (1994b) Alzheimer β amyloid peptide 25-35: electrostatic interactions with phospholipid membranes. *Biochem.* 33, 7434-7441.

Tewari M. Dixit V. M. (1996) Signalling through members of the tumour necrosis factor receptor family. In '*Signal transduction*' (First Edition). Edited by Bradshaw R., Purton M. Chapman and Hall, New York, USA.

Thery C., Chamak B., Mallat M. (1991) Cytotoxic effect of brain macrophages on developing neurons. *Eur. J. Neurosci.* 3, 1155-1164.

Thomas W. E. (1992) Brain macrophages: evaluation of microglia and their functions. *Brain Res. Rev.* 17, 61-74.

Thornberry N. A., Lazebnik Y. (1998) Caspases: Enemies within. *Science.* 281, 1312-1316.

Thornberry N. A., Bull H. G., Calaycay J. R., Chapman K. T., Howard A. D., Kostura M. J., Miller D. K., Molineaux S. M., Weidner J. R., Aunins J., Elliston K. O., Ayala J. M., Casano F. J., Chin J., Ding G., Egger L A., Gaffney E. P., Limjuco G., Palyha O. C., Raju S. M., Rolando A. M., Saliey P. J., Yamin T. T., Lee T. D., Shively J. E., MacCross M., Mumford R. A., Schmidt J. A., Tocci M. J. (1992) A novel heterodimeric cysteine protease is required for interleukin 1β processing in monocytes. *Nature.* 356, 768, 774.

Thuret G., Chiquet C., Herrag S., Dumollard J. M., Bednarz J., Campos L. (2003) Mechanisms of staurosporine induced apoptosis in a human corneal endothelial cell line. *Br. J. Ophthalmol.* 87, 346-352.

Tibbles L. A., Woodgett J. R. (1999) The stress activated protein kinase pathways. *Cell. Mol. Life Sci.* 55, 1230-1254.

Tiffany H. L., Lavigne M. C., Cui Y. H., Wang J. M., Leto T. L., Gao J. L., Murphy P. M. (2001) Amyloid β induces chemotaxis and oxidant stress by acting at formylpeptide receptor 2, a G protein coupled receptor expressed in phagocytes and brain. *J. Biol. Chem.* 276, 23645-23652.

Tikka T., Fiebich B. L., Goldstein G., Keinanen R., Koistinaho J. (2001) Minocycline, a tetracycline derivative is neuroprotective against excitotoxicity by inhibiting activation and proliferation of microglia. *J. Neurosci.* 21, 2580-2588.

Titus M. A. (1999) A class VII unconventional myosin is required for phagocytosis. *Curr. Biol.* 9, 1297-1303.

Tokmakov A. A., Sato K. I., Iwasaki T., Fukami Y. (2002) Src kinase induces calcium release in xenopus egg extracts via PLCγ and IP_3 dependent mechanism. *Cell Calcium*. 32, 11-20.

Torigoe K., Tanaka H. F., Takahashi A., Awaya A., Hashimoto K. (1996) Basic behaviour of migratory schwann cells in peripheral nerve regeneration. *Exp. Neurol.* 137, 301-308.

Troadec J. D., Thirion S., Petturiti D., Bohn M, T., Poujeol P. (1999) ATP acting on P_{2Y} receptors triggers calcium mobilisation in primary cultures of rat neurohypophysial astrocytes (pituicytes). *Eur. J. Physiol.* 437, 745-753.

Troy C. M., Rabacchi S. A., Friedman W. J., Frappier T. F., Brown K., Shelanski M. L. (2000) Caspase 2 mediates neuronal cell death induced by β amyloid. *J. Neurosci.* 20, 1386-1392.

Tsien R. Y. (1988) Fluorescence measurement and photochemical manipulation of cytosolic free calcium. *Trends Neurosci.* 11, 419-424.

Tsubuki S., Takaki Y., Saido T. C. (2003) Dutch, Flemish, Italian and Artic mutations of APP and resistance to physiologically relevant proteolytic degradation. *Lancet.* 361, 1957-1958.

Ueda T., Rieu P., Brayer J., Arnaout A. (1994) Identification of the complement iC3b binding site in the β2 integrin CR3 (Cd11b/CD18). *Proc. Natl. Acad. Sci.* 91, 10680-10684.

Uetsuki T., Takemoto K., Nishimura I., Okamoto M., Ninobe M., Momoi T., Miura M., Yoshikawa K. (1999) Activation of neuronal caspase 3 by intracellular accumulation of wild type Alzheimer amyloid precursor protein. *J. Neurosci.* 19, 6955-6964.

Vairano M., Dello Russo C., Pozzoli G., Battaglia A., Scambia G., Tringali G., Aloe-Spiriti M. A., Preziosi P., Navarra P. (2002) Erythropoietin exerts anti-apoptotic effects on rat microglial cell *in vitro*. *Eur. J. Neurosci.* 16, 584-592.

van Broeckhoven C. L. (1995) Molecular genetics of Alzheimer's disease: identification of genes and gene mutations. *Eur. Neurol.* 35, 8-19.

Vane J. R., Bakhle Y. S., Botting R. M. (1998) Cycloxygenase 1 and 2. *Annu. Rev. Pharmacol. Toxicol.* 38, 97-120.

Vasser R., Bennet B. D., Babu-Khan S., Kahn S., Mendiaz E. A., Denis P., Teplow D. B., Ross S., Amarante P., Loeloff R., Luo Y., Fisher S., Fuller J., Edenson S., Lile J., Jarosinski M. A., Biere A. L., Curran E., Burgess T., Louis J. C., Collins F., Treanor J., Rogers G., Citron M. (1999) β-secretase cleavage of Alzheimer's amyloid precursor protein by the transmembrane aspartic protease BACE. *Science*. 286, 735-741.

Vaughan D. W., Peters A. (1974) Neuroglial cells in the cerebral cortex of rats from young adult to old age: an electron microscopy study. *J. Neurocytol.* 3, 405-429.

Vedler C., Ulvestad E., Grundt I., Conti G., Nyland H., Matre R., Pleasure D. (1994) Fc receptor for IgG (FcR) on rat microglia. *J. Neuroimmunol.* 49, 19-24.

Vehmas A. K., Kawas C. H., Stewart W. F., Troncoso J. C. (2003) Immune reactive cells in senile plaques and cognitive decline in Alzheimer's disease. *Neurobiol. Ageing*. 24, 321-331.

Vilcek J., Lee T. H. (1991) Tumour necrosis factor. New insights into the molecular mechanisms of its multiple actions. *J. Biol. Chem.* 266, 7313-7316.

Volknandt W., Schober M., Fischer-Colbrie R., Zimmermann H., Winkler H. (1987) Cholinergic nerve terminals in the rat diaphragm are chromogranin A immunoreactive. *Neurosci. Lett.* 81, 241-244.

von Kügelgen I., Wetter A. (2000) Molecular pharmacology of 2_{PY} receptors. *Naunyn Schmiedeberg's Arch. Pharmacol.* 362, 310-323.

Wallach T. M., Segal A. W. (1996) Stoichiometry of the subunits of flavocytochrome b558 of the NAPH oxidase of phagocytes. *Biochem. J.* 320, 33-38.

Walton K. M., DiRocco R., Bartlett B. A., Koury E., Marcy V. R., Jarvis B., Schaefer E. M., Bhat R. V. (1998) Activation of $p38^{MAPK}$ in microglia after ischaemia. *J. Neurochem.* 70, 1764-1767.

Wang H., Ubl J. J., Stricker R., Reiser G. (2002) Thrombin (PAR-1) induced proliferation in astrocytes via MAPK involved multiple signalling pathways. *Am. J. Physiol. Cell Physiol.* 283, 1351-1364.

Wang X., Yue T. L., Barone F. C., Feuerstein G. Z. (1995) Monocyte chemoattractant protein 1 messenger RNA expression in rat ischaemic cortex. *Stroke*. 26, 661-666.

Watanabe H., Abe H., Takeuchi S., Tanaka R. (2000) Protective effect of microglial conditioned medium on neuronal damage induced by glutamate. *Neurosci. Lett.* 289, 53-56.

Watt J. A., Pike C. J., Walencewicz-Wasserman A. J., Cotman C. W. (1994) Ultra-structural analysis of β amyloid induced apoptosis in cultures hippocampal neurons. *Brain Res.* 661, 147-156.

Wekerle H., Linington C., Lassmann H., Meyermann R. (1986) Cellular immune reactivity in the CNS. *Trends Neurosci.* 9, 271-277.

Weisiger R., Gollan J., Ockner R. (1981) Receptor for albumin on the liver cell surface may mediate uptake of fatty acids and other albumin bound substances. *Science.* 211, 1048-1051.

Whitman S. C., Daugherty A., Post S. R. (2000) Regulation of acetylated low density lipoprotein uptake in macrophages by pertussis toxin sensitive G proteins. *J. Lipid. Res.* 41, 807-813.

Whitson J. S., Glabe C. G., Shintani E., Abcar A., Cotman C. W. (1990) Beta-amyloid protein promotes neuritic branching in hippocampal cultures. *Neurosci. Lett.* 110, 319-324.

Willis W. D., Grossman R. G. (1981) *Medical Neurobiology.* Third edition. Edited by Lotz J. E. The C. V. Mosby company. Missouri, USA.

Wirth J. A., Jensen K. A., Post P. L., Bement W. M., Mooseker M. S. (1996) Human IXb, an unconventional myosin with a chimerin like rho/rac GTPase activating protein domain in its tail. *J. Cell Sci.* 109, 653-661.

Wisniewski K. E., Wisniewski H. M., Wen G. Y. (1985) Occurrence of neuropathological changes and dementia of Alzheimer's disease in Down's syndrome. *Ann. Neurol.* 17, 278-282.

Wisniewski T., Fragione B. (1992) Apolipoprotein E: a pathological chaperone protein in patients with cerebral and systemic amyloid. *Neurosci. Lett.*135, 235-238.

Wisniewski T., Palha J. A., Ghiso J., Fragione B. (1995) S182 protein in Alzheimer's disease neuritic plaques. *The Lancet.* 346, 1366.

Wolf P. A., D'Agostino R. B. Epidemiology of stroke. In '*Stroke, pathophysiology, diagnosis and management.*' Third edition. Edited by Barnett H. J.M., Mohr J. P., Stein B. M., Yatsu F. M. Churchill and Livingstone. Philadelphia, USA.

Wolfe M. S., Xia W., Ostaszewski B. L., Diehl T. S., Taylor Kimberly W., Selkoe D. J. (1999) Two transmembrane aspartates in presenilin-1 required for presenilin endoproteolysis and γ secretase activity. *Nature.* 398, 513-517.

Wood J. G., Zinsmeister P. (1991) Tyrosine phosphorylation systems in Alzheimer's disease pathology. *Neurosci. Lett.* 121, 12-16.

Xaus J., Comalada M., Valledor A. F., Lloberas J., Lopez-Soriano F., Argiles J. M., Bogdan C., Celada A. (2000) LPS induces apoptosis in macrophages mostly through the autocrine production of TNFα. *Blood*. 95, 3823-3831.

Xie Q., Cho H. J., Calaycay J., Mumford R. A., Swiderek K. M., Lee T. D., Ding A., Troso T., Nathan C. (1992) Cloning and characterisation of inducible nitric oxide synthase from mouse macrophages. *Science*. 256, 225-228.

Xu J., Chuang D. (1987) Serotonergic, adrenergic and histaminegic receptors coupled to phospholipase c in cultured cerebellar granule cells of rats. *Biochem. Pharmacol.* 36, 2353-2358.

Xu J., Chen S., Ahmed H., Chen H., Ku G., Goldberg M. P., Hsu C. Y. (2001) Amyloid β peptides are cytotoxic to oligodendrocytes. *J. Neurosci.* 21, 1-5.

Yan S. D., Chen X., Fu J., Chen M., Zhu H., Roher A., Slattery T., Zhao L., Nagashima M., Morser J., Migheli A., Nawroth P., Stern D., Schmidt A. M. (1996) RAGE and amyloid β peptide neurotoxicity in Alzheimer's disease. *Nature*. 382, 685-691.

Yan S. D., Zhu H., Fu J., Yam S. F., Roher A., Tiurtellotte W. W., Rajavashisth T., Chen X., Godman G. C., Stern D., Schmidt A. M. (1997) Amyloid β peptide - receptor for advanced glycation endproduct interaction elicits neuronal expression of macrophage colony stimulating factor: A proinflammatory pathway in Alzheimer's disease. *Proc. Natl. Acad. Sci.* 94, 5296-5301.

Yan Y. P., Yin K. J., Sun F. Y. (1998) Effect of glutamate transporter on neuronal damage induced by photochemical thrombotic brain ischaemia. *Neuroreport*. 9, 441-446.

Yang F., Sun X., Beech W., Teter B., Wu S., Sigel J., Vinters h. V., Frautschy S. A., Cole G. M. (1998) Antibody to caspase cleaved actin detects apoptosis in differentiated neuroblastoma and plaque associated neurones and microglia in Alzheimer's disease. *Am. J. Pathol.* 152, 379-389.

Yang J. C., Cortopassi G.A. (1998) Induction of the mitochondrial permeability transition causes release of the apoptogenic factor cytochrome c. *Free Radical Biol. Med.* 24, 624-631.

Yanker B. A., Duffy L. K., Kirschner D. A. (1990) Neurotrophic and neurotoxic effects of amyloid beta protein: reversal by tachykinin neuropeptides. *Science*. 250, 279-282.

Yasuhara O., Kawamata T., Aimi Y., McGeer E. G., McGeer P. L. (1994) Expression of chromogranin A in lesions in the central nervous system from patients with Alzheimer's disease. *Neurosci. Lett.* 170, 13-16.

Yates S. L., Burgess L. H., Kocsis-Angle J., Antal J. M., Dority M. D., Embury P. B., Pitrkowski A. M., Brunden K. R. (2000) Amyloid beta and amylin fibrils induce increases in proinflammatory cytokine and chemokine production by THP-1 cells and murine microglia. *J. Neurochem.* 74, 1017-1025.

Yeh C. H., Sturgis L., Haidacher J., Zhang X. N., Sherwood S. J., Bjercke R. J., Juhasz O., Crow M. T., Tilton R. G., Denner L. (2001) Requirement for p38 and p44/42 mitogen activated protein kinases in RAGE mediated nuclear factor κβ transcriptional activation and cytokine secretion. *Diabetes.* 50, 1495-1504.

Yenari M. A., Giffard R. G. (2001) Ischaemic vulnerability of primary murine microglial cultures. *Neurosci. Lett.* 298, 5-8.

You Y., Kaur C. (2000) Expression of induced nitric oxide synthase in amoeboid microglia in post natal rats following an exposure to hypoxia. *Neurosci. Lett.* 279, 101-104.

Young P. A., Young P. H. (1997) *Basic clinical neuroanatomy (First Edition).* Williams and Wilkins. Baltimore, USA.

Yu A. C., Chan P. H., Fishman R. A. (1987) Arachidonic acid inhibits uptake of glutamate and glutamine but not of GABA in cultured cerebellar granule cells. *J. Neurosci. Res.* 17, 424-427.

Yu A. C. H., Gregory G. A., Chan P. H. (1989) Hypoxia induced dysfunctions and injury of astrocytes in primary cell cultures. *J. Cereb. Blood Flow Metab.* 9, 20-28.

Yuchen H. Z., Liu X., Wang X. (1999) An APAF-1 cytochrome c multimeric complex is a functional apoptosome that activates pro-caspase 9. *J. Biol. Chem.* 274, 11549-11556.

Zamzami N., Marchetti P., Castedo M., Hirsch T., Susin S. A., Masse B., Kroemer G. (1996) Inhibitors of permeability transition interfere with the disruption of the mitochondrial transmembrane potential during apoptosis. *FEBS. Lett.* 384, 53-57.

Zhang H., Yang Y., Steinbrecher U. P. (1993) Structural requirements for the binding of modified proteins to the scavenger receptor of macrophages. *J. Biol. Chem.* 268, 5535-5542.

Zhang L., McLarnon J G., Goghari V., Lee Y. B., Kim S. U., Krieger C. (1998) Cholinergic agonists increase intracellular Ca^{2+} in cultured human microglia. *Neurosci. Lett.* 255, 33-36.

Zhao L., Eghhbali-Webb M. (2001) Release of pro- and anti- angiogenic factors by human cardiac fibroblasts: effects on DNA synthesis and protection under hypoxia in human endothelial cells. *Biochem. Biophys. Acta.* 1538, 273-282.

Zhu D. Y., Deng Q., Yao H. H., Wang D. C., Deng Y., Liu G. (2002) Inducible nitric oxide synthase expression in the ischaemic core and penumbra after transient focal cerebral ischaemia in mice. *Life Sci.* 71, 1985-1996.

Zhu W., Sano H., Nagai R., Fukuhara K., Miyazaki A., Horiuchi S. (2001) The role of galectin-3 endocytosis of advanced glycation end products and modified low density lipoproteins. *Biochem. Biophys. Res. Comm.* 280, 1183-1188.

Zhu Y., Xu H., Huang K. (2002) Mitochondrial permeability transition and cytochrome c release induced by selenite. *J. Inorg. Biochem.* 90, 43-50.

Zondag G. C. M., Postma F. R., Etten I. V., Verlaan I., Moolenaar W. H. (1998) Shingosine-1 phosphate signalling through the G protein coupled receptor Edg-1. *Biochem. J.* 330, 605-609.